

Complications of Hemorrhagic and
Ischemic Stroke:
a CT Perfusion Evaluation

Jan Willem Dankbaar

Complications of Hemorrhagic and Ischemic Stroke: a CT Perfusion Evaluation

Thesis, Utrecht University, the Netherlands

ISBN: 978-90-3935330-1

© Jan Willem Dankbaar, Utrecht, 2010

The copyright of the articles that have been published or accepted for publication has been transferred to the respective Journals

The research in this thesis was conducted at the departments of radiology, neurology and neurosurgery of the University Medical Center Utrecht, the Netherlands, and the department of radiology of the University of California San Francisco, USA. It was financially supported by the department of radiology of the University Medical Center Utrecht, ZonMw (Nederlandse organisatie voor gezondheidsonderzoek en zorginnovatie), NWO (Nederlandse organisatie voor wetenschappelijk onderzoek) and the Girard de Miolet van Coehoorn Stichting.

Lay-out: Roy Sanders

Cover design: Jan Willem Dankbaar

Printed by: Gildeprint Drukkerijen-Enschede, the Netherlands

Complications of Hemorrhagic and Ischemic Stroke: a CT Perfusion Evaluation

**Complicaties van Hemorragische en Ischemische Beroertes:
een Evaluatie met CT-Perfusie**

(met een samenvatting in het Nederlands)

Proefschrift

ter verkrijging van de graad van doctor aan de Universiteit Utrecht op gezag van
de rector magnificus, prof.dr. J.C. Stoof, ingevolge het besluit van
het college voor promoties in het openbaar te verdedigen
op vrijdag 21 mei 2010 des middags te 4.15 uur

door

Jan Willem Dankbaar
geboren op 1 juli 1979 te Amsterdam

Promotoren: Prof. dr. G.J.E. Rinkel
Prof. dr. W.P.Th.M. Mali

Co-promotoren: Dr. I.C. van der Schaaf
Dr. B.K. Velthuis

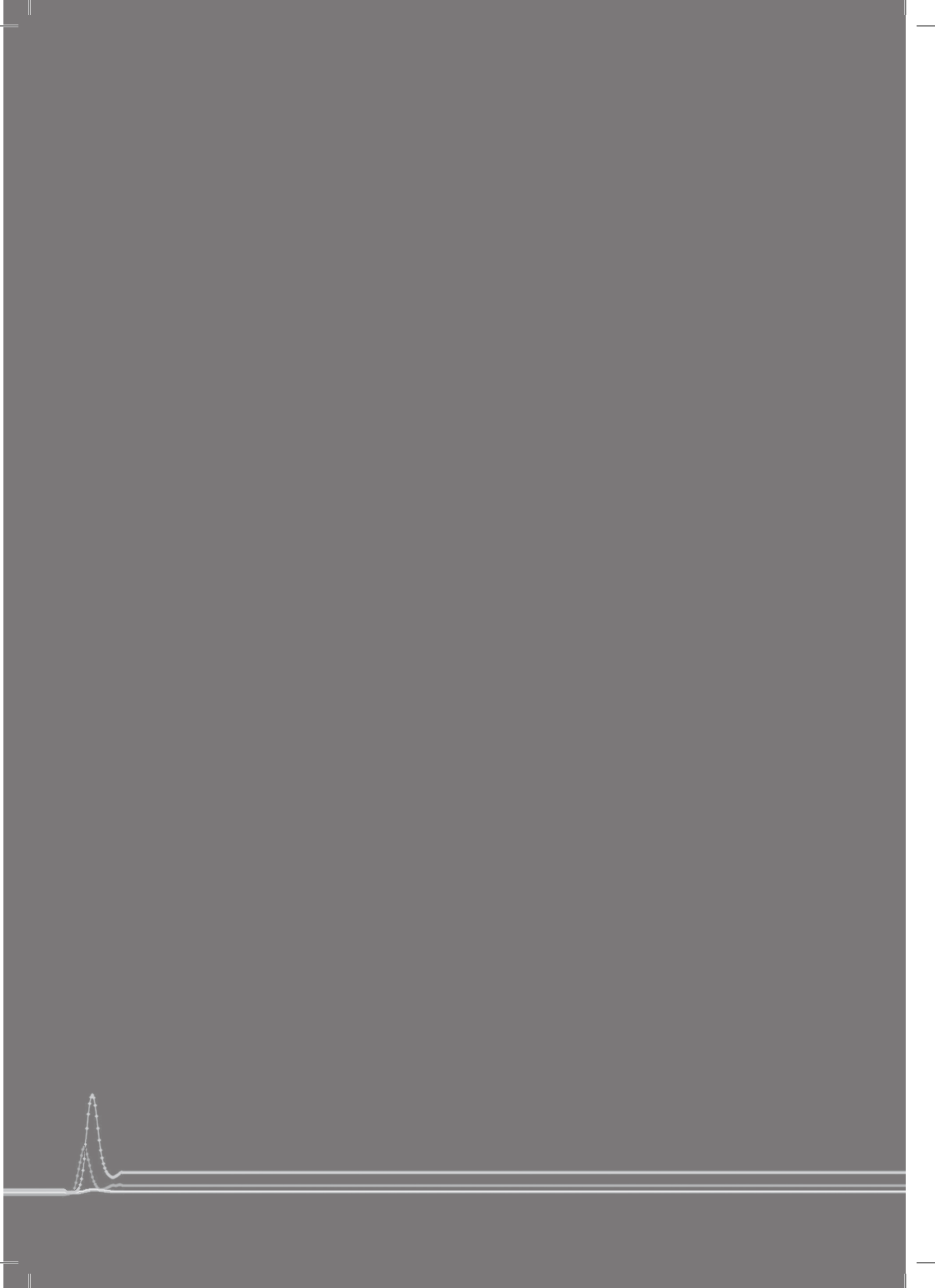
Financial support for the reproduction of this thesis was generously provided by:

Philips Healthcare, EV3 Benelux, Terumo Europe N.V., Röntgen Stichting Utrecht

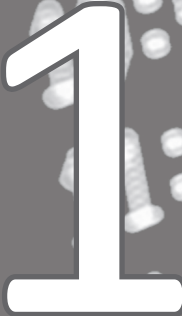
Contents

Chapter 1	General Introduction	9
Part 1	Complications of subarachnoid hemorrhage: a CT perfusion evaluation of delayed cerebral ischemia	17
Chapter 2	Normal values of cerebral perfusion measured with CT perfusion: absolute values and inter-territorial ratios.	19
Chapter 3	Relationship between vasospasm, cerebral perfusion and delayed cerebral ischemia after aneurysmal subarachnoid hemorrhage.	35
Chapter 4	Changes in cerebral perfusion around the time of delayed cerebral ischemia in subarachnoid hemorrhage patients.	49
Chapter 5	Diagnosing delayed cerebral ischemia with different CT modalities in SAH patients with clinical deterioration.	67
Chapter 6	Diagnostic threshold values of cerebral perfusion measured with CT for delayed cerebral ischemia after aneurysmal subarachnoid hemorrhage.	81
Chapter 7	Effect of different components of triple-H therapy on cerebral perfusion in patients with aneurysmal subarachnoid hemorrhage: a systematic review.	97

Part 2	Complications of ischemic stroke: a CT perfusion evaluation of blood-brain barrier damage	113
Chapter 8	Dynamic CT perfusion assessment of blood-brain barrier permeability: first-pass versus delayed acquisition.	115
Chapter 9	Accuracy and anatomical coverage of CT perfusion assessment of blood-brain barrier permeability: one bolus versus two boluses.	129
Chapter 10	Age- and anatomy-related values of blood-brain barrier permeability measured with CT perfusion in non-stroke patients.	139
Chapter 11	Dynamic CT perfusion assessment of early changes in blood-brain barrier permeability of acute ischaemic stroke patients.	155
Chapter 12	Blood-brain barrier permeability assessed by CT perfusion predicts symptomatic hemorrhagic transformation and malignant edema in acute ischemic stroke.	167
Chapter 13	General Discussion	185
	Nederlandse Samenvatting	201
	Dankwoord	211
	List of publications	217
	Curriculum Vitae	221
	Color figures	225



General introduction



1

Stroke is the second leading cause of death in industrialized countries and one of the leading causes of disability worldwide.¹ About a quarter of all stroke patients dies within a month and more than a third has died after one year.² The clinical outcome after stroke is negatively influenced by the occurrence of complications. Detecting and predicting complications has important consequences for treatment decision making and plays an important part in improving outcome. In this thesis the evaluation of complications of two important subtypes of stroke, being subarachnoid hemorrhage (SAH) and ischemic stroke, will be discussed. Each subtype has its own pathogenic mechanism and its own distinct population. The first part of this thesis will discuss a harmful complication of SAH and the second part the major complications of ischemic stroke.

Part 1

Complications of subarachnoid hemorrhage: a CT perfusion evaluation of delayed cerebral ischemia

Subarachnoid hemorrhage (SAH) covers about 5% of all strokes^{2, 3} with an incidence of 6 to 9 per 100,000 per year.^{2, 4} It has a case fatality of 40 to 50% in the first month.^{2, 5} The cause of SAH is mostly (85%) rupture of a cerebral aneurysm.⁶ Half of the SAH patients are less than 55 years old. Because of this young age and the poor prognosis, the population based loss of productive life years from SAH is relatively high.⁷ The prognosis of SAH patients can be worsened by a complication termed delayed cerebral ischemia (DCI). DCI occurs in about one third of SAH patients in the first two weeks after hemorrhage and causes a 1.5 to 3 fold increase in case fatalities.^{5, 6} Currently, triple-H and its separate components (hypertension, hypervolemia, hemodilution) are used to treat DCI.⁸ However, it has not equivocally been proven that this type of treatment improves neurological outcome, and the use has been associated with an increased risk of life threatening sequelae.⁹ Physicians are therefore quite reluctant to apply triple-H or its components if the diagnosis DCI is not certain. Thus, to evaluate current treatment and to develop new treatment options, it is necessary to properly understand the pathogenesis of DCI and to accurately diagnose DCI in SAH patients. This can however be extremely challenging.

The development of DCI can be gradual and a decrease in the level of consciousness is often the only symptom at hand.⁶ In SAH patients there is a long list of comorbidity that could cause a decrease in consciousness. Aneurysm rebleeding, intraparenchymal hemorrhage (often coinciding with SAH), hydrocephalus, infection, and metabolic abnormalities can all cause clinical deterioration. Currently the diagnosis DCI is mainly based on excluding these other causes.⁶ Non-contrast CT (NCT) scans are made to exclude rebleeding, hydrocephalus and increasing edema around intraparenchymal hemorrhage. Physical and laboratory exams help to exclude metabolic and infectious causes. If all other causes for deterioration are excluded the diagnosis DCI is assumed but hardly ever certain. Surely NCT made at a later time can identify ischemia that has led to infarction. This is however not useful for treatment decision making at the time of deterioration.

Another frequently applied method to confirm DCI is to visualize the presence of vasospasm (luminal narrowing of the cerebral arteries). Vasospasm is often suggested to be the main cause of ischemic symptoms after SAH and it seems to be a clear and simple explanation. However, brain ischemia may occur in patients without apparent vessel narrowing, and conversely documented vasospasm does not always lead to neurological deterioration.¹⁰⁻¹⁴

Other suggested pathogenetic mechanisms consist of a combination of large and small vessel vasospasm, disturbed cerebral autoregulation, which is often seen after SAH, absence of collateral blood supply, and increased platelet aggregation.^{12, 15-18} These processes may cause a decrease in cerebral perfusion resulting in ischemia or infarction. Cerebral perfusion measurements should reflect the net effect of all factors that contribute to the development of DCI.

A readily available, inexpensive, fast and accurate cerebral perfusion measuring technique is CT-perfusion (CTP).¹⁹⁻²¹ This technique involves rapid infusion of a bolus of contrast material with repetitive image acquisition over a short time at a fixed anatomic position. Currently CTP is mainly used in the evaluation of ischemic stroke patients and it can accurately identify ischemic and already infarcted brain tissue.²²⁻²⁵ For the purpose of diagnosing DCI in SAH patients CTP needs to be more thoroughly examined.

In this thesis we evaluate the use of CTP for the purpose of visualizing the pathogenesis of DCI, the diagnosis of DCI and the use of perfusion measurements for DCI treatment evaluation.

In *Chapter 2* of this thesis we present normal values of cerebral perfusion and an innovative way to tackle one of the difficulties encountered when using CTP for quantitative measurements. *Chapter 3 and 4* focuses on the use of CTP to evaluate the pathogenesis of DCI. The effect of vasospasm on cerebral perfusion is estimated and discussed in *Chapter 3*. *Chapter 4* shows the time-course of cerebral perfusion in patients with and without DCI. *Chapter 5 and 6* deal with the diagnosis of DCI using CTP, with the use of a visual assessment of CTP color maps in *Chapter 5* and the evaluation of quantitative diagnostic threshold values of perfusion in *Chapter 6*. In *Chapter 7* we present a review of the available literature on the effect of triple-H and its separate components on cerebral perfusion.

Part 2

Complications of ischemic stroke: a CT perfusion evaluation of blood-brain barrier damage

About 87% of all strokes are ischemic strokes, which makes it the most common subtype of stroke.³ Ischemic stroke has an incidence of 117 to 142 per 100,000 per year,^{2, 3} and results from vessel occlusion caused by either cardioemboli, emboli from an atherosclerotic plaque or small vessel disease.²⁶ With a mean age of 75 years, ischemic stroke occurs at a relatively high age compared to the subtype SAH.² The overall case fatality rate is about 30% after 1 year² and like in SAH, the prognosis of ischemic stroke patients radically worsens due to complications of the disease itself.

One major complication is the occurrence of hemorrhage in the ischemic region. This complication is termed hemorrhagic transformation (HT).²⁷ Severe HT with mass effect occurs in about 3.5% of all ischemic stroke patients and can cause an eleven fold increase in case fatalities.^{27, 28} A consistently identified risk factor for HT is the treatment for ischemic stroke, systemic administration of recombinant tissue plasminogen activator (rtPA).^{28, 29} Thus, rtPA on the one hand saves brain tissue but on the other can also induce further brain damage. Differentiation of patients that will benefit from this treatment from patients that will be harmed is needed. Many different predictors for HT have been investigated.^{30, 31} The predictor with the highest predictive value is the presence of a large infarcted area indicating severe brain damage.^{30, 31} It would be desirable to identify patients at risk for HT before the brain is severely damaged.

A second major complication is the occurrence of severe swelling in the ischemic area. This severe swelling is termed malignant edema (ME).³² ME occurs in 1-5% of all stroke patients and leads to case fatality rates up to 78%.³² Since no medical treatment has yet been proven to be effective for patients with ME,³³ treatment with surgical decompression (removal of part of the skull and duraplasty) is applied in an attempt to reduce fatality and improve outcome.³⁴ Surgical decompression seems beneficial if performed within 48 hours after stroke onset.³⁵ However, all patients included in studies on the effect of decompression already had a large ischemic area with space occupying effect.^{32, 35-37} Being able to select patients destined to develop ME on admission, before irreversible damage to the brain has occurred may result in a faster, earlier treatment and improved outcome.³⁸

For both HT and ME more sensitive methods to identify patients at risk for these complications at an early stage are thus needed.

Both HT and ME have been associated with a damaged blood-brain barrier (BBB), which causes an increase in BBB permeability (BBBP).³⁹⁻⁴² Before ischemic stroke occurs the BBB can be degraded by cardiovascular risk factors such as diabetes and hypertension;^{43, 44} after stroke onset the BBB can be (further) damaged by ischemia,⁴⁰ reperfusion of brain tissue after recanalization of the occluded vessel, and by rtPA treatment itself.^{45, 46} Therefore, accurate measurement of BBB integrity and evaluation of factors that influence BBB integrity may be an important step in identifying patients destined to develop HT,^{47, 48} and ME.⁴²

BBBP can be calculated from CT-perfusion (CTP) data.⁴⁹⁻⁵¹ CTP is a fast and readily available dynamic imaging technique⁵² that is already frequently obtained as standard stroke care. With CTP the infarct core and the penumbra (brain tissue at risk for infarction) can be identified to decide what patient may benefit from reperfusion treatment.²³⁻²⁵ Adding BBBP measurements would be a useful new application of CTP to identify patients at risk for complications. The Patlak model can be applied to calculate BBBP from CTP.^{51, 53} This is a relatively simple mathematical model to describe progressive contrast extravasation out of the cerebral vessels.^{54, 55}

In this thesis we evaluate the use of CTP for BBBP measurements in stroke and non-stroke patients in order to identify factors that influence BBB integrity and to predict which patients are likely to develop HT or ME.

Chapter 8 and 9 discuss the optimal use of the Patlak model for BBBP measurement. *Chapter 10* outlines the normal variations in BBBP measurements and factors that can influence BBBP in non-stroke individuals. *Chapter 11* outlines in what way BBBP varies in patients with acute ischemic stroke. It provides an overview of BBBP values in infarcted, ischemic, and non-ischemic tissue and the influence of several patient characteristics on BBBP. *Chapter 12* combines the gained knowledge from our observations in non-stroke and stroke patients regarding BBBP, to create a predictive model for the complications HT and ME in ischemic stroke patients.

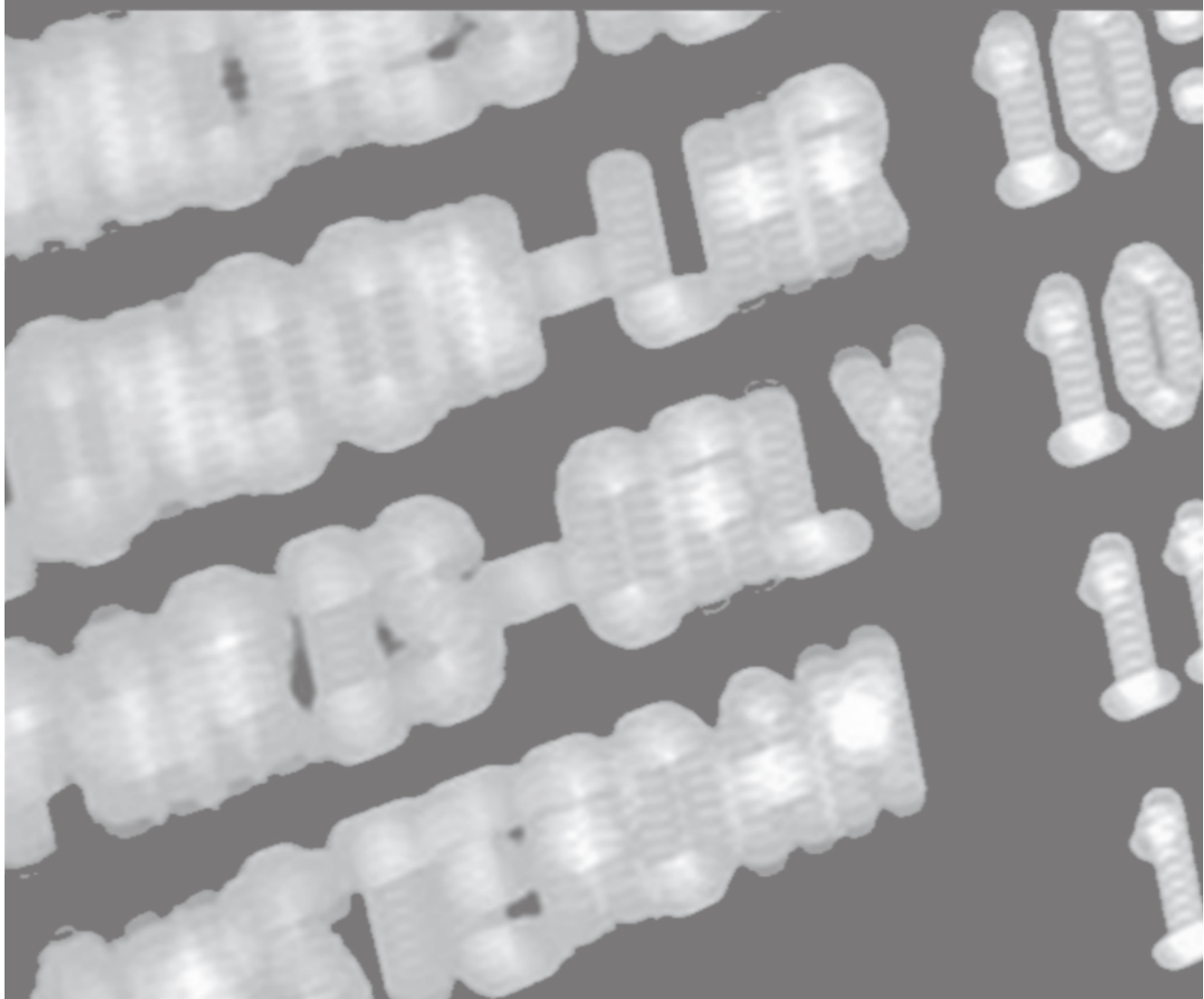
References

1. World Health Organization. World health report 2004 changing history. 2004:(Statistical Annex)
2. Thrift AG, Dewey HM, Sturm JW, Srikanth VK, Gilligan AK, Gall SL, Macdonell RA, McNeil JJ, Donnan GA. Incidence of stroke subtypes in the north east Melbourne stroke incidence study (Nemesis): Differences between men and women. *Neuroepidemiology*. 2009;32:11-18
3. Lloyd-Jones D, Adams R, Carnethon M, De Simone G, Ferguson TB, Flegal K, Ford E, Furie K, Go A, Greenlund K, Haase N, Hailpern S, Ho M, Howard V, Kissela B, Kittner S, Lackland D, Lisabeth L, Marelli A, McDermott M, Meigs J, Mozaffarian D, Nichol G, O'Donnell C, Roger V, Rosamond W, Sacco R, Sorlie P, Stafford R, Steinberger J, Thom T, Wasserthiel-Smoller S, Wong N, Wylie-Rosett J, Hong Y. Heart disease and stroke statistics--2009 update: A report from the American Heart Association Statistics Committee and Stroke Statistics Subcommittee. *Circulation*. 2009;119:480-486
4. de Rooij NK, Linn FH, van der Plas JA, Algra A, Rinkel GJ. Incidence of subarachnoid haemorrhage: A systematic review with emphasis on region, age, gender and time trends. *J Neurol Neurosurg Psychiatry*. 2007;78:1365-1372
5. Nieuwkamp DJ, Setz LE, Algra A, Linn FH, de Rooij NK, Rinkel GJ. Changes in case fatality of aneurysmal subarachnoid haemorrhage over time, according to age, sex, and region: A meta-analysis. *Lancet Neurol*. 2009;8:635-642
6. van Gijn J, Kerr RS, Rinkel GJ. Subarachnoid haemorrhage. *Lancet*. 2007;369:306-318
7. Johnston SC, Selvin S, Gress DR. The burden, trends, and demographics of mortality from subarachnoid hemorrhage. *Neurology*. 1998;50:1413-1418
8. Treggiari MM, Deem S. Which is the most important in triple-h therapy for cerebral vasospasm? *Curr Opin Crit Care*. 2009;15:83-86
9. Sen J, Belli A, Albon H, Morgan L, Petzold A, Kitchen N. Triple-h therapy in the management of aneurysmal subarachnoid haemorrhage. *Lancet Neurol*. 2003;2:614-621
10. Aralasmak A, Akyuz M, Ozkaynak C, Sindel T, Tuncer R. Ct angiography and perfusion imaging in patients with subarachnoid hemorrhage: Correlation of vasospasm to perfusion abnormality. *Neuroradiology*. 2009;51:85-93
11. Binaghi S, Colleoni ML, Maeder P, Uske A, Regli L, Dehdashti AR, Schnyder P, Meuli R. Ct angiography and perfusion ct in cerebral vasospasm after subarachnoid hemorrhage. *AJNR AmJNeuroradiol*. 2007;28:750-758
12. Stein SC, Levine JM, Nagpal S, LeRoux PD. Vasospasm as the sole cause of cerebral ischemia: How strong is the evidence? *NeurosurgFocus*. 2006;21:E2
13. Sviri GE, Britz GW, Lewis DH, Newell DW, Zaaroor M, Cohen W. Dynamic perfusion computed tomography in the diagnosis of cerebral vasospasm. *Neurosurgery*. 2006;59:319-325
14. Wintermark M, Dillon WP, Smith WS, Lau BC, Chaudhary S, Liu S, Yu M, Fitch M, Chien JD, Higashida RT, Ko NU. Visual grading system for vasospasm based on perfusion ct imaging: Comparisons with conventional angiography and quantitative perfusion ct. *Cerebrovasc Dis*. 2008;26:163-170
15. Kozniowska E, Michalik R, Rafalowska J, Gadamski R, Walski M, Frontczak-Baniewicz M, Piotrowski P, Czernicki Z. Mechanisms of vascular dysfunction after subarachnoid hemorrhage. *J Physiol Pharmacol*. 2006;57 Suppl 11:145-160

16. Ng WH, Moochhala S, Yeo TT, Ong PL, Ng PY. Nitric oxide and subarachnoid hemorrhage: Elevated level in cerebrospinal fluid and their implications. *Neurosurgery*. 2001;49:622-626; discussion 626-627
17. Romano JG, Rabinstein AA, Arheart KL, Nathan S, Campo-Bustillo I, Koch S, Forteza AM. Microemboli in aneurysmal subarachnoid hemorrhage. *J Neuroimaging*. 2008;18:396-401
18. Weidauer S, Vatter H, Beck J, Raabe A, Lanfermann H, Seifert V, Zanella F. Focal laminar cortical infarcts following aneurysmal subarachnoid haemorrhage. *Neuroradiology*. 2008;50:1-8
19. Hoeffner EG, Case I, Jain R, Gujar SK, Shah GV, Deveikis JP, Carlos RC, Thompson BG, Harrigan MR, Mukherji SK. Cerebral perfusion ct: Technique and clinical applications. *Radiology*. 2004;231:632-644
20. Wintermark M, Thiran JP, Maeder P, Schnyder P, Meuli R. Simultaneous measurement of regional cerebral blood flow by perfusion ct and stable xenon ct: A validation study. *AJNR AmJ-Neuroradiol*. 2001;22:905-914
21. Adams HP, Jr., del Zoppo G, Alberts MJ, Bhatt DL, Brass L, Furlan A, Grubb RL, Higashida RT, Jauch EC, Kidwell C, Lyden PD, Morgenstern LB, Qureshi AI, Rosenwasser RH, Scott PA, Wijdicks EF. Guidelines for the early management of adults with ischemic stroke: A guideline from the american heart association/american stroke association stroke council, clinical cardiology council, cardiovascular radiology and intervention council, and the atherosclerotic peripheral vascular disease and quality of care outcomes in research interdisciplinary working groups: The american academy of neurology affirms the value of this guideline as an educational tool for neurologists. *Circulation*. 2007;115:e478-534
22. Nabavi DG, Dittrich R, Kloska SP, Nam EM, Klotz E, Heindel W, Ringelstein EB. Window narrowing: A new method for standardized assessment of the tissue at risk-maximum of infarction in ct based brain perfusion maps. *Neurol Res*. 2007;29:296-303
23. Parsons MW, Pepper EM, Bateman GA, Wang Y, Levi CR. Identification of the penumbra and infarct core on hyperacute noncontrast and perfusion ct. *Neurology*. 2007;68:730-736
24. Schaefer PW, Roccatagliata L, Ledezma C, Hoh B, Schwamm LH, Koroshetz W, Gonzalez RG, Lev MH. First-pass quantitative ct perfusion identifies thresholds for salvageable penumbra in acute stroke patients treated with intra-arterial therapy. *AJNR Am J Neuroradiol*. 2006;27:20-25
25. Wintermark M, Flanders AE, Velthuis B, Meuli R, van Leeuwen M, Goldsher D, Pineda C, Serena J, van der Schaaf I, Waaijer A, Anderson J, Nesbit G, Gabriely I, Medina V, Quiles A, Pohlman S, Quist M, Schnyder P, Bogousslavsky J, Dillon WP, Pedraza S. Perfusion-ct assessment of infarct core and penumbra: Receiver operating characteristic curve analysis in 130 patients suspected of acute hemispheric stroke. *Stroke*. 2006;37:979-985
26. Donnan GA, Fisher M, Macleod M, Davis SM. Stroke. *Lancet*. 2008;371:1612-1623
27. Berger C, Fiorelli M, Steiner T, Schabitz WR, Bozzao L, Bluhmki E, Hacke W, von KR. Hemorrhagic transformation of ischemic brain tissue: Asymptomatic or symptomatic? *Stroke*. 2001;32:1330-1335
28. Hacke W, Donnan G, Fieschi C, Kaste M, von KR, Broderick JP, Brott T, Frankel M, Grotta JC, Haley EC, Jr., Kwiatkowski T, Levine SR, Lewandowski C, Lu M, Lyden P, Marler JR, Patel S, Tilley BC, Albers G, Bluhmki E, Wilhelm M, Hamilton S. Association of outcome with early stroke treatment: Pooled analysis of atlantis, ecass, and ninds rt-pa stroke trials. *Lancet*. 2004;363:768-774
29. Hacke W, Kaste M, Bluhmki E, Brozman M, Davalos A, Guidetti D, Larrue V, Lees KR, Medeghri Z, Machnig T, Schneider D, von Kummer R, Wahlgren N, Toni D. Thrombolysis with alteplase 3 to 4.5 hours after acute ischemic stroke. *N Engl J Med*. 2008;359:1317-1329

30. Khatri P, Wechsler LR, Broderick JP. Intracranial hemorrhage associated with revascularization therapies. *Stroke*. 2007;38:431-440
31. Paciaroni M, Agnelli G, Corea F, Ageno W, Alberti A, Lanari A, Caso V, Micheli S, Bertolani L, Venti M, Palmerini F, Biagini S, Comi G, Previdi P, Silvestrelli G. Early hemorrhagic transformation of brain infarction: Rate, predictive factors, and influence on clinical outcome: Results of a prospective multicenter study. *Stroke*. 2008;39:2249-2256
32. Hofmeijer J, Algra A, Kappelle LJ, van der Worp HB. Predictors of life-threatening brain edema in middle cerebral artery infarction. *Cerebrovascular Diseases*. 2008;25:176-184
33. Hofmeijer J, van der Worp HB, Kappelle LJ. Treatment of space-occupying cerebral infarction. *Crit Care Med*. 2003;31:617-625
34. Rieke K, Schwab S, Krieger D, von Kummer R, Aschoff A, Schuchardt V, Hacke W. Decompressive surgery in space-occupying hemispheric infarction: Results of an open, prospective trial. *Crit Care Med*. 1995;23:1576-1587
35. Hofmeijer J, Kappelle LJ, Algra A, Amelink GJ, van Gijn J, van der Worp HB. Surgical decompression for space-occupying cerebral infarction (the hemicraniectomy after middle cerebral artery infarction with life-threatening edema trial [hamlet]): A multicentre, open, randomised trial. *Lancet Neurol*. 2009;8:326-333
36. Juttler E, Schwab S, Schmiedek P, Unterberg A, Hennerici M, Woitzik J, Witte S, Jenetzky E, Hacke W. Decompressive surgery for the treatment of malignant infarction of the middle cerebral artery (destiny): A randomized, controlled trial. *Stroke*. 2007;38:2518-2525
37. Vahedi K, Vicaut E, Mateo J, Kurtz A, Orabi M, Guichard JP, Boutron C, Couvreur G, Rouanet F, Touze E, Guillon B, Carpentier A, Yelnik A, George B, Payen D, Bousser MG. Sequential-design, multicenter, randomized, controlled trial of early decompressive craniectomy in malignant middle cerebral artery infarction (decimal trial). *Stroke*. 2007;38:2506-2517
38. Schwab S, Steiner T, Aschoff A, Schwarz S, Steiner HH, Jansen O, Hacke W. Early hemicraniectomy in patients with complete middle cerebral artery infarction. *Stroke*. 1998;29:1888-1893
39. Serena J, Blanco M, Castellanos M, Silva Y, Vivancos J, Moro MA, Leira R, Lizasoain I, Castillo J, Davalos A. The prediction of malignant cerebral infarction by molecular brain barrier disruption markers. *Stroke*. 2005;36:1921-1926
40. Sandoval KE, Witt KA. Blood-brain barrier tight junction permeability and ischemic stroke. *Neurobiol Dis*. 2008;32:200-219
41. Wang X, Lo EH. Triggers and mediators of hemorrhagic transformation in cerebral ischemia. *MolNeurobiol*. 2003;28:229-244
42. Lampl Y, Sadeh M, Lorberboym M. Prospective evaluation of malignant middle cerebral artery infarction with blood-brain barrier imaging using tc-99m dtpa spect. *Brain Res*. 2006;1113:194-199
43. Nag S, Kilty DW. Cerebrovascular changes in chronic hypertension. Protective effects of enalapril in rats. *Stroke*. 1997;28:1028-1034
44. Starr JM, Wardlaw J, Ferguson K, MacLulich A, Deary IJ, Marshall I. Increased blood-brain barrier permeability in type ii diabetes demonstrated by gadolinium magnetic resonance imaging. *J Neural Neurosurg Psychiatry*. 2003;74:70-76
45. Su EJ, Fredriksson L, Geyer M, Folestad E, Cale J, Andrae J, Gao Y, Pietras K, Mann K, Yepes M, Strickland DK, Betsholtz C, Eriksson U, Lawrence DA. Activation of pdgf-cc by tissue plasminogen activator impairs blood-brain barrier integrity during ischemic stroke. *Nat Med*. 2008;14:731-737

46. Warach S, Latour LL. Evidence of reperfusion injury, exacerbated by thrombolytic therapy, in human focal brain ischemia using a novel imaging marker of early blood-brain barrier disruption. *Stroke*. 2004;35:2659-2661
47. Aviv RI, d'Esterre CD, Murphy BD, Hopyan JJ, Buck B, Mallia G, Li V, Zhang L, Symons SP, Lee TY. Hemorrhagic transformation of ischemic stroke: Prediction with ct perfusion. *Radiology*. 2009;250:867-877
48. Bang OY, Saver JL, Alger JR, Shah SH, Buck BH, Starkman S, Ovbiagele B, Liebeskind DS. Patterns and predictors of blood-brain barrier permeability derangements in acute ischemic stroke. *Stroke*. 2009;40:454-461
49. Bisdas S, Hartel M, Cheong LH, Koh TS, Vogl TJ. Prediction of subsequent hemorrhage in acute ischemic stroke using permeability ct imaging and a distributed parameter tracer kinetic model. *JNeuroradiol*. 2007;34:101-108
50. Dankbaar JW, Hom J, Schneider T, Cheng SC, Lau BC, van der Schaaf I, Virmani S, Pohlman S, Dillon WP, Wintermark M. Dynamic perfusion ct assessment of the blood-brain barrier permeability: First pass versus delayed acquisition. *AJNR Am J Neuroradiol*. 2008;29:1671-1676
51. Lin K, Kazmi KS, Law M, Babb J, Peccerelli N, Pramanik BK. Measuring elevated microvascular permeability and predicting hemorrhagic transformation in acute ischemic stroke using first-pass dynamic perfusion ct imaging. *AJNR AmJNeuroradiol*. 2007;28:1292-1298
52. Wintermark M, Sesay M, Barbier E, Borbely K, Dillon WP, Eastwood JD, Glenn TC, Grandin CB, Pedraza S, Soustiel JF, Nariai T, Zaharchuk G, Caille JM, Dousset V, Yonas H. Comparative overview of brain perfusion imaging techniques. *Stroke*. 2005;36:e83-99
53. Cianfoni A, Cha S, Bradley WG, Dillon WP, Wintermark M. Quantitative measurement of blood-brain barrier permeability using perfusion-ct in extra-axial brain tumors. *J Neuroradiol*. 2006;33:164-168
54. Patlak CS, Blasberg RG. Graphical evaluation of blood-to-brain transfer constants from multiple-time uptake data. Generalizations. *J Cereb Blood Flow Metab*. 1985;5:584-590
55. Patlak CS, Blasberg RG, Fenstermacher JD. Graphical evaluation of blood-to-brain transfer constants from multiple-time uptake data. *J Cereb Blood Flow Metab*. 1983;3:1-7

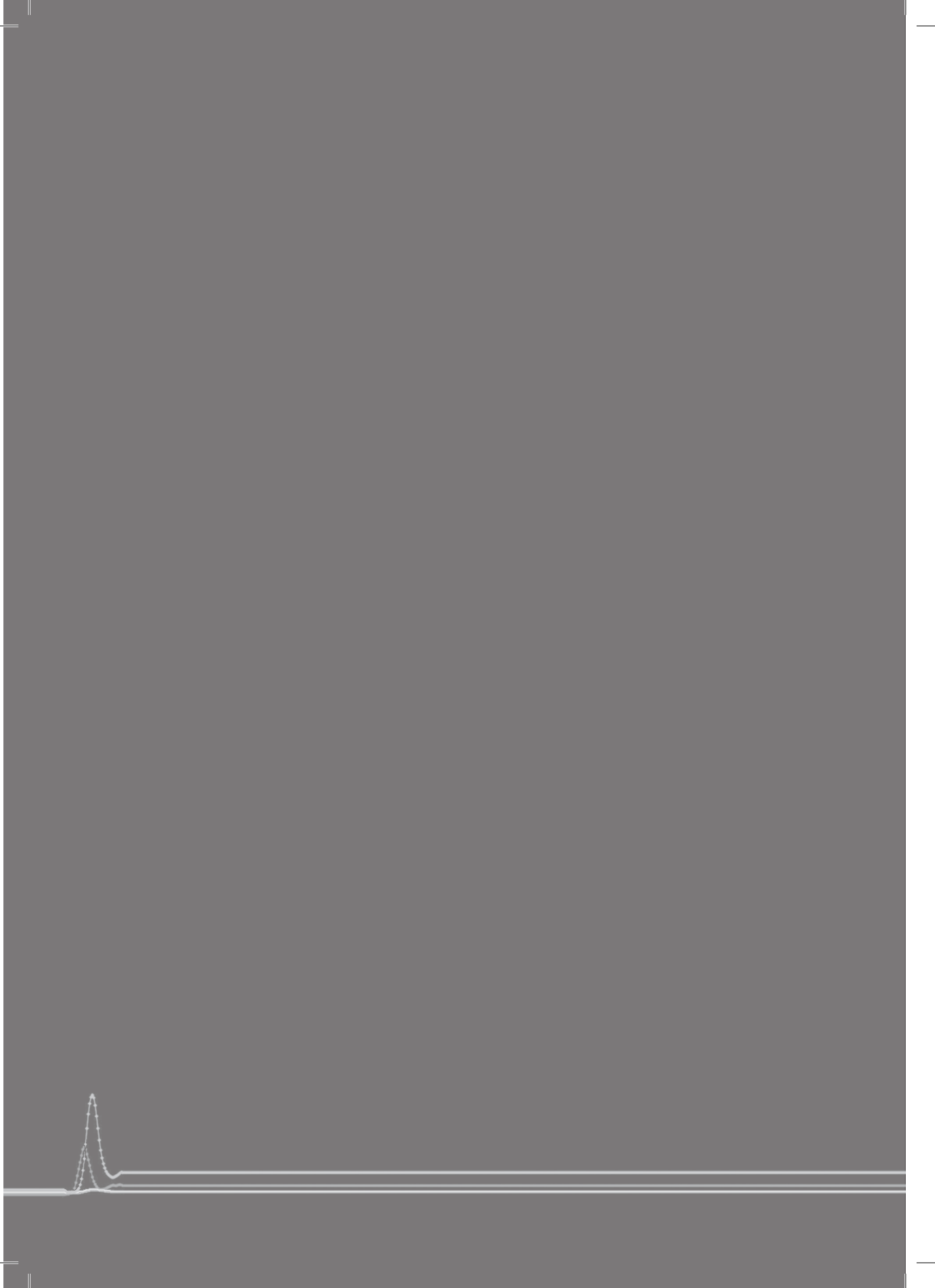




Part 1

**Complications of
subarachnoid hemorrhage:
a CT perfusion evaluation of
delayed cerebral ischemia**





Normal values of cerebral perfusion measured with CT- perfusion: absolute values and inter-territorial ratios



2

J.W. Dankbaar, F.A. Franssen, A.M. Tiehuis, B.K. Velthuis, I.C. van der Schaaf

Abstract

Background and purpose

Normal reference values for cerebral perfusion measured with CT-perfusion (CTP) are lacking in the literature. The purpose of this study is to obtain reference values of absolute perfusion and ratios between flow-territories in normal individuals.

Methods

We retrospectively identified patients who presented with headache and in whom CT (NCT, CTP, CTA, and post-contrast CT) and clinical follow up excluded intracranial pathology. Mean absolute perfusion values with their 95% CI were determined in cortical gray matter, basal ganglia, and white matter, and compared using ANOVA with Bonferroni corrections. The effect of age on perfusion was analyzed using linear regression. Relative perfusion values were determined by calculating mean ratios (with 95% CI) of ACA to MCA and PCA to MCA perfusion of cortical gray matter. If the 95% CI did not contain 1, the difference was considered significant.

Results

47 patients (median age 41) met our inclusion criteria, of which 6 had unevaluable CTP studies. Mean CBF and 95% CI in cortical gray matter, basal ganglia, and white matter were 56.4(51.5↔61.3), 64.4(57.9↔70.8) (higher than cortex: $p=0.06$), and 24.5(22.3↔26.7) (lower than cortex: $p<0.001$) respectively. The effect of age on CBF was non-significant. The mean ACA to MCA and PCA to MCA CBF ratios were 0.92(0.89↔0.96) and 0.96(0.91↔1.01) respectively.

Conclusion

We provided reference values of absolute cerebral perfusion with CTP, useful for group comparison and relative values for individual measurements.

Introduction

CT-perfusion (CTP) of the brain is a widely available diagnostic tool that provides quick and minimally invasive assessment of brain perfusion.¹ Currently CTP is mainly used in acute ischemic stroke to discriminate potentially salvageable tissue from infarcted tissue.²⁻⁴ CTP can also be applied to characterize the grade or invasiveness of tumors,¹ to test the cerebrovascular reserve,⁵ and to evaluate delayed cerebral ischemia in patients with subarachnoid hemorrhage.^{6,7}

Evaluation of CTP images can be either qualitative, by interpretation of color-coded perfusion maps, or quantitative.¹ The quantitative measurement of cerebral perfusion is frequently mentioned as a great advantage of CTP over other dynamic imaging techniques.⁸ In order to identify pathologic perfusion values, proper reference values of absolute perfusion measured in individuals without brain pathology are needed. These values are currently not available for CTP.

A difficulty of comparing absolute CTP values is the variability caused by observer-dependent post processing steps.^{9,10} This variability can range from 15 to 30% when ROI-based techniques are used.¹¹⁻¹³ A frequently applied solution to correct for this variability of absolute perfusion values is the use of relative perfusion measurement. In cerebral perfusion analysis, this relative measurement is mostly based on the ratio between values of the symptomatic and asymptomatic hemisphere.^{4,14} However, these left to right ratios may not be accurate in non-unilateral and diffuse perfusion abnormalities as seen for example in patients with delayed cerebral ischemia after subarachnoid hemorrhage^{15,16} or bilateral carotid artery stenosis. This issue could be solved by a relative method in which different flow territories within the same hemisphere are compared.

The purpose of this study is to obtain absolute cerebral perfusion values from CTP and to present an alternative relative method by calculating ratios of different ipsilateral flow-territories in the brains of normal individuals.

Methods

Design

Patients presenting to our emergency department with headache, without decreased consciousness or focal deficits and no history of renal insufficiency or contrast allergy frequently undergo a CT survey including non-contrast CT (NCT), CTP, CT-angiography (CTA), and post-contrast CT of the head. Some of these patients show no pathology and their headache resolves without recurrent symptoms. They can therefore be considered to be normal control subjects with an incidental unspecific headache.

We retrospectively identified all patients with unspecific headache that underwent CT-imaging to exclude intracranial pathology in our hospital between November 2005 and November 2008. Patients were excluded if they had: (a) a decreased level of consciousness or focal deficits on presentation, (b) unavailable clinical data, or (c) a final diagnosis or previous history of venous sinus thrombosis, stroke, transient ischemic attack, intracerebral hemorrhage, tumors or other

intracranial abnormalities, epilepsy, migraine, pre-eclampsia, cluster headache, drug-intoxication, or carotid artery pathology.

Patients' charts, imaging studies and discharge reports were reviewed for demographic data and the final diagnosis.

CTP scanning

Cerebral perfusion was assessed with CTP imaging. CTP imaging measures cerebral perfusion on tissue level and provides accurate and reliable data compared to the gold standard Xenon-CT.¹⁷ CTP gives information on cerebral blood volume (CBV), mean transit time (MTT), cerebral blood flow (CBF), and time to peak (TTP). All imaging studies were executed on a 16-slice or 64 slice spiral CT scanner (Philips Mx8000 LDT, Best, the Netherlands). CTP source data were derived from sequential scans covering a 2.4 cm slab (16 slice) or a 4 cm slab (64 slice), both angulated parallel to the meato-orbital line at the level of the basal ganglia. For the CTP scan 40 ml of non-ionic contrast agent (Iopromide, Ultravist, 300mg iodine/ml, Schering, Berlin, Germany) was injected into the cubital vein (18 gauge needle) at a rate of 5 ml/s followed by a 40 ml saline flush at a rate of 5 ml/s using a dual power injector (Stellant Dual CT injector, Medrad Europe BV, Beek, the Netherlands). The following parameters were used: 16 slice, 90 kVp, 150 mAs, 8x3 mm collimation, 512x512 matrix, 200 mm field of view, 1 image per 2 seconds during 60 seconds, UB filter and standard resolution; 64 slice, 80 kVp, 150 mAs, 64x0.625 mm collimation, 512x512 matrix, 220 mm FOV, 1 image per 2 seconds during 60 seconds, UB filter and standard resolution.

CTP post-processing

CTP scans were reconstructed at 6 mm (16 slice) and 5 mm (64 slice) contiguous axial images. Data were transferred to a Philips workstation equipped with Extended Brilliance Workstation 3.x software, for post processing. This software relies on the central volume principle, which is the most accurate for low injection rates of iodinated contrast material.¹⁸ The software obtains mathematical descriptions of the time-density curves for each pixel, by applying curve fitting by least mean squares, after correcting for motion and noise reduction through an anisotropic, edge-preserving spatial filter. The CBV map is calculated from the area under the time-density curves.¹⁹ A closed-form (non-iterative) deconvolution is then applied to calculate the MTT and CBF (= CBV/MTT) map.²⁰ The deconvolution operation requires a reference arterial input function (most often within the anterior cerebral artery), that is automatically selected by the CTP software within a region of interest (ROI) drawn by the user.

CBV, MTT, CBF, and TTP were measured in different ROIs in both hemispheres (*Figure 1*). ROIs were drawn by hand by one observer with vast experience in CT-perfusion image reading (JWD), in the cortical gray matter of the flow-territory of the ACA, MCA, and PCA, in the white matter (region of the flow-territory of the MCA), and in the basal ganglia, which contained caudate head (ACA), lenticular nucleus (MCA) and thalamus (PCA). This results in 14 ROIs per patient (*Figure 1*).

Before all measurements a CBV threshold was applied removing vessels from the measured region.

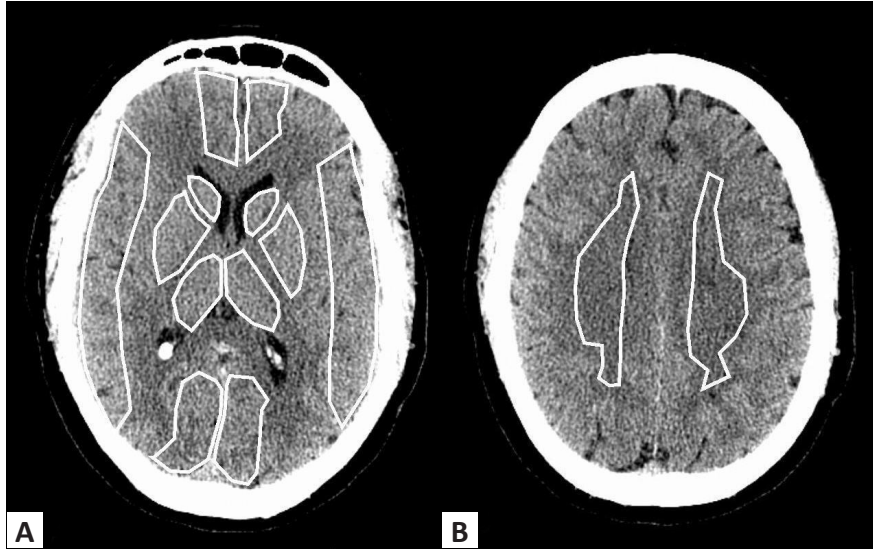


Figure 1 Regions of Interest (ROIs) for cerebral perfusion measurement drawn by hand in (A) the cortical gray matter and basal ganglia of the flow-territories of the anterior cerebral artery (ACA), the middle cerebral artery (MCA), and the posterior cerebral artery (PCA); (B) cerebral white matter.

Data analysis

Mean absolute perfusion values for cortical gray matter (mean value of all cortical ROIs per patient), white matter, and the basal ganglia (mean value of all basal ganglia ROIs per patient) were calculated with their 95% CI. The differences between the three tissue types were analyzed by using a 1-way ANOVA with a Bonferroni correction for multiple comparisons. Since an inverse relation between age and cerebral perfusion has been previously described,²¹⁻²³ the relation between age and CBF was analyzed using linear regression and calculating the effect size (B in ml/100g/min per year) and squared regression coefficient (R^2). An R^2 of 1 indicates a perfect linear relation. Additionally relative perfusion measurements were performed. In each patient we calculated for CBV, CBF, MTT, and TTP: 1) the ACA to MCA ratio and 2) the PCA to MCA ratio of cortical gray matter. Mean values with their 95% CI were calculated for the different ratios. If the 95% CI contained 1, the difference between the compared regions was considered to be non-significant.

Results

Patients

132 patients with unspecific headache were scanned with NCT, CTP and CTA between November 2005 and November 2008. 47 of these patients met our inclusion criteria. Their patient characteristics are summarized in *Table 1*. The CTP studies of six patients could not be processed due to improper bolus timing or movement artifacts.

Table 1 Patient characteristics

N = 47	
Age:	
Median	41
Full range	19-73
Interquartile range	31-48
Number of Men	14 (29.8%)
Final Diagnosis:	
Unspecific headache	44 (93.6%)
BPPV	2 (4.3%)
Sinusitis	1 (2.1%)

BPPV = benigne paroxysmal positional vertigo

The mean absolute perfusion measurements of cortical gray matter, basal ganglia and white matter are presented in *Table 2*. There was a trend towards higher perfusion (higher CBF and lower MTT) in the basal ganglia compared to cortical gray matter, and cerebral perfusion was significantly lower (lower CBV and CBF and higher MTT) in white matter compared to cortical gray matter. There was no significant difference between TTP in the different tissue types.

Table 2 Mean values and 95% confidence intervals of absolute cerebral perfusion parameters in different types of brain tissue.

N=41	ANOVA p-value	Cortex	Basal Ganglia	Post Hoc p-value	White Matter	Post Hoc p-value
CBV (ml/100g)	<0.001	3.32 (3.17↔3.46)	3.35 (3.16↔3.54)	1.000	1.96 (1.84↔2.08)	<0.001
MTT (sec)	<0.001	3.73 (3.47↔3.98)	3.33 (3.09↔3.57)	0.093	4.98 (4.69↔5.27)	<0.001
CBF (ml/100g/min)	<0.001	56.37 (51.48↔61.27)	64.37 (57.94↔70.80)	0.059	24.50 (22.30↔26.70)	<0.001
TTP (sec)	0.163	20.62 (19.61↔21.64)	20.31 (19.29↔21.34)	1.000	21.62 (20.62↔22.62)	0.494

ANOVA (1-way analysis of variance) p-values and p-values compared to cortical gray matter (cortex) of post hoc tests for multiple comparisons with Bonferroni correction.

The effect of age on CBF was non-significant in all tissue types, with an effect size (B) of -0.149 ml/100g/min per year (95% CI: -0.511 ↔ 0.214; p-value: 0.412) in cortical gray matter; B = -0.079 (-0.559 ↔ 0.401; p-value: 0.740) in the basal ganglia; and B = 0.064 (-0.099 ↔ 0.227; p-value: 0.431) in white matter.

The mean ratios of CBV, MTT, and CBF in the ACA flow-territory to perfusion in the MCA territory were significantly lower than 1 (CBV ratio = 0.88 (95% CI: 0.85 ↔ 0.91); MTT ratio = 0.96 (0.94 ↔ 0.99); CBF ratio = 0.92 (0.89 ↔ 0.96)), indicating that CBV, MTT and CBF are lower in the ACA flow-territory (Figure 2A). The mean ratio of TTP in ACA versus MCA was 0.99 (0.99 ↔ 1.00) (Figure 2A).

The mean ratios of CBV, MTT, and TTP in the PCA flow-territory to the MCA territory were significantly higher than 1 (CBV ratio = 1.05 (1.02 ↔ 1.08); MTT ratio = 1.12 (1.08 ↔ 1.17); TTP ratio = 1.02 (1.02 ↔ 1.03)), indicating that CBV, MTT, and TTP are higher in the PCA flow-territory (Figure 2B). The mean ratio of CBF in PCA versus MCA was not significantly different from 1 (CBF ratio = 0.96 (0.91 ↔ 1.01)), indicating no difference in CBF between PCA and MCA flow-territories (Figure 2B).

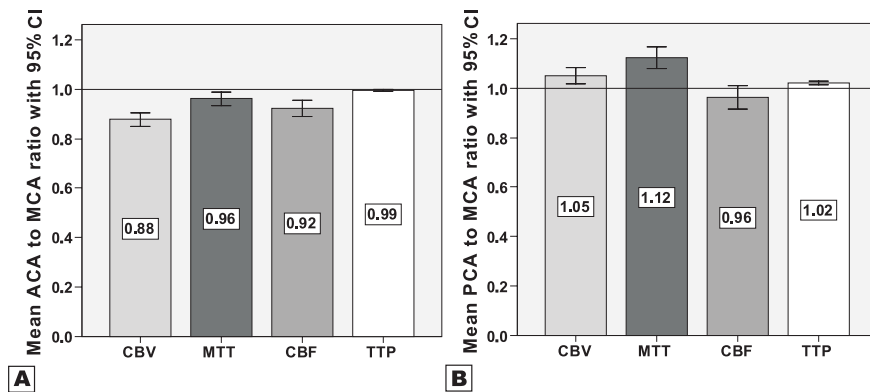


Figure 2. Mean ratio with 95% confidence interval (95% CI) of cerebral perfusion parameters in the flow-territories of (A) the anterior cerebral artery (ACA) versus the middle cerebral artery (MCA); (B) the posterior cerebral artery (PCA) versus the middle cerebral artery (MCA). If the 95% CI does not contain 1 (horizontal dotted line) the difference in perfusion between the two flow-territories is considered to be significant.

CBV = cerebral blood volume; MTT = mean transit time; CBF = cerebral blood flow, TTP = time to peak

Discussion

In this study we presented reference values of absolute cerebral perfusion measured with CTP in cortical gray matter, basal ganglia, and white matter showing that white matter has significantly lower perfusion than cortical gray matter and perfusion in the basal ganglia is slightly higher than in the cortex. The effect of age on CBF was non-significant. We furthermore presented an alternative relative measurement, comparing perfusion in the three different ipsilateral cerebral flow territories.

The higher CBF in cortical gray matter compared to white matter has been previously reported using other perfusion measuring techniques.²¹⁻²⁵ This difference in CBF can be explained by the fact that the microvascular density in cerebral gray matter is higher than in white matter.²⁶⁻²⁸ We detected that the basal ganglia had a slightly higher CBF ($p=0.06$) compared to cortical tissue. This has not previously been reported. However, in situations of global cerebral ischemia and chronic vascular disease it is known that the basal ganglia remain relatively spared.^{29, 30} This may indicate that the microvascular structure of the basal ganglia is also different from the cortex.

The mean CTP values we obtained in our population are similar to measurements with the gold standard ¹³³Xe inhalation and arterial spin labeling in normal individuals. ¹³³Xe inhalation shows CBF values of 57 ml/100g/min in cortical gray matter compared to 56 in our results, 60 ml/100g/min in the basal ganglia (64 in our results), and 20 ml/100g/min in white matter (25 in our results).²³ Arterial spin labeling shows CBF values of about 60 ml/100g/min in cortical gray matter, and 20 to 25 ml/100g/min in white matter.^{21, 25}

Previous studies report a decreasing CBF with age of 0.45% to 0.5% per year.^{21, 24, 25} In our study we could not confirm this very small age effect. The reason for this may lie in the fact that the interquartile range of age in our population was quite narrow (31-48) and therefore a small decrease or increase in CBF may not be significant or even not observable.

The confidence intervals of our mean values are relatively narrow, indicating that these values are clinically very well applicable as reference values for comparing groups of patients.

However, absolute perfusion measurements on an individual level can be quite variable due to observer dependent post processing steps.^{9, 10} We therefore additionally focused on normal within patient ratios of perfusion of different ipsilateral flow-territories of the brain.

According to our results perfusion is somewhat lower in the ACA flow-territory compared to the MCA flow-territory and a ratio for CBF up to 0.90 could be considered to be normal in the individual patient. The PCA to MCA ratios of CBV and MTT were both slightly higher than 1, the CBF ratio however was not.

The central volume principle, which was used in our CTP analysis, states that CBF depends on CBV and MTT. When looking at CBV one has to be aware of the fact that partial volume of large veins in the measured region can cause an overestimation of this parameter, even if a CBV threshold is applied to remove pixels that most likely represent vascular structures. Differences in MTT between the different flow territories may be a result of AIF selection which is required for a deconvolution based CT-perfusion software. The AIF is typically selected in the ACA since the ACA is relatively large and perpendicular to the axial plane.^{31, 32} Due to dispersion and delayed arrival relative to the AIF, the MTT may be overestimated in areas that are distant to the AIF,³³ like the PCA flow territory, especially since the PCA territory is mostly fed by the basilar artery. However since the selection of the ACA as an input function is commonly applied in CTP measurements our findings should be generally applicable. Also, time independent perfusion models are currently being developed.³³

TTP, being a measurement of arrival to the tissue, is of course also influenced by travelled distance of contrast agent, however the relative differences are much smaller since the absolute values are quite large.

Our alternative relative measurement has an advantage over conventional left to right comparison when studying (possible) bilaterally present perfusion abnormalities like delayed cerebral ischemia after subarachnoid hemorrhage^{15,16} or bilateral carotid artery stenosis. Surely more than one flow territory can be affected within one hemisphere. In that case the conventional left to right comparison may be more helpful. However, in these types of complicated cases, visual interpretation may prove to be the only possible way to analyze the CTP data.

We acknowledge some limitations to this study. For the obvious reason of increased radiation exposure and use of intravenous contrast, we did not use healthy volunteers to obtain the reference values in this study. By selecting individuals from a group of patients that were evaluated for headache without decreased consciousness or focal neurologic deficits, we attempted to obtain a proper reference population. We are confident that all pathological conditions that are known to influence cerebral perfusion were excluded and the selected individuals were reported to have only an unspecific headache. A recent study on long term ischemic consequences of migraine and nonmigraine headaches showed that nonmigraine headache, in contrast to migraine with aura, is not associated with infarct like lesions on late MR follow up.³⁴ Recent evaluations with functional imaging of patients with migraine and clusterheadache actually show that the headache component is most likely caused by structural abnormalities in functional brain anatomy and only the aura symptoms may be caused by perfusion abnormalities.³⁵ These findings support our assumption that unspecific headache does not influence cerebral perfusion. Another headache entity which may influence perfusion is reversible cerebral vasoconstriction syndrome. Our patients are very unlikely to have had this condition since they did not experience recurrent thunderclap headaches and there were no multifocal reversible arterial vasoconstrictions reported on CTA examinations.³⁶

Conclusion

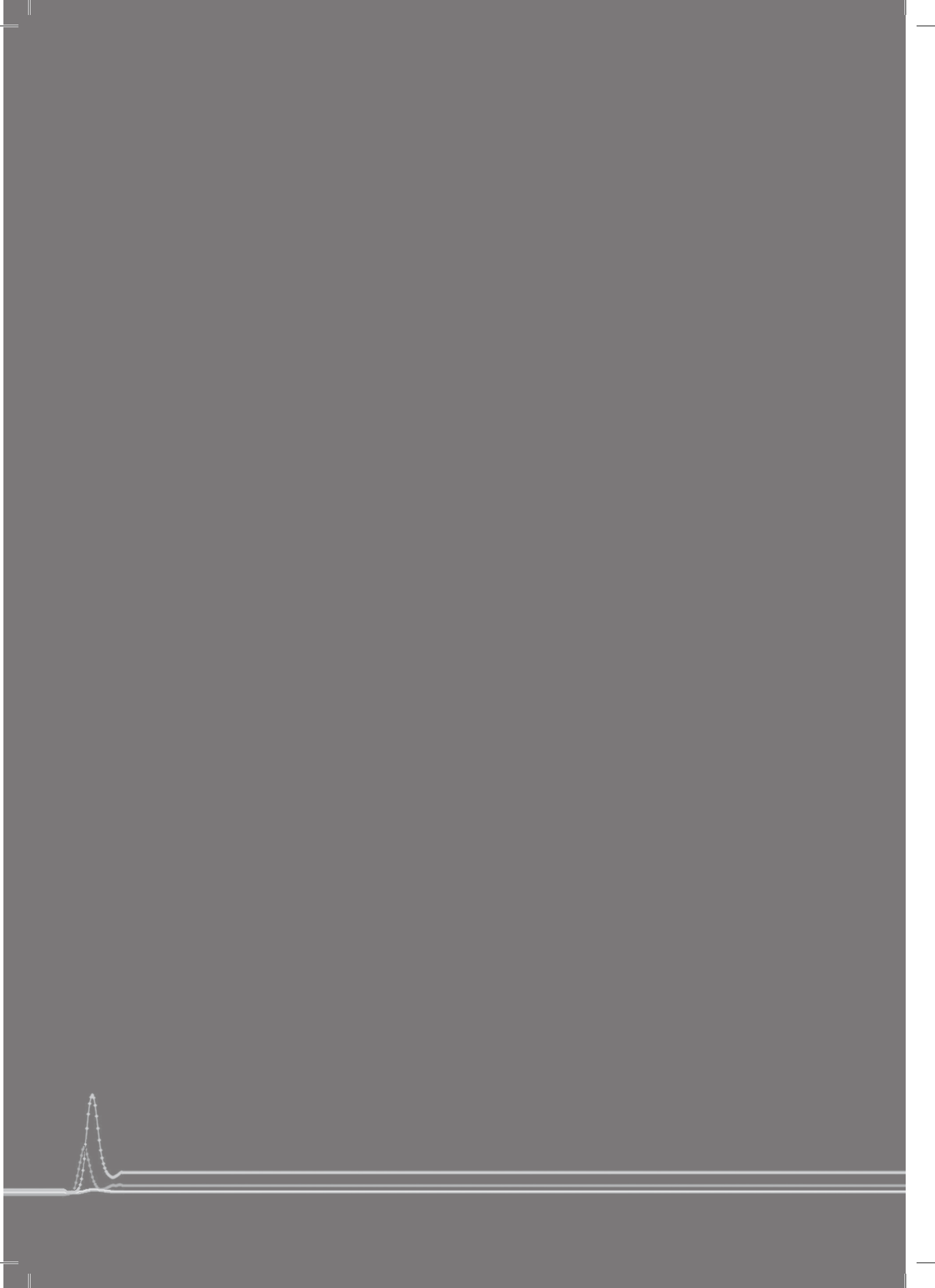
We presented reference values for CTP of absolute cerebral perfusion and an alternative relative analysis, in which we calculated ratios of perfusion between the different cerebral flow-territories. Our absolute values in cortical gray matter, basal ganglia, and white matter are comparable to values measured with other techniques and have a relatively narrow confidence interval. Our alternative relative values may be useful to overcome observer dependent variability in the individual patient when evaluating regional but bilaterally present perfusion abnormalities like delayed ischemia after subarachnoid hemorrhage or bilateral carotid artery stenosis.

References

1. Hoeffner EG, Case I, Jain R, Gujar SK, Shah GV, Deveikis JP, Carlos RC, Thompson BG, Harrigan MR, Mukherji SK. Cerebral perfusion ct: Technique and clinical applications. *Radiology*. 2004;231:632-644
2. Parsons MW, Pepper EM, Bateman GA, Wang Y, Levi CR. Identification of the penumbra and infarct core on hyperacute noncontrast and perfusion ct. *Neurology*. 2007;68:730-736
3. Schaefer PW, Roccatagliata L, Ledezma C, Hoh B, Schwamm LH, Koroshetz W, Gonzalez RG, Lev MH. First-pass quantitative ct perfusion identifies thresholds for salvageable penumbra in acute stroke patients treated with intra-arterial therapy. *AJNR Am J Neuroradiol*. 2006;27:20-25
4. Wintermark M, Flanders AE, Velthuis B, Meuli R, van Leeuwen M, Goldsher D, Pineda C, Serena J, van der Schaaf I, Waaijer A, Anderson J, Nesbit G, Gabriely I, Medina V, Quiles A, Pohlman S, Quist M, Schnyder P, Bogousslavsky J, Dillon WP, Pedraza S. Perfusion-ct assessment of infarct core and penumbra: Receiver operating characteristic curve analysis in 130 patients suspected of acute hemispheric stroke. *Stroke*. 2006;37:979-985
5. Rim NJ, Kim HS, Shin YS, Kim SY. Which ct perfusion parameter best reflects cerebrovascular reserve?: Correlation of acetazolamide-challenged ct perfusion with single-photon emission ct in moyamoya patients. *AJNR Am J Neuroradiol*. 2008;29:1658-1663
6. Dankbaar JW, de Rooij NK, Velthuis BK, Frijns CJ, Rinkel GJ, van der Schaaf IC. Diagnosing delayed cerebral ischemia with different ct modalities in patients with subarachnoid hemorrhage with clinical deterioration. *Stroke*. 2009; 40(11):3493-3498
7. Dankbaar JW, Rijdsdijk M, van der Schaaf IC, Velthuis BK, Wermer MJ, Rinkel GJ. Relationship between vasospasm, cerebral perfusion, and delayed cerebral ischemia after aneurysmal subarachnoid hemorrhage. *Neuroradiology*. 2009; 51(12):813-819
8. Latchaw RE, Yonas H, Hunter GJ, Yuh WT, Ueda T, Sorensen AG, Sunshine JL, Biller J, Wechsler L, Higashida R, Hademenos G. Guidelines and recommendations for perfusion imaging in cerebral ischemia: A scientific statement for healthcare professionals by the writing group on perfusion imaging, from the council on cardiovascular radiology of the american heart association. *Stroke*. 2003;34:1084-11049.
9. Kealey SM, Loving VA, DeLong DM, Eastwood JD. User-defined vascular input function curves: Influence on mean perfusion parameter values and signal-to-noise ratio. *Radiology*. 2004;231:587-593
10. van der Schaaf I, Vonken EJ, Waaijer A, Velthuis B, Quist M, van Osch T. Influence of partial volume on venous output and arterial input function. *AJNR Am J Neuroradiol*. 2006;27:46-50
11. Fiorella D, Heiserman J, Prenger E, Partovi S. Assessment of the reproducibility of postprocessing dynamic ct perfusion data. *AJNR Am J Neuroradiol*. 2004;25:97-107
12. Soares BP, Dankbaar JW, Bredno J, Cheng S, Bhogal S, Dillon WP, Wintermark M. Automated versus manual post-processing of perfusion-ct data in patients with acute cerebral ischemia: Influence on interobserver variability. *Neuroradiology*. 2009;51:445-451
13. Waaijer A, van der Schaaf IC, Velthuis BK, Quist M, van Osch MJ, Vonken EP, van Leeuwen MS, Prokop M. Reproducibility of quantitative ct brain perfusion measurements in patients with symptomatic unilateral carotid artery stenosis. *AJNR Am J Neuroradiol*. 2007;28:927-932
14. van der Schaaf I, Wermer MJ, van der Graaf Y, Hoff RG, Rinkel GJ, Velthuis BK. Ct after subarachnoid hemorrhage: Relation of cerebral perfusion to delayed cerebral ischemia. *Neurology*. 2006;66:1533-1538

15. Romano JG, Rabinstein AA, Arheart KL, Nathan S, Campo-Bustillo I, Koch S, Forteza AM. Microemboli in aneurysmal subarachnoid hemorrhage. *J Neuroimaging*. 2008;18:396-401
16. Stein SC, Levine JM, Nagpal S, LeRoux PD. Vasospasm as the sole cause of cerebral ischemia: How strong is the evidence? *NeurosurgFocus*. 2006;21:E2
17. Wintermark M, Thiran JP, Maeder P, Schnyder P, Meuli R. Simultaneous measurement of regional cerebral blood flow by perfusion ct and stable xenon ct: A validation study. *AJNR AmJ-Neuroradiol*. 2001;22:905-914
18. Wintermark M, Maeder P, Thiran JP, Schnyder P, Meuli R. Quantitative assessment of regional cerebral blood flows by perfusion ct studies at low injection rates: A critical review of the underlying theoretical models. *Eur Radiol*. 2001;11:1220-1230
19. Ladurner G, Zilkha E, Iliff D, du Boulay GH, Marshall J. Measurement of regional cerebral blood volume by computerized axial tomography. *JNeuroNeurosurgPsychiatry*. 1976;39:152-158
20. Axel L. Tissue mean transit time from dynamic computed tomography by a simple deconvolution technique. *Invest Radiol*. 1983;18:94-99
21. Biagi L, Abbruzzese A, Bianchi MC, Alsop DC, Del Guerra A, Tosetti M. Age dependence of cerebral perfusion assessed by magnetic resonance continuous arterial spin labeling. *J Magn Reson Imaging*. 2007;25:696-702
22. Ito H, Kanno I, Kato C, Sasaki T, Ishii K, Ouchi Y, Iida A, Okazawa H, Hayashida K, Tsuyuguchi N, Kuwabara Y, Senda M. Database of normal human cerebral blood flow, cerebral blood volume, cerebral oxygen extraction fraction and cerebral metabolic rate of oxygen measured by positron emission tomography with 15o-labelled carbon dioxide or water, carbon monoxide and oxygen: A multicentre study in japan. *Eur J Nucl Med Mol Imaging*. 2004;31:635-643
23. Kawamura J, Meyer JS, Ichijo M, Kobari M, Terayama Y, Weathers S. Correlations of leuko-ariosis with cerebral atrophy and perfusion in elderly normal subjects and demented patients. *J Neurol Neurosurg Psychiatry*. 1993;56:182-187
24. Leenders KL, Perani D, Lammertsma AA, Heather JD, Buckingham P, Healy MJ, Gibbs JM, Wise RJ, Hatazawa J, Herold S, et al. Cerebral blood flow, blood volume and oxygen utilization. Normal values and effect of age. *Brain*. 1990;113 (Pt 1):27-47
25. Parkes LM, Rashid W, Chard DT, Tofts PS. Normal cerebral perfusion measurements using arterial spin labeling: Reproducibility, stability, and age and gender effects. *Magn Reson Med*. 2004;51:736-743
26. Cavaglia M, Dombrowski SM, Drazba J, Vasanji A, Bokesch PM, Janigro D. Regional variation in brain capillary density and vascular response to ischemia. *Brain Res*. 2001;910:81-93
27. Nonaka H, Akima M, Hatori T, Nagayama T, Zhang Z, Ihara F. Microvasculature of the human cerebral white matter: Arteries of the deep white matter. *Neuropathology*. 2003;23:111-118
28. Suzuki M, Obara K, Sasaki Y, Matoh K, Kitabatake A, Sasaki K, Nunosawa F. Comparison of perivascular astrocytic structure between white matter and gray matter of rats. *Brain Res*. 2003;992:294-297
29. Kavanagh EC. The reversal sign. *Radiology*. 2007;245:914-915
30. O'Brien JT. Role of imaging techniques in the diagnosis of dementia. *Br J Radiol*. 2007;80 Spec No 2:S71-77
31. Sanelli PC, Lev MH, Eastwood JD, Gonzalez RG, Lee TY. The effect of varying user-selected input parameters on quantitative values in ct perfusion maps. *Acad Radiol*. 2004;11:1085-1092

32. Wintermark M, Lau BC, Chien J, Arora S. The anterior cerebral artery is an appropriate arterial input function for perfusion-ct processing in patients with acute stroke. *Neuroradiology*. 2008;50:227-236
33. Kudo K, Sasaki M, Ogasawara K, Terae S, Ehara S, Shirato H. Difference in tracer delay-induced effect among deconvolution algorithms in ct perfusion analysis: Quantitative evaluation with digital phantoms. *Radiology*. 2009
34. Scher AI, Gudmundsson LS, Sigurdsson S, Ghambaryan A, Aspelund T, Eiriksdottir G, van Buchem MA, Gudnason V, Launer LJ. Migraine headache in middle age and late-life brain infarcts. *JAMA*. 2009;301:2563-2570
35. May A. New insights into headache: An update on functional and structural imaging findings. *Nat Rev Neurol*. 2009;5:199-209
36. Ducros A, Boukobza M, Porcher R, Sarov M, Valade D, Bousser MG. The clinical and radiological spectrum of reversible cerebral vasoconstriction syndrome. A prospective series of 67 patients. *Brain*. 2007;130:3091-3101



Relationship between vasospasm, cerebral perfusion and delayed cerebral ischemia after aneurysmal subarachnoid hemorrhage



3

J.W. Dankbaar, M. Rijdsdijk, I.C. van der Schaaf, B.K. Velthuis, M.J.H. Wermer, G.J.E. Rinkel

Neuroradiology. 2009 Dec;51(12):813-9.

Abstract

Background and purpose

Vasospasm after aneurysmal subarachnoid hemorrhage (SAH) is thought to cause ischemia. To evaluate the contribution of vasospasm to delayed cerebral ischemia (DCI), we investigated the effect of vasospasm on cerebral perfusion and the relationship of vasospasm with DCI.

Methods

We studied 37 consecutive SAH patients with CT-angiography (CTA) and CT-perfusion (CTP) on admission, and within 14 days after admission or at time of clinical deterioration. CTP values (cerebral blood volume (CBV) and -flow (CBF), and mean transit time), degree of vasospasm on CTA, and occurrence of DCI were recorded. Vasospasm was categorized in: no spasm (0-25% decrease in vessel diameter); moderate spasm (25-50% decrease); and severe spasm (>50% decrease). The correspondence of the flow-territory of the most spastic vessel with the least perfused region was evaluated, and differences in perfusion values and occurrence of DCI between degrees of vasospasm were calculated with 95% confidence intervals (95%CI).

Results

Fourteen patients had no vasospasm, 16 moderate and 7 severe. In 65% of patients with spasm, the flow-territory of the most spastic vessel corresponded with the least perfused region. There was significant CBF (ml/100g/min) difference (-21.3; 95%CI:-37↔-5.3) between flow-territories of severe and no vasospasm. 4 of 7 patients with severe, 6 of 16 with moderate, and 3 of 14 patients with no vasospasm had DCI.

Conclusion

Vasospasm decreases cerebral perfusion, but corresponds with the least perfused region in only two thirds of our patients. Furthermore almost half of patients with severe vasospasm does not have DCI. Thus although severe vasospasm can decrease perfusion, it may not result in DCI.

Introduction

Delayed cerebral ischemia (DCI) is a serious complication of aneurysmal subarachnoid hemorrhage (SAH). It typically occurs 4-12 days after initial bleeding and increases the risk of poor outcome in patients that survive the first days.¹ The onset of DCI is characterised by a decrease in consciousness, new focal deficit or both. Presence or absence of angiographic vasospasm (luminal narrowing) is often used as a criterion for DCI. TCD measurements of flow velocities in the large cerebral vessels are performed daily in many hospitals, and SAH patients with neurological symptoms frequently undergo angiography to detect vasospasm. Furthermore, many strategies to treat DCI, such as induced hypertension and hypervolemia, or balloon angioplasty, are developed with the conviction that vasospasm is the main cause of deterioration and ischemia.²⁻⁴ However, vasospasm does not necessarily lead to cerebral infarcts (positive predictive value around 70%)⁵ and cerebral infarcts after SAH have been reported to occur in absence of vasospasm.⁶ In the development of DCI infarction is preceded by a decreased cerebral perfusion.^{7,8} It would therefore make sense to measure perfusion in an area that is fed by a spastic vessel to evaluate the contribution of vasospasm to DCI.

CT perfusion imaging (CTP) is an accurate tool to measure cerebral perfusion.⁹ Within the same imaging study CTP can be combined with CT-angiography (CTA), which can be used to accurately detect vasospasm.^{10,11} The combination of CTA and CTP makes it possible to study the relationship between vasospasm and perfusion deficits.

The purpose of this study was to investigate the effects of vasospasm (measured with CTA) on cerebral perfusion (measured with CTP) and its relation with DCI.

Methods

Design

All patients admitted to our hospital with SAH, proven on non-contrast CT (NCT) or CSF analysis, were prospectively enrolled. We included all patients who were admitted within 72 hours after SAH with written informed consent. Included patients were scanned on admission and at the time of clinical deterioration or within 14 days after admission if no deterioration occurred. Exclusion criteria for the present study were a) patients with a cause of SAH other than a ruptured aneurysm and b) patients younger than 18 years of age. For all patients the clinical status on admission (according to the World Federation of Neurological Surgeons (WFNS) scale)¹² and time to follow up was recorded. Informed consent for the study was obtained from all patients and the study was approved by the ethics committee of our institution. All patients were treated according to a standardized protocol that consisted of absolute bed rest until aneurysm treatment, oral administration of nimodipine, cessation of antihypertensive medication, and intravenous administration of fluid aiming for normovolemia.

Imaging technique

In our hospital all patients with SAH routinely undergo a CTA on admission to evaluate the presence and configuration of aneurysms. At the time of clinical deterioration or about one week after admission in clinically stable patients, included patients underwent a NCT, CTP and CTA scan (follow up scan). The CTP scan was performed prior to CTA and replaces the timing scan for the CTA. CTA can be used for detection of vasospasm with an accuracy equal to that of the gold standard DSA.^{10, 11} CTP imaging measures cerebral perfusion on tissue level and provides accurate and reliable data compared to the gold standard Xenon-CT.⁹ CTP gives information on cerebral blood volume (CBV), cerebral blood flow (CBF), mean transit time (MTT) and time-to-peak (TTP).

All imaging studies were executed on a 16-slice spiral CT scanner (Philips Mx8000 LDT, Best, the Netherlands). CTP source data were derived from sequential scans covering a slab of 2.4 cm thickness selected 3 cm above the sella turcica and angulated parallel to the meato-orbital line to contain the upper parts of the lateral ventricles and the basal ganglia. For the CTP scan 40 ml of nonionic contrast agent (Iopromide, Ultravist, 300mg iodine/ml, Schering, Berlin, Germany) was injected into the cubital vein (18 gauge needle) at a rate of 5 ml/s followed by a 40 ml saline flush at a rate of 5 ml/s using a dual power injector (Stellant Dual CT injector, Medrad Europe BV, Beek, the Netherlands). The following parameters were used: 90 kVp, 150 mAs, 8x3 mm collimation, 512x512 matrix, 200 mm FOV, 1 image per 2 seconds during 60 seconds (total 30 images), UB filter and standard resolution. For the CTA scan 70 ml of nonionic contrast agent was injected into the cubital vein; 50 ml at a rate of 5 ml/s, 20 ml at a rate of 4 ml/s followed by a 40 ml saline flush at a rate of 4 ml/s. Scanning was performed with: 120 kVp, 180 mAs, 16x0.75 mm collimation, 512x512 matrix, 160 FOV, rotation time 0.4 s, pitch 0.9, slice thickness 1 mm, reconstruction increment 0.5 mm, filter B and UF resolution. All CT angiograms were evaluated on a Philips MXView workstation.

CTA and CTP measurements and data processing

CTA scans were reconstructed at 10 mm contiguous axial, sagittal and coronal maximal intensity projection (MIP) images. The smallest diameters of both the proximal (A1) and distal (A2) segments of the anterior cerebral artery (ACA) and the proximal (M1) and distal (M2) segments of the middle cerebral artery (MCA) were measured by one of two observers blinded for the perfusion results and for the clinical condition of the patient (IvdS, MR) using the best projecting viewing plane.

The degree of vasospasm was assessed by dividing the vessel diameter on the follow up scan with the vessel diameter measured on the admission scan. We assumed that no vasospasm was present on the admission scan since vasospasm generally occurs more than three days after SAH.¹ Vasospasm was categorized as: 1) none: 0 to 25% decrease in vessel diameter on the follow up scan, 2) moderate: 25-50% decrease and 3) severe: >50% decrease.^{13, 14}

CTP scans were reconstructed at 6 mm contiguous axial images. Data were transferred to a Philips workstation for post processing. The CTP algorithm was based

upon the central volume principle and CBF was calculated by the deconvolution method.¹⁵ Perfusion was measured in regions of interest (ROIs) drawn by hand bilaterally in the cortical gray matter of the flow territories of the anterior and middle cerebral artery at the level of the basal ganglia (*Figure 1*). The ROIs were drawn by one observer blinded for the clinical condition and CTA images of the patient (MR). The posterior circulation was not included in this study.



Figure 1 Regions of interest (ROIs) drawn by hand bilaterally in the cortical gray matter of the flow territories of the anterior and middle cerebral artery at the level of the basal ganglia.

DCI

The occurrence of delayed cerebral ischemia (DCI) was assessed by a neurologist (MW) blinded for the CTP and CTA scan results. DCI was defined as a clinical deterioration (new focal deficit, decreased Glasgow Coma Scale, or both) lasting two hours or longer with no evidence for rebleeding or hydrocephalus on CT and no other medical causes, such as cardiovascular or pulmonary complications, infections or metabolic disturbances.

Analysis

To investigate the effect of vasospasm on cerebral perfusion, we assessed whether the flow territory of the most spastic vessel corresponded with the ROI with lowest perfusion. Additionally, differences in mean perfusion values and their respective 95% CIs, were calculated between flow territories of moderate and severe vasospastic vessels, and flow territories of vessels without spasm. The category of spasm was based on the most spastic vessel segment (proximal or distal) since flow territories are supplied by the proximal and distal segment which may both influence cerebral perfusion. Thus, per patient four vessels (proximal and distal MCA and ACA) with corresponding perfusion were incorporated in the analysis.

To investigate the relationship of vasospasm and DCI, we calculated differences (and their 95% CIs) in the percentage of patients with DCI between the different degrees of vasospasm (most spastic vessel).

For all analyses a difference was considered statistically significant if the 95% CI did not contain zero.

Results

Forty patients met our inclusion criteria. Three patients were excluded because the follow up scan could not be evaluated due to motion artefacts or improper timing of contrast bolus injection. The characteristics of the 37 remaining patients and time of follow up scanning are shown in *Table 1*.

Table 1 Patient characteristics

Number of patients	(total = 37)
Women (%)	28 (76%)
Mean age in years (range)	58 (range 32-77)
WFNS grade (number of patients)	
1	15 (41%)
2	8 (22%)
3	1 (3%)
4	6 (16%)
5	7 (19%)
Median days after SAH for follow up scan	7 (range 3- 12)
Delayed Cerebral Ischemia (DCI)	13 (35%)

WFNS grade = World Federation of Neurological Surgeons clinical grading scale.

Of all patients, 14 had no vasospasm, 16 had moderate vasospasm and 7 had severe vasospasm. In 15 of the 23 patients with moderate to severe vasospasm (65%), the flow territory of the vessel with most severe vasospasm corresponded with the least perfused region (*Figure 2*). With increasing degree of vasospasm, cerebral perfusion in the corresponding flow territory decreased (*Table 2*). Mean cerebral perfusion values were most favorable (highest CBV and CBF values and lowest MTT and TTP values) in the flow territories supplied by arteries without vasospasm and least favorable in flow territories supplied by arteries with severe vasospasm. Differences in perfusion were more prominent between none and severe vasospasm than between none and moderate vasospasm (*Table 2*). Differences in CBF between none and severe vasospasm were statistically significant (*Table 2*).

Four of 7 (57%) patients with severe vasospasm and 6 of 16 (38%) with moderate vasospasm had DCI compared to 3 of 14 (21%) of patients with no vasospasm. The difference in percentage DCI between no vasospasm and moderate vasospasm was 17% (95% CI: -15 ↔ 49), and between no and severe 36% (95% CI: 0 ↔ 68%).

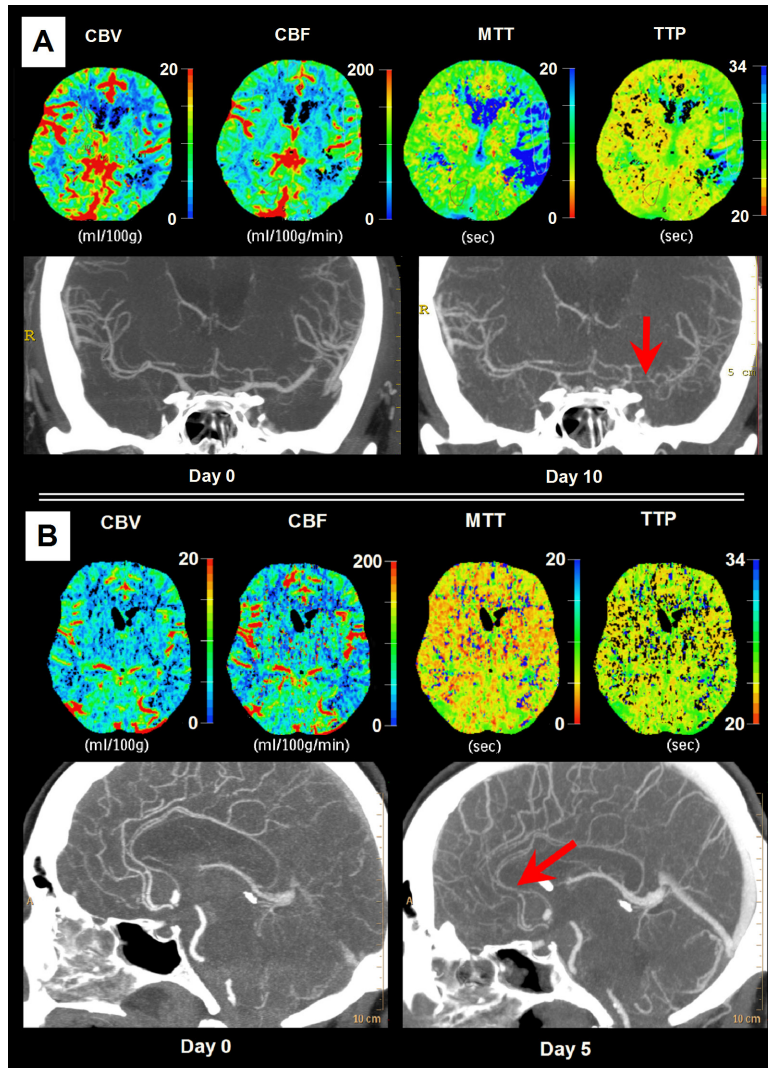


Figure 2 CTA vasospasm and its effect on cerebral perfusion as seen on CTP colour maps: (A) 43 year old man, 10 days after SAH with vasospasm (red arrow) in the left middle cerebral artery and an area of low perfusion in the flow territory of this artery (most visible on the MTT map); (B) 60 year old woman, 5 days after SAH with vasospasm (red arrow) in all anterior cerebral arteries (ACA; note the presence of an accessory ACA) and no areas of low perfusion in the flow territory of these arteries. *For color figure see page 227*

Table 2 Mean Cerebral perfusion values in the flow territories of vessels with no, moderate and severe vasospasm.

	Vasospasm				
	None (<25%) N = 14	Moderate (25-50%) N = 16	<i>Difference between moderate and none (95% CI)</i>	Severe (>50%) N = 7	<i>Difference between severe and none (95% CI)</i>
Number of flow territories*	94	46		8	
Mean CBV (ml/100g)	4.3	4.0	-0.3 (-0.7 ↔ 0.1)	3.5	-0.8 (-1.7 ↔ 0.1)
Mean CBF (ml/100g/min)	59.5	52.7	-6.8 (-14 ↔ 0.6)	38.2	-21.3 (-37 ↔ -5.3) [†]
Mean MTT (s)	4.8	5.0	0.2 (-0.6 ↔ 0.9)	8.1	3.3 (-2.5 ↔ 9.1)
Mean TTP (s)	22.8	23.5	0.7 (-1.1 ↔ 2.5)	27.0	4.2 (-6.0 ↔ 15)

CBV = Cerebral Blood Volume; CBF = Cerebral Blood Flow; MTT = Mean Transit Time; TTP = Time To Peak

*37 patients with 4 flow territories = total of 148 flow territories.

[†]statistically significant

Discussion

Our results show that cerebral perfusion decreases with increasing degree of vasospasm. Our results also show that patients with severe vasospasm more often experience DCI than patients without vasospasm. However, almost half of the patients with severe vasospasm does not experience DCI. This suggests that although vasospasm causes a decrease in perfusion in the area behind the spasm, severe vasospasm alone is not always sufficient to cause DCI. Most likely other factors play a role in decreasing cerebral perfusion to a level where DCI does occur.

We studied a relatively large consecutive series of symptomatic and asymptomatic SAH patients to evaluate the effect of vasospasm on cerebral perfusion. In the setting of vasospasm cerebral perfusion has previously been investigated, but rarely asymptomatic patients were included. Our findings that vasospasm affects cerebral perfusion to an increasing extent with increasing vasospasm, are in accordance with the results of other clinical and experimental studies.^{13, 16-19} Differences in quantitative perfusion values between severe and moderate to absent vasospasm were comparable to other studies quantifying perfusion in angiographic vasospasm.^{18, 19} A recent study showed that qualitative assessment of CTP color maps correlates well with vasospasm on DSA. However, this study also showed that in 70% of cases no vasospasm is present on DSA although the patients experienced neurological symptoms at that time.²⁰ In other studies 11-49 % of patients without vasospasm experienced neurological symptoms suggestive of DCI.^{16, 17, 19} However,

these studies did not look at asymptomatic patients. In a study where patients with and without symptoms of DCI were examined, 36% of patients had severe vasospasm (compared to 19% in our study) while 49% of all patients had DCI (compared to 35% in our study).¹⁸ A correlation between the two was not given. Our results show that although severe vasospasm decreases cerebral perfusion it does not cause DCI in almost half of our patients. This suggests that the decrease in perfusion caused by vasospasm, is not sufficient to cause DCI in all patients and the presence of vasospasm is not equivalent to DCI.

DCI is likely to be a focal problem^{21, 22} that is caused by a decrease in cerebral perfusion resulting in ischemia or infarction. Cerebral perfusion measurements reflect the net effect of all factors that contribute to the development of DCI. Failing compensatory mechanisms in the presence of vasospasm together with other pathogenic processes play a role. Firstly, cerebral autoregulation is often disturbed in SAH patients.^{23, 24} With disturbed autoregulation distal resistance vessels can not compensate sufficiently to maintain adequate CBF in a setting of vasospasm or other hemodynamic challenges.^{13, 23, 25} Secondly, blood flow through collateral circulation can compensate for the drop in CBF in flow territories behind a spastic vessel segment.²⁶ Absence of collateral flow consequently results in less compensation. Thirdly, there are other pathogenetic processes not visible on CTA that can contribute to a decrease of CBF and the development of DCI. These processes include small-artery spasm and platelet aggregation.^{6, 22, 27-29} All these factors can explain the discrepancy between the presence of vasospasm and presence of DCI, and also that the flow territory of the vessel with most severe vasospasm corresponds with the least perfused region in less than two thirds of our patients.

We acknowledge that the used imaging technique has some limitations.

Brain perfusion measurements with CTP are limited by its coverage (in this study only 2.4 cm). However, with increasing detectors this scan volume will expand. Also, CTP data of the posterior fossa can rarely be used and were excluded in this study since large veins in the posterior fossa influence CTP measurements due to partial volume effects.

Another limitation may be that we did not vary the region of perfusion measurements with the location of the spasm (distal or proximal in the feeding vessel). A small area of decreased perfusion due to distal spasm may therefore have been averaged with the larger region of normal perfusion. However, by not using information on spasm for the CTP assessment we reduced observer bias.

The strength of this study lies in the fact that a relatively large consecutive series of symptomatic and asymptomatic SAH patients was prospectively collected. A good comparison could thus be made between patients with different degrees of vasospasm with and without DCI.

Conclusion

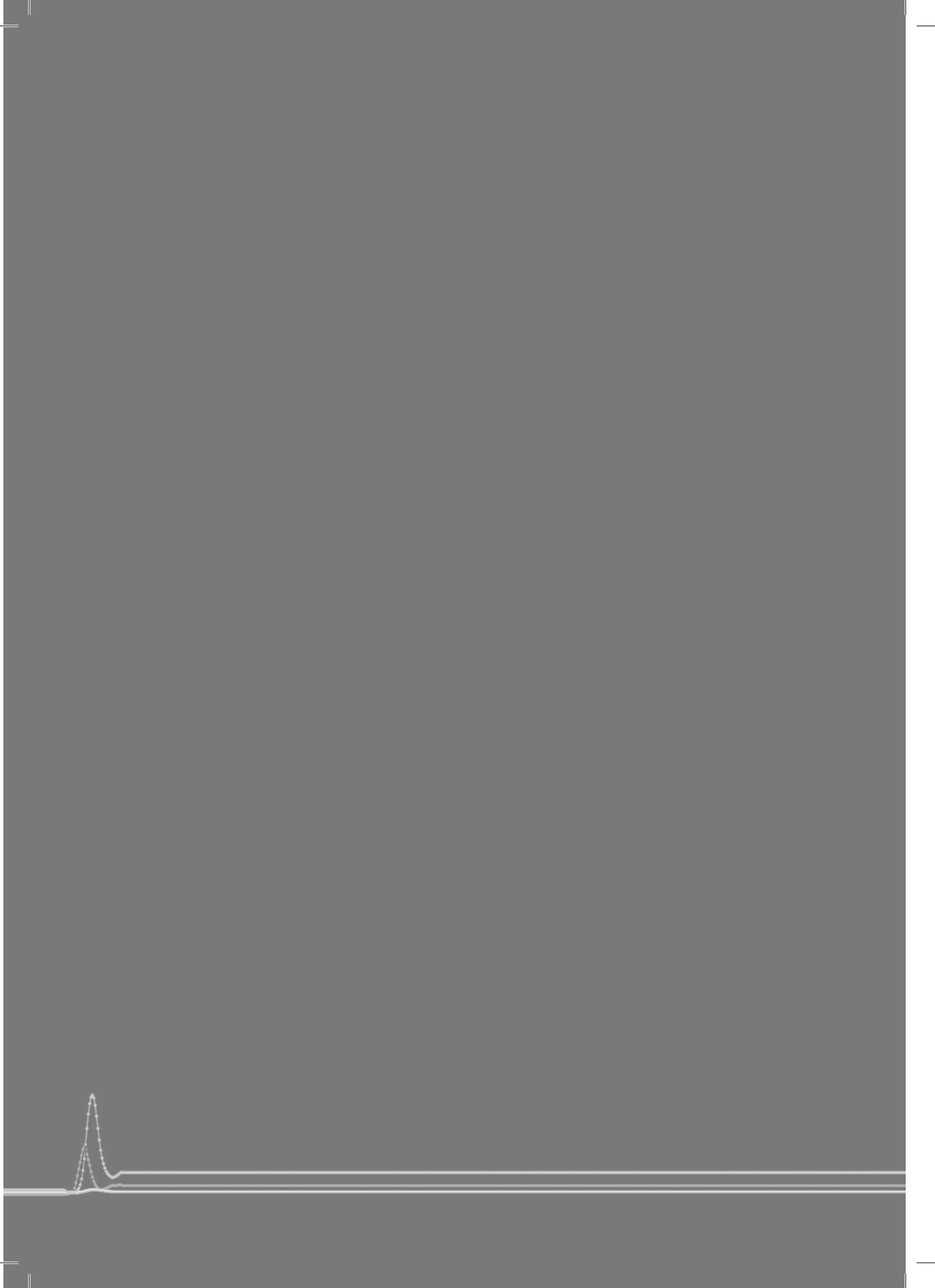
Our findings emphasize that although cerebral vasospasm does affect cerebral perfusion, it is by itself not sufficient to cause DCI. This reflects the multifactorial origin of DCI and affirms the poor diagnostic value of vasospasm for DCI. The net

effect on perfusion of mechanisms compensating for vasospasm and additional pathogenetic processes can be measured with CTP. Cerebral perfusion should therefore be more thoroughly evaluated as a diagnostic tool in the acute phase of DCI, and angiographic vasospasm on CTA may not be a proper gold standard for diagnosing DCI.

References

1. van Gijn J, Kerr RS, Rinkel GJ (2007) Subarachnoid haemorrhage. *Lancet* 369: 306-318
2. Myburgh JA (2005) "Triple h" Therapy for aneurysmal subarachnoid haemorrhage: Real therapy or chasing numbers? *Crit Care Resusc*. 7: 206-212
3. Qureshi AI, Suarez JJ, Bhardwaj A, Yahia AM, Tamargo RJ, Ulatowski JA (2000) Early predictors of outcome in patients receiving hypervolemic and hypertensive therapy for symptomatic vasospasm after subarachnoid hemorrhage. *Crit Care Med* 28: 824-829
4. Weyer GW, Nolan CP, Macdonald RL (2006) Evidence-based cerebral vasospasm management. *NeurosurgFocus* 21: E8
5. Rabinstein AA, Friedman JA, Weigand SD, McClelland RL, Fulgham JR, Manno EM, Atkinson JL, Wijidicks EF (2004) Predictors of cerebral infarction in aneurysmal subarachnoid hemorrhage. *Stroke* 35: 1862-1866
6. Stein SC, Levine JM, Nagpal S, LeRoux PD (2006) Vasospasm as the sole cause of cerebral ischemia: How strong is the evidence? *NeurosurgFocus* 21: E2
7. Harrod CG, Bendok BR, Batjer HH (2005) Prediction of cerebral vasospasm in patients presenting with aneurysmal subarachnoid hemorrhage: A review. *Neurosurgery* 56: 633-654
8. Pham M, Johnson A, Bartsch AJ, Lindner C, Mullges W, Roosen K, Solymosi L, Bendszus M (2007) Ct perfusion predicts secondary cerebral infarction after aneurysmal subarachnoid hemorrhage. *Neurology* 69: 762-765
9. Wintermark M, Thiran JP, Maeder P, Schnyder P, Meuli R (2001) Simultaneous measurement of regional cerebral blood flow by perfusion ct and stable xenon ct: A validation study. *AJNR AmJNeuroradiol* 22: 905-914
10. Chaudhary SR, Ko N, Dillon WP, Yu MB, Liu S, Cricqui GI, Higashida RT, Smith WS, Wintermark M (2008) Prospective evaluation of multidetector-row ct angiography for the diagnosis of vasospasm following subarachnoid hemorrhage: A comparison with digital subtraction angiography. *Cerebrovasc Dis* 25: 144-150
11. Yoon DY, Choi CS, Kim KH, Cho BM (2006) Multidetector-row ct angiography of cerebral vasospasm after aneurysmal subarachnoid hemorrhage: Comparison of volume-rendered images and digital subtraction angiography. *AJNR AmJNeuroradiol* 27: 370-377
12. Report of world federation of neurological surgeons committee on a universal subarachnoid hemorrhage grading scale. (1988) *JNeurosurg* 68: 985-986
13. Lodi CA, Ursino M (1999) Hemodynamic effect of cerebral vasospasm in humans: A modeling study. *Ann Biomed Eng* 27: 257-273
14. Voldby B, Enevoldsen EM, Jensen FT (1985) Regional cbf, intraventricular pressure, and cerebral metabolism in patients with ruptured intracranial aneurysms. *JNeurosurg* 62: 48-58
15. Axel L (1983) Tissue mean transit time from dynamic computed tomography by a simple deconvolution technique. *Invest Radiol* 18: 94-99
16. Aralasmak A, Akyuz M, Ozkaynak C, Sindel T, Tuncer R (2009) Ct angiography and perfusion imaging in patients with subarachnoid hemorrhage: Correlation of vasospasm to perfusion abnormality. *Neuroradiology* 51: 85-93
17. Binaghi S, Colleoni ML, Maeder P, Uske A, Regli L, Dehdashti AR, Schnyder P, Meuli R (2007) Ct angiography and perfusion ct in cerebral vasospasm after subarachnoid hemorrhage. *AJNR AmJNeuroradiol* 28: 750-758

18. Sviri GE, Britz GW, Lewis DH, Newell DW, Zaaroor M, Cohen W (2006) Dynamic perfusion computed tomography in the diagnosis of cerebral vasospasm. *Neurosurgery* 59: 319-325
19. Wintermark M, Ko NU, Smith WS, Liu S, Higashida RT, Dillon WP (2006) Vasospasm after subarachnoid hemorrhage: Utility of perfusion ct and ct angiography on diagnosis and management. *AJNR AmJNeuroradiol* 27: 26-34
20. Wintermark M, Dillon WP, Smith WS, Lau BC, Chaudhary S, Liu S, Yu M, Fitch M, Chien JD, Higashida RT, Ko NU (2008) Visual grading system for vasospasm based on perfusion ct imaging: Comparisons with conventional angiography and quantitative perfusion ct. *Cerebrovasc Dis* 26: 163-170
21. Rijdsdijk M, van der Schaaf IC, Velthuis BK, Wermer MJ, Rinkel GJ (2008) Global and focal cerebral perfusion after aneurysmal subarachnoid hemorrhage in relation with delayed cerebral ischemia. *Neuroradiology* 50: 813-820
22. Weidauer S, Vatter H, Beck J, Raabe A, Lanfermann H, Seifert V, Zanella F (2008) Focal laminar cortical infarcts following aneurysmal subarachnoid haemorrhage. *Neuroradiology* 50: 1-8
23. Jaeger M, Schuhmann MU, Soehle M, Nagel C, Meixensberger J (2007) Continuous monitoring of cerebrovascular autoregulation after subarachnoid hemorrhage by brain tissue oxygen pressure reactivity and its relation to delayed cerebral infarction. *Stroke* 38: 981-986
24. Hattingen E, Blasel S, Dettmann E, Vatter H, Pilatus U, Seifert V, Zanella FE, Weidauer S (2008) Perfusion-weighted mri to evaluate cerebral autoregulation in aneurysmal subarachnoid haemorrhage. *Neuroradiology* 50: 929-938
25. Pucher RK, Auer LM (1988) Effects of vasospasm in the middle cerebral artery territory on flow velocity and volume flow. A computersimulation. *Acta Neurochir (Wien)* 93: 123-128
26. Weidauer S, Lanfermann H, Raabe A, Zanella F, Seifert V, Beck J (2007) Impairment of cerebral perfusion and infarct patterns attributable to vasospasm after aneurysmal subarachnoid hemorrhage: A prospective mri and dsa study. *Stroke* 38:1831-1836
27. Kozniewska E, Michalik R, Rafalowska J, Gadamski R, Walski M, Frontczak-Baniewicz M, Piotrowski P, Czernicki Z (2006) Mechanisms of vascular dysfunction after subarachnoid hemorrhage. *J Physiol Pharmacol* 57 Suppl 11:145-160
28. Ng WH, Moochhala S, Yeo TT, Ong PL, Ng PY (2001) Nitric oxide and subarachnoid hemorrhage: Elevated level in cerebrospinal fluid and their implications. *Neurosurgery* 49:622-626 discussion 626-627
29. Romano JG, Rabinstein AA, Arheart KL, Nathan S, Campo-Bustillo I, Koch S, Forteza AM (2008) Microemboli in aneurysmal subarachnoid hemorrhage. *J Neuroimaging* 18:396-401



Changes in cerebral perfusion around the time of delayed cerebral ischemia in subarachnoid hemorrhage patients



4

*J.W. Dankbaar, N.K. de Rooij, E.J. Smit, B.K. Velthuis, C.J.M. Frijns,
G.J.E. Rinkel, I.C. van der Schaaf*

Abstract

Background and purpose

Because the pathogenesis of delayed cerebral ischemia (DCI) after subarachnoid hemorrhage (SAH) is unclear, we studied cerebral perfusion at different time points around the occurrence of DCI.

Methods

We prospectively enrolled 53 patients who underwent CT-perfusion (CTP) scans on admission, and within 2 weeks after hemorrhage on 2 scheduled time points or during clinical deterioration. The occurrence of DCI was assessed according to pre-defined criteria by two neurological observers blinded for perfusion results. Clinically stable patients (no-DCI) served as reference, and patients with other causes of deterioration (n=11) were excluded. In DCI patients, the day of DCI-onset and in no-DCI patients the median day of DCI was taken as t=0. Scans made before and after DCI were clustered into five additional time-points. At each time point, cerebral blood volume (CBV) and flow (CBF), and mean transit time (MTT) were measured, and absolute and relative (interhemispheric asymmetry) values were compared between DCI and no-DCI patients.

Results

Absolute CBF was lower and MTT higher in the 18 DCI patients than in the 24 no-DCI patients before, during and after DCI. MTT asymmetry increased during DCI and partially recovered afterwards in DCI patients while it remained constant in no-DCI patients. Absolute and relative CBV remained constant in both groups.

Conclusion

Our findings suggest that DCI patients already have diffusely worse perfusion (absolute values) than no-DCI patients before focal worsening (increased asymmetry) occurs and becomes symptomatic. The partial recovery in the measured areas suggests that DCI can be partially reversible.

Introduction

Delayed cerebral ischemia (DCI) is a serious complication of aneurysmal subarachnoid hemorrhage (SAH) that increases the risk of poor outcome in patients who survive the first hours after the initial hemorrhage.^{1,2} Despite many years of research the pathogenesis of DCI is still unclear.

Vasospasm is traditionally considered to be the main cause of DCI. The incidence of vasospasm peaks seven days after hemorrhage.^{3,4} Although up to 70% of patients with aneurysmal SAH develop vasospasm, only 20 to 30% have neurological symptoms compatible with DCI.¹ Presence of vasospasm alone is therefore an insufficient explanation for the development of DCI, and most likely a combination of factors plays a role.⁵ Disturbed cerebral autoregulation, often seen after SAH, together with large or small vessel vasospasm, absence of collateral blood supply, and microthrombosis may cause a decrease in cerebral perfusion resulting in ischemia or infarction.⁵⁻⁸ Since cerebral perfusion measurements are likely to reflect the net effect of all factors that contribute to the development of DCI,⁹ repeated measurement of cerebral perfusion in SAH patients at different time points may give new insights into what DCI is and why it occurs. CT perfusion imaging (CTP) is an accurate tool to measure cerebral perfusion¹⁰ and can be used to diagnose DCI.¹¹

The purpose of this study was to increase our understanding of DCI by comparing cerebral perfusion at different time points in SAH patients with and without DCI.

Methods

Design

We prospectively enrolled all SAH patients admitted to the University Medical Center Utrecht between May 2007 and September 2009 who underwent non-contrast CT (NCT), CTP, and CT-angiography (CTA) on admission and met the following inclusion criteria: (a) 18 years of age or older, (b) aneurysmal cause of SAH, (c) admitted within 72 hours after SAH, (d) written informed consent. Patients with impaired renal function (creatinine > 200 $\mu\text{mol/l}$) or other contra-indications for contrast enhanced CT-scans, as well as pregnant women, were excluded.

After the admission scan, all patients were planned to undergo at least two additional CTP scans planned at 2-4, 5-7 or 8-10 days after SAH. If patients developed clinical deterioration within 21 days after SAH the admission scanning protocol (NCT, CTP and CTA) was performed. This scan could replace one of the planned scans. Patients with clinical deterioration from other causes than DCI (11 patients) were excluded from further analyses. Patients without clinical deterioration were used as a reference group (no-DCI).

All patients were treated according to the SAH treatment protocol of our hospital, which includes oral nimodipine, fluid management to prevent hypovolemia, and evaluation for clinical deterioration (every 2-4 hours). Age, gender, clinical status on admission (according to the World Federation of Neurological Surgeons (WFNS) scale¹²), amount of blood on the admission scan (Hijdra score¹³), presence

of parenchymal hemorrhage, aneurysm location and treatment, time of clinical deterioration, and use of hypertensive treatment was recorded. The study was approved by the local ethics committee.

DCI

For the purpose of the study, the diagnosis of delayed cerebral ischemia (DCI) in patients who experienced clinical deterioration was assessed after completion of the clinical course. This assessment was based on prospectively collected data and done by a neurology resident (NKR) and a neurologist (CJMF) according to previously published criteria.¹¹ The two observers had full access to all clinical information concerning the patient's entire clinical course, both before and after clinical deterioration, all laboratory results, and all NCTs, but were blinded for the CTP. The NCTs were used to show ischemic changes, and to exclude rebleeding, hydrocephalus, edema around a hematoma and postoperative swelling. The clinical information and laboratory results were used to exclude infection or metabolic disturbances as a cause of the deterioration.

Imaging protocol

All patients underwent NCT and CTP imaging on admission and at least two other time points planned at 2-4, 5-7 or 8-10 days after SAH. A scan made at the time of clinical deterioration often replaced one of the planned scans. A CTA was only obtained on admission and at the time of deterioration.

CTP gives accurate information on cerebral blood volume (CBV), cerebral blood flow (CBF), and mean transit time (MTT) on tissue level.¹⁰ CTA can be used for detection of macrovascular vasospasm with accuracy equal to that of the gold standard digital subtraction angiography (DSA).¹⁴

All imaging studies were executed on a 64 slice spiral CT scanner (Philips Mx8000 LDT, Best, the Netherlands) using previously published scanning protocols.¹¹ The CTP scan covered a 4 cm slab selected at the level of the basal ganglia.

CTP and CTA post-processing and evaluation

CTP scans were reconstructed at 5 mm contiguous axial images and transferred to a Philips workstation for post processing. We used commercially available Philips software (Extended Brilliance Workspace 3) to calculate absolute perfusion maps of CBV, CBF, and MTT. Perfusion was measured in pre-defined regions of interest (ROIs) drawn by hand by one observer blinded for the clinical condition of the patient (JWD) bilaterally in the cortical gray matter and basal ganglia of the flow territories of the anterior, middle and posterior cerebral artery (*Figure 1*). If a parenchymal hemorrhage was present at that level a slice just above the hemorrhage was chosen. Since the ROIs were pre-defined, the perfusion measurements were not necessarily performed in the region with the lowest perfusion.

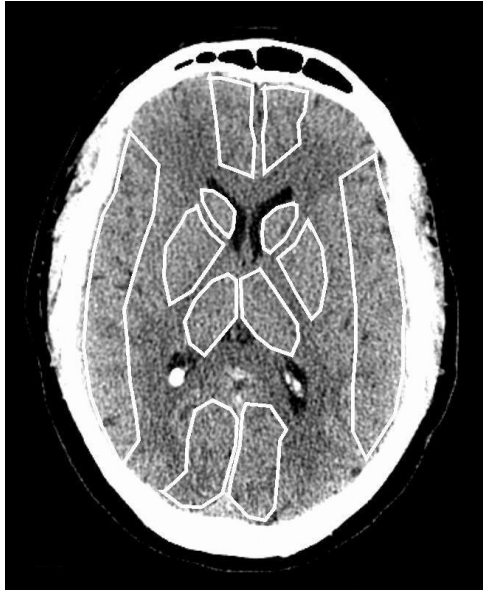


Figure 1 The twelve regions of interest for cerebral perfusion measurement drawn by hand in the cortical gray matter and basal ganglia of the flow-territories of the anterior, middle, and posterior cerebral artery.

The CTA made at the time of clinical deterioration was evaluated for the presence of vasospasm by visual comparison to the admission CTA scan on a Philips workstation by one of two observers (ICvdS, JWD). Vasospasm was assessed in the proximal and distal segments of the anterior, middle and posterior cerebral artery, and basilar artery, and for each segment categorized in: 1) none: 0-25% decrease in vessel diameter, 2) moderate: 26-50% decrease and 3) severe: >50% decrease.¹⁵

Analysis

We used scans made on the day of DCI as a time zero ($t=0$) in our analysis. In clinically stable patients (no-DCI group) we used the median day of DCI in the DCI patient group as $t=0$. The admission CTP scan and all other scans of each patient were numbered relative to $t=0$. The numbers were clustered (for example all first scans following DCI or median day of DCI in no-DCI patients) and for each cluster, the median day relative to $t=0$ was calculated. These median days were referred to as the time points.

At each time point we selected the ROIs with the lowest absolute values of CBV and CBF and highest absolute values of MTT (reflecting the least perfused flow territories) for each patient.

Since absolute perfusion values can be influenced by observer-dependent post processing steps^{16, 17} we also used a relative approach. For each ROI we calculated interhemispheric ratios (lowest to highest) for CBV and CBF, and interhemispheric differences for MTT. For each patient, the lowest CBV and CBF ratio, and the largest MTT difference (reflecting the largest asymmetry in perfusion between both hemispheres) were selected. For each time point the Mann Whitney U test (no

normal distribution in a small sample) was used to compare the absolute and relative values of DCI patients and no-DCI patients.

To assess the changes in cerebral perfusion before, during and after DCI, we plotted the median perfusion values of each time point for DCI and no-DCI patients.

Results:

We included 42 patients; 18 were diagnosed to have DCI and 24 patients remained clinically stable (no-DCI; reference group).

The patient characteristics of the DCI and no-DCI patients are summarized in *Table 1*.

Of the 18 DCI patients 11 (61%) had severe angiographic vasospasm in one or more vessel segments at the time of deterioration. Six (33%) DCI patients received hypertensive treatment after clinical deterioration.

The median day of onset of DCI was six days after SAH. Clustering of the additional scans resulted in five more time-points. The clusters of scans made before and after DCI were made at a median of ten, six and three days before DCI and three and four days after DCI.

Absolute CTP values

Figure 2 (left panel) illustrates the changes in lowest absolute cerebral perfusion values around the time of DCI in patients with and without DCI. *Table 2* shows the median of the absolute perfusion measurements used for each time-point, the interquartile range, and the p-value of the Mann Whitney U test for differences between DCI and no-DCI patients at that time point.

The median CBV remains relatively constant over time in the measured area, with no significant differences between DCI and no-DCI patients at any time-point.

In the measured areas CBF is at a constant lower level in DCI patients than in no-DCI patients, but this difference is only statistically significant at 3 days before DCI onset.

MTT gradually increases (indicating worsening perfusion) towards the time of DCI in DCI patients and decreases after DCI. The difference in MTT between DCI and no-DCI patients is statistically significant at the time of DCI, 3 days before and 3 days after DCI.

Relative CTP values

Figure 2 (right panel) illustrates the changes in perfusion asymmetry around the time of DCI in patients with and without DCI; *Table 3* shows the actual values. In the measured areas CBV asymmetry remained stable over time, with no significant differences between DCI and no-DCI patients at any time-point. The CBF asymmetry increased over time in DCI patients, while it decreased in no-DCI patients, but the differences between DCI and no-DCI patients were not statistically significant at any time-point. MTT asymmetry increased markedly in DCI patients at the time of DCI, and decreased thereafter, while it remained relatively constant in no-DCI patients. At the time of DCI and 3 days after DCI the differences were statistically significant.

Table 1 Patient characteristics

	DCI	No-DCI
Number of patients	18	24
Number of men	5(28%)	11(46%)
Median age (range)	57.5(26-81)	59(18-79)
Admission WFNS score		
1	3(17%)	16(67%)
2	5(27%)	3(12%)
3	3(17%)	0(0%)
4	4(22%)	5(21%)
5	3(17%)	0(0%)
Amount of blood (Hijdra score)		
Cisternal sum-score (median)	19	15
1-10	4(22%)	6(25%)
11-20	7(39%)	13(54%)
21-30	7(39%)	5(21%)
Intraventricular sum-score (median)	5	2
0	4(22%)	9(38%)
>0	14(78%)	15(62%)
Parenchymal hemorrhage	7 (39%)	7(30%)
Aneurysm location		
anterior cerebral artery	1(5.5%)	0(0%)
anterior communicating artery	7(39%)	8(33%)
carotid bifurcation	5(27.5%)	3(13%)
middle cerebral artery	3(17%)	8(33%)
posterior communicating artery	1(5.5%)	4(17%)
vertebrobasilar artery	0(0%)	1(4%)
posterior inferior cerebellar artery	1(5.5%)	0(0%)
Aneurysm treatment		
No	0(0%)	1(4%)
Coiling	12(67%)	11(46%)
Clipping	6(33%)	12(50%)
Median day of intervention (range)	2 (0-5)	1 (0-4)
Median day after SAH of occurrence of DCI (range)	6 (1-15)	
Vasospasm (% luminal narrowing) in one or more vessel segments		
0-25%	5 (28%)	*
26-50%	2 (11%)	*
> 50%	11 (61%)	*
Hypertensive treatment after suspected DCI	6 (33%)	

DCI: delayed cerebral ischemia

*In clinically stable patients no CTA was performed to minimize the total radiation dose.

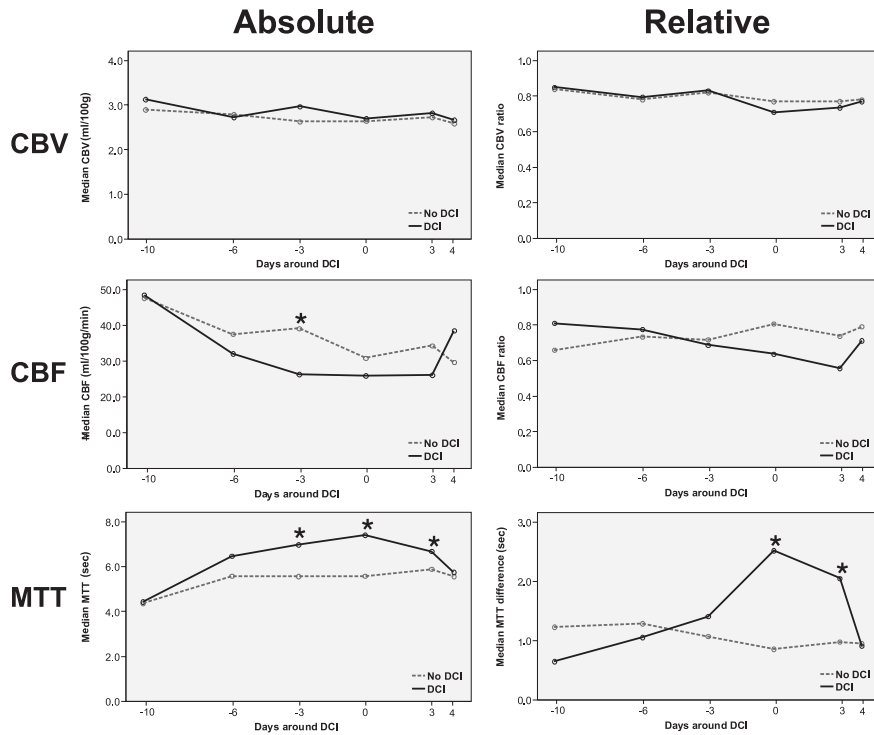


Figure 2 Time course of median absolute and relative cerebral perfusion parameters in relation to the median day of delayed cerebral ischemia (DCI) in patients with and without DCI. CBV = Cerebral Blood Volume; CBF = Cerebral Blood Flow; MTT = Mean Transit Time
* statistically significant difference between DCI and no-DCI

Figure 3 shows absolute maps of perfusion around the time of DCI in two patients. Patient A had reversible perfusion abnormalities while patient B had progressively increasing perfusion abnormalities leading to definite cerebral infarction.

Table 2 Absolute CT-perfusion values per time point (median days around DCI of scan cluster) in patients with and without delayed cerebral ischemia (DCI).

Absolute	-10 days		-6 days		-3 days		day of DCI		3 days		4 days	
	DCI: n=3 no-DCI: n=3	Median (iqr 25-75%)	DCI: n=10 no-DCI: n=15	Median (iqr 25-75%)	DCI: n=17 no-DCI: n=23	Median (iqr 25-75%)	DCI: n=17 no-DCI: n=8	Median (iqr 25-75%)	DCI: n=10 no-DCI: n=23	Median (iqr 25-75%)	DCI: n=6 no-DCI: n=5	Median (iqr 25-75%)
CBV (ml/100g)	DCI 3.13 (3.09-3.28)	0.51	2.73 (2.52-3.23)	0.87	2.97 (2.25-3.35)	0.37	2.70 (2.17-3.28)	0.73	2.82 (2.34-3.27)	0.60	2.67 (1.86-3.45)	0.93
	no-DCI 2.90 (2.41-3.73)		2.79 (2.32-3.12)		2.63 (2.16-3.14)		2.64 (2.31-2.94)		2.73 (2.50-2.90)		2.59 (2.06-3.12)	
CBF (ml/100g/sec)	DCI 48.4 (48.1-53.9)	0.28	32.1 (23.6-36.7)	0.07	26.3 (16.6-35.9)	0.02*	26.1 (19.1-33.6)	0.32	26.1 (19.1-35.7)	0.07	38.5 (22.1-40.5)	0.86
	no-DCI 47.6 (41.6-53.1)		37.5 (33.1-39.8)		39.1 (30.0-42.6)		30.9 (29.4-40.0)		34.3 (27.9-38.1)		29.64 (26.5-40.2)	
MTT (sec)	DCI 4.43 (4.40-4.88)	0.51	6.47 (4.82-8.83)	0.24	6.98 (6.12-10.97)	0.00*	7.41 (6.03-9.34)	0.04*	6.69 (5.86-9.21)	0.05*	5.76 (5.10-7.16)	1.00
	no-DCI 4.36 (3.66-5.67)		5.58 (5.17-5.93)		5.57 (4.68-6.02)		5.58 (4.69-7.18)		5.89 (5.04-7.26)		5.57 (4.98-7.48)	

CBV = Cerebral Blood Volume; CBF = Cerebral Blood Flow; MTT = Mean Transit Time; iqr 25-75%= interquartile range of 25th and 75th percentile.
* statistically significant p-value for Mann-Whitney U test

Table 3 Relative CT-perfusion values per time point (median days around DCI of scan cluster) in patients with and without delayed cerebral ischemia (DCI).

Relative	-10 days		-6 days		-3 days		day of DCI		3 days		4 days	
	DCI: n=3 no-DCI: n=3	Median (iqr 25-75%)	p-value	Median (iqr 25-75%)	p-value	DCI: n=10 no-DCI: n=15	Median (iqr 25-75%)	p-value	DCI: n=17 no-DCI: n=23	Median (iqr 25-75%)	p-value	DCI: n=6 no-DCI: n=5
CBV ratio	DCI	0.85 (0.71-0.90)	0.83	0.80 (0.76-0.84)	0.42	0.83 (0.66-0.86)	0.81	0.71 (0.57-0.83)	0.54	0.74 (0.63-0.78)	0.18	0.77 (0.58-0.83)
	no-DCI	0.84 (0.82-0.94)	0.78	0.78 (0.61-0.82)	0.82	0.82 (0.71-0.85)	0.82	0.77 (0.63-0.83)	0.77	0.77 (0.71-0.84)	0.78	0.78 (0.75-0.84)
CBF ratio	DCI	0.81 (0.74-0.81)	0.13	0.78 (0.67-0.87)	0.27	0.69 (0.54-0.82)	0.25	0.64 (0.36-0.75)	0.04*	0.56 (0.37-0.83)	0.23	0.71 (0.55-0.73)
	no-DCI	0.66 (0.50-0.81)	0.73	0.73 (0.53-0.82)	0.72	0.72 (0.68-0.83)	0.72	0.81 (0.62-0.89)	0.81	0.74 (0.68-0.79)	0.79	0.79 (0.72-0.84)
MTT difference	DCI	0.65 (0.47-1.1)	0.13	1.06 (0.64-1.72)	0.70	1.41 (0.98-2.75)	0.06	2.52 (1.29-3.86)	0.02*	2.05 (1.21-3.29)	0.02*	0.91 (0.59-1.54)
	no-DCI	1.23 (0.90-1.42)	1.29	1.29 (0.80-1.50)	1.07	1.07 (0.68-1.63)	1.07	0.86 (0.60-2.26)	0.86	0.98 (0.73-1.43)	0.95	0.95 (0.61-1.10)

CBV = Cerebral Blood Volume; CBF = Cerebral Blood Flow; MTT = Mean Transit Time; iqr 25-75%= interquartile range of 25th and 75th percentile.

* statistically significant p-value for Mann-Whitney U test

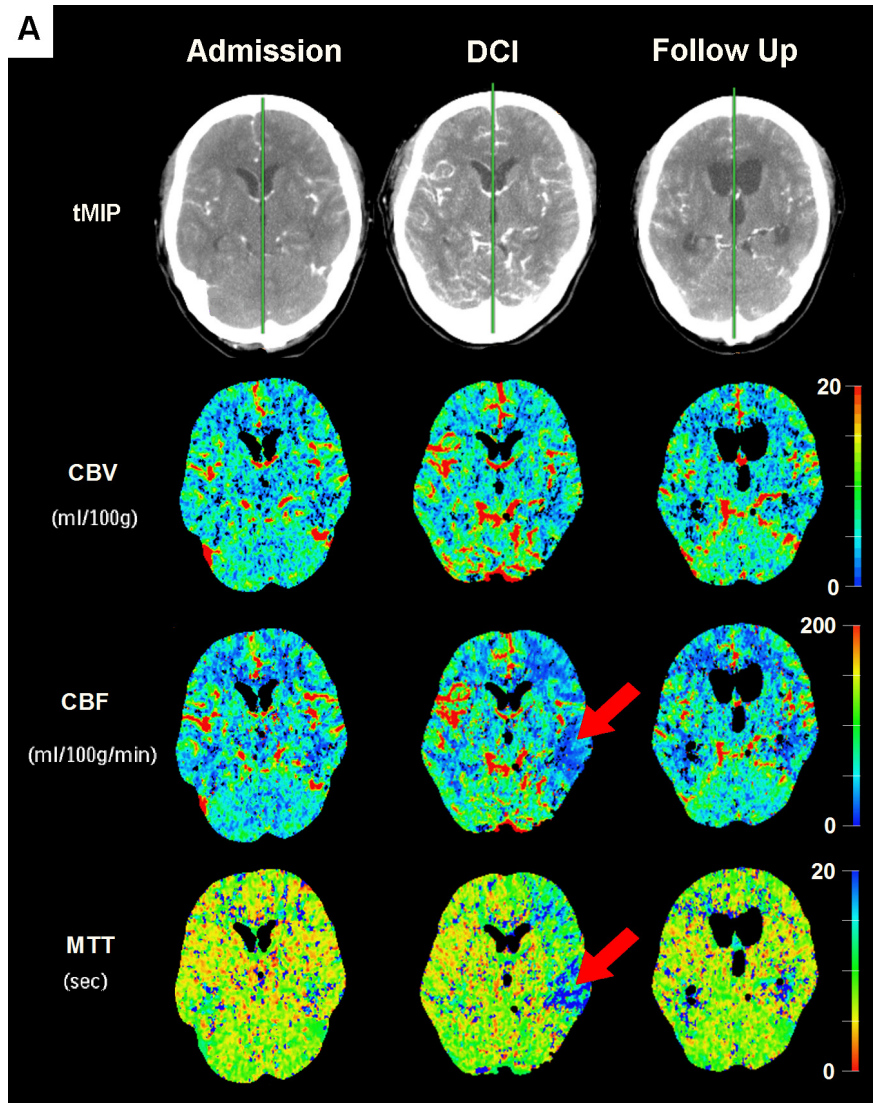


Figure 3 Example of reversible (A) and irreversible (B) ischemia in two patients with delayed cerebral ischemia (DCI). (A) A 49-year-old woman with a ruptured left carotid bifurcation aneurysm that was successfully treated with surgical clip placement. On day seven after hemorrhage the patient developed dysphasia due to DCI. The Cerebral Blood Flow (CBF) and Mean Transit Time (MTT) color map show a perfusion abnormality in the left middle cerebral artery flow territory (red arrows), and no apparent abnormalities on the Cerebral Blood Volume (CBV) map. The symptoms and the CTP abnormalities resolved in the following days, indicating reversible ischemia. *For color figure see page 228*

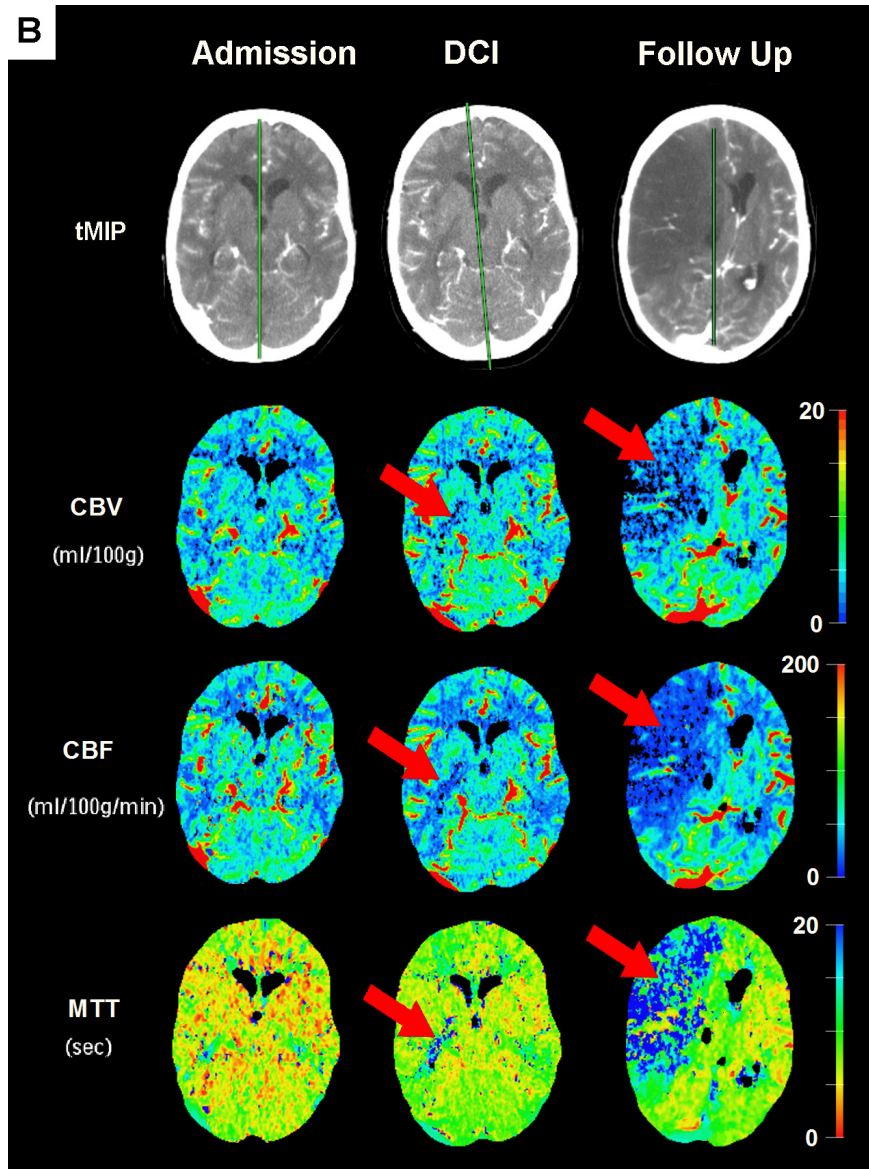


Figure 3 Example of reversible (A) and irreversible (B) ischemia in two patients with delayed cerebral ischemia (DCI). (B) A 52-year-old woman with a ruptured right carotid bifurcation aneurysm that was successfully treated by intravascular coil embolization. One day after embolization the patient developed new focal deficits from DCI, with a perfusion abnormality in the right internal capsule visible on the CBV, CBF and MTT color map (red arrows). The perfusion abnormality progressed to complete right middle cerebral artery infarction on follow up. tMIP = temporal maximal intensity projection. *For color figure see page 229*

Discussion

Our study on changes in cerebral perfusion around the time of DCI shows that CBF is lower and MTT higher in DCI patients compared to no-DCI patients before, during, and after DCI, with the largest difference between the groups at the time of DCI, while CBV remains relatively constant in both groups. Furthermore, MTT asymmetry develops in DCI patients at the time of DCI and decreases after DCI.

Auto-regulation is often disturbed in SAH patients.¹⁸ As a result CBV may not be adjusted appropriately to changes in MTT, which could explain the stable CBV, with increasing MTT and thereby decreasing CBF in DCI patients towards the time of DCI. In ischemic stroke a prolonged MTT in the absence of a decrease in CBV indicates areas of possibly reversible ischemia since blood is still flowing to the ischemic region.¹⁹⁻²¹ The increased MTT and constant CBV in our DCI patients could therefore also indicate that the ischemia is still reversible in the measured area at the time of DCI. This would explain why absolute and relative MTT and CBF partially recovered after DCI.^{4, 22} The partial recovery in the measured area can be either spontaneous or due to hypertensive treatment. Without a randomized assignment to treatment this is hard to differentiate.

The finding that absolute MTT only gradually increased towards DCI while the observed increase in MTT asymmetry was more prominent and occurred after absolute values had already worsened, suggests that patients with diffusely worse absolute perfusion parameters may be more susceptible to additional changes in perfusion. The worse absolute perfusion may be a result of increased intracranial pressure while factors like vasospasm, micro-thrombi, or a failing collateral blood supply may lead to additional focal perfusion abnormalities in these patients resulting in increased asymmetry and neurologic worsening.^{5, 7, 8} Patients without a compromised absolute perfusion do not develop symptoms which may explain why not all patients with vasospasm develop DCI.²³ The fact that of our DCI patients only 60% had severe angiographic vasospasm at the time of clinical deterioration makes clear that the other above mentioned factors have to be kept in mind as causes for DCI.

Future research may make it possible to separate different causes of DCI and see whether reversible and irreversible ischemia have different pathogenetic mechanisms.

Our study design differs essentially from previous studies describing the time course of cerebral perfusion in SAH patients. Firstly, we chose not to use angiographic vasospasm as a criterion for DCI because of the relatively weak association between vasospasm and DCI. Other studies categorized patients based on presence of angiographic vasospasm,^{4, 24, 25} rather than clinical course and symptoms suggestive of DCI. Secondly, we chose to use the time of occurrence of DCI as the center point (t=0) rather than the time of the admission scan which also varied up to 72 hours after onset of SAH. This is necessary to combine the time-course of perfusion of all patients with DCI, since DCI does not occur at the same day after SAH in each patient. To relate the time course of our reference group

(no-DCI) to the time course in DCI patients, we chose the median day of DCI as $t=0$. In this way perfusion changes before and after DCI are accurately visualized and compared to the changes of perfusion in the absence of DCI. The disadvantage of this design is that the scans made before DCI are made at different times after SAH and we can therefore not make any comments regarding the predictive value of CTP measurements before DCI. Predicting DCI was not a goal of this paper. The use of CTP for this purpose has however previously been evaluated, with the conclusion that CTP is a useful tool to predict DCI.^{26, 27}

In designing the study, we have deliberately chosen to measure perfusion in pre-defined ROIs at a standard level in the brain (level of the basal ganglia), and not to adjust measurements to least perfused area's. As a result we may have measured perfusion outside a possibly infarcted area (where CBV would be decreased) and only have detected ischemia surrounding infarction. We may thereby have found less abnormal perfusion measurements than in case of adjusted measurements. However, by selecting pre-defined ROIs we kept observer bias to a minimum.

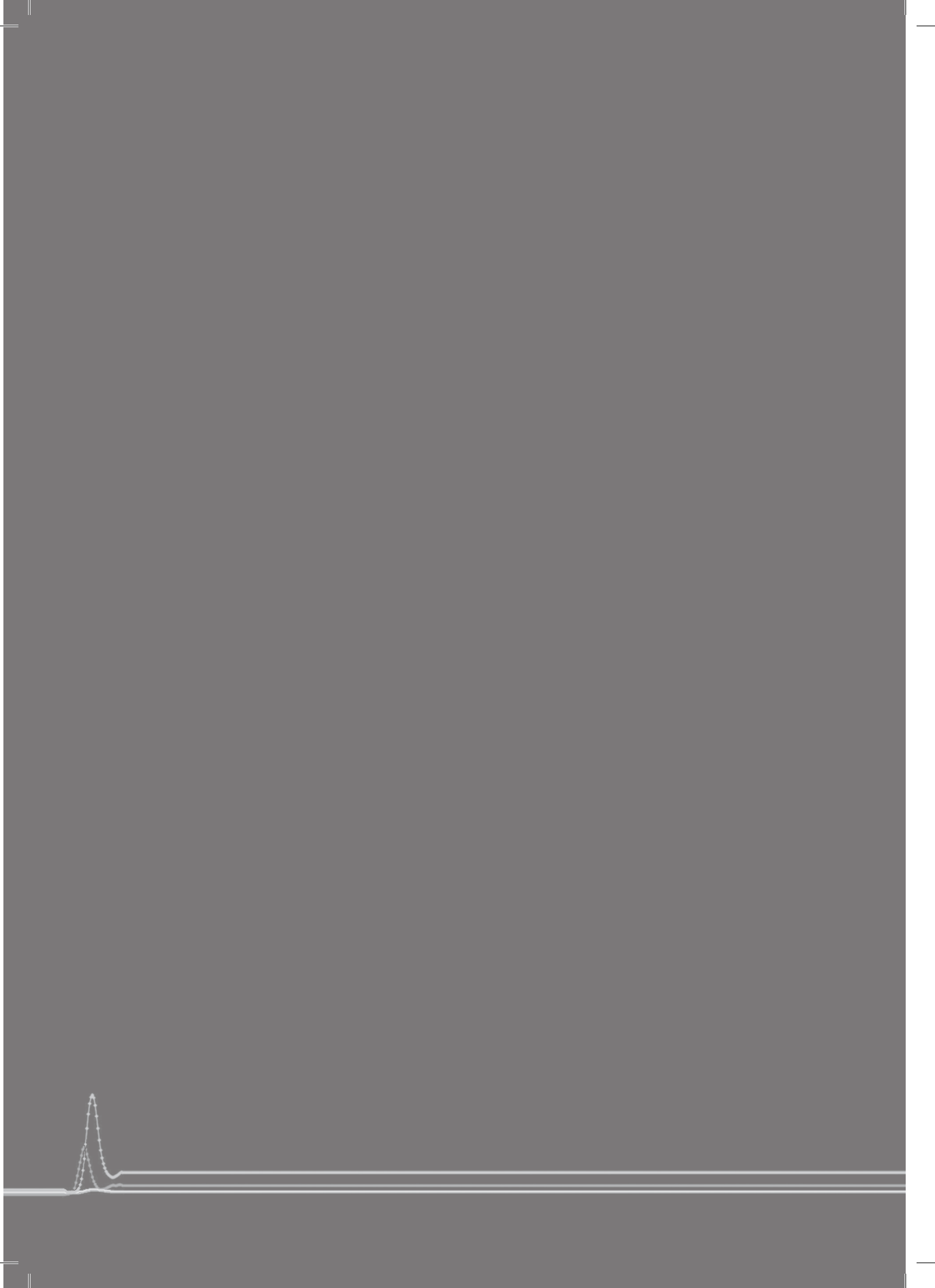
Conclusion

We observed worse absolute and relative CBF and MTT values before, during, and after DCI in DCI patients compared to no-DCI patients with SAH. Especially MTT asymmetry increased markedly towards the time of DCI and decreased afterwards in DCI patients while it remained constant in no-DCI patients. Both absolute and relative CBV remained constant over time without apparent differences between DCI and no-DCI patients. The less favorable perfusion before DCI with a clear increase in asymmetry during DCI suggests focal worsening of perfusion in an already compromised group of patients. The improvement of perfusion after DCI suggests a certain degree of reversibility in the measured areas.

References

1. van Gijn J, Kerr RS, Rinkel GJ. Subarachnoid haemorrhage. *Lancet*. 2007;369:306-318
2. Treggiari MM, Walder B, Suter PM, Romand JA. Systematic review of the prevention of delayed ischemic neurological deficits with hypertension, hypervolemia, and hemodilution therapy following subarachnoid hemorrhage. *J Neurosurg*. 2003;98:978-984
3. Charpentier C, Audibert G, Guillemin F, Civit T, Ducrocq X, Bracard S, Hepner H, Picard L, Laxenaire MC. Multivariate analysis of predictors of cerebral vasospasm occurrence after aneurysmal subarachnoid hemorrhage. *Stroke*. 1999;30:1402-1408
4. Weidauer S, Lanfermann H, Raabe A, Zanella F, Seifert V, Beck J. Impairment of cerebral perfusion and infarct patterns attributable to vasospasm after aneurysmal subarachnoid hemorrhage: A prospective mri and dsa study. *Stroke*. 2007;38:1831-1836
5. Stein SC, Levine JM, Nagpal S, LeRoux PD. Vasospasm as the sole cause of cerebral ischemia: How strong is the evidence? *NeurosurgFocus*. 2006;21:E2
6. Kozniowska E, Michalik R, Rafalowska J, Gadamski R, Walski M, Frontczak-Baniewicz M, Piotrowski P, Czernicki Z. Mechanisms of vascular dysfunction after subarachnoid hemorrhage. *J Physiol Pharmacol*. 2006;57 Suppl 11:145-160
7. Romano JG, Rabinstein AA, Arheart KL, Nathan S, Campo-Bustillo I, Koch S, Forteza AM. Microemboli in aneurysmal subarachnoid hemorrhage. *J Neuroimaging*. 2008;18:396-401
8. Vergouwen MD, Vermeulen M, Coert BA, Stroes ES, Roos YB. Microthrombosis after aneurysmal subarachnoid hemorrhage: An additional explanation for delayed cerebral ischemia. *J Cereb Blood Flow Metab*. 2008;28:1761-1770
9. Dankbaar JW, Rijdsijk M, van der Schaaf IC, Velthuis BK, Wermer MJ, Rinkel GJ. Relationship between vasospasm, cerebral perfusion, and delayed cerebral ischemia after aneurysmal subarachnoid hemorrhage. *Neuroradiology*. 2009
10. Wintermark M, Thiran JP, Maeder P, Schnyder P, Meuli R. Simultaneous measurement of regional cerebral blood flow by perfusion ct and stable xenon ct: A validation study. *AJNR AmJ Neuroradiol*. 2001;22:905-914
11. Dankbaar JW, de Rooij NK, Velthuis BK, Frijns CJ, Rinkel GJ, van der Schaaf IC. Diagnosing delayed cerebral ischemia with different ct modalities in patients with subarachnoid hemorrhage with clinical deterioration. *Stroke*. 2009
12. Rabinstein AA, Friedman JA, Weigand SD, McClelland RL, Fulgham JR, Manno EM, Atkinson JL, Wijdicks EF. Predictors of cerebral infarction in aneurysmal subarachnoid hemorrhage. *Stroke*. 2004;35:1862-1866
13. Hijdra A, Brouwers PJ, Vermeulen M, van GJ. Grading the amount of blood on computed tomograms after subarachnoid hemorrhage. *Stroke*. 1990;21:1156-1161
14. Yoon DY, Choi CS, Kim KH, Cho BM. Multidetector-row ct angiography of cerebral vasospasm after aneurysmal subarachnoid hemorrhage: Comparison of volume-rendered images and digital subtraction angiography. *AJNR AmJ Neuroradiol*. 2006;27:370-377
15. Voldby B, Enevoldsen EM, Jensen FT. Regional cbf, intraventricular pressure, and cerebral metabolism in patients with ruptured intracranial aneurysms. *J Neurosurg*. 1985;62:48-58
16. Kealey SM, Loving VA, Delong DM, Eastwood JD. User-defined vascular input function curves: Influence on mean perfusion parameter values and signal-to-noise ratio. *Radiology*. 2004;231:587-593

17. van der Schaaf I, Vonken EJ, Waaijer A, Velthuis B, Quist M, van Osch T. Influence of partial volume on venous output and arterial input function. *AJNR Am J Neuroradiol*. 2006;27:46-50
18. Jaeger M, Schuhmann MU, Soehle M, Nagel C, Meixensberger J. Continuous monitoring of cerebrovascular autoregulation after subarachnoid hemorrhage by brain tissue oxygen pressure reactivity and its relation to delayed cerebral infarction. *Stroke*. 2007;38:981-986
19. Parsons MW, Pepper EM, Bateman GA, Wang Y, Levi CR. Identification of the penumbra and infarct core on hyperacute noncontrast and perfusion ct. *Neurology*. 2007;68:730-736
20. Schaefer PW, Roccatagliata L, Ledezma C, Hoh B, Schwamm LH, Koroshetz W, Gonzalez RG, Lev MH. First-pass quantitative ct perfusion identifies thresholds for salvageable penumbra in acute stroke patients treated with intra-arterial therapy. *AJNR Am J Neuroradiol*. 2006;27:20-25
21. Wintermark M, Flanders AE, Velthuis B, Meuli R, van Leeuwen M, Goldsher D, Pineda C, Serena J, van der Schaaf I, Waaijer A, Anderson J, Nesbit G, Gabriely I, Medina V, Quiles A, Pohlman S, Quist M, Schnyder P, Bogousslavsky J, Dillon WP, Pedraza S. Perfusion-ct assessment of infarct core and penumbra: Receiver operating characteristic curve analysis in 130 patients suspected of acute hemispheric stroke. *Stroke*. 2006;37:979-985
22. Condet A, Auliac S, Bracard S, Anxionnat R, Schmitt E, Lacour JC, Braun M, Meloneto J, Cordebar A, Yin L, Picard L. Vasospasm after subarachnoid hemorrhage: Interest in diffusion-weighted mr imaging. *Stroke*. 2001;32:1818-1824
23. Svirni GE, Britz GW, Lewis DH, Newell DW, Zaaroor M, Cohen W. Dynamic perfusion computed tomography in the diagnosis of cerebral vasospasm. *Neurosurgery*. 2006;59:319-325
24. Talacchi A. Sequential measurements of cerebral blood flow in the acute phase of subarachnoid hemorrhage. *J Neurosurg Sci*. 1993;37:9-18
25. Nabavi DG, LeBlanc LM, Baxter B, Lee DH, Fox AJ, Lownie SP, Ferguson GG, Craen RA, Gelb AW, Lee TY. Monitoring cerebral perfusion after subarachnoid hemorrhage using ct. *Neuroradiology*. 2001;43:7-16
26. van der Schaaf I, Wermer MJ, van der Graaf Y, Hoff RG, Rinkel GJ, Velthuis BK. Ct after subarachnoid hemorrhage: Relation of cerebral perfusion to delayed cerebral ischemia. *Neurology*. 2006;66:1533-1538
27. van der Schaaf I, Wermer MJ, van der Graaf Y, Velthuis BK, van de Kraats CI, Rinkel GJ. Prognostic value of cerebral perfusion-computed tomography in the acute stage after subarachnoid hemorrhage for the development of delayed cerebral ischemia. *Stroke*. 2006;37:409-413



Diagnosing delayed cerebral ischemia with different CT modalities in SAH patients with clinical deterioration



5

*J.W. Dankbaar, N.K. de Rooij, B.K. Velthuis, C.J.M. Frijns,
G.J.E. Rinkel, I.C. van der Schaaf*

Stroke. 2009 Nov;40(11):3493-8.

Abstract

Background and purpose

Delayed cerebral ischemia (DCI) after aneurysmal subarachnoid hemorrhage (SAH) worsens the prognosis and is difficult to diagnose. We investigated the diagnostic value of non-contrast CT (NCT), CT-perfusion (CTP), and CT-angiography (CTA) for DCI after clinical deterioration in SAH patients.

Methods

We prospectively enrolled 42 SAH patients with clinical deterioration suspect for DCI (new focal deficit or GCS decrease ≥ 2 points) within 21 days after hemorrhage. All patients underwent NCT, CTP and CTA scans on admission and directly after clinical deterioration. The gold standard was the clinical diagnosis DCI, made retrospectively by two neurologists who interpreted all clinical data, except CTP and CTA, to rule out other causes for the deterioration. Radiologists interpreted NCT and CTP images for signs of ischemia (NCT) or hypoperfusion (CTP) not localized in the neurosurgical trajectory or around intracerebral hematomas, and CTA images for presence of vasospasm. Diagnostic values for DCI of NCT, CTP, and CTA were assessed by calculating sensitivities, specificities, positive predictive values (PPV), and negative predictive values (NPV) with 95% confidence intervals (CI).

Results

In three patients with clinical deterioration, imaging failed due to motion artifacts. Of the remaining 39 patients, 25 had DCI and 14 did not. NCT had a sensitivity of 0.56 (95%CI: 0.37-0.73), specificity = 0.71 (0.45-0.88), PPV = 0.78 (0.55-0.91), NPV = 0.48 (0.28-0.68); CTP: sensitivity = 0.84 (0.65-0.93), specificity = 0.79 (0.52-0.92), PPV = 0.88 (0.69-0.96), NPV = 0.73 (0.48-0.89); CTA: sensitivity = 0.64 (0.45-0.80), specificity = 0.50 (0.27-0.73), PPV = 0.70 (0.49-0.84), NPV = 0.44 (0.23-0.67).

Conclusion

As a diagnostic tool for DCI, qualitative assessment of CTP is overall superior to NCT and CTA, and could be useful for fast decision making and guiding treatment.

Introduction

Delayed cerebral ischemia (DCI) is a serious complication of aneurysmal subarachnoid hemorrhage (SAH). It typically occurs 4-12 days after initial bleeding and increases the risk of poor outcome in patients that survive the first days.¹ The onset of DCI is characterized by a decrease in consciousness, new focal deficit or both. There is however no good diagnostic test to confirm presence or absence of DCI at the time of clinical deterioration.

When clinical deterioration occurs, a non-contrast CT scan (NCT) is usually made to rule out rebleeding, swelling around an intracerebral hematoma, and hydrocephalus. NCT is however not very sensitive in showing early ischemia.² If NCT renders no explanation, and no clear signs of severe infection or metabolic disturbance are present, it is often assumed that the patient has DCI. This diagnosis is sometimes confirmed on later follow up imaging, showing one or more areas of cerebral infarction. However, when infarction is seen on these follow up images it is too late to treat the patient. Therefore, ischemia should be identified before it turns into infarction. To diagnose DCI when symptoms occur, presence of vasospasm shown with transcranial Doppler or angiography is frequently used. Although traditionally vasospasm is thought to be the main cause for DCI, vasospasm can be present without DCI and DCI can be present without vasospasm.³⁻⁵ Better diagnostic tools are thus needed to identify DCI at the time of deterioration, which is important to facilitate rapid treatment decision making.

In occlusive stroke patients, early ischemic changes can be accurately identified in the acute stage with CT-perfusion (CTP).^{6,7} Since infarction in DCI is preceded by a decreased cerebral perfusion,^{8,9} CTP may be a useful tool to identify ischemia as the cause of clinical deterioration.

The purpose of this study was to evaluate the diagnostic value of NCT, CTP, and CT-angiography (CTA) for DCI in SAH patients with clinical deterioration.

Methods

Design

We prospectively enrolled all SAH patients admitted to the University Medical Center Utrecht from May 2007 till June 2008 who underwent the SAH imaging protocol of our institution (NCT, CTP, and CTA) on admission and met the following inclusion criteria: (a) 18 years of age or older, (b) aneurysmal cause of SAH, (c) admitted within 72 hours after SAH, and (d) clinical deterioration (decreased Glasgow coma scale (GCS) of at least 2 points lasting more than 2 hours, or new focal deficit) within 21 days after hemorrhage.

Patients were treated according to the SAH treatment protocol of our hospital, which includes oral nimodipine, fluid management to prevent hypovolemia, and evaluation for clinical deterioration (every 2-4 hours). When deterioration occurred, patients were again scanned with our SAH imaging protocol. Patients with impaired renal function (Creatinine > 200 µmol/l) or other contra-indications for contrast enhanced CT-scans, as well as pregnant women, were excluded. For

all included patients age, gender, clinical status on admission (according to the World Federation of Neurological Surgeons (WFNS) scale⁵), amount of blood on the admission scan (Hijdra score¹⁰), aneurysm location and treatment, and time of clinical deterioration was recorded. The study was approved by our ethics committee.

DCI

The occurrence of delayed cerebral ischemia (DCI) was retrospectively assessed by two neurologists (NKR and CJMF), who had full access to all clinical information concerning the entire period of the patient's clinical course, both before and after clinical deterioration, all laboratory results, and the NCT performed at time of the clinical deterioration, but who were blinded for the CTP and CTA images. The NCT was used to exclude rebleeding, hydrocephalus, edema around a hematoma and postoperative swelling. The clinical information and lab findings were used to exclude infection or metabolic disturbances as a cause for the deterioration. Infection was defined as: fever, leucocytosis, increased C-reactive protein or positive cultures along with clinical signs of infection for which antibiotic treatment was indicated. Metabolic disturbances were defined as: hypo- or hypernatremia (< 125 mmol/L or >155 mmol/L), hypomagnesemia (< 0.6 mmol/L), or hypercalcemia (ionized calcium >1.3 mmol/L). This clinical diagnosis served as the gold standard.

Imaging protocol

All patients underwent NCT, CTP and CTA imaging on admission and at the time of clinical deterioration. CTP imaging measures cerebral perfusion on tissue level and provides accurate data compared with the gold standard Xenon-CT.¹¹ CTP gives information on cerebral blood volume (CBV), cerebral blood flow (CBF), and mean transit time (MTT). CTA can be used for detection of vasospasm with accuracy equal to that of the gold standard digital subtraction angiography (DSA).¹² All imaging studies were executed on a 64 slice spiral CT scanner (Philips Mx8000 LDT, Best, the Netherlands). The CTP scan covered a 4 cm slab selected at the level of the basal ganglia. For the CTP scan 40 ml of non-ionic contrast agent (Iopromide, Ultravist, 300mg iodine/ml, Schering, Berlin, Germany) was injected into the cubital vein at a rate of 5 ml/s followed by a 40 ml saline flush at a rate of 5 ml/s using a Stellant Dual CT injector (Medrad Europe BV, Beek, the Netherlands). The following parameters were used: 80 kVp, 150 mAs, 64x0.625 mm collimation, 512x512 matrix, 220 mm field of view, 1 image per 2 seconds during 60 seconds. For the CTA scan 70 ml of non-ionic contrast agent was injected into the cubital vein; 50 ml at a rate of 5 ml/s, followed by a 40 ml saline flush at a rate of 4 ml/s. Scanning was performed with: 80/120 kVp, 300/100 mAs, 64x0.625 mm collimation, 512x512 matrix, 200 field of view, slice thickness 0.67 mm, reconstruction increment 0.33 mm.

NCT, CTP and CTA post-processing and evaluation

NCT scans were evaluated on a PACS station by two independent radiologists (IvdS and BKV) who had information on the patient's state of consciousness and presence and location of focal deficits at time of the CT scan, which resembles the clinical situation, and who were blinded for the CTP and CTA results. Positive findings were ischemic changes not localized in the neurosurgical trajectory or around an intracerebral hematoma (ICH). Ischemic changes consisted of: hypodensities and loss of gray white matter differentiation. Consensus was reached for all images.

CTP scans were reconstructed at 5 mm contiguous axial images. Data were transferred to a Philips workstation for post processing. The CTP algorithm was based upon the central volume principle which is the most accurate for low injection rates of iodinated contrast material.¹³ CBF was calculated from CBV and MTT by the deconvolution method.¹⁴ CBV, CBF, and MTT color maps were interpreted visually (eyeballing) by two independent radiologists (JWD and IvdS), blinded for NCT and CTA results and for the clinical condition of the patient. Consensus reading was performed for discordant results. Positive findings were hypoperfused areas (lower CBV, higher MTT or lower CBF), indicating some degree of ischemia, that were not localized in the neurosurgical trajectory or around an ICH. No quantitative measurements were done in this study.

CTA scans were analyzed on a Philips workstation. The presence of vasospasm in both the proximal and distal (A1 and A2) segments of the anterior cerebral artery (ACA), the proximal and distal (M1 and M2) segments of the middle cerebral artery (MCA), the proximal and distal (P1 and P2) segments of the posterior cerebral artery (PCA), and the basilar artery was evaluated by two independent radiologists (JWD and IvdS), blinded for the NCT and CTP results, and for the clinical condition of the patient. Consensus reading was performed for discordant results. The degree of vasospasm was assessed by visual comparison of the admission and clinical deterioration images. We assumed that no vasospasm was present on the admission scan. Vasospasm was categorized in: 1) none: 0-25% decrease in vessel diameter at the time of clinical deterioration, 2) moderate: 26-50% decrease and 3) severe: >50% decrease.¹⁵ Positive findings were categorized in two ways: 1) any severe vasospastic vessel segments, 2) any moderate or severe segments.

Analysis

To evaluate the diagnostic value of NCT, CTP and CTA for DCI, two by two tables were made to calculate the sensitivity, specificity, negative predictive value (NPV), and positive predictive value (PPV) of the three modalities (with 95% confidence intervals calculated as Wilson score intervals¹⁶). From these values likelihood ratios graphs were created (*Figure 2*).¹⁷ These graphs are comparable to standard ROC-curves, which are designed to determinate the optimal diagnostic cut-off point of continuous variables. Since the determinants we used were not continuous but binary we used likelihood ratios graphs instead of ROC-curves. In these

graphs the difference in diagnostic quality of different tests (NCT, CTP, CTA) can be easily read by the relative position of their likelihood ratios graphs as explained in *Figure 2A*. This method takes into account all aspects (sensitivity, specificity, likelihood ratio of a negative test and likelihood ratio of a positive test) of differences in diagnostic quality, which is a great advantage over comparing areas under the ROC-curve, where only sensitivity and specificity are taken into account.

Results

42 patients met our inclusion criteria. Three patients were excluded because the images made at the time of clinical deterioration could not be evaluated due to motion artifacts. The characteristics of the 39 remaining patients and time of clinical deterioration are shown in *Table 1*.

25 patients were diagnosed with DCI and 14 patients were diagnosed with other causes for clinical deterioration than DCI. These causes were: progression of edema around an existing intracerebral hematoma (5 patients), the neurosurgical procedure (2 patients), rebleeding (2 patients), hydrocephalus (2 patients), and infectious/metabolic disturbance (3 patients).

The imaging findings of all patients are summarized in *Figure 1*. From the numbers in *Figure 1* sensitivities, specificities, NPV and PPV were calculated (*Table 2*) and likelihood ratios graphs were constructed (*Figure 2B*). *Figure 2B* shows that CTP has overall superior diagnostic quality for DCI compared to NCT and CTA, and NCT has overall superior diagnostic quality over CTA. Taking into account moderate vasospasm as well as severe vasospasm reduces the diagnostic quality of CTA for DCI compared to only severe vasospasm.

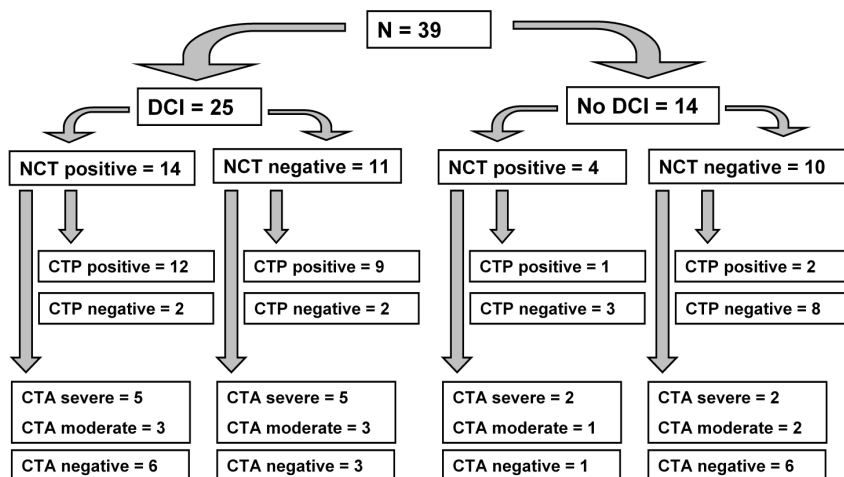


Figure 1 Flow chart of non-contrast CT (NCT), CT-perfusion (CTP), and CT-angiography (CTA) findings at the time of clinical deterioration in 25 patients with delayed cerebral ischemia (DCI) and 14 patients without DCI.

Table 1 Patient characteristics

	DCI	No DCI
Number of patients	25(64%)	14(36%)
Number of men	5(20%)	2(14%)
Median age (range)	54(32-77)	61(44-76)
Admission WFNS score		
1	9(36%)	3(21.5%)
2	10(40%)	2(14%)
3	1(4%)	2(14%)
4	3(12%)	4(29%)
5	2(8%)	3(21.5%)
Amount of blood (Hijdra score)		
Cisternal sum-score (median)	19	25*
1-10	5(20%)	3(21%)
11-20	9(36%)	2(14%)
21-30	11(24%)	8(57%)
Intraventricular sum-score (median)	2	5
0	9(36%)	2(14%)
1-12	16(64%)	11(79%)
Aneurysm location		
ACA	0(0%)	1(7%)
ACoA	14(56%)	4(29%)
Carotid Bifurcation	2(8%)	0(0%)
MCA	3(12%)	3(21.5%)
PCoA	5(20%)	1(7%)
PCA	0(0%)	1(7%)
VB	0(0%)	2(14%)
PICA	1(4%)	2(14%)
Intervention		
No	0(0%)	2(14%)
Coiling	16(64%)	6(43%)
Clipping	9(36%)	6(43%)
Median day of clinical deterioration after SAH (range)	6.0(1-17)	5.5(1-13)

DCI: delayed cerebral ischemia; ACA: anterior cerebral artery including pericallosal artery; ACoA: anterior communicating artery; PCoA: posterior communicating artery; MCA: middle cerebral artery; VB: vertebrobasilar artery; PICA: posterior inferior cerebellar artery

* Not evaluable in one case due to motion artifacts

Table 2 Sensitivity, specificity, positive predictive value (PPV) and negative predictive value (NPV) with 95% confidence intervals (95%CI: Wilson score interval¹⁶) for diagnosing delayed cerebral ischemia (DCI) of: positive findings on non-contrast CT (NCT), positive findings on CT-perfusion (CTP), moderate to severe vasospasm on CT-angiography (CTA), and severe vasospasm on CTA. CTP is overall superior to NCT and CTA.

	Sensitivity (95%CI)	Specificity (95%CI)	PPV (95%CI)	NPV (95%CI)
NCT	0.56 (0.37↔0.73)	0.71 (0.45↔0.88)	0.78 (0.55↔0.91)	0.48 (0.28↔0.68)
CTP	0.84 (0.65↔0.93)	0.79 (0.52↔0.92)	0.88 (0.69↔0.96)	0.73 (0.48↔0.89)
CTA moderate to severe spasm	0.64 (0.45↔0.80)	0.50 (0.27↔0.73)	0.70 (0.49↔0.84)	0.44 (0.23↔0.67)
CTA severe spasm	0.40 (0.23↔0.59)	0.71 (0.45↔0.88)	0.71 (0.45↔0.88)	0.40 (0.23↔0.45)

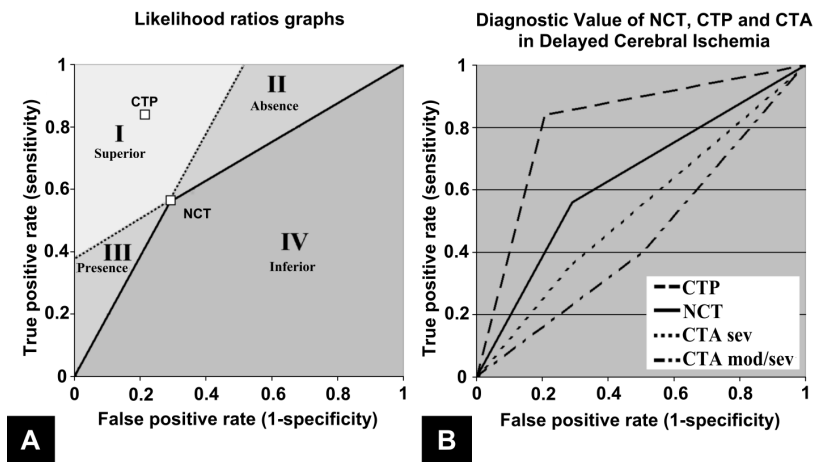


Figure 2 Comparing diagnostic values of non-contrast CT (NCT), CT-perfusion (CTP) and CT-angiography (CTA) with likelihood ratios graphs. These graphs are created by plotting “1 - specificities” (false-positive rate) against “sensitivities” (true-positive rate) and drawing lines through these points and the coordinates (0,0) and (1,1). The slope of the line through (0,0) is equal to the likelihood ratio of a positive test. Larger slopes indicate greater diagnostic ability. The slope of the line through (1,1) is equal to the likelihood ratio of a negative test. Smaller slopes indicate greater diagnostic ability: (A) regions of comparison: compared to NCT, a diagnostic test in region I (CTP) is superior overall, region II is superior for confirming absence of disease, region III is superior for confirming presence of disease, and region IV (both CTAs) is inferior overall. (B) Likelihood ratios graphs of NCT, CTP and CTA (sev = severe vasospasm; mod/sev = moderate to severe vasospasm).

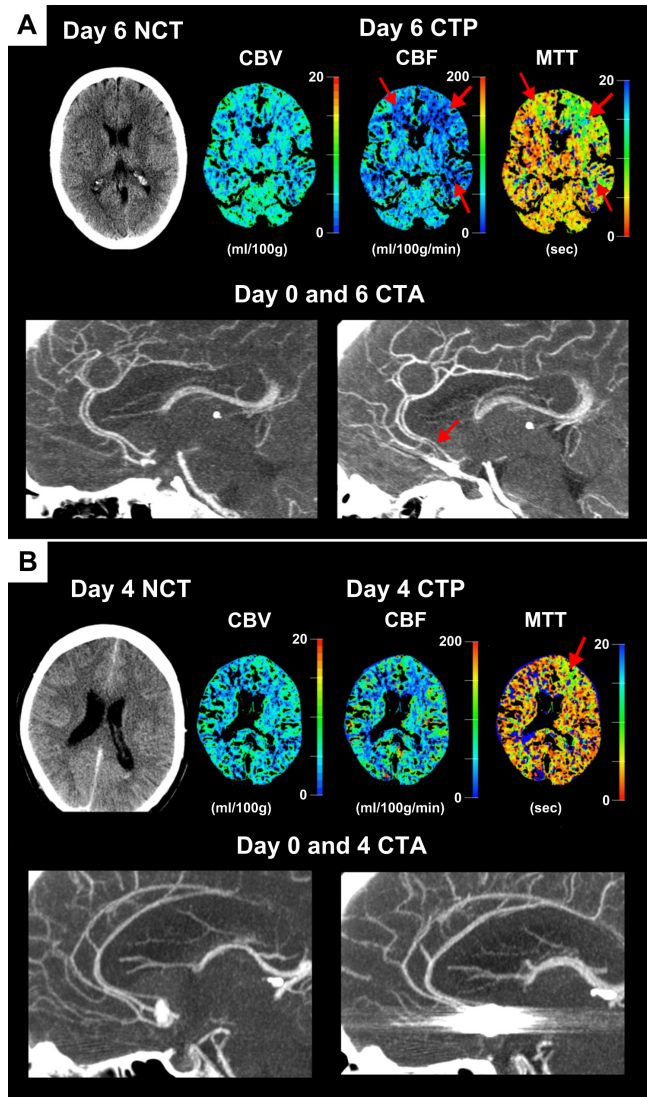


Figure 3 Example of non-contrast CT (NCT), CT-perfusion (CTP) and CT-angiography (CTA) findings in two patients with delayed cerebral ischemia (DCI): (A) 47 year old woman with clinical deterioration 6 days after subarachnoid hemorrhage (SAH) and: no ischemic changes on NCT; low perfusion in the flow territories of both anterior cerebral arteries (ACA) and the left middle cerebral artery on CTP (most visible on the MTT map); and vasospasm in the left ACA on CTA.

(B) 59 year old man with clinical deterioration 4 days after SAH and: no ischemic changes on NCT; areas of low perfusion in the flow territory of the left ACA on CTP (most visible on the MTT map); but no vasospasm on CTA.

For colorfigure see page 230

Discussion

In this study we used a qualitative interpretation of NCT, CTP color maps, and CTA to diagnose delayed cerebral ischemia (DCI) in SAH patients with clinical deterioration. Our results show that the diagnostic value of areas of low perfusion on CTP is superior to ischemic findings on NCT and far superior to vasospasm on CTA, in diagnosing DCI in SAH patients with clinical deterioration.

A positive diagnosis of DCI is clinically very relevant to guide treatment. Hyperdynamic therapy (hypertension, hypervolemia, hemodilution, or Triple-H) is frequently used to treat DCI. However, it has not equivocally been proven that hyperdynamic therapy improves neurological outcome, and the use of this therapy has been associated with an increased risk of severe complications.¹⁸ Therefore, physicians are quite reluctant to apply hyperdynamic therapy if the diagnosis is not certain. Certainty in the diagnosis DCI will increase with the large positive predictive value (0.88) of CTP, and in a much lesser extent with NCT and CTA.

Our results emphasize the known limitations of the diagnostic value of NCT in detecting early ischemia.² Of note is that the NCT at the time of deterioration was also part of our gold standard to define DCI, mainly to exclude rebleeding and hydrocephalus. The gold standard was furthermore based on clinical signs, blood analysis, and short term clinical follow up. However, we cannot rule out the possibility that ischemic lesions on the NCT were used to qualify the patient as having DCI. Therefore, incorporation bias may have caused an overestimation of the diagnostic value of NCT for DCI.

Our results also show that presence of vasospasm on CTA is not very helpful in diagnosing DCI. This confirms the findings of other investigators who showed that the positive predictive value of vasospasm for DCI is only 0.67.⁵ Although the degree of vasospasm is related to cerebral perfusion,^{3, 19, 20} presence of vasospasm does not mean that there is ischemia,¹⁹ and absence of vasospasm does not mean that there is no ischemia.^{3, 4, 20} Vasospasm may therefore not be the sole cause of DCI and using angiographic vasospasm as a gold standard for DCI may cause many missed cases of DCI in SAH patients with clinical deterioration.

Cerebral perfusion as seen on CTP reflects the net effect of all factors that contribute to the development of DCI. In stroke, CTP is already being used to show hypoperfused areas that are at risk for infarction.^{6, 7} Hypoperfused areas in SAH patients should in our opinion be interpreted in the same way. The false positive and false negative CTP findings in our results can be explained in the following ways. Firstly, false positive CTP findings can be a result of our definition of DCI in which we did not take into account that DCI could co-exist with other pathology. For example if no ischemic changes were seen on NCT and there clearly was other pathology that could cause clinical deterioration, like hydrocephalus, the deterioration was classified as other than DCI, whereas in fact DCI could have co-existed. This may have biased the results towards a lower diagnostic value of CTP. Secondly, false negative findings can be a result of the limited brain coverage with 64-slice CTP when abnormalities are outside of the scanned area. Scanners with

an increased detector range are currently coming on the market. False negative CTP findings can also result from the fact that CTP color maps were interpreted without knowledge of clinical condition. A radiologist will generally find more abnormalities when knowing what to look for. In contrast to this, information about the patient's state of consciousness and presence and location of focal deficits was available for the interpretation of NCT images.

Some limitations of our study should be considered.

Firstly, we did not use hypodensities on follow up imaging as an obligatory criterion for DCI. Although hypodensities on follow up may prove that ischemia has occurred, one can not be sure at what time point this has occurred. Also, the absence of hypodensities does not rule out the possibility that DCI has occurred; the hypoperfused areas on CTP or vasospasm on CTA may have been only transient,²¹ either because the patient received treatment or because it spontaneously resolved. We have seen patients with large perfusion deficits at the time of deterioration that resolved and left no hypodensities on follow up imaging. These aspects make follow up imaging less relevant when looking for a diagnostic tool to identify the cause of deterioration in SAH patients. Another limitation concerns the use of dynamic imaging techniques in the studied population. SAH patients are often restless, which can result in suboptimal images. Two patients were excluded for this reason.

One of our goals was to see whether CTP could be helpful in diagnosing DCI at time of clinical deterioration. Although the sample size of our study was relatively small, the current results show that CTP may indeed be a useful diagnostic tool in diagnosing DCI. However, before CTP can be implemented in clinical practice generalisability, including interobserver variability, and feasibility should be assessed. Finally, although our qualitative approach seems to be sufficient in identifying perfusion defects, future research should focus on calculating quantitative threshold values from CTP data, which will also make it possible to assess the effects of DCI treatment.

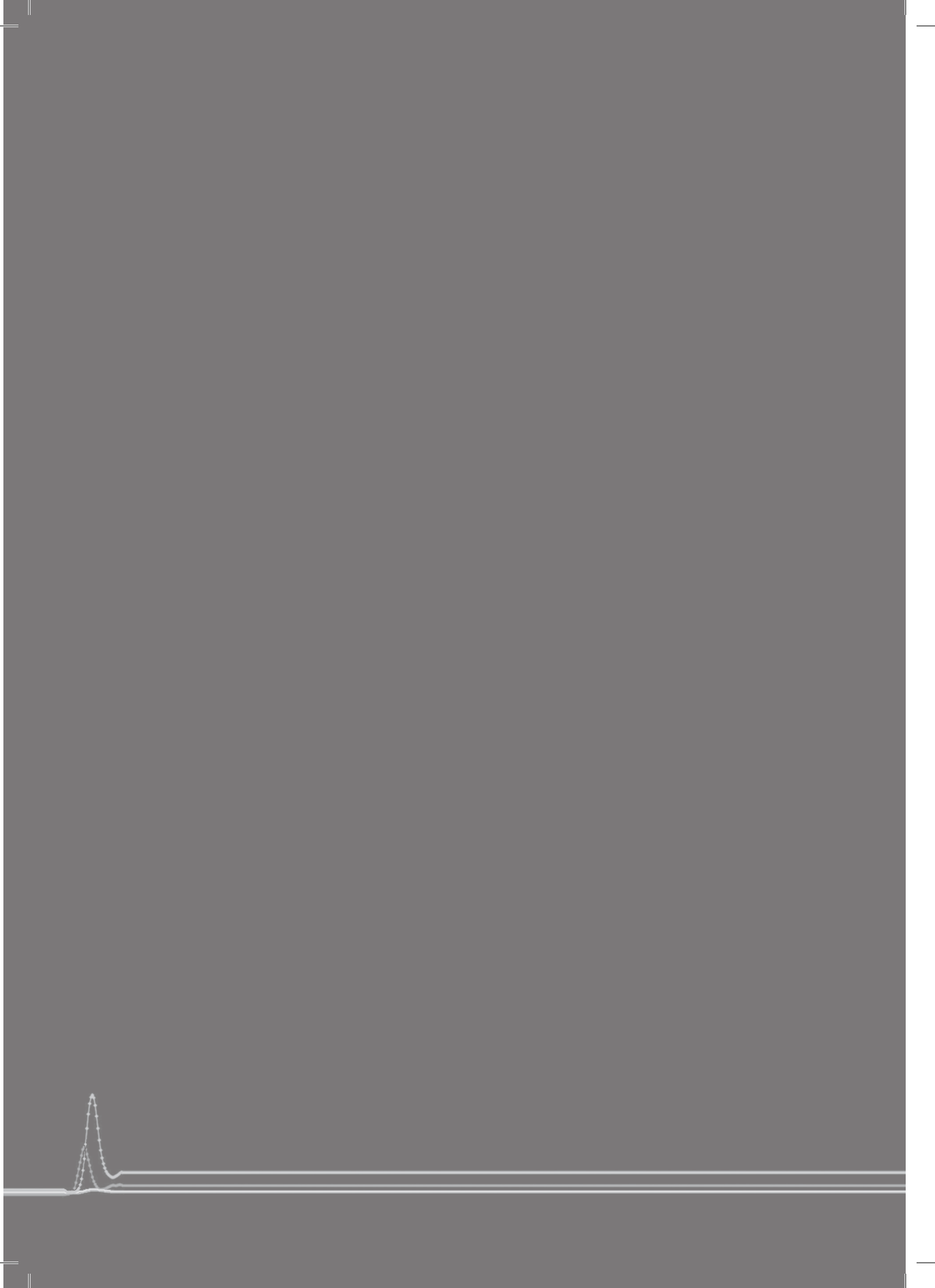
Conclusion

We evaluated several CT imaging modalities to add more certainty to the uncertain diagnosis of DCI at the time of clinical deterioration. According to our results CTP has superior diagnostic value compared to NCT and CTA. We therefore strongly suggest that future research on DCI should not focus on angiographic vasospasm but rather on perfusion abnormalities in combination with clinical findings. CTP can render a fast diagnosis of DCI, which could help the physician in his decision making and in guiding treatment.

References

1. van Gijn J, Kerr RS, Rinkel GJ. Subarachnoid haemorrhage. *Lancet*. 2007;369:306-318
2. Camargo EC, Furie KL, Singhal AB, Roccatagliata L, Cunnane ME, Halpern EF, Harris GJ, Smith WS, Gonzalez RG, Koroshetz WJ, Lev MH. Acute brain infarct: Detection and delineation with ct angiographic source images versus nonenhanced ct scans. *Radiology*. 2007;244:541-548
3. Aralasmak A, Akyuz M, Ozkaynak C, Sindel T, Tuncer R. Ct angiography and perfusion imaging in patients with subarachnoid hemorrhage: Correlation of vasospasm to perfusion abnormality. *Neuroradiology*. 2009;51:85-93
4. Binaghi S, Colleoni ML, Maeder P, Uske A, Regli L, Dehdashti AR, Schnyder P, Meuli R. Ct angiography and perfusion ct in cerebral vasospasm after subarachnoid hemorrhage. *AJNR AmJNeuroradiol*. 2007;28:750-758
5. Rabinstein AA, Friedman JA, Weigand SD, McClelland RL, Fulgham JR, Manno EM, Atkinson JL, Wijedicks EF. Predictors of cerebral infarction in aneurysmal subarachnoid hemorrhage. *Stroke*. 2004;35:1862-1866
6. Parsons MW, Pepper EM, Bateman GA, Wang Y, Levi CR. Identification of the penumbra and infarct core on hyperacute noncontrast and perfusion ct. *Neurology*. 2007;68:730-736
7. Wintermark M, Flanders AE, Velthuis B, Meuli R, van LM, Goldsher D, Pineda C, Serena J, van der Schaaf I, Waaijer A, Anderson J, Nesbit G, Gabriely I, Medina V, Quiles A, Pohlman S, Quist M, Schnyder P, Bogouslavsky J, Dillon WP, Pedraza S. Perfusion-ct assessment of infarct core and penumbra: Receiver operating characteristic curve analysis in 130 patients suspected of acute hemispheric stroke. *Stroke*. 2006;37:979-985
8. Harrod CG, Bendok BR, Batjer HH. Prediction of cerebral vasospasm in patients presenting with aneurysmal subarachnoid hemorrhage: A review. *Neurosurgery*. 2005;56:633-654
9. Pham M, Johnson A, Bartsch AJ, Lindner C, Mullges W, Roosen K, Solymosi L, Bendszus M. Ct perfusion predicts secondary cerebral infarction after aneurysmal subarachnoid hemorrhage. *Neurology*. 2007;69:762-765
10. Hijdra A, Brouwers PJ, Vermeulen M, van GJ. Grading the amount of blood on computed tomograms after subarachnoid hemorrhage. *Stroke*. 1990;21:1156-1161
11. Wintermark M, Thiran JP, Maeder P, Schnyder P, Meuli R. Simultaneous measurement of regional cerebral blood flow by perfusion ct and stable xenon ct: A validation study. *AJNR AmJNeuroradiol*. 2001;22:905-914
12. Yoon DY, Choi CS, Kim KH, Cho BM. Multidetector-row ct angiography of cerebral vasospasm after aneurysmal subarachnoid hemorrhage: Comparison of volume-rendered images and digital subtraction angiography. *AJNR AmJNeuroradiol*. 2006;27:370-377
13. Wintermark M, Maeder P, Thiran JP, Schnyder P, Meuli R. Quantitative assessment of regional cerebral blood flows by perfusion ct studies at low injection rates: A critical review of the underlying theoretical models. *Eur Radiol*. 2001;11:1220-1230
14. Axel L. Tissue mean transit time from dynamic computed tomography by a simple deconvolution technique. *Invest Radiol*. 1983;18:94-99
15. Voldby B, Enevoldsen EM, Jensen FT. Regional cbf, intraventricular pressure, and cerebral metabolism in patients with ruptured intracranial aneurysms. *JNeurosurg*. 1985;62:48-58
16. Brown LD CT, DasGupta A Interval estimation for a binomial proportion. *Statistical Science*. 2001;16:101-133

17. Biggerstaff BJ. Comparing diagnostic tests: A simple graphic using likelihood ratios. *Stat Med.* 2000;19:649-663
18. Sen J, Belli A, Albon H, Morgan L, Petzold A, Kitchen N. Triple-h therapy in the management of aneurysmal subarachnoid haemorrhage. *Lancet Neurol.* 2003;2:614-621
19. Sviri GE, Britz GW, Lewis DH, Newell DW, Zaaroor M, Cohen W. Dynamic perfusion computed tomography in the diagnosis of cerebral vasospasm. *Neurosurgery.* 2006;59:319-325
20. Wintermark M, Dillon WP, Smith WS, Lau BC, Chaudhary S, Liu S, Yu M, Fitch M, Chien JD, Higashida RT, Ko NU. Visual grading system for vasospasm based on perfusion ct imaging: Comparisons with conventional angiography and quantitative perfusion ct. *Cerebrovasc Dis.* 2008;26:163-170
21. Nabavi DG, LeBlanc LM, Baxter B, Lee DH, Fox AJ, Lownie SP, Ferguson GG, Craen RA, Gelb AW, Lee TY. Monitoring cerebral perfusion after subarachnoid hemorrhage using ct. *Neuroradiology.* 2001;43:7-16



Diagnostic threshold values of cerebral perfusion measured with CT for delayed cerebral ischemia after aneurysmal subarachnoid hemorrhage



6

*J.W. Dankbaar, N.K. de Rooij, M. Rijdsijk, B.K. Velthuis, C.J.M. Frijns,
G.J.E. Rinkel, I.C. van der Schaaf*

Accepted for publication in Stroke 2010

Abstract

Background and purpose

Delayed cerebral ischemia (DCI) after aneurysmal subarachnoid hemorrhage (SAH) is difficult to diagnose. We analyzed diagnostic threshold values of CT-perfusion (CTP) for DCI in SAH patients.

Methods

We prospectively enrolled 136 SAH patients with CTP on admission and at the time of clinical deterioration or after one week if no deterioration occurred. The gold standard was the clinical diagnosis DCI, based on all clinical, laboratory and imaging data, except CTP. Patients with failed imaging (n=6) and other causes of deterioration (n=45) were excluded for the current study. CTP values (cerebral blood volume (CBV) and -flow (CBF), mean transit time (MTT), and time to peak (TTP)) were measured in pre-defined regions of interest. For patients with and without DCI, we compared absolute perfusion and perfusion asymmetry (relative perfusion). Diagnostic threshold values for DCI were evaluated using receiver operating characteristics (ROC) curves. Sensitivity and specificity were calculated for optimal thresholds.

Results

Of the remaining 85 patients, 50 had DCI and 35 had no clinical deterioration (reference group). CBF was significantly lower, MTT higher, and perfusion asymmetry larger in DCI patients. Largest absolute MTT, and interhemispheric MTT difference had areas under the ROC curves >0.75 and are therefore considered good diagnostic tests. Optimal threshold values were: MTT 5.9 seconds with a sensitivity of 0.70(95%CI: 0.62-0.74), specificity=0.77(0.67-0.81); MTT difference 1.1 seconds with a sensitivity of 0.80(95%CI: 0.72-0.83), specificity=0.63(0.54-0.69).

Conclusion

Thresholds for absolute MTT values and interhemispheric MTT differences have good diagnostic properties to distinguish patients with DCI from clinically stable patients.

Introduction

Delayed cerebral ischemia (DCI) is a severe and frequent complication of aneurysmal subarachnoid hemorrhage (SAH). It typically occurs in the first two weeks after the initial hemorrhage and increases the risk of poor outcome in patients that survive the first days.¹ The onset of DCI is characterized by a gradual decrease in consciousness, new focal deficit or both. The clinical course of the symptoms and CT evaluation one or more days after onset of symptoms are often helpful in ruling DCI in or out. Establishing the diagnosis one or more days after onset is however not meaningful if treatment decisions need to be made. For these decisions diagnosing DCI early in its course is pivotal but notoriously difficult, since the onset of DCI is often insidious and there is a long list of other causes of deterioration. Increasing edema around a parenchymal hematoma (PH), rebleeding from the aneurysm, (increasing) hydrocephalus, cardiac insufficiency, pulmonary edema, infection, and metabolic disturbances may also cause a decrease in consciousness or focal deficit, and thus mimic DCI. When clinical deterioration occurs, a non-contrast CT scan (NCT) is routinely performed to rule out intracerebral causes other than DCI. However, NCT is not very sensitive in detecting early ischemia.² The presence of cerebral vasospasm identified with transcranial Doppler, digital subtraction angiography (DSA) or CT-angiography (CTA) is frequently used to confirm DCI. Presence of vasospasm however does not prove the presence of ischemia,³ and absence of vasospasm does not rule out ischemia.^{4, 5} Better diagnostic tests in the acute stage of deterioration, possibly caused by DCI, are therefore needed.

In ischemic stroke patients CT-perfusion (CTP) is an established tool to detect early ischemia.^{6, 7} In SAH patients CTP has recently been shown to be promising for this purpose.² Absolute threshold values would simplify the detection of DCI, but these values are not yet available.

The purpose of this study was to assess absolute and relative (interhemispheric ratios and differences) threshold values of CTP parameters for the diagnosis of DCI in SAH patients.

Methods

Design

In our hospital all patients with SAH routinely undergo non-contrast CT (NCT), CTP, and CT-angiography (CTA) on admission to evaluate the presence and configuration of aneurysms, and at the time of deterioration to identify the cause of deterioration. We prospectively enrolled all SAH patients admitted to our hospital between May 2007 and September 2009 who met the following inclusion criteria: (a) 18 years of age or older, (b) aneurysmal cause of SAH, (c) admitted within 72 hours after SAH, (d) written informed consent.

Patients without clinical deterioration underwent NCT and CTP about one week after admission. No CTA was performed in these clinically stable patients to limit the radiation dose. Patients with impaired renal function (Creatinine > 200 $\mu\text{mol/l}$) or other contra-indications for contrast enhanced CT-scans, including

pregnancy, were excluded. Included patients with a clinical deterioration during their clinical course from other causes than DCI were excluded from further analyses. Patients without clinical deterioration served as a reference group (no-DCI). For all included patients we recorded age, gender, clinical status on admission (according to the World Federation of Neurological Surgeons (WFNS) scale²), amount of blood on the admission scan (Hijdra score⁸), aneurysm location and treatment, and in patients with clinical deterioration presence of angiographic vasospasm on CTA. The study was approved by our hospital's ethics committee. All patients were treated according to the SAH treatment protocol of our hospital, consisting of absolute bed rest until aneurysm treatment, oral nimodipine, cessation of antihypertensive medication, intravenous administration of fluid aiming for normovolemia, and regular assessment of clinical status.

DCI

For the purpose of the study, the diagnosis of delayed cerebral ischemia (DCI) in patients who experienced clinical deterioration (decreased Glasgow coma scale (GCS) of at least 2 points lasting more than 2 hours, or a new focal deficit) was assessed after completion of the clinical course. This was based on prospectively collected data by two neurologists (NKR and CJMF) as described previously.² The two neurologists had full access to all clinical information concerning the patient's entire clinical course, both before and after clinical deterioration, all laboratory results, and all NCTs, but were blinded for the CTP. The NCTs were used to show ischemic changes, exclude rebleeding, hydrocephalus, edema around a hematoma and postoperative swelling. The clinical information and laboratory results were used to exclude infection or metabolic disturbances as a cause of the deterioration.

Imaging protocol

CTP imaging is an accurate technique to calculate information on cerebral blood volume (CBV), cerebral blood flow (CBF), mean transit time (MTT), and time to peak (TTP).⁹ CTA can be used to accurately detect vasospasm.¹⁰ Imaging studies were executed on a 16 slice or 64 slice spiral CT scanner (Philips Mx8000 LDT, Best, the Netherlands) using previously published scanning protocols.² The CTP scan covered a 2.4 to 4 cm slab selected at the level of the basal ganglia. The additional radiation dose from a the research scanning protocol (CTP and NCT) was about 3 mSv.¹¹

Image post-processing and evaluation

CTP scans were reconstructed at 6 mm (16-slice) and 5 mm (64 slice) contiguous axial images. Absolute perfusion maps of CBV, CBF, MTT and TTP were calculated using commercially available Philips software (Extended Brilliance Workspace 3.x). On all follow up scans perfusion was measured in regions of interest (ROIs) that were drawn by hand bilaterally in the cortical gray matter and the basal ganglia of the flow territories of the anterior and middle cerebral artery at the level of the basal ganglia (*Figure 1*). If a parenchymal hemorrhage was present at that level a slice just above that level was chosen. All ROIs were drawn by one of two



Figure 1 Regions of interest drawn by hand bilaterally in the cortical gray matter and basal ganglia of the flow territories of the anterior and middle cerebral artery.

observers blinded for the clinical condition and CTA images of the patient (MR, JWD). The flow territory of the posterior cerebral artery was not included in this study due to the high variability in quantitative values caused by partial volume effects of large veins in this region and inconsistent availability of this region in the scanned brain slab.

In patients with clinical deterioration, CTA scans were evaluated for the presence of vasospasm on a Philips workstation by comparison to the admission scan. Vasospasm was assessed in the proximal and distal segments of the anterior, middle and posterior cerebral artery, and the basilar artery, and categorized in: 1) none: 0-25% decrease in vessel diameter, 2) moderate: 26-50% decrease and 3) severe: >50% decrease.¹² For each patient the most severe spasm was noted.

Analysis

In all analyses we compared patients with DCI to clinically stable patients (no-DCI). For the analysis of absolute CTP threshold values we selected the ROI with the lowest absolute values of CBV and CBF and highest absolute values of MTT and TTP (reflecting the least perfused flow territories) in each patient. Since absolute perfusion values can be influenced by observer-dependent post processing steps¹³ we also used relative measurements. For each ROI we calculated inter-hemispheric ratios (lowest to highest) for CBV, CBF, and interhemispheric differences (highest minus lowest) for MTT and TTP for all ROIs. For each patient, the lowest (closest to zero) CBV and CBF ratio, and the largest MTT and TTP difference (reflecting the largest asymmetry in perfusion between both hemispheres) were selected. Since both absolute and relative values were not normally distributed, the median and the interquartile range for each parameter were calculated. The

values of DCI and no-DCI patients were compared using the Mann Whitney U test. To obtain diagnostic threshold values of perfusion, we used receiver-operator characteristic (ROC) curves. These curves were made for absolute values of the least perfused ROI and for the relative values of the ROI with the largest perfusion asymmetry (ratio closest to zero or largest difference). An area under the curve of more than 0.75 is considered to be a good test.¹⁴ From the ROC curve, we derived optimal threshold values to distinguish between patients with and without DCI by seeking the best trade off between highest possible sensitivities and specificities of the threshold values. For the sensitivity and specificity of the optimal threshold value a 95% Wilson score interval was calculated. Sensitivity and specificity were used to create likelihood ratios graphs which make it possible to visually compare all diagnostic properties of a test.¹⁵

Results

136 patients were enrolled in the study, of which six were excluded because the follow up images could not be evaluated due to motion artifacts. Of the remaining 130 patients 50 had DCI; 35 patients remained clinically stable and served as our reference group (no-DCI); and 45 patients were excluded from further analyses because the cause of clinical deterioration was not DCI but: progression of edema around an existing intracerebral hematoma (8), the neurosurgical/coiling procedure (15), rebleeding (3), hydrocephalus (9), severe infectious/metabolic disturbance (8), epilepsy (1), and increasing subdural hygroma (1).

The patient characteristics of the 50 DCI patients and the 35 no-DCI patients are shown in *Table 1*. Of all patients with DCI 66% had moderate or severe vasospasm in one or more vessel segments on CTA.

The median absolute (ROIs with lowest CBF and CBV and highest MTT and TTP) and relative (lowest CBF and CBV ratios and largest MTT and TTP differences between hemispheres) CTP values with their interquartile ranges for patients with and without DCI are summarized in *Table 2*. CBF was significantly lower and MTT significantly higher in DCI patients ($p < 0.05$). Perfusion asymmetries were significantly larger in DCI patients (smaller CBV and CBF ratios and larger MTT and TTP differences, $p < 0.05$).

The ROC curves of lowest CBF and CBV and highest MTT and TTP per patient are shown in *Figure 2A*. The ROC curves of lowest interhemispheric CBV and CBF ratios and largest interhemispheric MTT and TTP differences are shown in *Figure 2B*. The optimal threshold values for diagnosing DCI extracted from the ROC curves (*Figure 2A and 2B*) were used to create likelihood ratios graphs (*Figure 2C and 2D*). The areas under the ROC curves and the optimal threshold values with their sensitivity and specificity are shown in *Table 3*. Largest absolute MTT, and largest MTT and TTP difference had AUCs larger than 0.75 and can therefore be considered to be a good diagnostic test. The threshold for absolute MTT and MTT differences had the best diagnostic properties (*Figure 2D*).

Figure 3 shows an example of how the MTT difference threshold can be applied to make perfusion abnormalities more easily visible in an SAH patient with reversible and irreversible areas of DCI.

Table 1 Patient characteristics

	DCI	No DCI
Number of patients	50	35
Number of men	12 (24%)	12 (34%)
Median age (range)	55 (26-81)	57 (18-79)
Admission WFNS score		
1	12 (24%)	25 (71.5%)
2	17 (34%)	4 (11%)
3	4 (8%)	0 (0%)
4	10 (20%)	6 (17.5%)
5	7 (14%)	0 (0%)
Amount of blood (Hijdra score)		
Cisternal sum-score (median)	19	15
1-10	11 (22%)	11 (31%)
11-20	17 (34%)	16 (46%)
21-30	22 (44%)	8 (23%)
Intraventricular sum-score (median)	2	2
0-2	26 (52%)	24 (69%)
2-12	24 (48%)	11(31%)
Aneurysm location		
anterior cerebral artery	2 (4%)	2 (6%)
anterior communicating artery	19 (38%)	11 (31%)
carotid bifurcation	8 (16%)	4 (11%)
middle cerebral artery	8 (16%)	10 (29%)
posterior communicating artery	9 (18%)	5 (14%)
vertebrobasilar artery	1 (2%)	1 (3%)
posterior inferior cerebellar artery	3 (6%)	2(6%)
Aneurysm treatment		
No	0 (0%)	1 (3%)
Coiling	27 (54%)	14 (40%)
Clipping	23 (46%)	20 (57%)
Vasospasm (% luminal narrowing)		
in one or more vessel segments		
0-25%	17 (34%)	*
26-50%	13 (26%)	*
> 50%	20 (40%)	*
Median day after SAH (range) of clinical deterioration/follow up scan	6 (1-15)	7 (3-14)

*In clinically stable patients no CTA was performed to minimize the additional radiation dose.

Table 2 Median values and p-value (Mann-Whitney U test) of differences between patients with and without delayed cerebral ischemia (DCI) of absolute (ROIs with lowest CBF (Cerebral Blood Flow) and Cerebral Blood Volume (CBV) and highest Mean Transit Time (MTT) and Time to Peak (TTP)) and relative (lowest CBF and CBV ratios and largest MTT and TTP differences between hemispheres).

	Median (interquartile range 25-75%)		
	DCI	No DCI	p-value
CBV (ml/100g)	2.77 (2.32-3.32)	2.85 (2.52-3.31)	0.262
CBF (ml/100g/min)	30.6 (20.7-37.6)	38.4 (31.2-45.4)	0.001
MTT (sec)	6.65 (5.62-8.75)	5.34 (4.51-5.62)	<0.001
TTP (sec)	26.5 (22.6-29.7)	24.3 (23.1-26.6)	0.119
CBV ratio	0.74 (0.63-0.84)	0.82 (0.71-0.87)	0.031
CBF ratio	0.67 (0.45-0.77)	0.78 (0.69-0.84)	0.001
MTT difference (sec)	1.91 (1.10-3.89)	0.96 (0.67-1.47)	<0.001
TTP difference (sec)	1.34 (0.80-2.89)	0.70 (0.47-1.22)	<0.001

Table 3 Sensitivity and specificity with 95% confidence intervals (95%CI) of optimal CTP threshold values for diagnosing delayed cerebral ischemia.

	AUC (95%CI)	Threshold	Sensitivity (95%CI)	Specificity (95%CI)
CBV (ml/100g)	0.57 (0.45 ↔ 0.70)	2.78	0.52 (0.45 ↔ 0.58)	0.63 (0.54 ↔ 0.69)
CBF (ml/100g/min)	0.71 (0.60 ↔ 0.82)	36.3	0.74 (0.66 ↔ 0.78)	0.63 (0.54 ↔ 0.69)
MTT (sec)	0.76 (0.66 ↔ 0.86)	5.85	0.70 (0.62 ↔ 0.74)	0.77 (0.67 ↔ 0.81)
TTP (sec)	0.60 (0.48 ↔ 0.72)	25.2	0.54 (0.47 ↔ 0.60)	0.63 (0.54 ↔ 0.69)
CBV ratio	0.64 (0.52 ↔ 0.76)	0.80	0.64 (0.57 ↔ 0.69)	0.63 (0.54 ↔ 0.69)
CBF ratio	0.72 (0.61 ↔ 0.83)	0.77	0.76 (0.68 ↔ 0.80)	0.63 (0.54 ↔ 0.69)
MTT difference (sec)	0.78 (0.68 ↔ 0.87)	1.08	0.80 (0.72 ↔ 0.83)	0.63 (0.54 ↔ 0.69)
TTP difference (sec)	0.75 (0.65 ↔ 0.86)	0.99	0.70 (0.62 ↔ 0.74)	0.66 (0.57 ↔ 0.72)

CBV = Cerebral Blood Volume; CBF = Cerebral Blood Flow; MTT = Mean Transit Time; TTP = Time to Peak

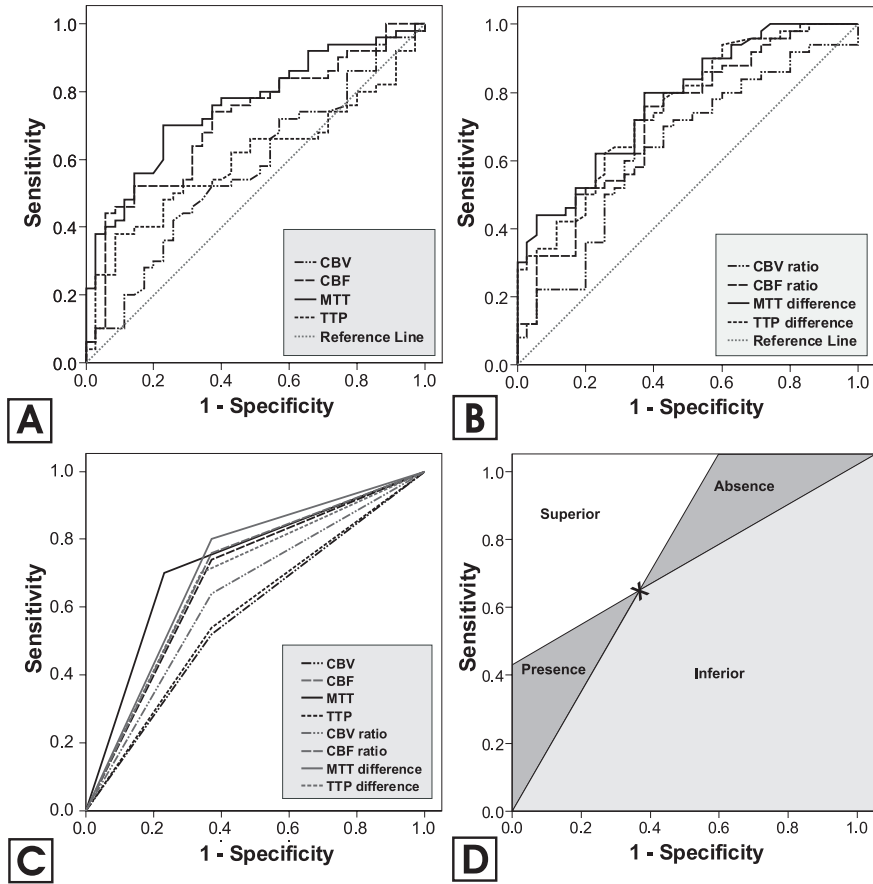


Figure 2 Receiver Operating Characteristics (ROC) Curves of absolute (A) and relative (B) CTP values. (C) Likelihood ratios graphs created from the optimal threshold values extracted from A and B. (D) diagnostic test qualities of a diagnostic test (superior in showing absence or presence of disease or superior or inferior overall quality) in different areas relative to a test X.

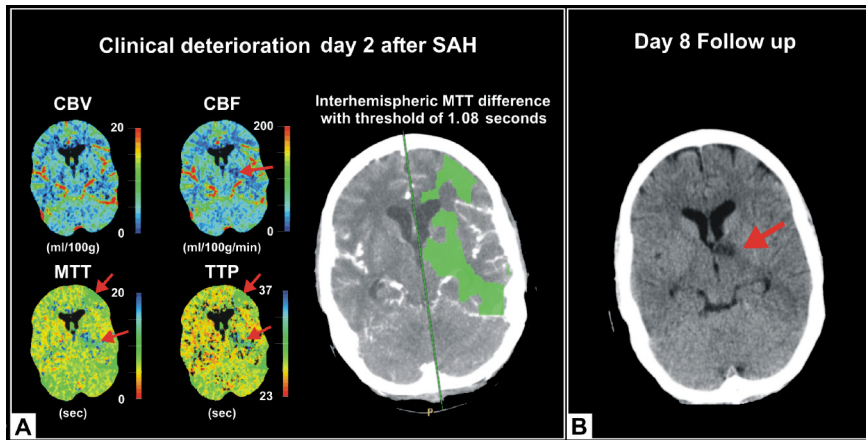


Figure 3 A 51 year old woman who developed dysphasia and a right sided paresis two days after aneurysmal subarachnoid hemorrhage (SAH). The deterioration was eventually diagnosed as delayed cerebral ischemia (DCI). (A) The CBF, MTT and TTP map at time of the clinical deterioration show a small perfusion defect in the left internal capsule. The MTT and TTP map furthermore show subtle abnormalities in the left frontal region. Applying the MTT difference threshold shows the perfusion asymmetries more clearly. The patient was not treated with hypertensive treatment. (B) On the follow up non-contrast CT 6 days later (day 8 after hemorrhage) permanent infarction is seen in the internal capsule but not in the anterior frontal region, indicating that the ischemia has partially resolved.

CBV = cerebral blood volume; CBF = cerebral blood flow; MTT = mean transit time; TTP = time to peak.

For colorfigure see page 231

Discussion

We assessed absolute and relative (interhemispheric ratios and differences) CT-perfusion threshold values to discriminate between patients with DCI and clinically stable patients (no-DCI). Patients with DCI had significantly larger perfusion asymmetry, lower CBF and longer MTT than no-DCI patients. MTT showed the best diagnostic values for DCI with highest areas under the ROC curve for both absolute and relative MTT measurements.

In agreement with previous studies,^{3,16} our results show that there are differences in cerebral perfusion and perfusion asymmetry between patients with DCI and clinically stable patients. Differences between the two groups are however not adequate enough for diagnostic purposes in the individual patient. The threshold values presented in this paper can distinguish DCI patients from clinically stable patients and are an important step towards individual diagnostics, necessary to guide treatment. Thresholds for absolute and relative MTT had the best diagnostic properties while CBV had the worst properties. Apparently, MTT abnormalities occur in DCI patients with CBV remaining relatively stable and almost equal to the CBV in no-DCI patients. This is comparable to the penumbral tissue in acute ischemic stroke indicating that the ischemia may still be reversible in the measured area.^{6,7} The fact that CBV is not increased in the presence of a prolonged MTT is

compatible with disturbed cerebral autoregulation in DCI patients.¹⁷ Overall relative threshold values had better diagnostic properties than absolute measurements. The reason for this may be that relative measurements reduce the variability caused by (observer-dependent) post-processing steps.¹³ Determining threshold values with good diagnostic properties for DCI in SAH patients is quite challenging. Firstly, perfusion measurements may be blurred by other pathological conditions inherent to SAH and SAH treatment.^{18, 19} Although these conditions were not the cause of deterioration in our DCI group, the presence of hydrocephalus, parenchymal hemorrhage, temporary vessel occlusion during surgical or angiographic interventions, and edema may have affected cerebral perfusion in addition to DCI. Secondly, the duration and extent of DCI most likely influences our results. DCI can be transient and multifocal.^{20, 21} For example, in some patients the neurological condition was already improving at the time of scanning and thus perfusion deficits may have diminished. Also, some of our patients had visually apparent bilateral ischemia on CTP resulting in less asymmetry than in patients with unilateral ischemia. In these patients the absolute threshold values may be more useful, indicating that both threshold values should always be applied for optimal results. Thirdly, we performed measurements of perfusion in pre-defined regions of interest. This is necessary to objectively test the diagnostic ability of CTP and minimize observer bias. However, differences may be less conspicuous due to perfusion measurements not being centered to the ischemic area. Selecting the region of interest in visible areas of hypoperfusion would probably result in better diagnostic performance. Studies reporting on absolute perfusion measured in visually selected ROIs showed lower CBF and higher MTT values than reported in our study.^{3, 16} A recent study using only visual assessment of CTP color maps without absolute or relative measurements found a positive and negative predictive value of 0.88 and 0.73 for DCI in a population of SAH patients with clinical deterioration.² However, interpreting CTP color maps in SAH patients requires experienced readers, which reduces generalisability and usage during out-of-office hours. The presented diagnostic thresholds may simplify the diagnosis (*Figure 3*). The color coded map in *Figure 3*, indicating DCI based on thresholds for relative MTT measurements, could be used in future research to see if other pathology causing decreased perfusion can be distinguished from DCI by visual interpretation. In this way objective measurements and knowledge on clinical condition and features can be combined. Furthermore, future research is needed to assess whether DCI can be identified before symptoms occur, to predict whether ischemia at the time of deterioration is reversible or will lead to permanent infarction, and to study the influence of therapeutic interventions on tissue fate.

There are some issues to our study that need further explanation.

Since all patients with other causes for deterioration than DCI were excluded we could not calculate predictive values from our threshold values. Moreover, the absolute and relative values of perfusion overlap considerably between DCI and no-DCI patients in our population. For any chosen threshold value there will thus be a considerable number of false positive and false negative measurements.

These problems regarding the practical application of perfusion values have also been described in ischemic stroke where identification of the ischemic penumbra (salvageable brain tissue) is the main goal. Reported optimal threshold values for the penumbra vary widely and are not yet generally applicable.²² Clearly, our threshold values will also need to be validated and tested for reproducibility in another series of patients including all patients with serious co-morbidity.

Another issue is that our gold standard for DCI did not require the presence of hypodensities on follow up imaging. We thereby identified all patients with symptomatic ischemia and not just patients with ischemia that turns into permanent infarction. The absence of hypodensities does not rule out the possibility that DCI has occurred, since the hypoperfusion may have been transient,²⁰ due to treatment or spontaneous resolution. The lack of performing CTA to assess the presence of vasospasm in patients without clinical deterioration might be considered a weakness of our study. However, in our opinion presence of vasospasm is not relevant in the absence of clinical symptoms.²

The use of CTP for the evaluation of DCI results in an additional exposure to radiation ranging between 1.1 to 5.0 mSv, depending on the used parameters.²³ An effective dose of 5 mSv results in an additional risk of cancer of 0.025% compared to unexposed individuals.²³ However, since diagnosing DCI with CTP facilitates adequate treatment of DCI, resulting in reduced mortality and morbidity,¹ this additional risk may be justified.²⁴ Perfusion imaging with MRI is possible without radiation²⁵ but less suited for intensive care patients, slower, more expensive, and less available outside regular working hours.

Conclusion

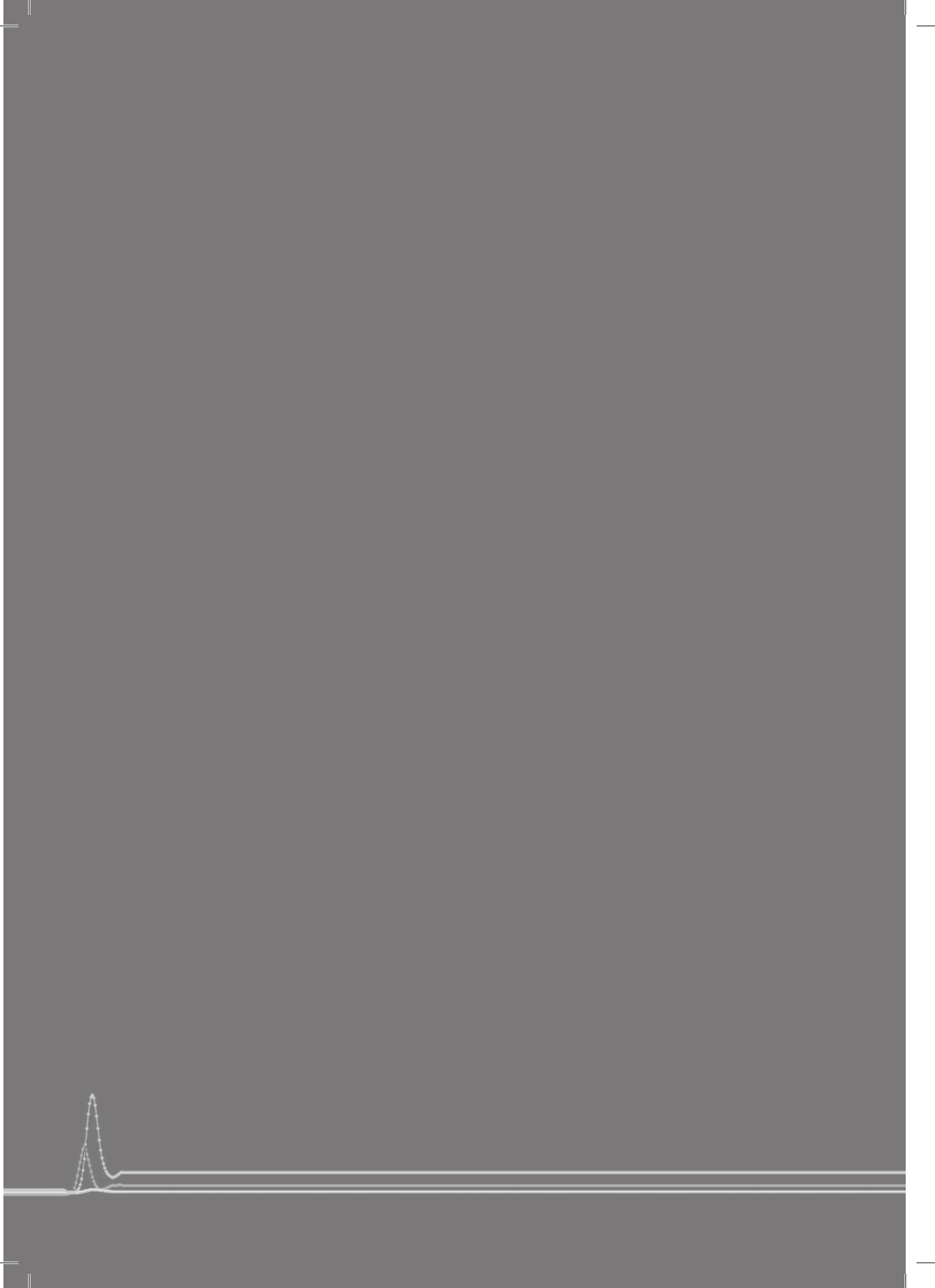
DCI patients have larger perfusion asymmetry and decreased absolute perfusion than patients with no deterioration after SAH. Threshold values of absolute and relative perfusion measurements in SAH patients can be used to diagnose DCI. Absolute MTT values and interhemispheric MTT differences have good diagnostic properties to distinguish patients with DCI from clinically stable patients.

The presented threshold values are an important step towards individualized diagnostics of DCI in SAH patients, but require further validation.

References

1. van Gijn J, Kerr RS, Rinkel GJ. Subarachnoid haemorrhage. *Lancet*. 2007;369:306-318
2. Dankbaar JW, de Rooij NK, Velthuis BK, Frijns CJ, Rinkel GJ, van der Schaaf IC. Diagnosing delayed cerebral ischemia with different ct modalities in patients with subarachnoid hemorrhage with clinical deterioration. *Stroke*. 2009;40:3493-3498
3. Sviri GE, Britz GW, Lewis DH, Newell DW, Zaaroor M, Cohen W. Dynamic perfusion computed tomography in the diagnosis of cerebral vasospasm. *Neurosurgery*. 2006;59:319-325
4. Aralasmak A, Akyuz M, Ozkaynak C, Sindel T, Tuncer R. Ct angiography and perfusion imaging in patients with subarachnoid hemorrhage: Correlation of vasospasm to perfusion abnormality. *Neuroradiology*. 2009;51:85-93
5. Wintermark M, Dillon WP, Smith WS, Lau BC, Chaudhary S, Liu S, Yu M, Fitch M, Chien JD, Higashida RT, Ko NU. Visual grading system for vasospasm based on perfusion ct imaging: Comparisons with conventional angiography and quantitative perfusion ct. *Cerebrovasc Dis*. 2008;26:163-170
6. Schaefer PW, Roccatagliata L, Ledezma C, Hoh B, Schwamm LH, Koroshetz W, Gonzalez RG, Lev MH. First-pass quantitative ct perfusion identifies thresholds for salvageable penumbra in acute stroke patients treated with intra-arterial therapy. *AJNR Am J Neuroradiol*. 2006;27:20-25
7. Wintermark M, Flanders AE, Velthuis B, Meuli R, van Leeuwen M, Goldsher D, Pineda C, Serena J, van der Schaaf I, Waaijer A, Anderson J, Nesbit G, Gabriely I, Medina V, Quiles A, Pohlman S, Quist M, Schnyder P, Bogousslavsky J, Dillon WP, Pedraza S. Perfusion-ct assessment of infarct core and penumbra: Receiver operating characteristic curve analysis in 130 patients suspected of acute hemispheric stroke. *Stroke*. 2006;37:979-985
8. Dupont SA, Wijndicks EF, Manno EM, Lanzino G, Rabinstein AA. Prediction of angiographic vasospasm after aneurysmal subarachnoid hemorrhage: Value of the hijdra sum scoring system. *Neurocrit Care*. 2009
9. Wintermark M, Thiran JP, Maeder P, Schnyder P, Meuli R. Simultaneous measurement of regional cerebral blood flow by perfusion ct and stable xenon ct: A validation study. *AJNR AmJ-Neuroradiol*. 2001;22:905-914
10. Yoon DY, Choi CS, Kim KH, Cho BM. Multidetector-row ct angiography of cerebral vasospasm after aneurysmal subarachnoid hemorrhage: Comparison of volume-rendered images and digital subtraction angiography. *AJNR AmJNeuroradiol*. 2006;27:370-377
11. Imaging Performance Assessment of CT Scanners an MDA Evaluation centre. ImpACT CT Patient Dosimetry Calculator. 2004; [0.99v]
12. Voldby B, Enevoldsen EM, Jensen FT. Regional cbf, intraventricular pressure, and cerebral metabolism in patients with ruptured intracranial aneurysms. *JNeurosurg*. 1985;62:48-58
13. Kealey SM, Loving VA, DeLong DM, Eastwood JD. User-defined vascular input function curves: Influence on mean perfusion parameter values and signal-to-noise ratio. *Radiology*. 2004;231:587-593
14. van der Schaaf I, Wermer MJ, van der Graaf Y, Hoff RG, Rinkel GJ, Velthuis BK. Ct after subarachnoid hemorrhage: Relation of cerebral perfusion to delayed cerebral ischemia. *Neurology*. 2006;66:1533-1538
15. Biggerstaff BJ. Comparing diagnostic tests: A simple graphic using likelihood ratios. *Stat Med*. 2000;19:649-663

16. Ohkuma H, Suzuki S, Kudo K, Islam S, Kikkawa T. Cortical blood flow during cerebral vasospasm after aneurysmal subarachnoid hemorrhage: Three-dimensional n-isopropyl-p-[(123)I]iodoamphetamine single photon emission ct findings. *AJNR Am J Neuroradiol*. 2003;24:444-450
17. Jaeger M, Schuhmann MU, Soehle M, Nagel C, Meixensberger J. Continuous monitoring of cerebrovascular autoregulation after subarachnoid hemorrhage by brain tissue oxygen pressure reactivity and its relation to delayed cerebral infarction. *Stroke*. 2007;38:981-986
18. Pasco A, Ter Minassian A, Chapon C, Lemaire L, Franconi F, Darabi D, Caron C, Benoit JP, Le Jeune JJ. Dynamics of cerebral edema and the apparent diffusion coefficient of water changes in patients with severe traumatic brain injury. A prospective mri study. *Eur Radiol*. 2006;16:1501-1508
19. van Asch CJ, van der Schaaf IC, Rinkel GJ. Acute hydrocephalus and cerebral perfusion after aneurysmal subarachnoid hemorrhage. *AJNR Am J Neuroradiol*. 2009
20. Nabavi DG, LeBlanc LM, Baxter B, Lee DH, Fox AJ, Lownie SP, Ferguson GG, Craen RA, Gelb AW, Lee TY. Monitoring cerebral perfusion after subarachnoid hemorrhage using ct. *Neuroradiology*. 2001;43:7-16
21. Romano JG, Rabinstein AA, Arheart KL, Nathan S, Campo-Bustillo I, Koch S, Forteza AM. Microemboli in aneurysmal subarachnoid hemorrhage. *J Neuroimaging*. 2008;18:396-401
22. Bandera E, Botteri M, Minelli C, Sutton A, Abrams KR, Latronico N. Cerebral blood flow threshold of ischemic penumbra and infarct core in acute ischemic stroke: A systematic review. *Stroke*. 2006;37:1334-1339
23. Mnyusiwalla A, Aviv RI, Symons SP. Radiation dose from multidetector row ct imaging for acute stroke. *Neuroradiology*. 2009;51:635-640
24. International Commission on Radiological Protection. Radiological protection in biomedical research. *Annals of the ICRP*. 1993:11-13
25. Weidauer S, Lanfermann H, Raabe A, Zanella F, Seifert V, Beck J. Impairment of cerebral perfusion and infarct patterns attributable to vasospasm after aneurysmal subarachnoid hemorrhage: A prospective mri and dsa study. *Stroke*. 2007;38:1831-1836



Effect of different components of
triple-H therapy on cerebral perfusion in
patients with aneurysmal
subarachnoid hemorrhage:
a systematic review



7

J.W. Dankbaar, A.J.C. Slooter, G.J.E. Rinkel, I.C. van der Schaaf

Critical Care. 2010 Feb;14(1):R23

Abstract

Background and purpose

Triple-H therapy and its separate components (hypervolemia, hemodilution, and hypertension) aim to increase cerebral perfusion in subarachnoid hemorrhage (SAH) patients with delayed cerebral ischemia. We systematically reviewed the literature on the effect of triple-H components on cerebral perfusion in SAH patients.

Methods

We searched medical databases to identify all articles till October 2009 (except case reports) on treatment with triple-H components in SAH patients with evaluation of the treatment using cerebral blood flow (CBF in ml/100g/min) measurement. We summarized study design, patient and intervention characteristics, and calculated differences in mean CBF before and after intervention.

Results

Eleven studies (4-51 patients per study) were included (one randomized trial). Hemodilution did not change CBF. One of seven studies on hypervolemia showed statistically significant CBF increase compared to baseline, there was no comparable control group. Two of four studies applying hypertension and one of two applying triple-H showed significant CBF increase, none used a control group. The large heterogeneity in interventions and study populations prohibited meta-analyses.

Conclusions

There is no good evidence from controlled studies for a positive effect of triple-H or its separate components on CBF in SAH patients. In uncontrolled studies hypertension seems to be more effective in increasing CBF than hemodilution or hypervolemia.

Introduction

Aneurysmal subarachnoid hemorrhage (SAH) is a subset of stroke that occurs at a relatively young age (median 55 years), and has a high rate of morbidity (25%) and case fatality (35%).¹ In SAH patients who survive the first days after bleeding, delayed cerebral ischemia (DCI) is an important contributor to poor outcome.²

In patients with SAH cerebral autoregulation is often disturbed.³ Disturbed cerebral autoregulation, in the presence of vasospasm or microthrombosis may result in decreased cerebral blood flow (CBF) and thereby DCI.³⁻⁶ When autoregulation is affected, CBF becomes dependent on cerebral perfusion pressure and blood viscosity. To increase CBF different combinations of hemodilution, hypervolemia, and hypertension have been used for many years.⁷ When all three components are used, the treatment combination is called triple-H.⁸

There is no sound evidence for effectiveness of triple-H or its components on clinical outcome, while triple-H and its components are associated with increased complications and costs.^{8,9} To assess the potential of triple-H or its components in improving neurological outcome, knowledge of its effects on its intended substrate, cerebral perfusion, is pivotal.

We aimed to systematically review the literature on the effect of triple-H and its components on CBF in SAH patients and to provide a quantitative summary of this effect.

Methods

Search strategy

The Entrez PubMed NIH and EMBASE online medical databases, and the central COCHRANE Controlled Trial Register were searched using the following key terms and MeSH terms: subarachnoid hemorrhage AND (delayed ischemic neurological deficit OR delayed cerebral ischemia OR neurologic deficits OR vasospasm) AND (volume expansion therapy OR hyperdynamic OR hypervolem* OR hemodilution OR hypertens* OR Triple-H therapy) AND (cerebral perfusion OR cerebral blood flow). Reference lists from the retrieved reports were checked for completeness. The last search was performed in October 2009.

Selection criteria

Studies were considered for this review when the investigation was based on human subjects older than 18 years with proven aneurysmal SAH. At least part of the studied population had to be treated with one or more triple-H components and evaluated with a technique measuring CBF. Treatment with triple-H components was considered to be any intervention that aimed to increase blood pressure, to increase circulating blood volume, to cause hemodilution or to result in a combination of these three effects. CBF measurement had to be assessed before and after intervention. Studies from which mean CBF values before and after intervention could not be calculated were excluded. Case reports, reviews and articles that were not obtainable in English, German, French or Dutch were also excluded.

Data extraction

Two investigators independently assessed eligibility of studies and extracted data by means of a standardized data extraction form. In case of disagreement, both observers reviewed the article in question together until consensus was reached. We extracted data on 1.) study design, 2.) population characteristics, 3.) characteristics of the intervention with triple-H components, and 4.) cerebral perfusion. The following items were listed on the standardized extraction form: *Study design*: first year of study, prospective or retrospective design, consecutive series of patients, presence or absence of a control group, and randomization; *Population characteristics*: number of included patients, age, gender, clinical condition (Hunt & Hess grade¹⁰ or WFNS¹¹ score) on admission, and clinical outcome; *Characteristics of the intervention*: type and composition of triple-H components, prophylactic or therapeutic intervention, and intra-cranial and systemic complications; *Cerebral perfusion*: measurement technique, measured part of the brain, time between baseline and follow up CBF measurement (clustered in: <24 hours, 5 to 7 days, and 12 to 14 days), and difference in CBF between baseline and follow up.

Analysis

The outcome measurement in this review was the difference in mean CBF between pre- and post-intervention measurements. The 95% confidence intervals (95% CI) of these differences in means were calculated if the sample variance and sample size of the mean pre- and post-intervention measurements were available.¹² The Review Manager software (RevMan5) for preparing and maintaining Cochrane reviews was used for this purpose. If an intervention was done several times, the perfusion measurements around the intervention closest to 7 days after SAH were used. Differences in pre- and post-intervention CBF were studied in relation to the time since the start of the intervention (<24 hours after baseline measurement, 5 to 7 days, or 12 to 14 days after baseline measurement), intention of the intervention (prophylactic or therapeutic (i.e. confirmed angiographic vasospasm or symptomatic vasospasm) and type of intervention (isovolemic hemodilution, hypervolemia, hypertension, or triple-H).

Results

Our literature search resulted in 172 articles. Screening by title and abstract resulted in 13 original studies and 10 review articles on the topic. One more article was identified by reviewing the reference lists of the included studies and the reviews. Of the resulting fourteen original studies eleven fulfilled all selection criteria and were used for further analyses (*Figure 1*).

Study design and population characteristics

The study design and population characteristics are summarized in *Table 1*. The 11 included studies were published between 1987 and 2007; 8 (73%) of these were prospective. Two studies (18%)^{13,14} compared the effect of triple-H compo-

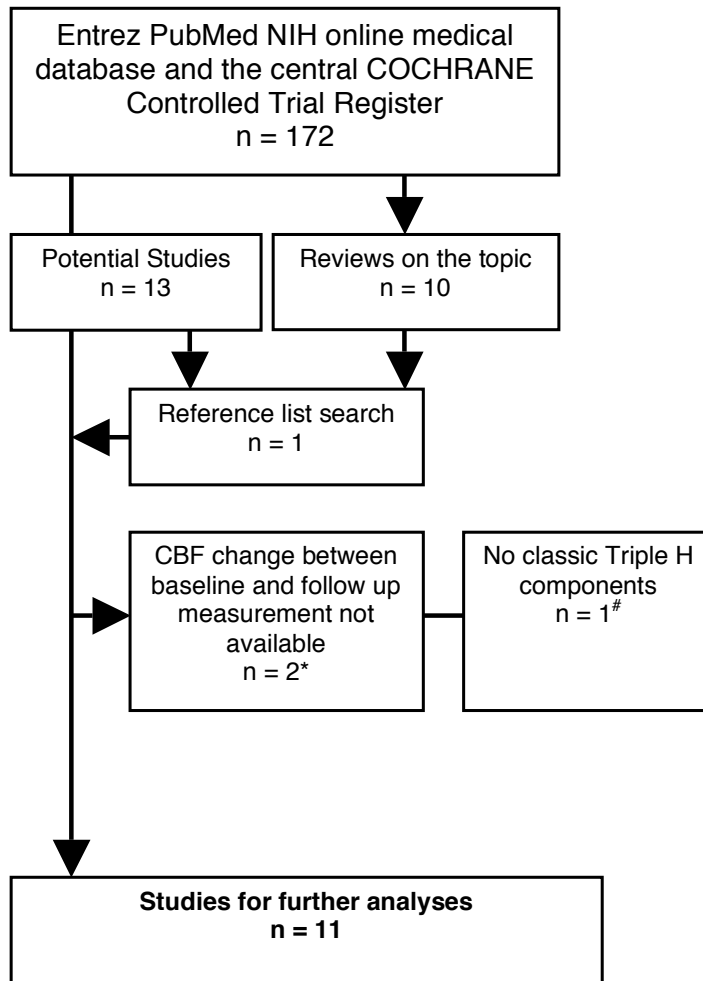


Figure 1 Flow chart showing the search process for included studies.
Subscript: * Joseph et al ³¹ and Egge et al ⁹, # Hadeishi et al ³²

nents on cerebral perfusion with an independent control group; in one of these interventions allocation was randomized (using hypervolemia as a prophylactic intervention, *Table 2*), in the other study the intervention and control group differed both in intervention (hypervolemia versus no hypervolemia) and in domain (angiographically confirmed vasospasm versus patients without vasospasm).¹⁴ Two studies (18%) mentioned that they used a consecutive series of patients.^{13, 15} The number of included patients varied from 4 to 51 with an average age of 42 to 59 years. In the 9 (82%) studies that used the Hunt and Hess scale to classify the clinical condition on admission, the median H&H varied between 2 and 4. One study (9%) used the World Federation of Neurological Societies (WFNS) grading

Table 1 Study design and population characteristics:

Reference	Study design	Population Characteristics										
		Intervention type	Prophylactic/Therapeutic	Prospective	Consecutive series	Randomized	Control group	Nr. Int/nont	Mean age	Men	Clinical condition on admission: Type, median Int/no Int (range)	Good Recovery or moderate Disability: Int/no Int
Ekelund, 2002 ¹⁸	isovolemic hemodilution or hypovolemic hemodilution	Therapeutic	+	unknown	-	-	8/0	42	13%	H&H, 2 (1-3)	100%	0%
Mori, 1995 ¹⁴	hypervolemic hemodilution	Therapeutic	+	unknown	-	+	51/47	56	38%	H&H, 2/2 (1-4)	82%/ unknown	18%/ unknown
Yamakami, 1987 ²¹	hypervolemia	Prophylactic	+	unknown	-	-	35/0	51	31%	H&H, ? (1-4)	86%	14%
Lennihan, 2000 ¹³	hypervolemia	Prophylactic	+	+	+	+	41/41	48.5	41%	H&H, 2/2 (1-4)	80%/76%	17%/20%
Tseng, 2003 ²³	hypervolemia	Therapeutic	+	unknown	-	-	6/0	50	unknown	WFNS, ? (4-5)	unknown	unknown
Jost, 2005 ²²	hypervolemia	Therapeutic	+	-	-	-	6/0	49	50%	unknown	unknown	unknown
Muizelaar, 1986 ²⁵	hypertension	Therapeutic	unknown	-	-	-	4/0	44	0%	H&H, 4 (2-5)	100%	0%
Touho, 1992 ²⁰	hypertension	Both	unknown	unknown	-	-	20/0	55	55%	H&H, 2 (2-4)	90%	10%
Darby, 1994 ²⁴	hypertension	Therapeutic	-	-	-	-	13/0	59	23%	H&H, 2.5 (1-5)	unknown	unknown
Origitano, 1990 ¹⁵	Triple-H	Prophylactic	+	+	-	-	43/0	46	35%	H&H, 2 (1-4)	84%	16%
Muench, 2007 ¹⁹	Triple-H or hypervolemic hemodilution	Prophylactic	+	unknown	-	-	10/0	53	20%	H&H, ? (2-5)	unknown	unknown

Int = Intervention; H&H = Hunt and Hess grading scale for subarachnoid hemorrhage (10); WFNS = World Federation of Neurological Surgeons score (11); DCI = delayed cerebral ischemia.

scale including only patients with WFNS 4 and 5. Clinical outcome was described in seven studies (64%), three using the Glasgow outcome scale,¹⁶ one using the neurologic outcome by Allen et al,¹⁷ and three using not further specified outcome definitions. Eighty to 100% of treated patients showed good recovery or moderate disability.

Characteristics of the intervention

The details of the intervention are summarized in *Table 2*. One study used isovolemic hemodilution, seven used hypervolemia (of which three with hemodilution), four induced hypertension, and two triple-H. Two studies applied several triple-H components in succession within the same patient and compared their effect on CBF.^{18, 19} Four (36%) studies applied the intervention in SAH patients without DCI or vasospasm (prophylactically), six (55%) in SAH patients with DCI or vasospasm (therapeutically), and 1(9%) applied the intervention both therapeutically and prophylactically. To achieve isovolemic hemodilution venasection was simultaneously performed with infusion of 70% dextran and 4% albumin. To achieve hypervolemia a 4-5% albumin solution was most commonly used. The total volume of administered fluids was not always provided in the study reports; in those who provided this item, it varied between 250 - 4000 ml per day. To induce hypertension either phenylephrine or dopamine was used. This resulted in an average increase in mean arterial pressure (MAP) of 21 to 33 mmHg. Four studies mentioned the occurrence of complications during intervention with triple-H components, with systemic complications (congestive heart failure, pulmonary oedema, diabetes insipidus, electrolyte disturbances) being less frequently present (0-9%) than intracranial complications (cerebral oedema, 0-17%). None of the complications were fatal.

Cerebral perfusion

Cerebral perfusion measurement details are summarized in *Table 3*. Different perfusion measurement techniques were used: five (45%) studies used an external scintillation counter (e.s.c.) technique, one (9%) used SPECT, three (27%) used Xenon-CT (XeCT), one used (9%) PET and one (9%) study thermal diffusion microprobes (validated by XeCT). Four (36%) studies did not report whole brain perfusion measurements, but only measurements from the hemisphere ipsilateral to craniotomy or in the flow territory distal to the aneurysm.^{14, 19-21} Nine (82%) studies measured CBF within 24 hours after the start of the intervention and two at a later time. These two studies both measured after five to seven days and one also after 12 to 14 days. Differences in mean CBF before and after intervention with their 95% confidence intervals are plotted in *Figure 2 and 3*. Weighted total effects could not be calculated due to the large heterogeneity in the used intervention, the studied populations and the applied methods.

Table 2 Characteristics of the intervention:

Reference	Triple-H components		Composition		Complications	
	type	Prophylactic/ Therapeutic	Intervention group	Control group	Intracranial Int/no Int	Systemic Int/no Int
Ekelund, 2002 ¹⁸	isovolemic hemodilution or hypervolemic hemodilution	Therapeutic	Isovolemic: Venasection with simultaneous infusion of 70% dextran and 4% albumin in equal volumes Hypervolemic (after isovolemic): Autotransfusion and infusion of 70% dextran and 4% albumin	-	unknown	unknown
Mori, 1995 ¹⁴	hypervolemic hemodilution	Therapeutic	500 ml human albumin solution, 500 ml low molecular dextran per day	900 ml 10% glycerol per day	0%/ unknown	4%/ unknown
Yamakami, 1987 ²¹	hypervolemia	Prophylactic	500 ml 5% albumin in 30 minutes	-	unknown	unknown
Lennihan, 2000 ¹³	hypervolemia	Prophylactic	250 ml 5% albumin in 2 hours	80 ml 5% dextrose and 0.9% saline in 1 hour	15%/17%	7%/5%
Tseng, 2003 ²³	hypervolemia	Therapeutic	2 ml/kg 23.5% saline in 20 minutes	-	unknown	unknown
Jost, 2005 ²²	hypervolemia	Therapeutic	15ml/kg 0.9% saline in 1 hour	-	unknown	unknown
Muizelaar, 1986 ²⁵	hypertension	Therapeutic	Phenylephrine (mean MAP increase of 33 mmHg) hypervolemia with Ht around 32%	-	0%	0%
Touho, 1992 ²⁰	hypertension	Both	Continuous infusion of dopamine 7-15 µg/kg/min (mean MAP increase of 22 mmHg)	-	unknown	unknown
Darby, 1994 ²⁴	hypertension	Therapeutic	dopamine 6.4-20 µg/kg/min (mean MAP increase of 21 mmHg)	-	unknown	unknown
Origitano, 1990 ¹⁵	Triple-H	Prophylactic	Venasection to Ht of 30 in increments of 150-250 ml every 8 hours within 12-24 hours	-	0%	9%
Muench, 2007 ¹⁹	Triple-H or hypertension or hypervolemic hemodilution	Prophylactic	infusion of 250-500 ml 5% albumin every 6 hours dopamine or labetalol (mean MAP increase not written) norepinephrine to raise MAP above 130 mmHg (mean MAP increase not written) 1000 ml hydroxyethyl-starch and 1000-3000 ml crystalloids	-	unknown	unknown

Int = Intervention; Ht = hematocrit

Table 3 Cerebral Perfusion Measurement

Reference	Triple-H components	Prophylactic/ Therapeutic	CBF Technique	Measuring location	Timing after Intervention
Ekelund, 2002 ¹⁸	isovolemic hemodilution or hypervolemic hemodilution	Therapeutic	¹³³ Xe SPECT	Whole brain	<24 hours
Mori, 1995 ¹⁴	hypervolemic hemodilution	Therapeutic	¹²³ I-IMP e.s.c.	Ipsilateral to craniotomy	5-7 days
Yamakami, 1987 ²¹	hypervolemia	Prophylactic	¹³³ Xe e.s.c.	Ipsilateral to craniotomy	<24 hours
Lennihan, 2000 ¹³	hypervolemia	Prophylactic	¹³³ Xe e.s.c.	Whole brain	<24 hours 5-7 days 12-14 days
Tseng, 2003 ²³	hypervolemia	Therapeutic	XeCT	Whole brain	<24 hours
Jost, 2005 ²²	hypervolemia	Therapeutic	PET	Whole brain	<24 hours
Muizelaar, 1986 ²⁵	hypertension	Therapeutic	¹³³ Xe e.s.c.	Whole brain	<24 hours
Touho, 1992 ²⁰	hypertension	Both	XeCT	Ipsilateral to craniotomy	<24 hours
Darby, 1994 ²⁴	hypertension	Therapeutic	XeCT	Whole brain	<24 hours
Origitano, 1990 ¹⁵	Triple-H	Prophylactic	¹³³ Xe e.s.c.	Whole brain	<24 hours
Muench, 2007 ¹⁹	Triple-H or hypertension or hypervolemic hemodilution	Prophylactic	thermal diffusion microprobe	in flow territory distal to aneurysm	<24 hours

e.s.c. = external scintillation counter; CBF = cerebral blood flow

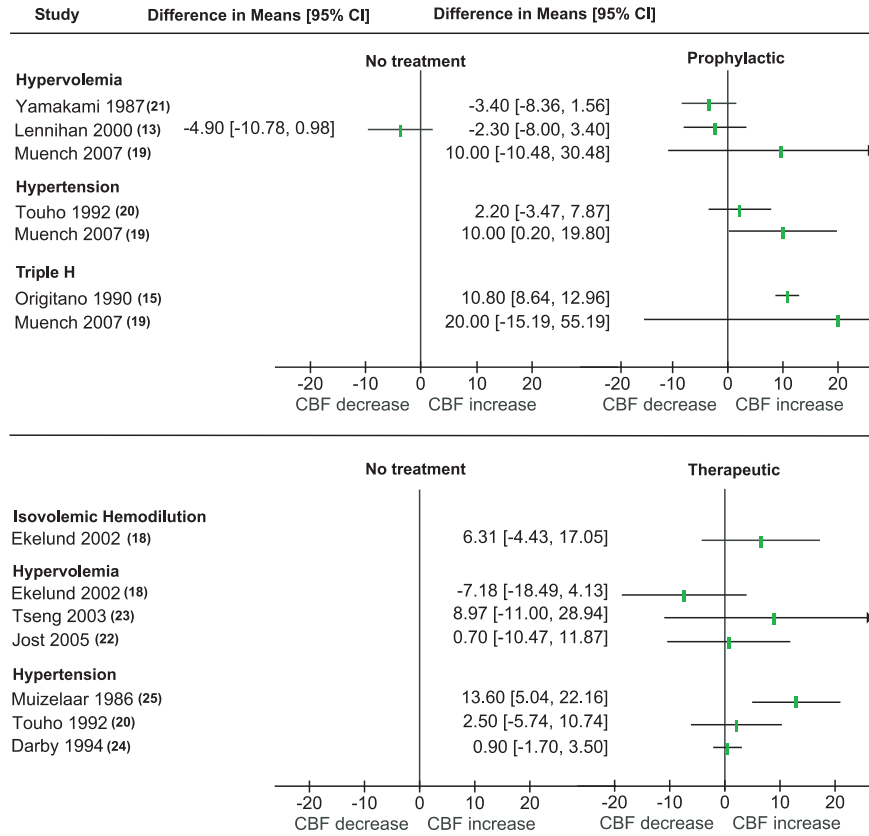


Figure 2 Short term (within 24 hours) difference in mean CBF (ml/100g/min) before and after baseline measurement (start of intervention) with 95% confidence interval (CI) calculated from sample variances and sample sizes, of prophylactic (upper) or therapeutic (lower) interventions, stratified by triple-H component.

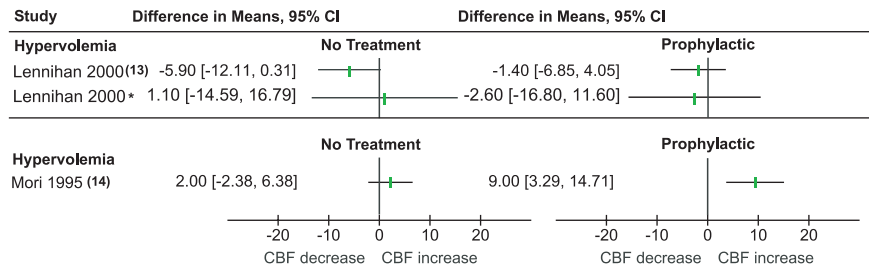


Figure 3 Long term (5 to 7 days and 12-14* days) difference in mean CBF (ml/100g/min) before and after baseline measurement (start of intervention) with 95% confidence interval (CI) calculated from sample variances and sample sizes, of prophylactic (upper) or therapeutic (lower) interventions, stratified by triple-H component.

- Short term (within 24 hours) effects of prophylactic use of triple-H components:

When compared to baseline measurement, hypervolemia led to a non-significant CBF decrease in two studies^{13,21} and a non-significant CBF increase in one study.¹⁹ Hypertension was associated with an increase in CBF in two studies, this was statistically significant in one (increase of 10 ml/100gr/min);¹⁹ triple-H led to CBF increase in two studies,^{15, 19} this was statistically significant in one (increase of 11 ml/100gr/min).¹⁵ The study that compared hypervolemia to a control group found no statistically significant difference between both groups.¹³

- Short term (within 24 hours) effects of therapeutic use of triple-H components:

Isovolemic hemodilution resulted in a non-significant CBF increase.¹⁸ Hypervolemia was associated with a non-significant increase in two studies^{22, 23} and decrease in one,¹⁸ and hypertension resulted in a CBF increase in three studies^{20, 24, 25} which was significant in one (increase of 13 ml/100gr/min).²⁵ All these changes were compared to baseline values. None of these studies compared the effects to a control group.

- Long term (5-7 days and 12-14 days) effects of triple-H components:

When compared to baseline measurement, prophylactic hypervolemia resulted in a non-significant CBF decrease in the intervention group both after 5-7 days and 12-14 days, in the control group a non-significant decrease after 5-7 days and increase after 12-14 days was seen.¹³ Therapeutic hypervolemia resulted in a significant CBF increase (mean increase of 9 ml/100gr/min) compared to baseline values; the untreated control group without vasospasm showed no significant CBF increase.¹⁴

Discussion

Triple-H and its separate components aim to increase cerebral perfusion and thereby improve outcome. Given the lack of randomized clinical trials on triple-H and clinical outcome, we evaluated the evidence on the effect of triple-H components on CBF. Due to the large heterogeneity in study design, CBF measurement, and composition of triple-H components, it was not possible to perform a meta-analysis of treatment effects of the included studies. We therefore assessed the results of the individual studies separately.

There is no good evidence that isovolemic hemodilution or hypervolemia improve CBF in the initial days. One study found a remote effect of hypervolemia compared to baseline, but did not use a proper control group.¹⁴ Induction of hypertension, alone or combined with hypervolemia did improve CBF compared to baseline levels in three separate studies. It could be concluded that this component is the most promising. However, without a control group within the same population, one can not be sure that the observed changes in CBF do not just reflect the natural course of cerebral perfusion after SAH.

Apart from lack of properly controlled studies, there are other potential drawbacks of the presented evidence from the literature. Firstly, we are likely dealing with publication bias since positive studies have a greater chance of being report-

ed. Secondly, several of the included studies had small sample sizes (<10 patients) and are therefore likely to represent a selection of successful cases. Thirdly, there was a large heterogeneity in methods of CBF measurement making generalized conclusions and meta-analyses impossible. Although the used CBF measurement techniques have been validated,²⁶ small changes in CBF may not be picked up equally well by the different techniques. Furthermore, in some studies CBF was not measured in the entire brain but only in the separate hemispheres. In these studies we chose to analyze the CBF change in the hemisphere ipsilateral to craniotomy or in the flow territory distal to the aneurysm, since the risk of ischemia is highest in that region.²⁷ The changes induced by triple-H therapy are likely to be larger in that part of the brain, compared to the measurements in both hemispheres combined. Another issue is the composition of triple-H. The different triple-H components aim to influence perfusion pressure and blood viscosity in order to increase CBF.²⁸ Whether induction of hypertension is successful in terms of raising blood pressure is easily controlled, although there is no consensus on the degree and duration of induced hypertension. The discrepancies in effects on CBF within the different studies on hypertension may therefore be explained at least in part by different hypertension strategies. Whether strategies aiming for hemodilution and hypervolemia actually achieve these effects is unsure.²⁹ Triple-H combines hypertension, hemodilution and hypervolemia, and should theoretically result in the largest CBF increase, but we could not confirm this in this review.

We acknowledge the fact that an increase in CBF does not imply that the outcome of SAH improves. Firstly, this increase may only be transient or not sufficient to prevent ischemia and infarction. Secondly, oxygen delivery may not be increased despite the increase in CBF. This has been described in a study on the effect of hypervolemia on brain oxygenation and is most likely caused by hemodilution resulting from the volume expansion.¹⁹ However, since an increase in CBF is the mechanism by which triple-H and its components should improve outcome, explanatory (phase II) randomized trials showing an increase in CBF measurements from triple-H or its components are crucial before large effectiveness trials are undertaken. The estimated sample size needed for such a phase II trial to properly analyze the effect of triple-H on CBF is not too large. The data in this review show that the size of significant CBF changes in the presented studies was approximately 10 ml/100gr/min and that the mean standard deviation (based on the confidence intervals in *Figure 2*) for CBF differences was about 18 ml/100gr/min. To detect an effect size of 10 ml/100gr/min difference in CBF change between treated and untreated DCI patients (with a standard deviation of 18 ml/100gr/min) 104 patients (52 in each group) are needed to obtain a statistical power of 80% with an α of 0.05.

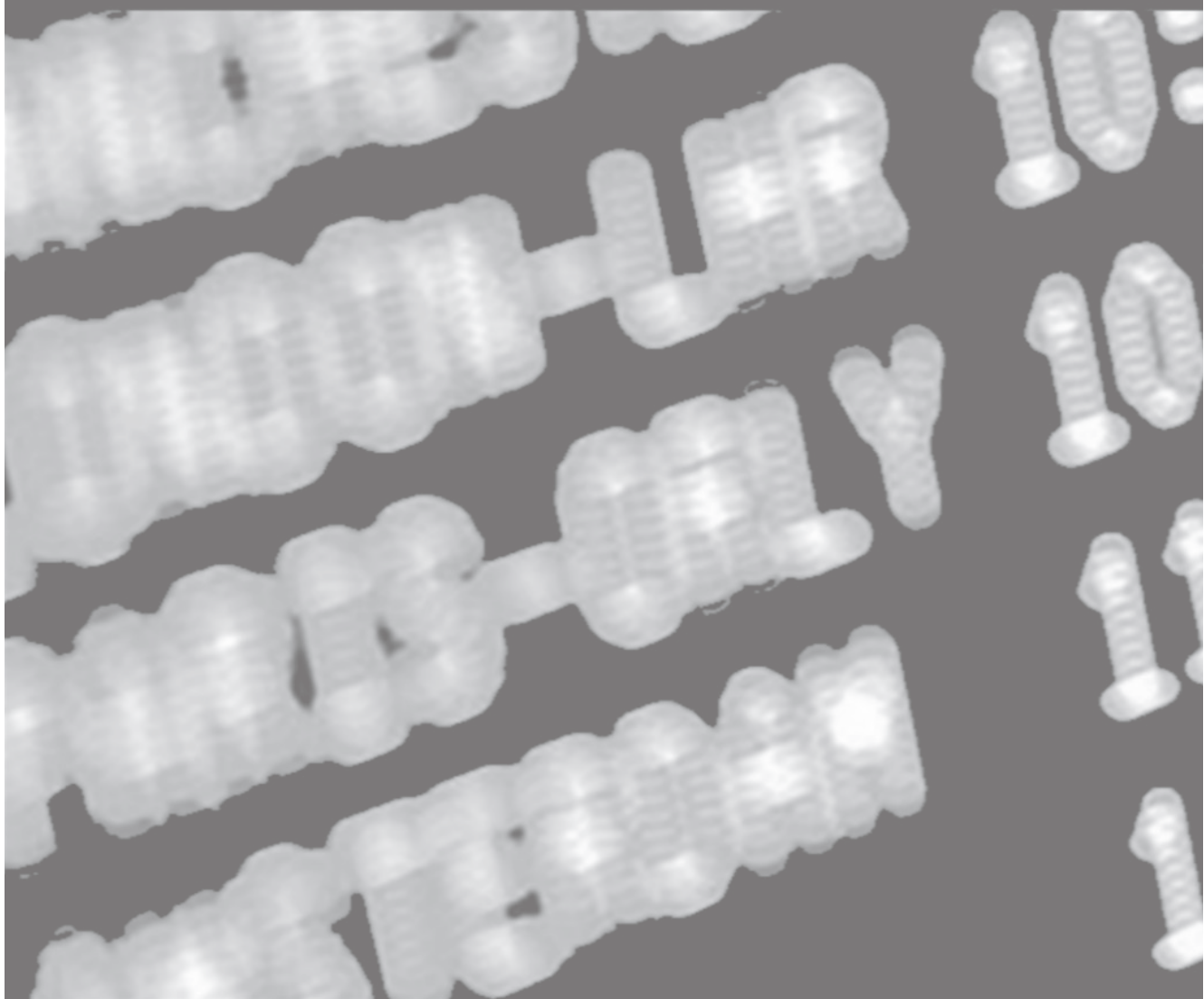
Conclusion

This review of the literature gives a quantitative summary of the effect of triple-H and its components on CBF, the intended substrate of this intervention. We showed that there is no good evidence that CBF improves due to the intervention. From all components of triple-H, induced hypertension seems to be the most promising triple-H component. A pivotal first step is to conduct a randomized controlled trial in SAH patients with DCI on the effect of induced hypertension on CBF.

References

1. Nieuwkamp DJ, Setz LE, Algra A, Linn FH, de Rooij NK, Rinkel GJ. Changes in case fatality of aneurysmal subarachnoid hemorrhage over time, according to age, sex, and region: A meta-analysis. *Lancet Neurol.* 2009;8:635-642
2. van Gijn J, Kerr RS, Rinkel GJ. Subarachnoid hemorrhage. *Lancet.* 2007;369:306-318
3. Jaeger M, Schuhmann MU, Soehle M, Nagel C, Meixensberger J. Continuous monitoring of cerebrovascular autoregulation after subarachnoid hemorrhage by brain tissue oxygen pressure reactivity and its relation to delayed cerebral infarction. *Stroke.* 2007;38:981-986
4. Vergouwen MD, Vermeulen M, Coert BA, Stroes ES, Roos YB. Microthrombosis after aneurysmal subarachnoid hemorrhage: An additional explanation for delayed cerebral ischemia. *J Cereb Blood Flow Metab.* 2008;28:1761-1770
5. Kozniowska E, Michalik R, Rafalowska J, Gadamski R, Walski M, Frontczak-Baniewicz M, Piotrowski P, Czernicki Z. Mechanisms of vascular dysfunction after subarachnoid hemorrhage. *J Physiol Pharmacol.* 2006;57 Suppl 11:145-160
6. Stein SC, Levine JM, Nagpal S, LeRoux PD. Vasospasm as the sole cause of cerebral ischemia: How strong is the evidence? *NeurosurgFocus.* 2006;21:E2
7. Kosnik EJ, Hunt WE. Postoperative hypertension in the management of patients with intracranial arterial aneurysms. *J Neurosurg.* 1976;45:148-154
8. Sen J, Belli A, Albon H, Morgan L, Petzold A, Kitchen N. Triple-h therapy in the management of aneurysmal subarachnoid hemorrhage. *Lancet Neurol.* 2003;2:614-621
9. Egge A, Waterloo K, Sjöholm H, Solberg T, Ingebrigtsen T, Romner B. Prophylactic hyperdynamic postoperative fluid therapy after aneurysmal subarachnoid hemorrhage: A clinical, prospective, randomized, controlled study. *Neurosurgery.* 2001;49:593-605
10. Hunt WE, Hess RM. Surgical risk as related to time of intervention in the repair of intracranial aneurysms. *J Neurosurg.* 1968;28:14-20
11. Report of world federation of neurological surgeons committee on a universal subarachnoid hemorrhage grading scale. *J Neurosurg.* 1988;68:985-986
12. Normand SL. Meta-analysis: Formulating, evaluating, combining, and reporting. *Stat Med.* 1999;18:321-359
13. Lennihan L, Mayer SA, Fink ME, Beckford A, Paik MC, Zhang H, Wu YC, Klebanoff LM, Raps EC, Solomon RA. Effect of hypervolemic therapy on cerebral blood flow after subarachnoid hemorrhage: A randomized controlled trial. *Stroke.* 2000;31:383-391
14. Mori K, Arai H, Nakajima K, Tajima A, Maeda M. Hemorheological and hemodynamic analysis of hypervolemic hemodilution therapy for cerebral vasospasm after aneurysmal subarachnoid hemorrhage. *Stroke.* 1995;26:1620-1626
15. Oritano TC, Wascher TM, Reichman OH, Anderson DE. Sustained increased cerebral blood flow with prophylactic hypertensive hypervolemic hemodilution ("Triple-h" Therapy) after subarachnoid hemorrhage. *Neurosurgery.* 1990;27:729-739
16. Jennett B, Snoek J, Bond MR, Brooks N. Disability after severe head injury: Observations on the use of the glasgow outcome scale. *J Neural Neurosurg Psychiatry.* 1981;44:285-293
17. Allen GS, Ahn HS, Preziosi TJ, Battye R, Boone SC, Chou SN, Kelly DL, Weir BK, Crabbe RA, Lavik PJ, Rosenbloom SB, Dorsey FC, Ingram CR, Mellits DE, Bertsch LA, Boisvert DP, Hundley MB, Johnson RK, Strom JA, Transou CR. Cerebral arterial spasm--a controlled trial of nimodipine in patients with subarachnoid hemorrhage. *N Engl J Med.* 1983;308:619-624

18. Ekelund A, Reinstrup P, Ryding E, Andersson AM, Molund T, Kristiansson KA, Romner B, Brandt L, Saveland H. Effects of iso- and hypervolemic hemodilution on regional cerebral blood flow and oxygen delivery for patients with vasospasm after aneurysmal subarachnoid hemorrhage. *Acta Neurochir(Wien)*. 2002;144:703-712
19. Muench E, Horn P, Bauhuf C, Roth H, Philipps M, Hermann P, Quintel M, Schmiedek P, Vajkoczy P. Effects of hypervolemia and hypertension on regional cerebral blood flow, intracranial pressure, and brain tissue oxygenation after subarachnoid hemorrhage*. *Crit Care Med*. 2007
20. Touho H, Karasawa J, Ohnishi H, Shishido H, Yamada K, Shibamoto K. Evaluation of therapeutically induced hypertension in patients with delayed cerebral vasospasm by xenon-enhanced computed tomography. *NeuroIMedChir (Tokyo)*. 1992;32:671-678
21. Yamakami I, Isobe K, Yamaura A. Effects of intravascular volume expansion on cerebral blood flow in patients with ruptured cerebral aneurysms. *Neurosurgery*. 1987;21:303-309
22. Jost SC, Diringner MN, Zazulia AR, Videen TO, Aiyagari V, Grubb RL, Powers WJ. Effect of normal saline bolus on cerebral blood flow in regions with low baseline flow in patients with vasospasm following subarachnoid hemorrhage. *JNeurosurg*. 2005;103:25-30
23. Tseng MY, Al-Rawi PG, Pickard JD, Rasulo FA, Kirkpatrick PJ. Effect of hypertonic saline on cerebral blood flow in poor-grade patients with subarachnoid hemorrhage. *Stroke*. 2003;34:1389-1396
24. Darby JM, Yonas H, Marks EC, Durham S, Snyder RW, Nemoto EM. Acute cerebral blood flow response to dopamine-induced hypertension after subarachnoid hemorrhage. *JNeurosurg*. 1994;80:857-864
25. Muizelaar JP, Becker DP. Induced hypertension for the treatment of cerebral ischemia after subarachnoid hemorrhage. Direct effect on cerebral blood flow. *SurgNeurol*. 1986;25:317-325
26. Latchaw RE, Yonas H, Hunter GJ, Yuh WT, Ueda T, Sorensen AG, Sunshine JL, Biller J, Wechsler L, Higashida R, Hademenos G. Guidelines and recommendations for perfusion imaging in cerebral ischemia: A scientific statement for healthcare professionals by the writing group on perfusion imaging, from the council on cardiovascular radiology of the american heart association. *Stroke*. 2003;34:1084-1104
27. Rabinstein AA, Friedman JA, Weigand SD, McClelland RL, Fulgham JR, Manno EM, Atkinson JL, Wijdicks EF. Predictors of cerebral infarction in aneurysmal subarachnoid hemorrhage. *Stroke*. 2004;35:1862-1866
28. Archer DP, Shaw DA, Leblanc RL, Tranmer BI. Haemodynamic considerations in the management of patients with subarachnoid hemorrhage. *Can J Anaesth*. 1991;38:454-470
29. Hoff R, Rinkel G, Verweij B, Algra A, Kalkman C. Blood volume measurement to guide fluid therapy after aneurysmal subarachnoid hemorrhage: A prospective controlled study. *Stroke*. 2009;40:2575-2577
30. Hoff RG, Rinkel GJ, Verweij BH, Algra A, Kalkman CJ. Nurses' prediction of volume status after aneurysmal subarachnoid hemorrhage: A prospective cohort study. *Crit Care*. 2008;12:R153
31. Joseph M, Ziadi S, Nates J, Dannenbaum M, Malkoff M. Increases in cardiac output can reverse flow deficits from vasospasm independent of blood pressure: A study using xenon computed tomographic measurement of cerebral blood flow. *Neurosurgery*. 2003;53:1044-1051
32. Hadeishi H, Mizuno M, Suzuki A, Yasui N. Hyperdynamic therapy for cerebral vasospasm. *Neurol Med Chir (Tokyo)*. 1990;30:317-323

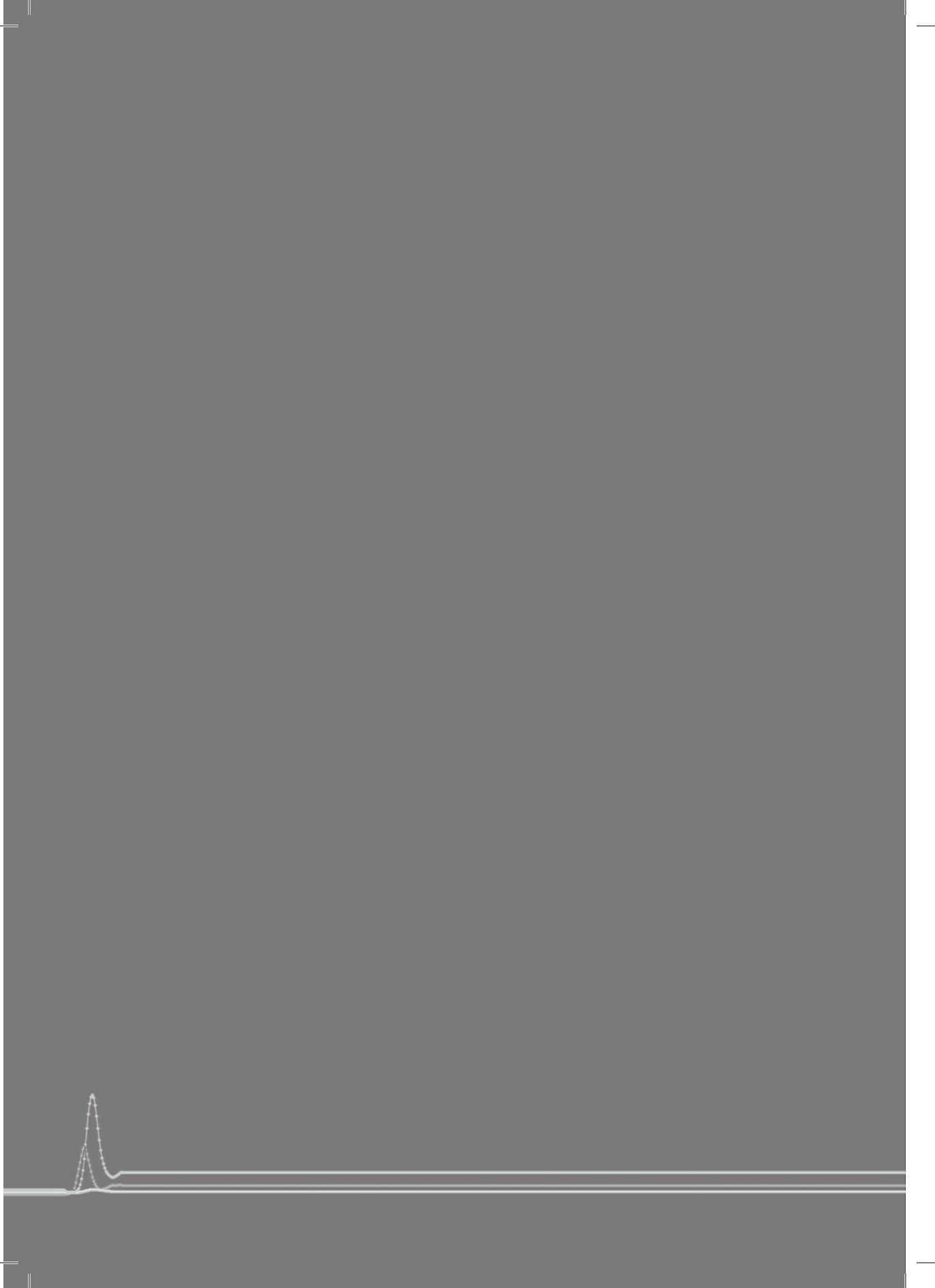




Part 2

Complications of ischemic stroke: a CT perfusion evaluation of blood-brain barrier damage





Dynamic CT perfusion assessment of blood-brain barrier permeability: first-pass versus delayed acquisition



8

*J.W. Dankbaar, J. Hom, T. Schneider, S.C. Cheng, B.C. Lau, I.C. van der Schaaf, S. Virmani,
S. Pohlman, W.P. Dillon, M. Wintermark*

AJNR Am J Neuroradiol. 2008 Oct;29(9):1671-6.

Abstract

Background and purpose

The Patlak model has been applied to first-pass CT-perfusion (CTP) data to extract information on blood-brain barrier permeability (BBBP) in order to predict hemorrhagic transformation in acute stroke patients. However, the Patlak model was originally described for the delayed, steady-state phase of contrast circulation. The goal of this study was to assess whether the first-pass or the delayed phase of a contrast bolus injection better respects the assumptions of the Patlak model for the assessment of BBBP in acute stroke patients using CTP.

Methods

We retrospectively identified 125 consecutive patients (29 with acute hemispheric stroke and 96 without) who underwent a CTP study using a prolonged acquisition time up to 3 minutes. The Patlak model was applied to calculate BBBP, in ischemic and non-ischemic brain tissue. Linear regression of the Patlak plot was performed separately for the first-pass and for the delayed phase of the contrast bolus injection. Patlak linear regression models for the first-pass and the delayed phase were compared in terms of their respective square root mean squared errors ($\sqrt{\text{MSE}}$) and correlation coefficients (R) using generalized estimating equations with robust variance estimation.

Results

BBBP values calculated from the first-pass were significantly higher than BBBP values from the delayed phase, both in non-ischemic brain tissue (2.81 ml/100g/min for first-pass versus 1.05 ml/100g/min for delayed phase, $p < 0.001$) and in ischemic tissue (7.63 ml/100g/min for first-pass versus 1.31 ml/100g/min for delayed phase, $p < 0.001$). Compared to regression models from first-pass, Patlak regression models obtained from delayed data were of significantly better quality, showing a significantly lower $\sqrt{\text{MSE}}$ and higher R.

Conclusion

Only the delayed phase of CTP acquisition respects the assumptions of linearity of the Patlak model in stroke and non-stroke patients.

Introduction

Hemorrhagic transformation (HT) is a serious complication of ischemic stroke which can increase the risk of mortality up to 11 times.¹ Combined data from six major stroke trials showed that severe hemorrhage with mass effect occurs in 4.8% of stroke patients treated with tPA within 3 hours after symptom onset and up to 6.4% in patients treated between 3-6 hours.² Damage to the blood-brain barrier (BBB) is considered one of the contributing mechanisms to HT.³ Early detection of a damaged BBB could potentially be used to identify patients who are more likely to develop HT, and might therefore represent a contraindication to acute reperfusion therapy.⁴ BBB damage manifested as parenchymal enhancement⁵ or CSF enhancement⁴ after contrast administration has been shown to be more frequently present in acute stroke patients who develop HT. Direct measurement of BBB permeability (BBBP) using CT-perfusion (CTP) has also been attempted.⁶⁻¹⁴

A relatively simple and frequently applied model to calculate BBBP is the Patlak model.^{15,16} Applying this model to CTP data^{6,9-13} means using arterial and parenchymal contrast enhancement curves to calculate the rate of contrast transfer from an intravascular to an extravascular compartment, which is a measure of BBBP. In several of the referenced studies on CTP, the Patlak model was applied to the first-pass of the contrast injection necessary for CTP.^{9,10,12} However, the original description of the Patlak model¹⁶ clearly states that it can be applied only once a steady state phase of contrast transfer between the compartments has been reached and the graphical analysis of the Patlak model becomes linear. The Patlak model and its assumptions are described in the Appendix.

The purpose of this study was to assess whether the first-pass or the delayed phase of a contrast bolus injection better respects the assumptions of linearity of the Patlak model for the assessment of blood-brain barrier permeability (BBBP) in acute stroke and non-stroke patients using CT-perfusion (CTP).

Methods

Design

Imaging data obtained as part of standard clinical stroke care at our institution were retrospectively reviewed with the approval of the institutional review board. At our institution, patients with suspicion of acute stroke and no history of significant renal insufficiency or contrast allergy routinely undergo a stroke CT survey including: noncontrast CT (NCT) of the brain, CTP at two cross-sectional positions, CT-angiogram (CTA) of the cervical and intracranial vessels, and post-contrast cerebral CT, obtained in this chronological sequence.

We retrospectively identified a consecutive series of 130 patients admitted to UCSF Medical Center from January 2006 to June 2007 who met the following inclusion criteria: (a) admission to the emergency room with signs and symptoms suggesting hemispheric stroke within 12 hours after symptom onset; and (b) no evidence of intracerebral hemorrhage on the admission NCT. Patients' charts were reviewed for demographic and clinical data.

Imaging protocol

CTP studies were obtained on 16-slice (95 patients) and 64-slice (35 patients) CT scanners. Each CTP study involved successive gantry rotations performed in cine mode during intravenous administration of iodinated contrast material. Images were acquired and reconstructed at a temporal sampling rate of 1 image per second for the first 45 seconds. Additional gantry rotations were obtained at 60, 90, 120, 150 and 180 seconds. Acquisition parameters were 80 kVp and 100 mAs. Two successive CTP series at two different levels were performed following the non-contrast CT and prior to the CTA. At each CTP level, 4 5-mm-thick slices (16-slice CT scanners) or 8 5-mm-thick slices (64-slice CT scanners) were assessed. The first CTP series was obtained at the level of the third ventricle and the basal ganglia and the second CTP series above the lateral ventricles. For each CTP series, a 40 ml bolus of iohexol (Omnipaque, Amersham Health, Princeton, NJ; 300 mg/ml of iodine) was administered into an antecubital vein using a power injector at an injection rate of 5 ml per second for all patients. CT scanning was initiated 7 seconds after start of the injection of the contrast bolus. Because there are no established measurements on how BBBP measurements from the second series are influenced by the contrast bolus of the first series, the second CTP series was not used for the purpose of this study.

Image post-processing

CTP data were analyzed utilizing CTP software developed by Philips Medical Systems (Cleveland, OH). This software relies on the central volume principle, which is the most accurate for low injection rates of iodinated contrast material¹⁷. The software obtains mathematical descriptions of the time-density curves for each pixel, by applying curve fitting by least mean squares, after correcting for motion and noise reduction through an anisotropic, edge-preserving spatial filter. A closed-form (non-iterative) deconvolution is then applied to calculate the mean transit time (MTT) map.¹⁸ The deconvolution operation requires a reference arterial input function (most often within the anterior cerebral artery), automatically selected by the CTP software within a region of interest drawn by the user. The cerebral blood volume (CBV) map is calculated from the area under the time-density curves.¹⁹ The CTP infarct core and salvageable brain tissue are automatically calculated by the software using MTT and CBV reported in the literature as the most accurate (CT-perfusion salvageable brain tissue: $MTT > 145\%$ of the contralateral side values plus $CBV \geq 2.0$ ml/100g; CT-perfusion infarct core: $MTT > 145\%$ of the contralateral side values plus $CBV < 2.0$ ml/100g).²⁰

BBBP measurements were extracted from CTP data using a second, prototype software developed by Philips Medical Systems. This software is based on the Patlak model,¹⁶ which is described in detail in the Appendix. Applying the Patlak model to CTP involves performing linear regression using data calculated from the CTP datasets. The slope of these regression lines is used as an indicator of BBBP. The prototype software used for this study allowed us to performed linear regression separately for CTP data from the first-pass and from the delayed phase

of the contrast injection. The cut-off point between the first-pass and the delayed phase was automatically detected by the software.

Two variables measuring the quality of the linear fit were used to quantify how well the assumptions of the Patlak model were met by data extracted from the first-pass and the delayed phase of the CTP acquisition. One of these variables is the square root mean squared error, which is a measure of variability of data points around a straight line: a value close to 0 indicates a smaller spread of data points around the line, corresponding to a better fit. The other variable is the correlation coefficient (R), which measures the strength of a linear relationship: an R value closer to 1 indicates stronger linearity.

Slopes, square root mean squared errors (VMSE), and correlation coefficients (R) were measured in regions of interest (ROIs) corresponding to vascular territories, drawn on each CTP slice. For the purpose of the statistical analysis, ROIs located within non-ischemic brain parenchyma (both in stroke and non-stroke patients) were distinguished from ROIs in ischemic brain parenchyma (only present in stroke patients). ROIs in ischemic hemisphere in stroke patients ("ischemic" ROIs) matched the areas delineated as abnormal (infarct core or salvageable brain tissue) by the software using the thresholds listed above. ROIs located within bilateral hemispheres in non-stroke patients and in non-ischemic hemisphere in stroke patients ("non-ischemic" ROIs) were drawn on an anatomical basis (cortical gray matter, white matter, basal ganglia).

Statistical analysis

Slopes, VMSE and R extracted from first-pass and delayed phase of CTP acquisitions in ischemic and non-ischemic ROIs were compared using generalized estimating equations (GEE) models with robust variance estimation, with fixed effects for patients, type of CT scanner and type of ROIs. Because the distribution of the parameters were not normal but skewed, rather than reporting simple means we described estimated mean values of the slopes (obtained by log transformation of the data), VMSE and R from fitting clustered log values. For all values, 95% confidence intervals (CI) were also calculated.

Results

Patients and imaging studies

One hundred and thirty patients matched our inclusion criteria. 29 of these patients showed an acute ischemic hemispheric stroke on their CTP studies and 101 did not have evidence of any abnormalities (non-stroke patients). Final diagnoses in non-stroke patients were: transient ischemic attacks in 12, vertigo in 9, migraine in 7, other neurological disorder in 9, adverse drug reaction in 3, other non-neurological disorders in 12, undetermined in 49. Five patients were excluded from the non-stroke group, because of CTP data that could not be analyzed due to motion artifacts or improper timing of contrast bolus injection. The patient characteristics of both groups are summarized in *Table 1*. In stroke patients, the median time from symptom onset to CTP was 3 hours (range: 1.5 – 12). The radia-

tion dose for the prolonged CTP acquisition protocol (cine mode for 45 seconds, followed by additional gantry rotations at 60, 90, 120, 150 and 180 seconds) was 10% (0.25 mSv) greater than the radiation dose of the conventional CTP protocol (cine mode for 45 seconds with no additional rotations).

The Patlak analyses for the 29 stroke patients and 96 non-stroke patients were performed in a total number of 290 ischemic ROIs and 1560 non-ischemic ROIs.

Table 1 Patient characteristics

	Stroke patients	Non-stroke patients
No. of patients	29	96
No. of men (%)	13 (45%)	42 (44%)
Median age (years)	median = 72 interquartile range = 66 - 82 range = 52 - 93	median = 55 interquartile range = 45 - 70 range = 17 - 91
Time from stroke to CTP (hours)	median = 3 interquartile range = 2 - 6 range = 1.5 - 12	median = 3.5 interquartile range = 2 - 7 range = 1 - 12
Stroke location:		
ACA & MCA territories	3	
MCA territory	24	
ACA territory	2	
PCA territory	0	

ACA = anterior cerebral artery; MCA = middle cerebral artery; PCA = posterior cerebral artery.

Table 2 Estimated means and 95% confidence intervals of BBBP measurements according to the Patlak model, and the parameters describing the quality of the linear regression. A square root mean squared error ($\sqrt{\text{MSE}}$) close to 0 indicates a smaller spread of data points around the line, corresponding to a better fit. A correlation coefficient (R) close to 1 indicates a stronger linearity.

	First Pass	Delayed phase	p-value
Ischemic ROIs			
(N = 290)			
BBBP (95% CI)	7.63 (4.78-12.19)	1.31 (1.03-1.68)	<0.001
$\sqrt{\text{MSE}} * 10^3$ (95% CI)	0.59 (0.36-0.96)	0.089 (0.073-0.11)	<0.001
R (95% CI)	0.53 (0.46-0.61)	0.69 (0.59-0.78)	<0.001
Non-ischemic ROIs			
(N = 1560)			
BBBP (95% CI)	2.81 (2.42-3.27)	1.05 (0.97-1.14)	<0.001
$\sqrt{\text{MSE}} * 10^3$ (95% CI)	0.18 (0.14-0.24)	0.041 (0.035-0.048)	<0.001
R (95% CI)	0.57 (0.52-0.61)	0.85 (0.81-0.88)	<0.001

ROI = regions of interest, BBBP = blood-brain barrier permeability, $\sqrt{\text{MSE}}$ = square root mean squared error, R = correlation coefficient, CI = confidence interval

BBBP measurements and parameters describing the quality of the linear regression according to the Patlak model

Compared to BBBP values from the delayed, steady-state phase BBBP values calculated from the first-pass were 5.8 (CI 3.3-10.1) times higher in ischemic ROIs, and 2.7 (CI 2.3-3.1) times higher in non-ischemic ROIs (*Table 2 & Figure 1*). Confidence intervals for the first-pass BBBP measurements were considerably larger than those from the delayed phase. For both the delayed phase and the first-pass, BBBP values were significantly higher ($p < 0.05$) in ischemic ROIs compared to non-ischemic ROIs.

The quality of the linear fit as part of the application of the Patlak model to the CTP data was significantly better for the delayed phase compared to the first-pass, with significantly lower $\sqrt{\text{MSE}}$ values and higher correlation coefficients (R) (*Table 2*). $\sqrt{\text{MSE}}$ values from the delayed phase were 6.6 (CI 4.1-10.6) times lower than corresponding values from the first-pass in ischemic ROIs, and 4.5 (CI 3.4-5.9) times lower in non-ischemic ROIs. Correlation coefficients (R) from the delayed phase were 1.29 (CI 1.11 – 1.47) times higher than corresponding values from the first-pass in ischemic ROIs, and 1.50 (CI 1.36 – 1.63) times higher in non-ischemic ROIs.

Discussion

The Patlak model^{15,16} is a relatively simple and frequently applied model to calculate BBBP and can be used to extract BBBP measurements from CTP data.^{6,9-13} BBBP is calculated from the slope of a graphical analysis (the Patlak plot) of parenchymal and arterial enhancement curves to calculate BBBP values, provided that the plot is linear. Our analysis shows that only Patlak plots calculated from the delayed phase of CTP acquisition (and not from the first-pass) are linear and verify the assumptions of the Patlak model. The Patlak model can thus be applied to CTP only if a delayed phase (3 minutes in our protocol) is obtained. The selection of an appropriate, relatively low temporal resolution allows adequate reconstruction of the linear part of the Patlak plots, while minimizing the additional radiation dose to the patients (10% in our protocol).

The absence of linearity of Patlak plots constructed from first-pass data indicates that first-pass data do not respect the Patlak model assumptions. BBBP measurements extracted from the first-pass model using the Patlak model are thus inaccurate. This observation has important repercussions, since BBBP measurements obtained from first-pass were significantly higher (overestimated) compared to BBBP measurements from the delayed phase. It challenges the results and conclusions of all previous studies that used the Patlak model and applied it to first-pass CTP data.^{9,10,12}

The graphs in *Figure 1* demonstrate the non-linearity of the Patlak plots calculated from first-pass CTP data, primarily in the salvageable brain tissue. The enhancement in the salvageable brain tissue is clearly delayed compared to

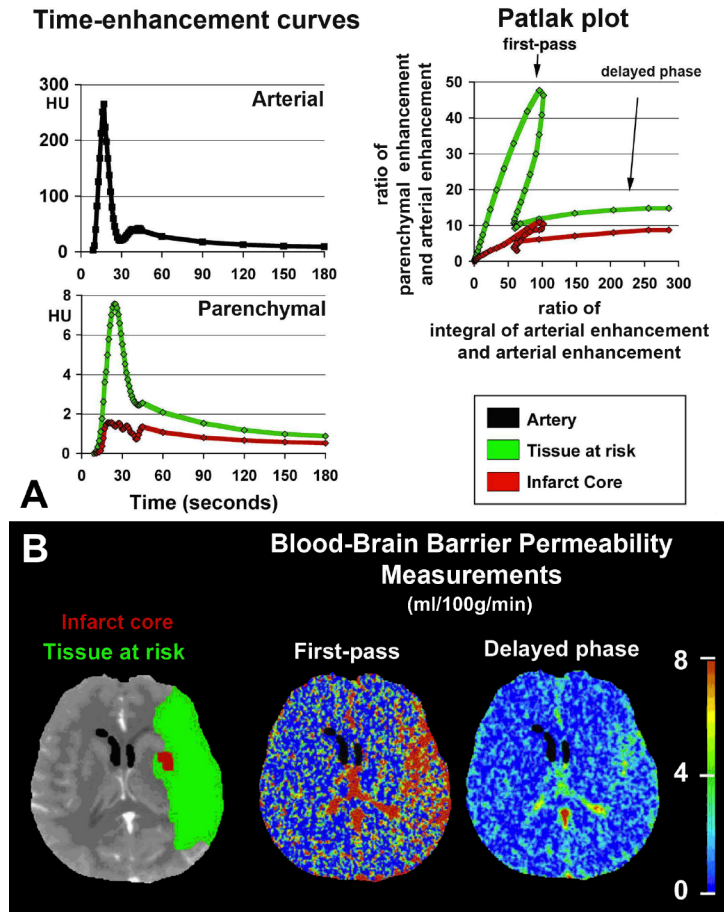


Figure 1 Graphical illustration of the calculation of blood-brain barrier permeability (BBBP) using the Patlak model. **(A)** The Patlak plots are constructed from the arterial and parenchymal time-enhancements curves. The first-pass component of the Patlak plots is clearly not linear, especially within the tissue at risk (shown in green in **(B)**), while the delayed phase respects the linear, steady-state assumption of the Patlak model. **(B)** BBBP maps, at the level of the basal ganglia, are shown. They are extracted from the Patlak plots and performed pixel-by-pixel. The first-pass BBBP map is noisier than delayed phase BBBP map because the quality of the linear fit is less, and results in BBBP values that are overestimated compared to the delayed phase BBBP values. This is true again especially within the tissue at risk (shown in green). The CTP infarct core (shown in red) and at risk brain tissue (shown in green) are automatically calculated by the software using MTT and CBV reported in the literature as the most accurate (CT-perfusion salvageable brain tissue: $MTT > 145\%$ of the contralateral side values plus $CBV \geq 2.0$ ml/100g; CT-perfusion infarct core: $MTT > 145\%$ of the contralateral side values plus $CBV < 2.0$ ml/100g).²⁰ For colorfigure see page 232

the arterial enhancement, reflecting the fact that the salvageable brain tissue receives its blood supplies from collaterals.²¹ The intensity of the enhancement in the salvageable brain tissue, on the other hand, is preserved, or even increased.²⁰ In salvageable brain tissue the delay in enhancement together with the relatively high enhancement cause the Patlak plot to rise steeply during the first-pass and to recede just as steeply at the end of the first-pass. A linear regression can be performed, but is meaningless as the steep line fitted to the first-pass data results from half of the points going down instead of up, and merely reflects a delay in enhancement. Permeability maps extracted from first-pass CTP data are thus actually images of delayed, increased contrast enhancement (as typically encountered in the salvageable brain tissue) rather than true images of BBBP. The same observations apply to Patlak plots extracted from first-pass CTP data in the infarct core, but the changes are not as dramatic, for there is hardly any blood arriving either through the occluded vessel or through collaterals.²¹ As a result, BBBP values measured from the first-pass and from the delayed phase do not differ as much in the infarct core as they do in the salvageable brain tissue. We acknowledge the following limitations to this study. Firstly, the goal of the study was to evaluate how the Patlak model could be applied to CTP data. We did not assess other models that have been applied to CTP data to calculate BBBP, such as the distributed parameter model.^{7, 22} Future studies are needed to determine whether our conclusions regarding the delayed acquisition required to apply the Patlak model to CTP data, also hold true for these alternative models. Secondly, brain perfusion is very different in ischemic brain (low CBF, high MTT) and in non-ischemic brain (high CBF, low MTT). In previous studies addressing different topics such as reproducibility or quantitative accuracy of CTP results, ischemic brain has been considered separately from non-ischemic brain, based on the concept that the same variation in CTP measurements can result in different relative errors when applied to different CTP values. Following this standard approach, we compared first-pass and delayed phase both in “ischemic ROIs” (with low brain perfusion) and in “non-ischemic” (with preserved perfusion). Finally, we limited our analysis to the first CTP bolus, and we did not include data from the second CTP bolus obtained routinely as part of our stroke CT protocol. This was motivated by the lack of research on the impact of the first bolus of contrast on the measurements of BBBP values from the second bolus. Saturation of the parenchymal compartment by the contrast from the first bolus could theoretically decrease the amount of contrast extravasation during the second bolus, and the corresponding BBBP measurements. Such theoretical considerations will need to be verified by additional appropriate studies.

Conclusion

Only the delayed phase of the CTP acquisition (and not the first-pass) respects the assumptions of the Patlak model. BBBP measurements extracted from first-pass CTP data overestimate BBBP values obtained from the delayed phase. Further research is required to investigate the relevance of delayed phase CTP BBBP values

in terms of predictive value for hemorrhagic transformation in acute stroke patients, however, it can be concluded that first-pass data from CTP studies should not be used to calculate BBB permeability in patients with acute stroke.

Appendix

The model described by Patlak et al.^{15, 16} is a theoretical model of blood-brain exchange. It is a multi-compartment model that assumes the unidirectional transfer of a tracer from a reversible (arterial) compartment to an irreversible tissue compartment (in this case the brain parenchyma) for a certain period of time. Transfer of tracer is assumed to be unidirectional when a steady-state phase is reached between reversible compartments (intravascular space and the blood-brain barrier complex). Such a steady-state phase can only occur after the initial, rapid changes in tracer concentration have subsided, so the arterial concentration changes slowly enough for the tissue compartment to follow.

The graphical representation of the Patlak model is called Patlak plot (*Figure 1*). When the Patlak plot is linear, unidirectional transfer is said to be present. The slope of the plot indicates the rate of transfer between the reversible and the irreversible compartments. When applied to CTP, the Patlak model uses iodinated contrast as the tracer, and takes advantage of the Hounsfield density to be directly proportional to the iodinated contrast concentration. Enhancement within the arterial input function (reversible compartment) and within the parenchyma (irreversible compartment) over time is used to construct the Patlak plot. The plot is described by the following equation:

$$T(t) / A(t) = Ki \times \left(\int_0^t A(t) dt \right) / A(t) + V$$

In this equation $T(t)$ is the tissue enhancement at time t ; $A(t)$ is the arterial enhancement at time t ; Ki is the rate constant of net contrast transfer; and V is the distribution volume, which is typically considered to be equal to the cerebral blood volume (CBV) in the considered region of interest (ROI). The ratio of $T(t)$ to $A(t)$, which is plotted on the y-axis, is called “apparent distribution volume”. The ratio of the *integral* of $A(t^0 \leq t \leq t')$ to $A(t)$, which is plotted on the x-axis, is called “normalized plasma integral”. The slope of a regression line fit to the linear part of the Patlak plot is an approximation of Ki (the rate of transfer) at that time. This value represents the amount of accumulated tracer in relation to the amount of tracer that has been available in plasma, and is a measurement of BBBP, expressed in ml/100g/min. The y-axis intercept is equal to the CBV. An example of a Patlak plot can be seen in *Figure 1*.

References

1. Berger C, Fiorelli M, Steiner T, Schabitz WR, Bozzao L, Bluhmki E, Hacke W, von KR. Hemorrhagic transformation of ischemic brain tissue: Asymptomatic or symptomatic? *Stroke*. 2001;32:1330-1335
2. Hacke W, Donnan G, Fieschi C, Kaste M, von KR, Broderick JP, Brott T, Frankel M, Grotta JC, Haley EC, Jr., Kwiatkowski T, Levine SR, Lewandowski C, Lu M, Lyden P, Marler JR, Patel S, Tilley BC, Albers G, Bluhmki E, Wilhelm M, Hamilton S. Association of outcome with early stroke treatment: Pooled analysis of atlantis, ecast, and ninds rt-pa stroke trials. *Lancet*. 2004;363:768-774
3. Wang X, Lo EH. Triggers and mediators of hemorrhagic transformation in cerebral ischemia. *MolNeurobiol*. 2003;28:229-244
4. Latour LL, Kang DW, Ezzeddine MA, Chalela JA, Warach S. Early blood-brain barrier disruption in human focal brain ischemia. *AnnNeurol*. 2004;56:468-477
5. Kim EY, Na DG, Kim SS, Lee KH, Ryoo JW, Kim HK. Prediction of hemorrhagic transformation in acute ischemic stroke: Role of diffusion-weighted imaging and early parenchymal enhancement. *AJNR AmJNeuroradiol*. 2005;26:1050-1055
6. Bartolini A, Gasparetto B, Furlan M, Sullo L, Trivelli G, Albano C, Roncallo F. Functional perfusion and blood-brain barrier permeability images in the diagnosis of cerebral tumors by angio ct. *Comput Med Imaging Graph*. 1994;18:145-150
7. Bisdas S, Hartel M, Cheong LH, Koh TS. Detection of early vessel leakiness in acute ischemic stroke using computed tomography perfusion may indicate hemorrhagic transformation. *Acta Radiol*. 2007;48:341-344
8. Bisdas S, Hartel M, Cheong LH, Koh TS, Vogl TJ. Prediction of subsequent hemorrhage in acute ischemic stroke using permeability ct imaging and a distributed parameter tracer kinetic model. *JNeuroradiol*. 2007;34:101-108
9. Cianfoni A, Cha S, Bradley WG, Dillon WP, Wintermark M. Quantitative measurement of blood-brain barrier permeability using CT-perfusion in extra-axial brain tumors. *J Neuroradiol*. 2006;33:164-168
10. Goh V, Halligan S, Bartram CI. Quantitative tumor perfusion assessment with multidetector ct: Are measurements from two commercial software packages interchangeable? *Radiology*. 2007;242:777-782
11. Leggett DA, Miles KA, Kelley BB. Blood-brain barrier and blood volume imaging of cerebral glioma using functional ct: A pictorial review. *Eur J Radiol*. 1999;30:185-190
12. Lin K, Kazmi KS, Law M, Babb J, Peccerelli N, Pramanik BK. Measuring elevated microvascular permeability and predicting hemorrhagic transformation in acute ischemic stroke using first-pass dynamic perfusion ct imaging. *AJNR AmJNeuroradiol*. 2007;28:1292-1298
13. Yeung WT, Lee TY, Del Maestro RF, Kozak R, Brown T. In vivo ct measurement of blood-brain transfer constant of iopamidol in human brain tumors. *J Neurooncol*. 1992;14:177-187
14. Bisdas S, Yang X, Lim CC, Vogl TJ, Koh TS. Delineation and segmentation of cerebral tumors by mapping blood-brain barrier disruption with dynamic contrast-enhanced ct and tracer kinetics modeling-a feasibility study. *Eur Radiol*. 2008;18:143-151
15. Patlak CS, Blasberg RG. Graphical evaluation of blood-to-brain transfer constants from multiple-time uptake data. Generalizations. *J Cereb Blood Flow Metab*. 1985;5:584-590
16. Patlak CS, Blasberg RG, Fenstermacher JD. Graphical evaluation of blood-to-brain transfer constants from multiple-time uptake data. *J Cereb Blood Flow Metab*. 1983;3:1-7

17. Wintermark M, Maeder P, Thiran JP, Schnyder P, Meuli R. Quantitative assessment of regional cerebral blood flows by perfusion ct studies at low injection rates: A critical review of the underlying theoretical models. *Eur Radiol.* 2001;11:1220-1230
18. Axel L. Tissue mean transit time from dynamic computed tomography by a simple deconvolution technique. *Invest Radiol.* 1983;18:94-99
19. Ladurner G, Zilkha E, Iliff D, du Boulay GH, Marshall J. Measurement of regional cerebral blood volume by computerized axial tomography. *JNeurolNeurosurgPsychiatry.* 1976;39:152-158
20. Wintermark M, Flanders AE, Velthuis B, Meuli R, van Leeuwen M, Goldsher D, Pineda C, Serena J, van der Schaaf I, Waaijer A, Anderson J, Nesbit G, Gabriely I, Medina V, Quiles A, Pohlman S, Quist M, Schnyder P, Bogousslavsky J, Dillon WP, Pedraza S. CT-perfusion assessment of infarct core and penumbra: Receiver operating characteristic curve analysis in 130 patients suspected of acute hemispheric stroke. *Stroke.* 2006;37:979-985
21. Tan JC, Dillon WP, Liu S, Adler F, Smith WS, Wintermark M. Systematic comparison of CT-perfusion and ct-angiography in acute stroke patients. *Ann Neurol.* 2007;61:533-543
22. Johnson JA, Wilson TA. A model for capillary exchange. *Am J Physiol.* 1966;210:1299-1303



Accuracy and anatomical coverage of CT-perfusion assessment of blood-brain barrier permeability: one bolus versus two boluses



9

*J.W. Dankbaar, J. Hom, T. Schneider S.C. Cheng, B.C. Lau¹, I.C. van der Schaaf, S. Virmani,
S. Pohlman, W.P. Dillon, M. Wintermark*

Cerebrovasc Dis. 2008;26(6):600-5.

Abstract

Background and purpose

To assess whether blood-brain barrier permeability (BBBP) values extracted with the Patlak model from the second CT-perfusion (CTP) contrast bolus, are significantly lower than the values extracted from the first bolus in the same patient.

Methods

125 consecutive patients (29 with acute hemispheric stroke and 96 without stroke) who underwent a CTP study using a prolonged acquisition time up to 3 minutes were retrospectively identified. As an indicator of BBBP we used the slope of a regression line fit to Patlak plots obtained in multiple regions of interest drawn in ischemic brain tissue and in non-ischemic brain tissue. Square root mean squared errors ($\sqrt{\text{MSE}}$) and correlation coefficients (R) were used to describe the quality of the linear regression model. This was performed separately for the first and the second CTP bolus. Results from the first and the second bolus were compared in terms of BBBP values and the quality of the linear model fitted to the Patlak plot, using generalized estimating equations with robust variance estimation.

Result

BBBP values from the second bolus were not lower than BBBP values from the first bolus in either non-ischemic brain tissue (estimated mean with 95% CI: 1.42 (1.10-1.82) ml/100g/min for the first bolus versus, 1.64 (1.31-2.05) ml/100g/min for the second bolus, $p=1.00$) or in ischemic tissue (1.04 (0.97-1.12) ml/100g/min for the first bolus versus 1.19 (1.11-1.28) ml/100g/min for the second bolus, $p=0.79$). Compared to regression models from the first bolus, the Patlak regression models obtained from the second bolus were of similar or slightly better quality. This was true both in non-ischemic and ischemic brain tissue.

Conclusion

The contrast material from the first bolus of contrast for CTP does not negatively influence measurements of BBBP values from the second bolus. The second bolus can thus be used to increase anatomical coverage of BBBP assessment using CTP.

Introduction

Brain CT-perfusion (CTP) is currently used for the evaluation of patients with symptoms of acute stroke^{1,2} where it helps to identify infarct core and brain tissue at risk for infarction.³⁻⁷ More recently, CTP data were also used to characterize blood-brain barrier permeability (BBBP),⁸⁻¹⁰ in an effort to predict which stroke patients are going to develop hemorrhagic transformation.

A well-known limitation of CTP is its limited anatomic coverage, which is typically 2-4 cm. One of the approaches to overcome this limitation is to scan at two consecutive levels with two separate contrast bolus injections.¹¹ In terms of BBBP measurements, it was suggested in a recent study⁹ that the contrast material from the first bolus, could saturate the interstitial compartment, by extravasating from the vascular compartment to the interstitial compartment. Theoretically this would impede further extravasation of contrast during the second bolus. BBBP values calculated from the second bolus would then turn out to be lower than they are in reality.

The goal of this study was to assess whether BBBP values extracted with the Patlak model from the second CTP contrast bolus, are lower than the values extracted from the first bolus in stroke and non-stroke patients.

Methods

Design

Imaging data obtained as part of standard clinical stroke care at our institution were retrospectively reviewed with the approval of the institutional review board. At our institution, patients with suspicion of acute stroke and no history of significant renal insufficiency or contrast allergy routinely undergo a stroke CT survey including: non-contrast CT (NCT) of the brain, CTP at two cross-sectional positions, CT-angiogram (CTA) of the cervical and intracranial vessels, and post-contrast cerebral CT, obtained in this chronological sequence.

We retrospectively identified a consecutive series of 130 patients admitted to UCSF Medical Center from January 2006 to June 2007 who met the following inclusion criteria: (a) admission to the emergency room with signs and symptoms suggesting hemispheric stroke within 12 hours after symptom onset; and (b) no evidence of intracerebral hemorrhage on the admission NCT. Presence of acute hemispheric stroke was evaluated by using the admission NCT, CTP and CTA studies. Absence of stroke was confirmed with follow up MR or CT imaging. Patients' charts were reviewed for demographic and clinical data and final diagnosis on discharge.

Imaging protocol

Each CTP study involved successive gantry rotations performed in cine mode during intravenous administration of iodinated contrast material. Images were acquired and reconstructed at a temporal sampling rate of 1 image per second for the first 45 seconds. Additional gantry rotations were obtained at 60, 90, 120, 150

and 180 seconds. Acquisition parameters were 80 kVp and 100 mAs. Two successive CTP series at two different levels were performed following the non-contrast CT and prior to the CTA. The first CTP series was obtained at the level of the third ventricle and the basal ganglia; and the second CTP series above the lateral ventricles. For each CTP series, a 40 ml bolus of iohexol (Omnipaque, Amersham Health, Princeton, NJ; 300 mg/ml of iodine) was administered into an antecubital vein using a power injector at an injection rate of 5 ml per second for all patients. The interval between both bolus injections was approximately 4 minutes. CT scanning was initiated 7 seconds after start of the injection of the contrast bolus.

Image post-processing

CTP data were analyzed utilizing CTP software developed by Philips Medical Systems (Cleveland, OH). This software relies on the central volume principle, which is the most accurate for low injection rates of iodinated contrast material.¹² After motion correction and noise reduction by an anisotropic, edge-preserving spatial filter, the software applies curve fitting by least mean squares to obtain mathematical descriptions of the time-density curves for each pixel. A closed-form (non-iterative) deconvolution is then applied to calculate the mean transit time (MTT) map.¹³ The deconvolution operation requires a reference arterial input function (most often within the anterior cerebral artery), automatically selected by the CTP software within a region of interest drawn by the user. The cerebral blood volume (CBV) map is calculated from the area under the time-density curves.¹⁴ The CTP infarct core and brain tissue at risk are automatically calculated by the software using CBV and MTT thresholds reported in the literature as the most accurate (CT-perfusion tissue at risk: $MTT > 145\%$ of the contralateral side values, $CBV \geq 2.0$ ml/100g; CT-perfusion infarct core: $MTT > 145\%$ of the contralateral side values, $CBV < 2.0$ ml/100g).⁵

BBBP measurements were extracted from CTP data using a second, prototype software developed by Philips Medical Systems. This software is based on the Patlak model.^{9,15} Applying the Patlak model to CTP involves performing a linear regression using data calculated from the delayed phase (not first-pass) of the CTP datasets.⁹ The slopes of the acquired regression lines are used as an indicator of BBBP. Two variables measuring the quality of the linear fit were used to assess whether the CTP data from the second bolus met the assumptions of the Patlak model just as well as CTP data from the first bolus: 1) the square root mean squared errors (\sqrt{VMSE}) are a measure of variability around a straight line: a value close to 0 indicates a smaller spread of datapoints around the line, corresponding to a better fit; 2) the correlation coefficients (R) measure the strength of a linear relationship: an R value closer to 1 indicates a stronger linearity. Slopes, \sqrt{VMSE} and R were measured in regions of interest (ROIs) corresponding to vascular territories, drawn on each CTP slice. For the purpose of the statistical analysis ROIs located within non-ischemic brain parenchyma (both in stroke and non-stroke patients) were distinguished from ROIs in ischemic brain parenchyma (i.e. infarct core and tissue at risk, only present in stroke patients).

Statistical analysis

The three parameters, slopes, $\sqrt{\text{MSE}}$ and R, extracted from CTP data from the first and the second bolus in ischemic and non-ischemic ROIs were compared using generalized estimating equations (GEE) models with robust variance estimation. The tested null hypotheses were that BBBP measurements (slopes) were not lower for the second bolus compared to the first bolus, and that linear regression fitting was not worse (higher square root mean squared errors - $\sqrt{\text{MSE}}$ - and lower correlation coefficients - R) for the second bolus compared to the first bolus. Because the distribution of the three mentioned parameters were not normal but skewed, estimated mean values were reported rather than simple means. For all values, 95% confidence intervals (CI) were also calculated.

Results

Patients and imaging studies

One hundred and thirty patients matched our inclusion criteria. 29 of these patients had an acute ischemic hemispheric stroke and 101 did not have any abnormalities on their CTP studies (non-stroke patients). Final diagnoses in non-stroke patients were: transient ischemic attacks in 12, vertigo in 9, migraine in 7, other neurological disorder in 9, adverse drug reaction in 3, other non-neurological disorders in 12, undetermined in 49. In these 101 patients, the absence of hemispheric, ischemic stroke or major hemispheric abnormality was confirmed on follow-up CT or MR imaging, and clinical work-up. 5 patients were excluded from the non-stroke group, because of CTP data that could not be analyzed due to motion artifacts or improper timing of contrast bolus injection. The patient characteristics of the 29 stroke and the 96 non-stroke patients are summarized in *Table 1*. The radiation dose for the prolonged CTP acquisition (cine mode over 45 seconds, then additional gantry rotations at 60, 90, 120, 150 and 180 seconds) was only 10% (0.25 mSv) higher than the dose for the conventional CTP protocol (cine mode over 45 seconds).

The Patlak analyses for the 29 stroke patients and 96 non-stroke patients were performed in a total number of 504 ischemic ROIs and 2194 non-ischemic ROIs.

BBBP measurements and parameters describing the quality of the linear regression according to the Patlak model

BBBP values were calculated from the slope of the regression line fit to the Patlak plots of (*Table 2, Figure 1*). BBBP values from the second bolus were not significantly lower than values calculated from the first bolus. This was true both in ischemic ($p=0.79$) and non-ischemic ROIs ($p=1.00$).

The quality of the linear regression, as part of the application of the Patlak model to the CTP data for BBBP measurement, was expressed in $\sqrt{\text{MSE}}$ and R (*Table 2*). $\sqrt{\text{MSE}}$ values from the second bolus were not higher (variability around the regression line was not worse) than values from the first bolus. This was true both in ischemic ROIs ($p=0.87$) and in non-ischemic ROIs ($p=0.63$). Correlation coef-

ficients (R) from the second bolus were not lower (linearity was not worse) than coefficients from the first bolus. This was true both in ischemic ROIs ($p=0.90$) and in non-ischemic ROIs ($p=0.99$).

Table 1 Patient demographics

	Stroke patients	Non-stroke patients
No. of patients	29	96
No. of men (%)	12 (43%)	42 (44%)
Median age (years)	median = 72 interquartile range = 66 - 82 range = 52 - 93	median = 55 interquartile range = 45 - 70 range = 17 - 91
Time from symptom to CTP (hours)	median = 3 interquartile range = 2 - 6 range = 1.5 - 12	median = 3.5 interquartile range = 2 - 7 range = 1 - 12
Stroke location:		
ACA & MCA territories	3	
MCA territory	24	
ACA territory	2	
PCA territory	0	

ACA = anterior cerebral artery; MCA = middle cerebral artery; PCA = posterior cerebral artery.

Table 2 Estimated means and 95% confidence intervals for the BBBP measurements according to the Patlak model, and the parameters describing the quality of the linear regression ($\sqrt{\text{MSE}}$, R), both for the first bolus (bolus 1) and the second bolus (bolus 2), in ischemic and non-ischemic ROIs. The square root mean squared error ($\sqrt{\text{MSE}}$) is a measure of variability around a straight line: a value close to 0 indicates a smaller spread of datapoints around the line, corresponding to a better fit. The correlation coefficient R measures the strength of a linear relationship: an R value closer to 1 indicates stronger linearity.

	Bolus 1	Bolus 2	p-value
Ischemic ROIs			
BBBP (95% CI)	1.42 (1.10-1.82)	1.64 (1.31-2.05)	0.79
Quality of linear regression:			
$\sqrt{\text{MSE}} * 10^4$ (95% CI)	0.96 (0.74-1.24)	0.73 (0.48-1.13)	0.87
R (95% CI)	0.69 (0.58-0.80)	0.79 (0.68-0.90)	0.90
Non-ischemic ROIs			
BBBP (95% CI)	1.04 (0.97-1.12)	1.19 (1.11-1.28)	1.0
Quality of linear regression:			
$\sqrt{\text{MSE}} * 10^4$ (95% CI)	0.42 (0.35-0.49)	0.41 (0.33-0.49)	0.63
R (95% CI)	0.84 (0.81-0.87)	0.87 (0.84-0.90)	0.99

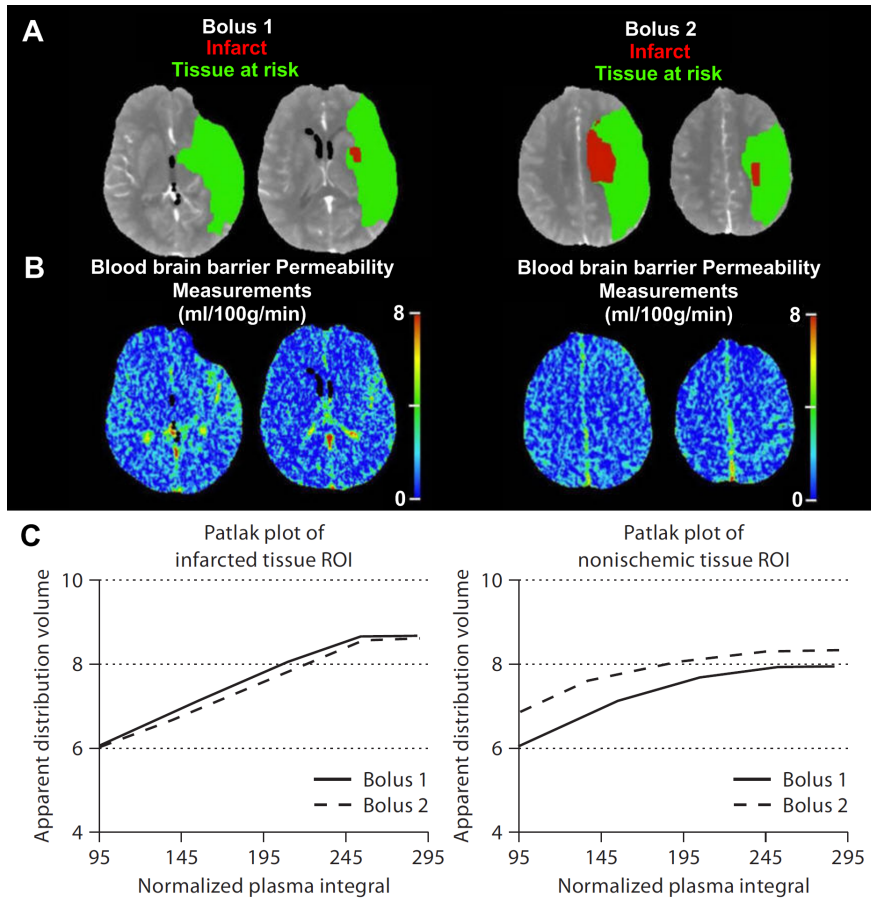


Figure 1 Example of graphical illustration of blood-brain barrier permeability (BBBP), calculated from the slope of a regression line fit to the Patlak plot: (A) CTP infarct core and tissue at risk threshold maps; (B) BBBP color maps, BBBP values from the second bolus (bolus 2) were not lower than the values from the first bolus (bolus 1); (C) Patlak plots that were constructed from arterial and parenchymal time-enhancements curves, in an infarcted tissue ROI and a non-ischemic tissue ROI. These Patlak plots illustrate how small the differences in slope (BBBP) and linearity between bolus 1 and 2 are. Of note, the slope of the plot from the infarcted tissue ROI is steeper than the slope of the non-ischemic tissue ROI. *For colorfigure see page 233*

Discussion

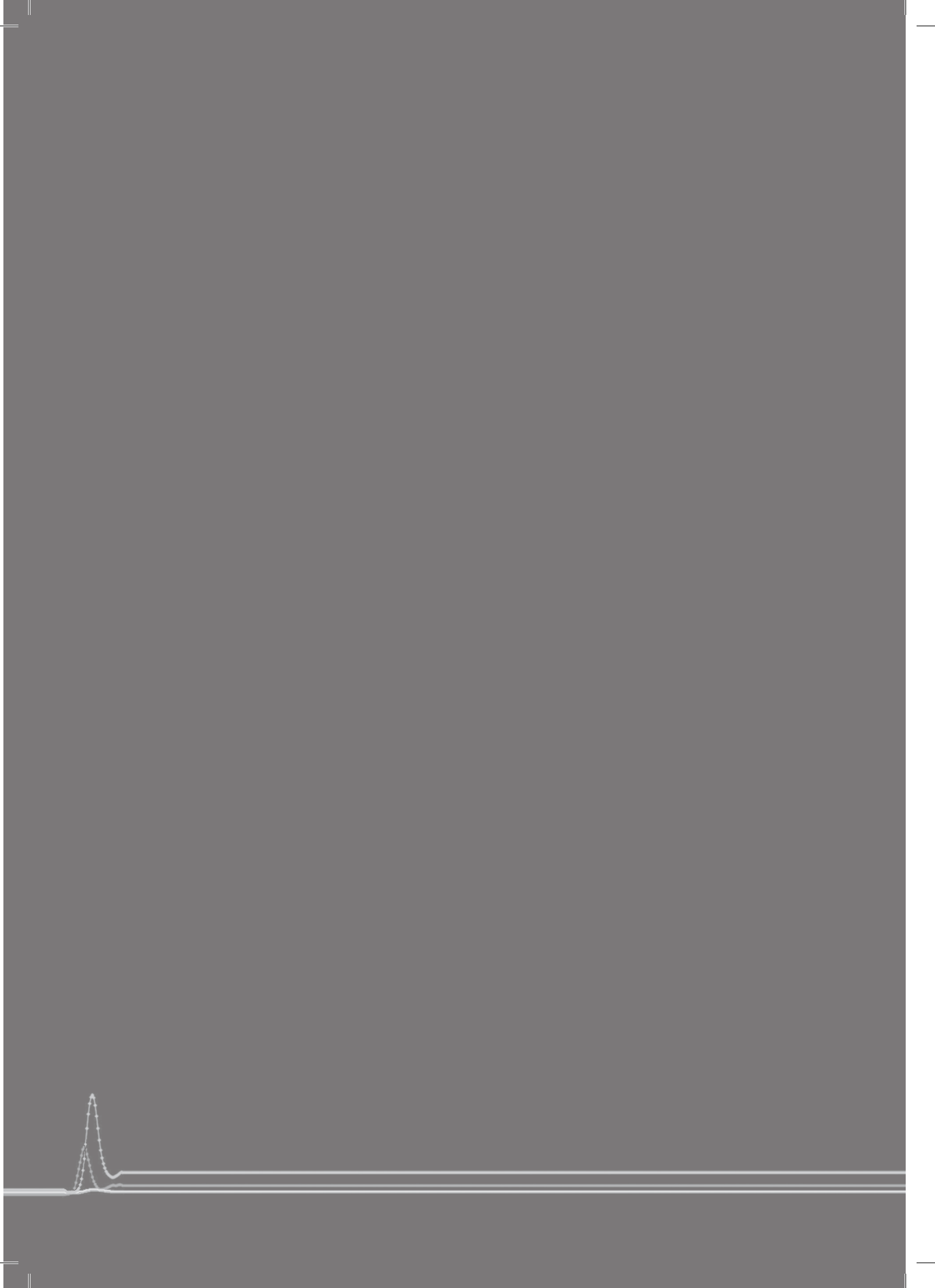
Recently, there has been an interest in using CTP imaging to assess BBBP alterations that may be a predisposing condition for hemorrhagic transformation in acute stroke patients.^{8, 10} In the pursuit of this objective, whole brain coverage would be desirable, which in the case of CTP is achieved by obtaining two successive CTP series with two successive injections of a contrast bolus. In this study, we demonstrated that the contrast material injected for the first bolus does not interfere with the BBBP measurements from the second bolus. BBBP measurements from the second bolus are not lower than BBBP values measured from the first bolus. The assumptions of the Patlak model are met equally well by the two boluses. This was true both for the ischemic brain tissue and for the non-ischemic brain tissue. We acknowledge several limitations to our study. For evident ethical reasons related to radiation dose, it was not possible to image the same levels twice with the two consecutive CTP contrast boluses. Instead, we decided to compare two boluses obtained at two different levels of the brain using generalized estimating equations (GEE) models with robust variance estimation, to account for within-patient correlations in addition to fixed effects for the two boluses, ischemic/nonischemic ROIs and their interaction. The different anatomical levels of the two CTP series could have influenced the amount of ischemic brain tissue in each of them (because of differences in gray-white matter ratio, hemodynamics, collaterals, etc), which in turn could have influenced the comparison between the two boluses in terms of BBBP values. However, the quality of the linear regression required by the Patlak model was not different for the two boluses, and the values from the second bolus were not lower than those from the first bolus, both in the non-ischemic and in the ischemic brain parenchyma. Finally, we limited our analysis to the Patlak model. The goal of this study was to evaluate how the Patlak model could be applied to CTP data. We did not assess other models that have been applied to CTP data to calculate BBBP, such as the distributed parameter model.^{8, 16} Future studies are needed to determine whether our conclusions regarding the acceptable use of a second CTP bolus hold for these alternative models.

Conclusion

The contrast material from the first bolus of contrast for CTP does not negatively influence measurements of BBBP values of the second bolus. The second bolus can thus be used to increase anatomical coverage of BBBP assessment using CTP. Further research is required to investigate the relevance of these BBBP measurements in terms of their predictive value for hemorrhagic transformation in acute stroke patients.

References

1. Fisher M. The ischemic penumbra: Identification, evolution and treatment concepts. *Cerebrovasc Dis.* 2004;17 Suppl 1:1-6
2. Meuli RA. Imaging viable brain tissue with ct scan during acute stroke. *Cerebrovasc Dis.* 2004;17 Suppl 3:28-34
3. Nabavi DG, Dittrich R, Kloska SP, Nam EM, Klotz E, Heindel W, Ringelstein EB. Window narrowing: A new method for standardized assessment of the tissue at risk-maximum of infarction in ct based brain perfusion maps. *Neurol Res.* 2007;29:296-303
4. Kloska SP, Nabavi DG, Gaus C, Nam EM, Klotz E, Ringelstein EB, Heindel W. Acute stroke assessment with ct: Do we need multimodal evaluation? *Radiology.* 2004;233:79-86
5. Wintermark M, Flanders AE, Velthuis B, Meuli R, van Leeuwen M, Goldsher D, Pineda C, Serena J, van der Schaaf I, Waaijer A, Anderson J, Nesbit G, Gabriely I, Medina V, Quiles A, Pohlman S, Quist M, Schnyder P, Bogousslavsky J, Dillon WP, Pedraza S. Perfusion-ct assessment of infarct core and penumbra: Receiver operating characteristic curve analysis in 130 patients suspected of acute hemispheric stroke. *Stroke.* 2006;37:979-985
6. Parsons MW, Pepper EM, Bateman GA, Wang Y, Levi CR. Identification of the penumbra and infarct core on hyperacute noncontrast and perfusion ct. *Neurology.* 2007;68:730-736
7. Schaefer PW, Roccatagliata L, Ledezma C, Hoh B, Schwamm LH, Koroshetz W, Gonzalez RG, Lev MH. First-pass quantitative ct perfusion identifies thresholds for salvageable penumbra in acute stroke patients treated with intra-arterial therapy. *AJNR Am J Neuroradiol.* 2006;27:20-25
8. Bisdas S, Hartel M, Cheong LH, Koh TS, Vogl TJ. Prediction of subsequent hemorrhage in acute ischemic stroke using permeability ct imaging and a distributed parameter tracer kinetic model. *JNeuroradiol.* 2007;34:101-108
9. Dankbaar JW, Hom J, Schneider T, Cheng SC, Lau BC, van der Schaaf I, Virmani S, Pohlman S, Dillon WP, Wintermark M. Dynamic perfusion ct assessment of the blood-brain barrier permeability: First pass versus delayed acquisition. *AJNR Am J Neuroradiol.* 2008;29:1671-1676
10. Lin K, Kazmi KS, Law M, Babb J, Peccerelli N, Pramanik BK. Measuring elevated microvascular permeability and predicting hemorrhagic transformation in acute ischemic stroke using first-pass dynamic perfusion ct imaging. *AJNR Am J Neuroradiol.* 2007;28:1292-1298
11. Eastwood JD, Lev MH, Provenzale JM. Perfusion ct with iodinated contrast material. *AJR Am J Roentgenol.* 2003;180:3-12
12. Wintermark M, Maeder P, Thiran JP, Schnyder P, Meuli R. Quantitative assessment of regional cerebral blood flows by perfusion ct studies at low injection rates: A critical review of the underlying theoretical models. *Eur Radiol.* 2001;11:1220-1230
13. Axel L. Tissue mean transit time from dynamic computed tomography by a simple deconvolution technique. *Invest Radiol.* 1983;18:94-99
14. Ladurner G, Zilkha E, Iliff D, du Boulay GH, Marshall J. Measurement of regional cerebral blood volume by computerized axial tomography. *JNeuroNeurosurgPsychiatry.* 1976;39:152-158
15. Patlak CS, Blasberg RG, Fenstermacher JD. Graphical evaluation of blood-to-brain transfer constants from multiple-time uptake data. *JCerebBlood Flow Metab.* 1983;3:1-7
16. Johnson JA, Wilson TA. A model for capillary exchange. *Am J Physiol.* 1966;210:1299-1303



Age- and anatomy-related values
of blood-brain barrier permeability
measured with CT-perfusion in
non-stroke patients



10

*J.W. Dankbaar, J. Hom, T. Schneider, S.C. Cheng, B.C. Lau¹, I.C. van der Schaaf, S. Virmani,
S. Pohlman, W.P. Dillon, M. Wintermark*

J Neuroradiol. 2009 Oct;36(4):219-27.

Abstract

Background and purpose

The goal of this study was to determine blood-brain barrier permeability (BBBP) values, and possible variations related to age, gender, race, vascular risk factors and their treatment, and anatomy in non-stroke patients with CT-perfusion (CTP).

Methods

We retrospectively identified 96 non-stroke patients who underwent a CTP study using a prolonged acquisition time up to 3 minutes. Patients' charts were reviewed for demographic data, vascular risk factors and their treatment. The Patlak model was applied to calculate BBBP values in regions of interest drawn within the basal ganglia and the gray and white matter of the different cerebral lobes. Differences in BBBP values were analyzed using a multivariate analysis considering clinical variables and anatomy.

Results

Mean absolute BBBP values were 1.2 ml/100g/min, and relative BBBP/CBF values were 3.5%. Statistical differences between gray and white matter were observed, but were not clinically relevant. BBBP values were influenced by age, history of diabetes and/or hypertension, and aspirin intake.

Conclusion

This study reports ranges of BBBP values in non-stroke patients calculated from delayed phase CTP data using the Patlak model. These ranges will be useful to detect abnormal BBBP values when assessing patients with cerebral infarction for the risk of hemorrhagic transformation.

Introduction

Hemorrhagic transformation (HT) is a serious complication of ischemic stroke.¹ According to the combined data from six major stroke trials, severe hemorrhage with mass effect occurs in 4.8% of stroke patients treated with tPA within 3 hours after symptom onset and up to 6.4% in patients treated between 3-6 hours.² One of the contributing mechanisms to HT is damage to the blood-brain barrier (BBB).³ Early detection of a damaged BBB could potentially be used to identify patients who are more likely to develop HT, and might therefore represent a contraindication to acute reperfusion therapy.⁴ Dynamic CT-perfusion (CTP) is a well established tool in the evaluation of acute stroke. With this technique, irreversibly damaged brain tissue and brain tissue at risk can be identified.⁵⁻⁸ In addition, blood-brain barrier permeability (BBBP) can be derived from CTP data.⁹⁻¹⁵ A relatively simple and frequently applied model to calculate BBBP is the Patlak model.^{16, 17} Applying this model to CTP data^{9, 10, 12-15, 18} means using arterial and parenchymal contrast enhancement curves to calculate the rate of contrast transfer from an intravascular to an extravascular compartment, which is a measure of BBBP. In order to identify abnormal BBBP predicting hemorrhagic transformation in stroke patients, one must first know the normal range of BBBP values in a control non-stroke population.

The goal of this study was to determine BBBP values in non-stroke patients extracted from CTP, and possible variations related to age, gender, race, vascular risk factors and their treatment, and anatomy.

Methods

Design

Imaging data obtained as part of standard clinical stroke care at our institution were retrospectively reviewed with the approval of the institutional review board. At our institution, patients with suspicion of acute stroke and no history of significant renal insufficiency or contrast allergy routinely undergo a stroke CT survey including: noncontrast CT (NCT) of the brain, CTP at two cross-sectional positions, CT-angiogram (CTA) of the cervical and intracranial vessels, and post-contrast cerebral CT, obtained in this chronological sequence.

We retrospectively identified a consecutive series of 101 patients admitted to UCSF Medical Center from January 2006 to June 2007 who met the following inclusion criteria: (a) admission to the emergency room with signs and symptoms suggesting hemispheric stroke within 12 hours after symptom onset; (b) no evidence of hemispheric stroke, intracerebral hemorrhage or other brain abnormalities on the admission NCT, follow-up CT or MR imaging, or clinical work-up.

Patient characteristics

Patients' charts were retrospectively reviewed for demographic and clinical data of the day of admission as entered by the clinician. Information was collected on:

age, gender, race, history of hypertension, diabetes mellitus, hyperlipidemia or cardiac disease, alcohol use, tobacco use, use of aspirin and other non-steroidal anti-inflammatory drugs (NSAIDs), anticoagulants anti-hypertensive drugs, diabetes treatment, statins and/or steroids. The final diagnoses for the patients were extracted from the discharge reports.

Imaging protocol

CTP studies were obtained on 16-slice (72 patients) and 64-slice (29 patients) CT scanners. Each CTP study involved successive gantry rotations performed in cine mode during intravenous administration of iodinated contrast material. Images were acquired and reconstructed at a temporal sampling rate of 1 image per second for the first 45 seconds. Additional gantry rotations were obtained at 60, 90, 120, 150 and 180 seconds. Acquisition parameters were 80 kVp and 100 mAs. Two successive CTP series at two different levels were performed following the NCT and prior to the CTA. At each CTP level, four 5-mm-thick slices (16-slice CT scanners) or eight 5-mm-thick slices (64-slice CT scanners) were assessed. The first CTP series was obtained at the level of the third ventricle and the basal ganglia and the second CTP series above the lateral ventricles. For each CTP series, a 40 ml bolus of iohexol (Omnipaque, Amersham Health, Princeton, NJ; 300 mg/ml of iodine) was administered into an antecubital vein using a power injector at an injection rate of 5 ml per second for all patients. CT scanning was initiated 7 seconds after start of the injection of the contrast bolus.

Image post-processing

CTP data were analyzed utilizing CTP software developed by Philips Medical Systems (Cleveland, OH). This software relies on the central volume principle, which is the most accurate for low injection rates of iodinated contrast material.¹⁹ The software obtains mathematical descriptions of the time-density curves for each pixel, by applying curve fitting by least mean squares, after correcting for motion and noise reduction through an anisotropic, edge-preserving spatial filter. A closed-form (non-iterative) deconvolution is then applied to calculate the mean transit time (MTT) map.²⁰ The deconvolution operation requires a reference arterial input function (most often selected within the anterior cerebral artery), automatically selected by the software within a region of interest drawn by the user. The cerebral blood volume (CBV) map is calculated from the area under the time-density curves.²¹

BBBP measurements were extracted from CTP data using a second, prototype software developed by Philips Medical Systems. This software is based on the Patlak model.¹⁷ Applying the Patlak model to CTP involves performing linear regression using data calculated from the CTP datasets. The slope of these regression lines was used as an indicator of BBBP. For the calculation of these BBBP values, only the delayed phase (and not the first-pass) of the contrast injection was used, because the assumptions of linearity of the Patlak model are only met in the delayed phase.⁹ The cut-off point between the first-pass and the delayed

phase was automatically detected by the software.

BBBP values (slopes of the regression lines) were measured in regions of interest (ROIs) drawn to encompass the gray matter of the hemispheric lobes (temporal, occipital, frontal, parietal, and insular ribbon), the white matter of the hemispheric lobes (temporal, occipital, frontal, parietal) and the basal ganglia (caudate, lenticular nucleus and thalamus), as represented in *Figure 1*. Frontal and parietal ROIs were drawn on CTP slices from the second CTP series/injection, while the other ROIs were drawn on CTP slices from the first CTP series/injection. Both CTP boluses could be used, in agreement with a recent study that demonstrated that the contrast material injected during the first CTP series does not affect BBBP measurements extracted from the second CTP series.²²

No ROIs were drawn in the posterior fossa because of the selection of the CTP slices above the orbits. In addition to BBBP values, BBBP/CBF ratios were recorded in all ROIs.

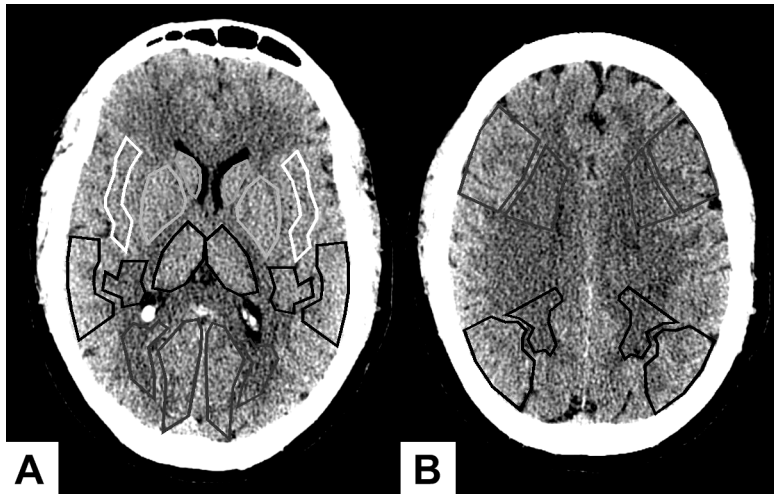


Figure 1 Graphical illustration of the regions of interest (ROI) drawn on CTP slices: (A), gray and white matter of the temporal and occipital lobe, caudate and lenticular nucleus, thalamus and insular ribbon; (B) gray and white matter of the frontal and parietal lobe.

Statistical analysis

As part of the statistical analysis, clustered log-BBBP values and log-BBBP/CBF ratios were modeled using a generalized estimating equations (GEE) model with robust variance estimation to account for within-patient correlations. Univariate analysis was done for all factors mentioned as patient characteristics and three different ROI clusters (gray matter, white matter and basal ganglia). Factors associated with a p value < 0.2 were retained in the subsequent multivariate analysis. History of hypertension and diabetes were a priori considered for the multivariate model because previous reports indicated their influence on BBBP.²³⁻²⁷ The only continuous factor, age effect, was modeled using a piecewise linear function after exploring scatter plots with median spline and local polynomial smooth

lines. Multivariate analysis involved forward-stepwise selection. Factors that were highly correlated with significant factors were also examined in the analysis. All non-significant factors in the multivariate analysis were dropped to create a final model that was used to estimate adjusted mean BBBP values and BBBP/CBF for the regions, as well as their 95% confidence intervals (CI).

Results

Patients

One hundred and one patients matched our inclusion criteria. Five patients were excluded, because of CTP data that could not be analyzed due to motion artifacts or improper timing of contrast bolus injection. The characteristics for the remaining 96 patients are summarized in *Table 1*. The Patlak analyses were performed in

Table 1 Patient characteristics

No. of patients	96
Age (range)	median = 55 interquartile range = 45 - 70 range = 17 - 91
Gender	42 (44%) males
Race:	
Black	12 (13%)
Asian	18 (19%)
Hispanic	11 (11%)
White	47 (49%)
Not reported	8 (8%)
Final diagnosis:	
TIA	11 (11%)
Vertigo	9 (9%)
Migraine	7 (7%)
Other neurological disorders	9 (9%)
Adverse drug reaction	3 (3%)
Other non-neurologic disorders	12 (13%)
No diagnosis (stroke excluded)	45 (47%)
Previous history of:	
Alcohol abuse	9 (9%)
Tobacco abuse	6 (6%)
Hypertension	24 (25%)
Diabetes	13 (14%)
Cardiac disease	3 (3%)
Hyperlipidemia	10 (10%)
Drugs:	
Aspirin	23 (24%)
Other NSAIDs	24 (25%)
Anticoagulants	7 (7%)
Anti-hypertensive	18 (19%)
Diabetes treatment	8 (8%)
Statins	11 (11%)
Steroids	2 (2%)

664 cortical gray matter ROIs, 664 white matter ROIs and 516 basal ganglia ROIs. Due to insufficient coverage, improper bolus timing and/or motion artifacts, 296 cortical gray matter ROIs, 104 white matter ROIs and 60 basal ganglia ROIs could not be obtained. The radiation dose for the prolonged CTP acquisition protocol (cine mode for 45 seconds, followed by additional gantry rotations at 60, 90, 120, 150 and 180 seconds) was only 10% (0.25 mSv) higher than the radiation dose of the conventional CTP protocol (cine mode for 45 seconds with no additional rotations).

Adjusted BBBP and BBBP/CBF values in different anatomical regions

The results of the univariate analysis (*Table 2*) were used to build the multivariate model. The final multivariate model contained: anatomical region, age, aspirin use and previous history of hypertension or diabetes (*Table 3*). Mean absolute BBBP values and BBBP/CBF ratios estimated from the multivariate model are reported in *Table 4*. Absolute BBBP values were similar in white matter and cortical gray matter, and lower in the basal ganglia. BBBP/CBF ratios were similar in white matter and basal ganglia, and lower in the cortical gray matter.

Factors influencing BBBP and BBBP/CBF ratios

Increasing age was associated with a decrease in absolute BBBP values and BBBP/CBF ratios. Absolute BBBP values and BBBP/CBF ratios were the highest in patients with hypertension and/or diabetes in the 40-55 age group (*Figure 2* and *Table 4*). The effect of hypertension and diabetes were similar and highly correlated (62% of all diabetic also had hypertension). They were therefore combined to be one factor. Hypertension and/or diabetes were associated with higher BBBP values, particularly pronounced in the 40-55 age group (factor of 1.2 to 2.4). Multivariate analysis showed that history of hypertension or diabetes interacted with age and aspirin use effects. Aspirin was associated with lower BBBP values in patients with hypertension and/or diabetes. Gender, race and other demographic and clinical factors were not found to influence BBBP measurements.

Table 2 Univariate analyses for patient characteristics and anatomical region. Factors with a significant effect (p -value < 0.2) were considered in the multivariate analysis. History of hypertension or diabetes, cardiac disease and/or hyperlipidemia were a priori considered for a multivariate model because previous reports indicated their influence on BBBP.

	Absolute BBBP Values			BBBP/CBF Ratios		
	<i>effect size</i>	<i>CI</i>	<i>p-value</i>	<i>effect size</i>	<i>CI</i>	<i>p-value</i>
Anatomy (vs white matter):						
Cortical gray matter	1.00	0.98-1.03	0.702	0.92	0.86-0.97	0.003
Basal ganglia	0.94	0.91-0.97	<0.001	0.95	0.89-1.02	0.143
Age (slope) with p-value for overall age effect:						
40-55 (vs <40)	0.96	0.94-0.99	0.011	0.95	0.92-0.99	0.010
55-70 (vs 40-55)	1.01	0.98-1.04	0.606	1.01	0.98-1.04	0.487
>70 (vs 55-70)	1.00	0.97-1.06	0.920	1.01	0.97-1.06	0.482
Male (vs female)	0.99	0.86-1.14	0.937	1.13	0.95-1.34	0.168
Race (vs white) with p-value for overall race effect:						
Hispanic	1.19	0.91-1.56		1.12	0.79-1.60	
Black	1.15	0.95-1.40		1.07	0.86-1.33	
Asian	0.99	0.83-1.17		0.87	0.70-1.08	
Not reported	0.99	0.73-1.33		0.93	0.62-1.41	
Previous history of (vs no history):						
Alcohol abuse	1.01	0.79-1.28	0.942	0.99	0.76-1.30	0.945
Tobacco abuse	0.89	0.60-1.34	0.583	0.88	0.56-1.37	0.566
Hypertension	1.03	0.86-1.24	0.745	1.03	0.82-1.31	0.772
Diabetes	1.08	0.88-1.33	0.476	1.07	0.77-1.47	0.691
Cardiac disease	0.76	0.67-0.87	<0.001	0.84	0.63-1.13	0.253
Hyperlipidemia	0.86	0.64-1.16	0.321	0.87	0.62-1.22	0.413
Drugs (vs no drugs):						
Aspirin	0.81	0.69-0.95	0.011	0.82	0.67-1.00	0.050
Other NSAIDs	0.96	0.82-1.12	0.600	0.93	0.74-1.16	0.505
Anticoagulants	0.90	0.64-1.25	0.518	1.10	0.72-1.67	0.666
Anti-hypertensive	1.09	0.89-1.34	0.416	1.06	0.81-1.39	0.661
Diabetes treatment	1.03	0.79-1.33	0.832	0.93	0.59-1.46	0.749
Statins	0.85	0.66-1.08	0.188	0.78	0.55-1.12	0.177
Steroids	1.09	0.97-1.23	0.160	1.49	1.17-1.90	0.001

BBBP = blood brain barrier permeability; CBF = cerebral blood flow; CI = 95% confidence interval

Table 3 Comparison based on the multivariate model, and taking into consideration the interactions demonstrated by the statistical analysis. Age had a decreasing effect on absolute BBBP values and BBBP/CBF ratios, particularly pronounced in patients with hypertension and/or diabetes in the 40-55 age group. Hypertension and/or diabetes had an increasing effect on BBBP, while aspirin had a decreasing effect in patients with with hypertension and/or diabetes.

	Absolute BBBP Values			BBBP/CBF Ratios		
	<i>effect size</i>	<i>CI</i>	<i>p-value</i>	<i>effect size</i>	<i>CI</i>	<i>p-value</i>
Anatomy (vs white matter):						
Cortical gray matter	1.00	0.98-1.03	0.699	0.92	0.86-0.97	0.003
Basal ganglia	0.94	0.91-0.97	<0.001	0.95	0.89-1.02	0.148
Aspirin (use vs no use):						
no hypertension and no diabetes	0.91	0.75-1.09	0.298	0.88	0.71-1.10	0.275
hypertension and/or diabetes	0.72	0.54-0.97	0.032	0.74	0.53-1.04	0.084
Age (effect per 5-year increment):						
no hypertension and no diabetes	0.97	0.95-1.00	0.018	0.98	0.96-1.01	0.206
hypertension and/or diabetes age 40-55	0.84	0.76-0.93	0.001	0.71	0.63-0.80	<0.001
hypertension and/or diabetes aged 55-91	1.02	0.97-1.07	0.496	1.05	0.97-1.14	0.206
Hypertension and/or diabetes (with vs without):						
not taking aspirin, age 40	1.64	1.29-2.09	<0.001	2.39	1.90-2.99	<0.001
not taking aspirin, age 50	1.21	1.04-1.42	0.020	1.25	1.02-1.52	0.031
not taking aspirin, age 55	1.04	0.85-1.27	0.693	0.90	0.68-1.20	0.477
not taking aspirin, age 60	1.09	0.90-1.32	0.394	0.97	0.75-1.25	0.790
not taking aspirin, age 70	1.19	0.95-1.49	0.134	1.11	0.85-1.46	0.444
taking aspirin, age 40	1.31	0.90-1.92	0.161	2.00	1.35-2.98	0.001
taking aspirin, age 50	0.97	0.70-1.33	0.850	1.05	0.73-1.51	0.803
taking aspirin, age 55	0.83	0.59-1.17	0.291	0.76	0.50-1.15	0.188
taking aspirin, age 60	0.87	0.64-1.19	0.378	0.81	0.56-1.18	0.280
taking aspirin, age 70	0.95	0.72-1.26	0.727	0.93	0.66-1.33	0.697

BBBP = blood brain barrier permeability; CBF = cerebral blood flow; CI = 95% confidence interval

Table 4 Estimated mean absolute BBBP values and BBBP/CBF ratios for a 40 year old subject with no previous history of hypertension or diabetes and no aspirin use in white matter, cortical gray matter and basal ganglia, based on the effect sizes of the multivariate analysis reported in Table 3. Absolute BBBP values were similar in white matter and cortical gray matter, and lower in the basal ganglia. BBBP/CBF ratios were similar in white matter and basal ganglia, and lower in the cortical gray matter.

	White Matter	Cortical Gray Matter	Basal Ganglia
	Mean	Mean	Mean
	95%CI	95%CI	95%CI
		(p value to white matter)	(p value to white matter)
Absolute BBBP values (ml/100g/min)	1.19	1.19	1.12
	1.08 - 1.31	1.08 - 1.32	1.01 - 1.24
		(0.699)	(<0.001)
BBBP/CBF ratios (%)	3.66%	3.35%	3.47%
	3.23% - 4.14%	2.97% - 3.78%	3.03% - 3.98%
		(0.003)	(0.148)

BBBP = blood brain barrier permeability; CBF = cerebral blood flow; CI = 95% confidence interval

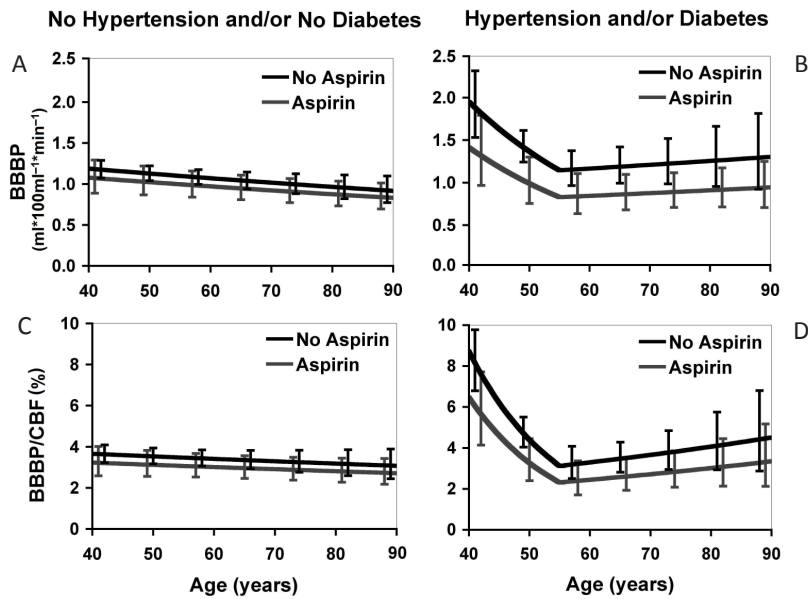


Figure 2 Differences in the effect of age and aspirin use on absolute BBBP values (A,B) and BBBP/CBF ratios (C,D) between patients with and without hypertension and/or diabetes. The error bars represent the 95% confidence interval at the considered age to illustrate differences between aspirin use and no aspirin use. Increasing age was associated with a decrease in absolute BBBP values and BBBP/CBF ratios. Absolute BBBP values and BBBP/CBF ratios were the highest in patients with hypertension and/or diabetes in the 40-55 age group. Hypertension and/or diabetes were associated with higher BBBP values, while aspirin was associated with lower BBBP values in patients with hypertension and/or diabetes.

Discussion

This study reports BBBP values extracted from CTP delayed phase data using the Patlak model in a consecutive series of 96 control, non-stroke patients. We found small but statistically significant differences in mean absolute BBBP and relative BBBP/CBF values between different cerebral tissue types. Relative values in cortical grey matter and absolute values in basal ganglia were lower than in white matter.

Our analysis assessed absolute BBBP values, but also BBBP/CBF ratios. The rationale for evaluating BBBP/CBF ratios, or relative BBBP values, was to consider the absolute BBBP values as the fraction (in percent) of the CBF extravasating from the intravascular compartment into the extracellular compartment. The same absolute BBBP value in the presence of a high or low CBF corresponds to a low or high fraction extravasating into the extracellular compartment, respectively. The slightly higher BBBP values we found in white matter have been related to the white matter having sparser vascular density than gray matter,²⁸ but also to morphological differences in white and gray matter astrocytes and their contact with endothelial cells.^{29, 30} This can also explain the preferential occurrence of brain edema within the white matter.³⁰ Our results furthermore show that BBBP values were influenced by age, history of diabetes and/or hypertension, and aspirin intake. Increasing age was associated with a decrease in BBBP, which is in disagreement with a prior meta-analysis that demonstrated an increase of BBBP in normal ageing patients.³¹ This disagreement may be related to the different populations and BBBP measuring techniques studied: our study focused on 96 subjects aged 40 and older using CTP, while the meta-analysis involved ten studies using biochemical measuring techniques or positron emission tomography. Furthermore, the number of normal controls in these studies ranged from 5 to 72 and the age ranged from 1 to 70, with three studies only having subjects older than 60.³¹ Patients with history of diabetes and/or hypertension showed increased BBBP values, particularly pronounced in the 40-55 age group (factor of 1.2 to 2.4). This finding is in agreement with previous reports that both hypertension^{23, 26} and diabetes^{24, 25, 27} are associated with BBBP breakdown and thus increased BBBP values. The effect of hypertension and/or diabetes on BBBP was reversed by aspirin intake. Experimental studies have shown that aspirin can decrease vascular permeability caused by inflammation.^{32, 33} Our results are the first to confirm this observation in a clinical population of patients. We acknowledge several limitations to our study. Firstly, the patients enrolled in this study were considered as control subjects based on the absence of ischemic stroke, major cerebral abnormality on baseline and follow-up CT and MR imaging, and clinical work-up. They were eventually diagnosed with a variety of clinical conditions, including transient ischemic attack (TIA), vertigo and migraine. The influence of such conditions on BBBP is unknown. However, for obvious ethical reasons, it was not possible to enroll completely normal subjects, because of the radiation and contrast administration. Secondly, in order to assess all lobes of

cerebral hemispheres, we used the spatial coverage offered by two successive CTP boluses. This was acceptable because of a recent study demonstrating that the contrast material injected during the first CTP bolus does not negatively affect BBBP measurements extracted from the second CTP bolus²². Whether the brain coverage obtained in this way is sufficient to estimate hemorrhagic potential of the whole brain in stroke patients needs to be further evaluated. Thirdly, there are some factors that have been reported to affect BBBP that could not be evaluated in the present study because of its retrospective nature. Alcohol³⁴ and nicotine³⁵ have been reported to damage the BBBP, while statins may have protective effects on BBBP.^{36, 37}

Conclusion

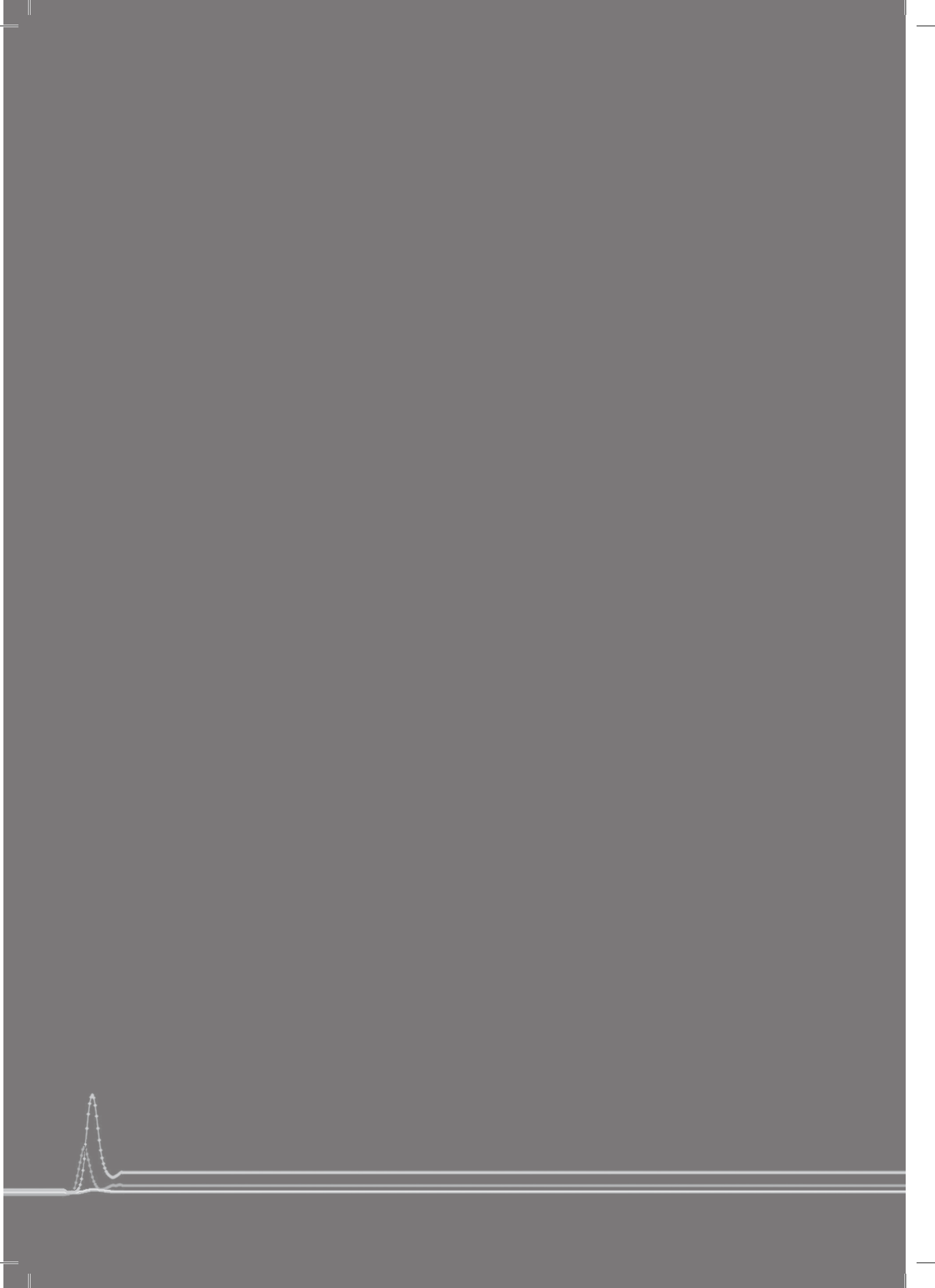
This study reports normal ranges of BBBP values calculated from delayed phase CTP data using the Patlak model. These normal ranges will be very useful to detect abnormal BBBP values when assessing patients with cerebral infarction for the risk of hemorrhagic transformation.

References

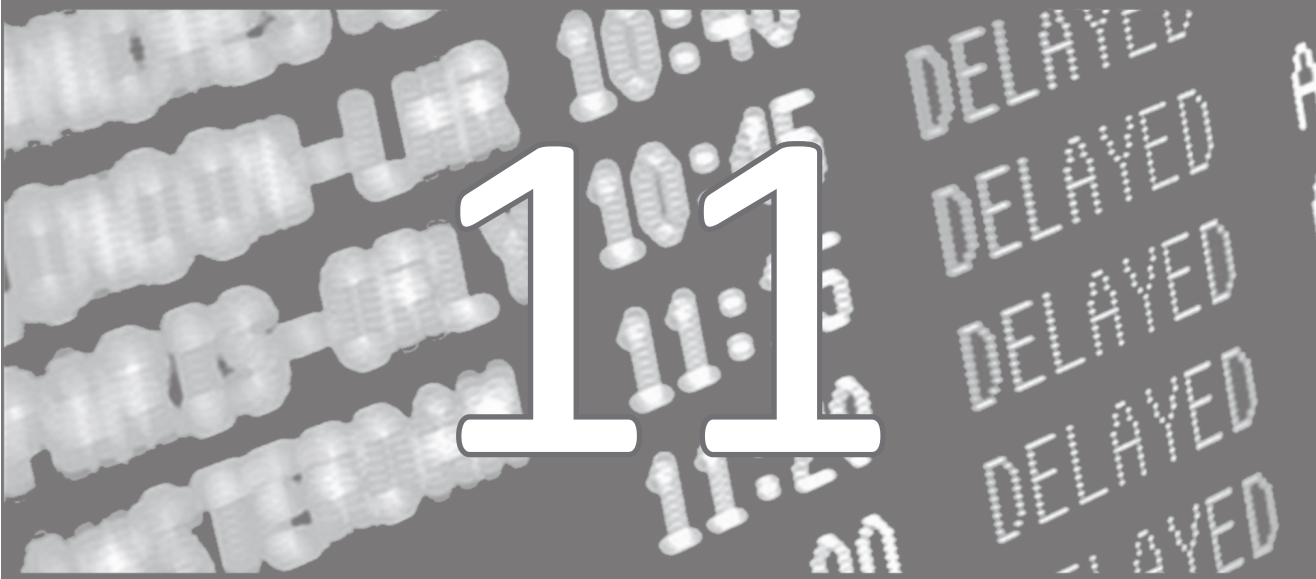
1. Berger C, Fiorelli M, Steiner T, Schabitz WR, Bozzao L, Bluhmki E, Hacke W, von KR. Hemorrhagic transformation of ischemic brain tissue: Asymptomatic or symptomatic? *Stroke*. 2001;32:1330-1335
2. Hacke W, Donnan G, Fieschi C, Kaste M, von KR, Broderick JP, Brott T, Frankel M, Grotta JC, Haley EC, Jr., Kwiatkowski T, Levine SR, Lewandowski C, Lu M, Lyden P, Marler JR, Patel S, Tilley BC, Albers G, Bluhmki E, Wilhelm M, Hamilton S. Association of outcome with early stroke treatment: Pooled analysis of atlantis, ecast, and ninds rt-pa stroke trials. *Lancet*. 2004;363:768-774
3. Wang X, Lo EH. Triggers and mediators of hemorrhagic transformation in cerebral ischemia. *MolNeurobiol*. 2003;28:229-244
4. Latour LL, Kang DW, Ezzeddine MA, Chalela JA, Warach S. Early blood-brain barrier disruption in human focal brain ischemia. *AnnNeurol*. 2004;56:468-477
5. Nabavi DG, Dittrich R, Kloska SP, Nam EM, Klotz E, Heindel W, Ringelstein EB. Window narrowing: A new method for standardized assessment of the tissue at risk-maximum of infarction in ct based brain perfusion maps. *Neurol Res*. 2007;29:296-303
6. Parsons MW, Pepper EM, Bateman GA, Wang Y, Levi CR. Identification of the penumbra and infarct core on hyperacute noncontrast and perfusion ct. *Neurology*. 2007;68:730-736
7. Schaefer PW, Roccatagliata L, Ledezma C, Hoh B, Schwamm LH, Koroshetz W, Gonzalez RG, Lev MH. First-pass quantitative ct perfusion identifies thresholds for salvageable penumbra in acute stroke patients treated with intra-arterial therapy. *AJNR Am J Neuroradiol*. 2006;27:20-25
8. Wintermark M, Flanders AE, Velthuis B, Meuli R, van Leeuwen M, Goldsher D, Pineda C, Serena J, van der Schaaf I, Waaijer A, Anderson J, Nesbit G, Gabriely I, Medina V, Quiles A, Pohlman S, Quist M, Schnyder P, Bogousslavsky J, Dillon WP, Pedraza S. Perfusion-ct assessment of infarct core and penumbra: Receiver operating characteristic curve analysis in 130 patients suspected of acute hemispheric stroke. *Stroke*. 2006;37:979-985
9. Dankbaar JW, Hom J, Schneider T, Cheng S, Lau B, van der Schaaf I, Virmani S, Pohlman S, Dillon WP, Wintermark M. Dynamic perfusion-ct assessment of the blood-brain barrier permeability: First-pass versus delayed acquisition. *AJNR (in press)*. 2008
10. Bartolini A, Gasparetto B, Furlan M, Sullo L, Trivelli G, Albano C, Roncallo F. Functional perfusion and blood-brain barrier permeability images in the diagnosis of cerebral tumors by angio ct. *Comput Med Imaging Graph*. 1994;18:145-150
11. Bisdas S, Hartel M, Cheong LH, Koh TS, Vogl TJ. Prediction of subsequent hemorrhage in acute ischemic stroke using permeability ct imaging and a distributed parameter tracer kinetic model. *JNeuroradiol*. 2007;34:101-108
12. Cianfoni A, Cha S, Bradley WG, Dillon WP, Wintermark M. Quantitative measurement of blood-brain barrier permeability using perfusion-ct in extra-axial brain tumors. *J Neuroradiol*. 2006;33:164-168
13. Goh V, Halligan S, Bartram CI. Quantitative tumor perfusion assessment with multidetector ct: Are measurements from two commercial software packages interchangeable? *Radiology*. 2007;242:777-782
14. Leggett DA, Miles KA, Kelley BB. Blood-brain barrier and blood volume imaging of cerebral glioma using functional ct: A pictorial review. *Eur J Radiol*. 1999;30:185-190
15. Yeung WT, Lee TY, Del Maestro RF, Kozak R, Brown T. In vivo ct measurement of blood-brain transfer constant of iopamidol in human brain tumors. *J Neurooncol*. 1992;14:177-187

16. Patlak CS, Blasberg RG. Graphical evaluation of blood-to-brain transfer constants from multiple-time uptake data. Generalizations. *J Cereb Blood Flow Metab.* 1985;5:584-590
17. Patlak CS, Blasberg RG, Fenstermacher JD. Graphical evaluation of blood-to-brain transfer constants from multiple-time uptake data. *J Cereb Blood Flow Metab.* 1983;3:1-7
18. Lin K, Kazmi KS, Law M, Babb J, Peccerelli N, Pramanik BK. Measuring elevated microvascular permeability and predicting hemorrhagic transformation in acute ischemic stroke using first-pass dynamic perfusion ct imaging. *AJNR AmJNeuroradiol.* 2007;28:1292-1298
19. Wintermark M, Maeder P, Thiran JP, Schnyder P, Meuli R. Quantitative assessment of regional cerebral blood flows by perfusion ct studies at low injection rates: A critical review of the underlying theoretical models. *Eur Radiol.* 2001;11:1220-1230
20. Axel L. Tissue mean transit time from dynamic computed tomography by a simple deconvolution technique. *Invest Radiol.* 1983;18:94-99
21. Ladurner G, Zilkha E, Iliff D, du Boulay GH, Marshall J. Measurement of regional cerebral blood volume by computerized axial tomography. *JNeuroNeurosurgPsychiatry.* 1976;39:152-158
22. Dankbaar JW, Hom J, Schneider T, Cheng S, Lau B, van der Schaaf I, Virmani S, Pohlman S, Dillon WP, Wintermark M. Accuracy and anatomical coverage of perfusion-ct assessment of the blood-brain barrier permeability: One bolus versus two boluses. *Submitted for Publication.* 2008
23. Al-Sarraf H, Philip L. Effect of hypertension on the integrity of blood brain and blood csf barriers, cerebral blood flow and csf secretion in the rat. *Brain Res.* 2003;975:179-188
24. Hawkins BT, Lundeen TF, Norwood KM, Brooks HL, Egleton RD. Increased blood-brain barrier permeability and altered tight junctions in experimental diabetes in the rat: Contribution of hyperglycaemia and matrix metalloproteinases. *Diabetologia.* 2007;50:202-211
25. Huber JD, VanGilder RL, Houser KA. Streptozotocin-induced diabetes progressively increases blood-brain barrier permeability in specific brain regions in rats. *Am J Physiol Heart Circ Physiol.* 2006;291:H2660-2668
26. Nag S, Kilty DW. Cerebrovascular changes in chronic hypertension. Protective effects of enalapril in rats. *Stroke.* 1997;28:1028-1034
27. Starr JM, Wardlaw J, Ferguson K, MacLulich A, Deary IJ, Marshall I. Increased blood-brain barrier permeability in type ii diabetes demonstrated by gadolinium magnetic resonance imaging. *J Neurol Neurosurg Psychiatry.* 2003;74:70-76
28. Duvernoy HM, Delon S, Vannson JL. Cortical blood vessels of the human brain. *Brain Res Bull.* 1981;7:519-579
29. Abbott NJ, Ronnback L, Hansson E. Astrocyte-endothelial interactions at the blood-brain barrier. *Nat Rev Neurosci.* 2006;7:41-53
30. Hirano A, Kawanami T, Llena JF. Electron microscopy of the blood-brain barrier in disease. *Microssc Res Tech.* 1994;27:543-556
31. Farrall AJ, Wardlaw JM. Blood-brain barrier: Ageing and microvascular disease - systematic review and meta-analysis. *Neurobiol Aging.* 2007
32. Alvarez-Guerra M, Hannaert P, Hider H, Chiavaroli C, Garay RP. Vascular permeabilization by intravenous arachidonate in the rat peritoneal cavity: Antagonism by antioxidants. *Eur J Pharmacol.* 2003;466:199-205
33. Serhan CN, Takano T, Chiang N, Gronert K, Clish CB. Formation of endogenous "Antiinflammatory" Lipid mediators by transcellular biosynthesis. Lipoxins and aspirin-triggered lipoxins inhibit neutrophil recruitment and vascular permeability. *Am J Respir Crit Care Med.* 2000;161:S95-S101

34. Haorah J, Knipe B, Gorantla S, Zheng J, Persidsky Y. Alcohol-induced blood-brain barrier dysfunction is mediated via inositol 1,4,5-triphosphate receptor (ip3r)-gated intracellular calcium release. *J Neurochem.* 2007;100:324-336
35. Hawkins BT, Abbruscato TJ, Egleton RD, Brown RC, Huber JD, Campos CR, Davis TP. Nicotine increases in vivo blood-brain barrier permeability and alters cerebral microvascular tight junction protein distribution. *Brain Res.* 2004;1027:48-58
36. Ifergan I, Wosik K, Cayrol R, Kebir H, Auger C, Bernard M, Bouthillier A, Mouldjian R, Duquette P, Prat A. Statins reduce human blood-brain barrier permeability and restrict leukocyte migration: Relevance to multiple sclerosis. *Ann Neurol.* 2006;60:45-55
37. Mooradian AD, Haas MJ, Batejko O, Hovsepian M, Feman SS. Statins ameliorate endothelial barrier permeability changes in the cerebral tissue of streptozotocin-induced diabetic rats. *Diabetes.* 2005;54:2977-2982



Dynamic perfusion-CT assessment of early changes in blood-brain barrier permeability of acute ischemic stroke patients



11

*J.W. Dankbaar, J. Hom, T. Schneider, S.C. Cheng, J. Bredno, B.C. Lau,
I.C. van der Schaaf, M. Wintermark*

Abstract

Background and purpose

Damage to the blood-brain barrier (BBB) may lead to hemorrhagic transformation after ischemic stroke. The purpose of this study was to evaluate the effect of patient characteristics and stroke severity on admission BBB permeability (BBBP) values measured with CT-perfusion (CTP) in acute hemispheric stroke patients.

Methods

We retrospectively identified 65 patients with proven ischemic stroke admitted within 12 hours after symptom onset. Patients' charts were reviewed for demographic variables and vascular risk factors. The Patlak model was applied to calculate BBBP values from the CTP data in the infarct core, penumbra and non-ischemic tissue in the contralateral hemisphere. Mean BBBP values and their 95% confidence intervals (CI) were calculated in the different tissue types. Effects of demographic variables and risk factors on BBBP were analyzed using a multivariate, generalized estimating equations (GEE) model.

Results

BBBP values in the infarct core (mean (95%CI): 2.48 (2.16-2.85)) and penumbra (2.48 (2.21-2.79)) were significantly higher than in non-ischemic tissue (2.12 (1.88-2.39)). Multivariate analysis demonstrated that only collateral filling has a significant effect on BBBP. Less elevated BBBP values were associated with more than 50% collateral filling.

Conclusions

BBBP values are increased in ischemic brain tissue on the admission CTP scan of acute ischemic stroke patients. Less abnormally elevated BBBP values were observed in patients with more than 50% collateral filling, possibly explaining why there is a relationship between more collateral filling and a lower incidence of hemorrhagic transformation.

Introduction

Stroke causes 9% of all deaths in industrialized countries and is the second most common cause of death after ischemic heart disease.¹ Hemorrhagic transformation (HT) is considered to be the most devastating complication of ischemic stroke and can increase the risk of mortality up to 11 times.² One of the mechanisms for the development of hemorrhagic transformation following an ischemic stroke is damage to the blood brain barrier (BBB).^{3, 4} The BBB can be degraded by age,⁵ conditions such as hypertension,⁶ high glucose levels,^{7, 8} and ischemia.³ Recombinant tissue plasminogen activator (rtPA), the only FDA-approved treatment of stroke, has also been reported to alter BBB integrity and is a well-known risk factor for hemorrhagic transformation.^{9, 10} There are thus factors both before and after the occurrence of ischemic stroke that can influence BBB permeability (BBBP). Assessing the amount of damage to the BBB and factors that influence BBBP at the time of stroke diagnosis may be helpful in assessing the risk of HT.

BBBP can be calculated from CT-perfusion (CTP) data.^{11, 12} CTP is a dynamic imaging technique that is frequently applied in stroke patients to identify the infarct core and penumbra.¹³⁻¹⁶

The purpose of this study was to evaluate the effect of patient characteristics and stroke severity on admission BBBP values measured with CTP in acute hemispheric stroke patients.

Methods

Design

With the approval of the institutional review board, we retrospectively reviewed imaging studies obtained as part of standard clinical stroke care at our institution. Patients suspected of acute stroke and no significant renal insufficiency or contrast allergy routinely undergo a stroke CT study at our institution. This stroke CT study consists of: noncontrast CT (NCT) of the brain, CTP at two cross-sectional positions, CT-angiogram (CTA) of the cervical and intracranial arteries, and contrast-enhanced cerebral CT, in this chronological sequence.

We retrospectively identified a consecutive series of patients admitted between July 2006 and August 2008 verifying the following inclusion criteria: (a) admission to the emergency room with a clinical presentation suggesting hemispheric stroke within 12 hours after symptom onset; (b) no evidence of intracerebral bleeding on the admission NCT; (c) evidence of ischemic stroke on admission NCT/CTP/CTA or follow-up imaging.

Patient characteristics

Patients' medical records were reviewed for clinical data on the day of admission, including: age, time from symptom onset to admission scan, NIH stroke scale (NIHSS), blood glucose levels on admission, and previous history of diabetes mellitus and/or hypertension.

Imaging protocol

Our CTP imaging protocol has been reported previously.¹⁷ It involves a cine mode CT acquisition, with a temporal sampling rate of 1 image per second for the first 37 seconds and 1 image every 2 seconds for the next 33 seconds. Additional gantry rotations are performed at 90, 120, 150, 180, 210 and 240 seconds. Acquisition parameters were 80 kVp and 100 mAs. Two successive CTP series were obtained at the level of the third ventricle and the basal ganglia and above the lateral ventricles, following the non-contrast CT and prior to the CTA. It has recently been shown that both CTP series can be used for BBBP measurements.¹⁷ For each CTP series, a bolus of 40 ml iohexol (Omnipaque, Amersham Health, Princeton, NJ; 300 mg/ml of iodine) was injected into an antecubital vein at an injection rate of 5 ml per second. CT scanning was initiated 7 seconds after start of the injection of the contrast bolus.

Image post-processing

To analyze the CTP data we used commercially available CTP software (Brain Perfusion, Philips Healthcare, Cleveland, OH, USA). This software applies a closed-form deconvolution to calculate the mean transit time (MTT) map.¹⁸ The reference arterial input function was automatically selected by the CTP software within a region of interest drawn by the user around the anterior cerebral artery. The cerebral blood volume (CBV) map is derived from the area under the time-density curves compared to a similarly obtained reference curve.¹⁹ The software automatically calculates the CTP infarct core and penumbra by applying thresholds reported in the literature (CTP penumbra: MTT > 145% of the contralateral side values, CBV \geq 2.0 ml/100g; CTP infarct core: MTT > 145% of the contralateral side values, CBV < 2.0 ml/100g).¹⁶

With a second, prototype software developed by Philips Healthcare, BBBP values (ml/100g/min) were calculated from the CTP data using the Patlak model²⁰ as described in previous publications.^{12, 17} In short, applying the Patlak model to CTP involves the fitting of a regression line to observations of time-density curves for each pixel and for an intravascular reference function. The blood-to-brain transfer constant for contrast agent can be calculated from the slope of these regression lines and used as an indicator of BBBP. The analysis was restricted to the delayed phase of the contrast injections,¹² with the cut-off point between the first-pass and the delayed phase being automatically detected by the software.

BBBP values were measured in several regions of interest (ROIs): infarct core and penumbra (as defined by CTP software thresholds), and ROIs in the contra lateral unaffected hemisphere.

Imaging review

All images were reviewed by an experienced neuroradiologist. On the admission NCT images the ASPECTS score was calculated for each patient. Patients were categorized in two categories: ASPECTS 0-7 and ASPECTS > 7.²¹

Admission CTA axial source images (1.25 mm thickness) were processed to obtain

axial, sagittal and coronal 20-mm-thick maximum intensity projections (MIP). CTA MIP images were evaluated for the site of occlusion and the presence of collateral filling. Collateral filling was categorized in three groups: collaterals filling <50% of the occluded territory, collaterals filling 50-100% of the occluded territory, according to a previously described approach.²²

Statistical analysis

BBBP values were considered as outcomes for the purpose of the statistical analysis, and the determinants were patient characteristics (age, blood glucose levels, previous history of diabetes mellitus and/or hypertension, NIHSS score, and time from symptom onset to admission CT) and stroke characteristics (CTP infarct volume, CTP penumbra volume, ASPECTS score on the admission NCT, and collateral filling on CTA). The effect size (regression coefficients) of the different determinants on BBBP was estimated by means of linear regression. Clustered log-BBBP values were modeled using a generalized estimating equations (GEE) model with robust variance estimation to account for within-patient correlations. First, a univariate analysis was performed. Effects associated with a p-value < 0.2 were retained in the subsequent multivariate analysis. Continuous determinants were modeled using a piecewise linear function after exploring scatter plots with median spline and local polynomial smooth lines. Multivariate analysis involved forward-stepwise selection. Factors that were highly correlated with significant factors were also examined in the analysis. All non-significant factors in the multivariate analysis were dropped to create a final model that was used to estimate adjusted mean BBBP values for the different types of ROI (infarct core, penumbra, non-ischemic tissue), as well as their 95% confidence interval (CI).

Results

Patients

Sixty-five patients matched our inclusion criteria. The patient characteristics are summarized in *Table 1*.

Absolute BBBP values in infarcted tissue and penumbra

BBBP values (*Table 2, Figure 1*) in infarcted tissue were higher ($p = 0.002$) than in non-ischemic tissue. BBBP values in the penumbra were higher ($p = 0.009$) than in non-ischemic tissue.

Univariate analyses and multivariate model (*Table 3*)

The univariate analyses showed that patient age, blood glucose, time since symptom onset, and collateral filling had an effect on BBBP with $p \leq 0.25$. These factors were included in the multivariate model, which demonstrated that only collateral filling had a borderline significant effect on BBBP ($p = 0.06$). Less abnormally elevated BBBP values were observed in patients with more than 50% collateral filling.

Table 1 Study patient characteristics

No. of patients	65
No. of men	28 (43%)
Median age (interquartile range; full range)	72 (61-81; 27-96)
Median blood glucose, mg/dl (interquartile range; full range)	116.0 (97.3-154.0; 66.0-237.0)
Previous history of:	
Diabetes	8 (12%)
Hypertension	24 (37%)
Median time (hours) between symptom onset and admission CT (interquartile range; full range)	2.25 (1.8-5.0; 1-12)
Median NIHSS (interquartile range; full range)	13 (7-16; 1-21)
Infarct Location:	
ACA&MCA	6 (9%)
MCA	58 (89%)
PCA	1 (2%)
Early CT changes*:	
ASPECTS 0-7	6 (9%)
ASPECTS > 7	56 (86%)
Collateral filling of occluded territory:	
<50%	19 (29%)
50-100%	20 (31%)
100%	26 (40%)
Mean infarct volume in mL (range)	22.5 (0-225)
Mean penumbra volume in mL (range)	58.8 (0.4-157)

NIHSS = National Institutes of Health Stroke Scale; ACA = anterior cerebral artery; MCA = middle cerebral artery; PCA = posterior cerebral artery; ASPECTS = Alberta Stroke Programme Early CT Score; * in three cases the ASPECTS was not assessable due to severe motion artifacts on the NCT.

Table 2 Mean absolute BBBP values (ml/100g/min) with 95% confidence intervals in the infarct core, the penumbra, and on the contralateral non-ischemic side.

	ROIs				
	<i>Infarct Core</i>	<i>p-value compared to non-ischemic</i>	<i>Penumbra</i>	<i>p-value compared to non-ischemic</i>	<i>Contralateral Non-ischemic Side</i>
BBBP:	2.48 (2.16-2.85)	0.002	2.48 (2.21-2.79)	0.009	2.12 (1.88-2.39)

BBBP = blood-brain barrier permeability; CBF = cerebral blood flow

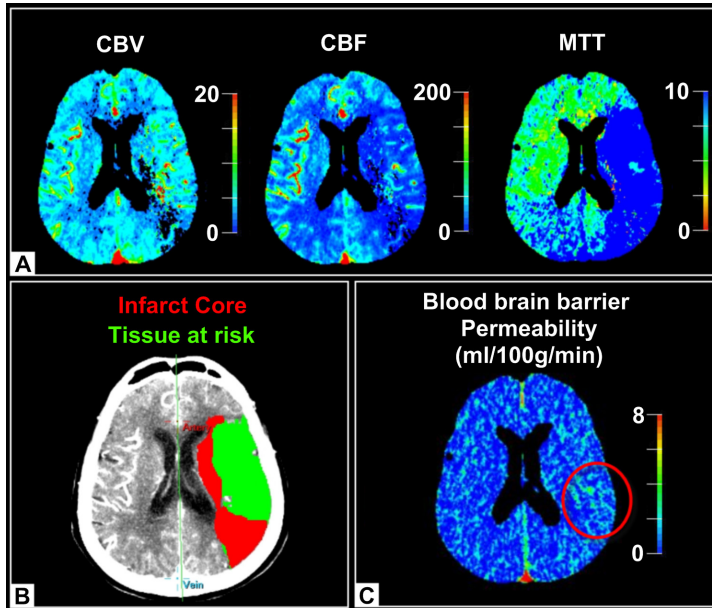


Figure 1 Illustrative case: 59 year old patient with an ischemic stroke in the left middle cerebral artery (MCA) flow territory, admitted within 5 hours after symptom onset with NIH-stroke scale of 14. (A) perfusion maps showing cerebral blood volume (CBV), cerebral blood flow (CBF), and mean transit time (MTT)); (B) infarct core in red and penumbra in green determined by perfusion threshold values¹⁶; (C) blood brain barrier permeability (BBBP) map calculated with the Patlak model from delayed phase perfusion data¹² showing an area of increased BBBP in the left MCA flow territory adjacent to the infarct core. For colorfigure see page 234

Table 3 Uni- and multivariate analysis for the absolute BBBP measurements, after adjustment for the type of ROI (infarct core, penumbra, contralateral non-ischemic side) where they were recorded. The variables noted with an asterix (*) were those retained for the multivariate analysis. The latter however demonstrated that only collateral filling was associated ($p = 0.06$) with BBBP measurements.

	Univariate Analyses			Multivariate Analysis		
	effect	CI	p-value	effect	CI	p-value
Age	0.99	0.98-1.01	0.25			
Blood glucose*	0.73	0.51-1.04	0.08	0.94	0.82-1.08	0.36
Diabetes	1.04	0.77-1.41	0.79			
Hypertension	0.99	0.79-1.25	0.95			
Time from symptom onset to CT scan*	0.94	0.86-1.04	0.25	0.94	0.85-1.05	0.27
NIHSS	1.00	0.99-1.03	0.50			
Early CT changes	1.03	0.68-1.58	0.88			
Collateral filling*	1.49	1.11-1.98	0.01	1.31	0.99-1.71	0.06
Penumbra volume	1.00	0.99-1.01	0.62			
Infarct volume	1.01	0.99-1.01	0.40			

CI = 95% confidence interval

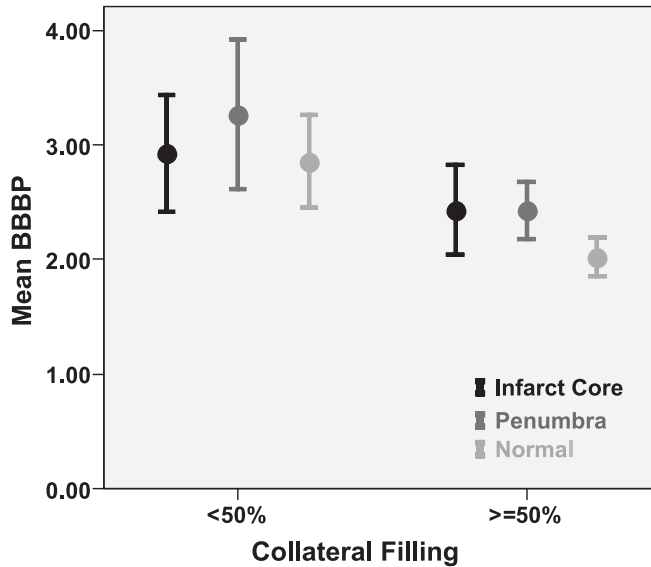


Figure 2 Blood-brain barrier permeability (BBBP) and collateral filling: Mean absolute BBBP values with 95% confidence intervals in the infarct core, penumbra and non-ischemic tissue in patients with less than (<) 50% collateral filling in the ischemic hemisphere and patients with equal or more than (>=) 50% collateral filling.

Discussion

Damage to the BBB is considered to be an important mechanism for the development of hemorrhagic transformation after stroke.^{3, 4} To describe the role of patient characteristics and ischemia on BBBP, we measured BBBP values in infarcted tissue, penumbra for infarction and non-ischemic tissue on the admission CTP scan of acute stroke patients.

Our results show that BBBP is higher in infarcted tissue compared to non-ischemic tissue. BBBP in penumbra is also higher than in non-ischemic tissue. This is in accordance with previous research²³ and the idea that ischemia and infarction disrupt BBB integrity and thereby cause hemorrhagic transformation.^{3, 4} In contrast, we did not find an association between BBBP values and the volume of penumbra or the infarct core volume. A recent study described only a non-significant association between the volume of lesions on diffusion weighted MRI and increased BBBP.⁷ Local BBBP changes thus seem to be independent of the total size of the ischemic area and BBBP may vary regionally within one area.²⁴ We also observed that less abnormally elevated BBBP values were observed in patients with more than 50% collateral filling. This finding may explain why more collateral filling has been previously associated with a lower incidence of hemorrhagic transformation.²⁵

The increase of BBBP in relation to a longer time from symptom onset to CT scan has recently been published.⁷ Our study did not confirm this finding. However, patients in our study were admitted and imaged on average several hours earlier compared to this previous study. The relationship between BBBP and time from symptom onset may be less profound in a very early stage.

In previous studies, age, blood glucose and previous history of diabetes and/or hypertension were associated with increased BBBP values.^{5, 6, 8, 26} However in our population these factors did not influence the baseline BBBP significantly. This is in agreement with a recent study demonstrating only a faint association (age and glucose) or no association (diabetes and hypertension) with BBBP in stroke patients.⁷

We acknowledge several limitations to our study.

We used the Patlak model to measure BBBP from CTP data. The Patlak model is a relatively simple²⁰ and accurate²⁷ model that has been frequently applied to extract BBBP measurements from CTP data.^{12, 28, 29} The Patlak model uses arterial and parenchymal contrast enhancement curves to measure the rate of contrast transfer from an intravascular to an extravascular compartment. The Patlak analysis can only be applied to the delayed phase of contrast injection.¹² It assumes unidirectional flow of contrast out of the vascular compartment while compensating for the amount of intravascular contrast agent.²⁰ Models for a bi-directional exchange between vascular and extravascular compartment have been presented in similar studies.^{11, 30} Different approaches to measure permeability do not yet compare well, such that our results on the BBBP values measured in the infarct core and in the penumbra, only apply to the Patlak analysis. The comparison of different approaches was beyond the scope of this paper.

Another limitation may be that we did not obtain follow-up imaging in all our patients, and as such we could not assess hemorrhagic transformation, and its relationship to BBBP measurements, in this study. Further research is required to investigate the relevance of these BBBP measurements in terms of their predictive value for hemorrhagic transformation in acute ischemic stroke patients.

Conclusion

We found increased BBBP in ischemic brain tissue on the admission CTP scan of acute ischemic stroke patients. We also found that less abnormally elevated BBBP values were observed in patients with more than 50% collateral filling, possibly explaining why there is a relationship between more collateral filling and a lower incidence of hemorrhagic transformation.

References

1. Donnan GA, Fisher M, Macleod M, Davis SM. Stroke. *Lancet*. 2008;371:1612-1623
2. Berger C, Fiorelli M, Steiner T, Schabitz WR, Bozzao L, Bluhmki E, Hacke W, von KR. Hemorrhagic transformation of ischemic brain tissue: Asymptomatic or symptomatic? *Stroke*. 2001;32:1330-1335
3. Sandoval KE, Witt KA. Blood-brain barrier tight junction permeability and ischemic stroke. *Neurobiol Dis*. 2008;32:200-219
4. Wang X, Lo EH. Triggers and mediators of hemorrhagic transformation in cerebral ischemia. *MolNeurobiol*. 2003;28:229-244
5. Farrall AJ, Wardlaw JM. Blood-brain barrier: Ageing and microvascular disease - systematic review and meta-analysis. *Neurobiol Aging*. 2007
6. Nag S, Kilty DW. Cerebrovascular changes in chronic hypertension. Protective effects of enalapril in rats. *Stroke*. 1997;28:1028-1034
7. Bang OY, Saver JL, Alger JR, Shah SH, Buck BH, Starkman S, Ovbiagele B, Liebeskind DS. Patterns and predictors of blood-brain barrier permeability derangements in acute ischemic stroke. *Stroke*. 2009;40:454-461
8. Kagansky N, Levy S, Knobler H. The role of hyperglycemia in acute stroke. *Arch Neurol*. 2001;58:1209-1212
9. Albers GW, Olivot JM. Intravenous alteplase for ischemic stroke. *Lancet*. 2007;369:249-250
10. Su EJ, Fredriksson L, Geyer M, Folestad E, Cale J, Andrae J, Gao Y, Pietras K, Mann K, Yepes M, Strickland DK, Betsholtz C, Eriksson U, Lawrence DA. Activation of pdgf-cc by tissue plasminogen activator impairs blood-brain barrier integrity during ischemic stroke. *Nat Med*. 2008;14:731-737
11. Bisdas S, Donnerstag F, Berding G, Vogl TJ, Thng CH, Koh TS. Computed tomography assessment of cerebral perfusion using a distributed parameter tracer kinetics model: Validation with h(2) ((15))o positron emission tomography measurements and initial clinical experience in patients with acute stroke. *J Cereb Blood Flow Metab*. 2008;28:402-411
12. Dankbaar JW, Hom J, Schneider T, Cheng SC, Lau BC, van der Schaaf I, Virmani S, Pohlman S, Dillon WP, Wintermark M. Dynamic perfusion ct assessment of the blood-brain barrier permeability: First pass versus delayed acquisition. *AJNR Am J Neuroradiol*. 2008;29:1671-1676
13. Nabavi DG, Dittrich R, Kloska SP, Nam EM, Klotz E, Heindel W, Ringelstein EB. Window narrowing: A new method for standardized assessment of the tissue at risk-maximum of infarction in ct based brain perfusion maps. *Neurol Res*. 2007;29:296-303
14. Parsons MW, Pepper EM, Bateman GA, Wang Y, Levi CR. Identification of the penumbra and infarct core on hyperacute noncontrast and perfusion ct. *Neurology*. 2007;68:730-736
15. Schaefer PW, Roccatagliata L, Ledezma C, Hoh B, Schwamm LH, Koroshetz W, Gonzalez RG, Lev MH. First-pass quantitative ct perfusion identifies thresholds for salvageable penumbra in acute stroke patients treated with intra-arterial therapy. *AJNR Am J Neuroradiol*. 2006;27:20-25
16. Wintermark M, Flanders AE, Velthuis B, Meuli R, van Leeuwen M, Goldsher D, Pineda C, Serena J, van der Schaaf I, Waaijer A, Anderson J, Nesbit G, Gabriely I, Medina V, Quiles A, Pohlman S, Quist M, Schnyder P, Bogousslavsky J, Dillon WP, Pedraza S. Perfusion-ct assessment of infarct core and penumbra: Receiver operating characteristic curve analysis in 130 patients suspected of acute hemispheric stroke. *Stroke*. 2006;37:979-985

17. Dankbaar JW, Hom J, Schneider T, Cheng SC, Lau BC, van der Schaaf I, Virmani S, Pohlman S, Dillon WP, Wintermark M. Accuracy and anatomical coverage of perfusion ct assessment of the blood-brain barrier permeability: One bolus versus two boluses. *Cerebrovasc Dis*. 2008;26:600-605
18. Axel L. Tissue mean transit time from dynamic computed tomography by a simple deconvolution technique. *Invest Radiol*. 1983;18:94-99
19. Ladurner G, Zilkha E, Iliff D, du Boulay GH, Marshall J. Measurement of regional cerebral blood volume by computerized axial tomography. *JNeurolNeurosurgPsychiatry*. 1976;39:152-158
20. Patlak CS, Blasberg RG, Fenstermacher JD. Graphical evaluation of blood-to-brain transfer constants from multiple-time uptake data. *JCerebBlood Flow Metab*. 1983;3:1-7
21. Barber PA, Demchuk AM, Zhang J, Buchan AM. Validity and reliability of a quantitative computed tomography score in predicting outcome of hyperacute stroke before thrombolytic therapy. Aspects study group. Alberta stroke programme early ct score. *Lancet*. 2000;355:1670-1674
22. Tan JC, Dillon WP, Liu S, Adler F, Smith WS, Wintermark M. Systematic comparison of perfusion-ct and ct-angiography in acute stroke patients. *Ann Neurol*. 2007;61:533-543
23. Bang OY, Buck BH, Saver JL, Alger JR, Yoon SR, Starkman S, Ovbiagele B, Kim D, Ali LK, Sanossian N, Jahan R, Duckwiler GR, Vinuela F, Salamon N, Villablanca JP, Liebeskind DS. Prediction of hemorrhagic transformation after recanalization therapy using t2*-permeability magnetic resonance imaging. *Ann Neurol*. 2007;62:170-176
24. Nagaraja TN, Karki K, Ewing JR, Croxen RL, Knight RA. Identification of variations in blood-brain barrier opening after cerebral ischemia by dual contrast-enhanced magnetic resonance imaging and t 1sat measurements. *Stroke*. 2008;39:427-432
25. Christoforidis GA, Karakasis C, Mohammad Y, Caragine LP, Yang M, Slivka AP. Predictors of hemorrhage following intra-arterial thrombolysis for acute ischemic stroke: The role of pial collateral formation. *AJNR Am J Neuroradiol*. 2009;30:165-170
26. Starr JM, Wardlaw J, Ferguson K, MacLulich A, Deary IJ, Marshall I. Increased blood-brain barrier permeability in type ii diabetes demonstrated by gadolinium magnetic resonance imaging. *J Neurol Neurosurg Psychiatry*. 2003;74:70-76
27. Ewing JR, Knight RA, Nagaraja TN, Yee JS, Nagesh V, Whitton PA, Li L, Fenstermacher JD. Patlak plots of gd-dtpa mri data yield blood-brain transfer constants concordant with those of 14c-sucrose in areas of blood-brain opening. *Magn Reson Med*. 2003;50:283-292
28. Bartolini A, Gasparetto B, Furlan M, Sullo L, Trivelli G, Albano C, Roncallo F. Functional perfusion and blood-brain barrier permeability images in the diagnosis of cerebral tumors by angio ct. *Comput Med Imaging Graph*. 1994;18:145-150
29. Leggett DA, Miles KA, Kelley BB. Blood-brain barrier and blood volume imaging of cerebral glioma using functional ct: A pictorial review. *Eur J Radiol*. 1999;30:185-190
30. Johnson JA, Wilson TA. A model for capillary exchange. *Am J Physiol*. 1966;210:1299-1303



Blood-brain barrier permeability
assessed by CT-perfusion as a predictor
for symptomatic hemorrhagic
transformation and malignant edema
after acute ischemic stroke



12

*J. Hom, J.W. Dankbaar, B.P. Soares, T. Schneider, S.C. Cheng, J. Bredno, B.C. Lau,
W. Smith, W.P. Dillon, M. Wintermark*

Abstract

Background and purpose

To evaluate the predictive value of admission blood-brain barrier permeability (BBBP) measurements derived from CT-perfusion (CTP) for the development of symptomatic hemorrhagic transformation (SHT) and malignant edema (ME) in acute ischemic stroke patients.

Methods

We retrospectively identified 32 consecutive acute ischemic MCA stroke patients with appropriate admission and follow-up imaging. The outcome measurements SHT and ME were defined according to ECASS III criteria. Admission BBBP was calculated using delayed acquisition CTP data and the Patlak model. Collateral flow was assessed on the admission CTA. Age, admission NIHSS score, time from symptom onset to scan, and treatment type were obtained from chart review. We incorporated both clinical and imaging variables, in a univariate and forward selection-based multivariate analysis for predictors of SHT and ME. Cut-off values for the optimal predictive properties of the variables in the multivariate model were determined and sensitivity, specificity, positive (PPV) and negative predictive (NPV) values calculated.

Results

Of the 32 patients, 3 developed SHT and 3 ME. Admission BBBP, age and rtPA were independent predictors of SHT and ME in our forward selection-based multivariate analysis. To predict SHT and ME, admission BBBP above threshold alone had a sensitivity of 1, specificity of 0.81, PPV of 0.55 and NPV of 1. The combination of admission BBBP above threshold, age ≥ 65 and rtPA had the best predictive properties (sensitivity=1, specificity=1, PPV=1, NPV=1).

Conclusion

A combination of admission BBBP above threshold and age ≥ 65 was a perfect predictor of SHT and ME in acute stroke patients receiving rtPA.

Introduction

Ischemic stroke is the 3rd leading cause of death and disability in the western world¹. Symptomatic hemorrhagic transformation (SHT)² and malignant edema (ME)³ are considered to be the most devastating complications of ischemic stroke. Systemic administration of rtPA is a highly effective treatment for acute ischemic stroke if administered within 4.5 hours after stroke onset.^{4,5} However, fewer than 2% of patients receive this treatment in most countries, primarily because of delayed admission to a stroke center.⁶ Moreover, rtPA is a consistently identified risk factor for SHT.⁴ SHT occurs in about 3.5% of all ischemic stroke patients and can cause an eleven fold increase in case fatalities.^{2,4} Thus, rtPA on the one hand saves brain tissue but on the other can also induce further brain damage. Differentiation of patients that will benefit from rtPA from patients that will be harmed is needed. ME occurs in 1-5% of all stroke patients and leads to case fatality rates up to 78%.³ Since no medical treatment has yet been proven to be effective for patients with ME,⁷ treatment with surgical decompression (removal of part of the skull and duraplasty) is applied in an attempt to reduce fatality and improve outcome.⁸ Surgical decompression seems beneficial if performed within 48 hours after stroke onset.⁹ However, all patients included in studies on the effect of decompression already had a large ischemic area with space occupying effect.^{3,9-11} Being able to select patients destined to develop ME on admission, before irreversible damage to the brain has occurred may result in a faster, earlier treatment and improved outcome.¹²

Blood-brain barrier (BBB) damage is the mechanism by which both hemorrhagic transformation (HT) and malignant edema (ME) occur after acute ischemic stroke.¹³⁻¹⁵ By assessing the permeability of the BBB (BBBP) direct knowledge is obtained on how much the BBB is damaged. BBBP measurements may therefore prove to be helpful in predicting complications and guiding treatment.¹⁶⁻¹⁹ CT-perfusion data, already acquired in ischemic stroke workup to predict whether recanalization treatment will be useful by distinguishing the amount of salvageable brain tissue from infarcted tissue,²⁰ can also be used to measure BBBP.^{21,22} These measurements may prove useful to predict which patients will develop complications.^{16,23}

The purpose of this study was to create a quantitative prediction algorithm based on CTP BBBP data, patient characteristics and treatment information, with the goal of identifying those patients destined for SHT or ME.

Methods

Study design

Clinical and imaging data obtained as part of standard clinical stroke care at our institution were retrospectively reviewed with the approval of the institutional review board. At our institution, patients with suspicion of acute stroke and no history of significant renal insufficiency or contrast allergy routinely undergo a stroke CT survey including noncontrast CT (NCT) of the brain, CTP at two cross-

sectional positions, CT-angiogram (CTA) of the cervical and intracranial vessels and post-contrast cerebral CT, obtained in this chronological sequence.

We retrospectively identified all consecutive patients admitted to UCSF from July 2006 to April 2009 who met the following inclusion criteria: (a) admission to the emergency room with signs and symptoms suggesting acute stroke within 12 hours after symptom onset; (b) documentation of acute ischemic MCA stroke by both admission stroke protocol and clinical examination; (c) no evidence of intracerebral hemorrhage on the admission NCT; (d) follow up imaging within 72 hours after the admission scan.

Patients' medical charts were reviewed for demographics, time from symptom onset to imaging, time to revascularization therapy, type of revascularization therapy (mechanical thrombectomy using MERCI retriever device or rtPA treatment (both intravenous and intra-arterial)), and NIH stroke scale (NIHSS) scores on admission, at 24 hours and on discharge.

Imaging protocol

CTP studies were obtained on 64-slice CT scanners. Each CTP study involved successive gantry rotations performed in cine mode during intravenous administration of iodinated contrast material. Images were acquired and reconstructed at a temporal sampling rate of 1 image per second for the first 37 seconds and 1 image every 2 seconds for the next 33 seconds. Additional gantry rotations were obtained at 90, 120, 150, 180, 210 and 240 seconds (delayed acquisition). Acquisition parameters were 80 kVp and 100 mAs. Two successive CTP series at two different levels were performed, with 8 5-mm-thick slices assessed at each CTP level. The first CTP series was obtained at the level of the third ventricle and the basal ganglia. The second CTP series was obtained above the lateral ventricles. For each CTP series, a 40 ml bolus of iohexol (Omnipaque, Amersham Health, Princeton, NJ; 300 mg/ml of iodine) was administered into an antecubital vein at an injection rate of 5 ml per second using a power injector. CT scanning was initiated 7 seconds after start of the injection of the contrast bolus. Data from both boluses was used as prior work has demonstrated that there is no significant parenchymal saturation effect from the first bolus and no underestimation of BBBP values from data from the second bolus.²⁴

Image post-processing

CTP data were analyzed utilizing commercially available CTP software (Brain Perfusion, Philips Healthcare, Cleveland, OH, USA).²⁵ The software applies a closed-form (non-iterative) deconvolution to calculate the mean transit time (MTT) map, using previously described methods.²⁶ The deconvolution operation requires a reference arterial input function (most often within the anterior cerebral artery), automatically selected by the CTP software within a region of interest drawn by the user. The cerebral blood volume (CBV) map is calculated from the area under the time-density curves compared to a similarly obtained venous reference curve. The CTP infarct core and salvageable brain tissue are automatically calcu-

lated by the software using CBV thresholds and MTT thresholds reported in the literature as the most accurate (CTP penumbra: MTT > 145% of the contralateral side values plus CBV \geq 2.0 ml /100g; CTP infarct core: MTT > 145% of the contralateral side values plus CBV < 2.0 ml /100g).²⁰

BBBP measurements were extracted from CTP data using a second, prototype software developed by Philips Healthcare. This software is based on the Patlak model.²⁷ Applying the Patlak model to CTP involves the fitting of a regression line to observations of time-density curves for each pixel and for an intravascular reference function. The slope of these regression lines was interpreted as a local blood-to-brain transfer constant and used as an indicator of BBBP values.

Image analysis

Volumes of the infarct core on the admission CTP were recorded, using the above described threshold CTP values.

CTP-derived BBBP maps were automatically segmented for all pixels with an absolute BBBP value > 5 ml /100g/min (a threshold defined by eye-balling all BBBP images). Values > 5 ml /100g/min were considered to be abnormally high. Next, we calculated the total volume of pixels with abnormally high (> 5ml /100g/min) BBBP values in each patient.

On the admission CTA, the collateral flow was graded according to a previously reported scoring system²⁸ on a scale from 0 to 3: 0= absent collaterals; 1= collaterals filling <50% of the occluded territory; 2= collaterals filling >50% but <100% of the occluded territory; 3= collaterals filling 100% of the occluded territory. The collateral score was then dichotomized into poor (score of 0 or 1) or good (score of 2 or 3).

We used the ECASS III criteria, which defines SHT as any extravasated blood associated with a NIHSS score increase of greater than 4 (or death), where the HT was the predominant cause of clinical deterioration⁵. To make this determination, all 24-hour images were reviewed for evidence of HT, and medical records were reviewed for documentation of an NIHSS increase > 4 that was causally attributed to the HT.

In addition to using the ECASS III criteria, all instances of HT were also graded based on a previously reported system using purely radiological definitions.²⁹ Parenchymal hematoma type-2 (PH-2), which was one of our outcomes of interest, was defined as dense hematoma >30% of the infarcted area with substantial space-occupying effect or as any hemorrhagic lesion outside the infarcted area.

Follow-up imaging was also reviewed for malignant edema (ME) as a primary complication, as was done in ECASS III.⁵ ME was defined as brain edema with mass effect as the predominant cause of clinical deterioration (a NIHSS score increase of greater than 4 or death).

Statistical analysis

Our outcome was significant clinical deterioration (a NIHSS score increase of greater than 4) related either to SHT or ME. We conducted a univariate analysis

to calculate the crude odds ratio (OR) of the proposed clinical and imaging predictors. In terms of clinical variables, we included age, admission NIHSS score, time from symptom onset to imaging, MERCI treatment and rtPA treatment. In terms of imaging variables, we included admission volume of abnormally high BBBP, volume of admission CTP-defined infarct, and collateral score.

Subsequently, a multivariate, mixed effect model involving forward-stepwise selection with a significant threshold set at 0.05 was built from the variables that had a univariate p value < 0.2 . Adjusted ORs of the remaining variables of the final multivariate model were calculated.

The values of variables in the multivariate model, were summarized for all patients and eye-balled to determine optimal cut-off point of each variable to identify patients with significant clinical deterioration related either to SHT or ME. The combination of cut-off points of the different variables with the best predictive properties for SHT and ME was also identified and sensitivities, specificities and positive and negative predictive values were calculated.

Results

Thirty-two patients admitted to our institution between July 2006 to April 2009 were identified that met the inclusion criteria. Patient characteristics, as well as imaging assessment of admission infarct core and collateral flow, are summarized in *Table 1*. Eight patients showed a significant clinical deterioration (a NIHSS score increase of greater than 4 or death). Three out of these 8 had SHT. In all cases SHT also qualified for the PH-2 criteria. Another three patients had ME. Two patients in our study had significant clinical deterioration due to a non-neurological cause - aspiration pneumonia and septicemia - without SHT/PH-2 or ME. The six patients with a significant clinical deterioration (a NIHSS score increase of greater than 4 or death) due to either SHT/PH-2 (3) or ME (3) were considered as those with a positive outcome. *Table 2* shows the results of the univariate analyses and the forward selection-based multivariate analysis. In the univariate analysis, age, NIHSS, rtPA treatment, admission CTP-defined infarct volume, and admission volume of abnormally high BBBP were associated with a p -value < 0.2 in terms of predicting a significant clinical deterioration due either to SHT or ME. The multivariate analysis showed that the optimal model to predict significant clinical deterioration related to either SHT/PH-2 or ME includes age, rtPA administration and admission volume of abnormally high absolute BBBP values.

Table 3 shows the admission volume of abnormally high absolute BBBP, rtPA and age in each patient. Eye-balling of the values in *Table 3* rendered an optimal threshold to dichotomize the volume of abnormally high absolute BBBP values of 7 ml and an optimal threshold to dichotomize age of 65 years. The predictive properties of the different combinations of these cut-off values and the use of rtPA are summarized in *Table 4*. The combination of admission BBBP above threshold (>7 ml), age ≥ 65 and rtPA (a triad of characteristics) had the best predictive properties, with a sensitivity, specificity, positive and negative predictive value of 1.

Median admission volumes of abnormally high absolute BBBP values were 8.9 (range: 7 - 17) in those patients who developed SHT/PH-2 or ME. Median admission volumes of abnormally high absolute BBBP values were 1.4 (range: 0 - 42) in those patients who did not develop SHT/PH-2 or ME.

Figure 1 shows an example of a patient with increased BBBP and subsequent hemorrhage.

Figure 2 shows a flow chart of our predictive algorithm. Of note, all patients with SHT/PH-2 had >50% collateral filling in the region of stroke and all patients with ME had <50% collateral filling.

Table 1 Patient characteristics.

Number of patients	32
Number of men (%)	13 (41%)
Age (years)	Median = 72 Interquartile range = 65 – 85
NIHSS (median with interquartile range)	
Admission	14 (10 – 17)
24h	9 (4 – 14)
Discharge	4 (2 – 10)
Treatment	
conservative	6
rtPA	13
MERC1	3
Both	10
Time (hours) from symptom onset to admission imaging (median with interquartile range)	2 (1.5 – 4.1)
Time (hours) from admission imaging to follow-up imaging (median with interquartile range)	24.8 (22.5 – 27.25)
Admission CTP findings	
mean volume of infarct core (ml ± standard deviation)	31.7 ± 33.1
Collateral flow on admission CTA	
absent collaterals	3
collateral filling <50%	6
collateral filling 50-99%	11
collateral filling 100%	12

Table 2 Univariate and multivariate analysis of clinical and imaging predictors of significant clinical deterioration, showing the crude odds ratio (OR) for the univariate analysis and the adjusted OR for the multivariate analysis. Variables with an asterisk (associated with a p value < 0.2) are those that were considered for inclusion in the multivariate analysis.

	Univariate Analysis (n = 32)	
	<i>Crude OR</i>	<i>P-Value</i>
Clinical		
Age	1.07	0.08*
Admission NIHSS score	1.26	0.07*
Time from symptom onset to scan	0.81	0.43
tPA treatment	>1000	0.03*
MERCI treatment	0.68	0.68
Imaging		
Admission CTP-defined infarct volume	1.02	0.08*
Admission blood-brain barrier permeability	1.71	0.01*
Collaterals to the region of the stroke	0.37	0.29
Forward Selection-Based Multivariate Analysis (n = 32)		
	<i>Adjusted OR</i>	<i>P-Value</i>
Age	>1000	<0.01
tPA administration	>1000	<0.01
Admission Blood-Brain Barrier Permeability	>1000	<0.01

Table 3 Admission volume of abnormally high absolute BBBP values, age, rtPA administration and development of SHT/PH-2 and ME in our study patients. For each patient, admission volume of abnormally high absolute BBBP > 7 ml , rtPA treatment (IA or IV), age ≥65 and a clinically significant complication (SHT/PH-2 or ME) are highlighted in gray. This graphically illustrates that only the patients with all three risk factors developed SHT/PH-2 or ME.

Patient	Admission volume of abnormally high absolute BBBP values (ml)	Treatment	Age	SHT/PH-2 or ME
1	11.7	IA rtPA + MERCI	65	ME
2	8.2	IV rtPA	73	ME
3	17.0	IV rtPA	96	ME
4	9.6	IV rtPA	75	SHT/PH-2
5	7.3	IV rtPA	85	SHT/PH-2
6	7.0	IA rtPA + MERCI	91	SHT/PH-2
7	29.7	IA rtPA + MERCI	39	No
8	19.5	IA rtPA + MERCI	49	No
9	16.5	Conservative	68	No
10	16.7	Conservative	69	No
11	42	MERCI	70	No
12	3	IA rtPA + MERCI	46	No
13	1.1	IV rtPA	63	No
14	1.6	IV rtPA	64	No
15	1.4	IA rtPA + MERCI	65	No
16	0	IV rtPA	68	No
17	3.9	IA rtPA + MERCI	71	No
18	0.3	IV rtPA	73	No
19	0.3	IV rtPA	73	No
20	1.3	IA rtPA + MERCI	74	No
21	0	IV rtPA	85	No
22	3.1	IA rtPA + MERCI	86	No
23	0.1	IV rtPA	86	No
24	0.5	IA rtPA + MERCI	87	No
25	0.1	IV rtPA	90	No
26	0	IV rtPA	91	No
27	1.7	MERCI	56	No
28	5.3	Conservative	61	No
29	0	Conservative	64	No
30	3.2	Conservative	69	No
31	1.0	Conservative	81	No
32	0.8	MERCI	90	No

Table 4 Predictive properties (with 95% confidence interval) for significant clinical deterioration of combinations of the variables in the multivariate model based on table 3.

	Sensitivity	Specificity	PPV	NPV
Volume of abnormal BBBP >7 ml	1.00 (0.64-1.00)	0.81 (0.62-0.92)	0.55 (0.28-0.79)	1.00 (0.86-1.00)
Volume of abnormal BBBP >7 ml and Age ≥65 years	1.00 (0.64-1.00)	0.88 (0.70-0.97)	0.67 (0.35-0.88)	1.00 (0.87-1.00)
Volume of abnormal BBBP >7 ml and rtPA treatment	1.00 (0.64-1.00)	0.92 (0.75-0.99)	0.75 (0.40-0.94)	1.00 (0.88-1.00)
Volume of abnormal BBBP >7 ml, rtPA treatment and age ≥65 years	1.00 (0.64-1.00)	1.00 (0.89-1.00)	1.00 (0.64-1.00)	1.00 (0.89-1.00)

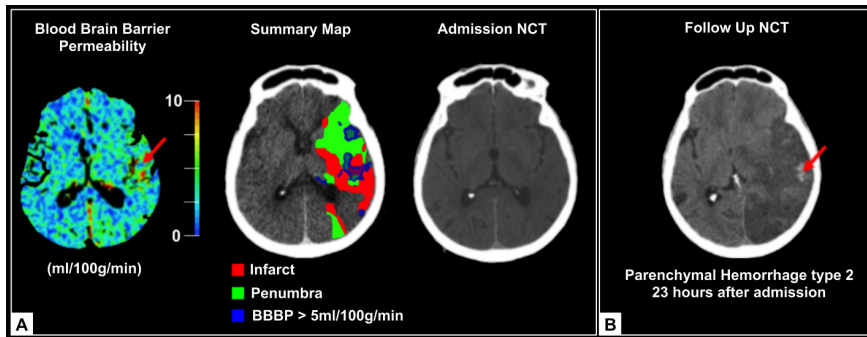


Figure 1 Illustrative case of abnormal permeability resulting in hemorrhagic transformation. (A) A 75 year-old woman with stroke CT imaging work-up approximately two hours after onset of a right sided hemiparesis. The blood brain barrier permeability (BBBP) map shows an area of increased BBBP (red arrow); applying the 5 ml/100gr/min threshold shows a “hotspot” of increased BBBP (automatically delineated in blue by the software) in the infarct core (red area) on the summary map; the non-contrast CT (NCT) revealed no evidence of intracranial hemorrhage. The patients was treated with IV rtPA. (B) 23 hours later, she was in critical condition in the ICU, and NCT imaging follow-up at that time demonstrated parenchymal hematoma type-2 (red arrow). Of note, permeability hotspots occur in both the infarct and penumbra, not just in the infarct, where the vasculature has presumably undergone the most severe ischemia-induced damage. This highlights that permeability imaging provides information above and beyond what is provided by the standard perfusion-CT parameters that can be used to define infarct and penumbra. *For colorfigure see page 235*

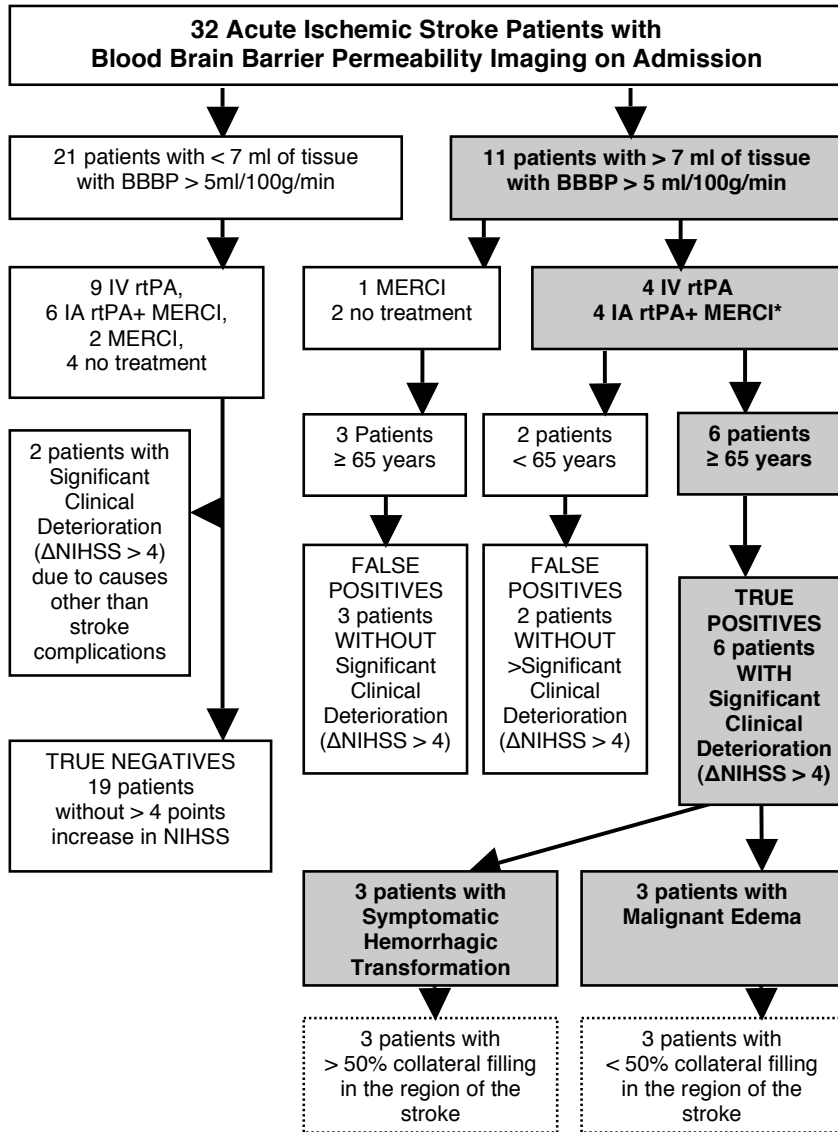


Figure 2 Flowchart of Our Predictive Algorithm for SHT and ME.

Discussion

This study highlights the promise of using quantitative blood-brain barrier permeability imaging in an automatable algorithm to predict subsequent development of symptomatic hemorrhagic transformation/parenchymal hematoma type-2 or malignant edema in acute ischemic stroke patients.

Using admission BBBP above a volume threshold as the sole predictor of SHT/PH-2 and ME, yields a sensitivity of 1 and specificity of 0.81 (5 false positives). This is in agreement with the critical role of ischemia-induced vascular damage in the pathogenesis of SHT/PH-2 and ME that has been previously reported.^{14, 15} Moreover, if we use the triad of admission BBBP above threshold, age ≥ 65 and rtPA administration, we can predict subsequent development of SHT/PH-2 or ME with 1 sensitivity and 1 specificity because 2 out of 5 of the false positives based on using BBBP imaging alone were younger than 65, and the remaining 3 false positives based on using BBBP imaging alone did not receive rtPA. These findings suggests that patients with elevated BBBP older than 65 years may not benefit from rtPA treatment.

The role of age ≥ 65 and rtPA administration in maximizing the specificity of our algorithm is consistent with prior studies that have discussed the relevance of these two variables in the development of SHT/PH-2. Older age in rtPA -treated patients has previously been associated with SHT.³⁰ The link between older age and ME that is suggested by our data is however not documented. The link is physiologically plausible given that the pathogenesis of SHT/PH-2 and ME share similarities regarding vascular damage.^{14, 15}

The role of rtPA in SHT/PH-2 pathogenesis has been unequivocally established and widely studied. Although rtPA offers an overall benefit in stroke patients,⁵ it also increases the risk of SHT/PH-2.^{2, 5, 31, 32} Furthermore, studies have suggested that rtPA not only increases the risk of SHT/PH-2 by promoting reperfusion but also by direct upregulation of MMP-9,³³⁻³⁵ a protease which damages the vasculature. Elevated MMP-9 levels have also been demonstrated in stroke patients who develop ME.³⁶

Our data on collaterals added a way to potentially distinguish SHT/PH-2 and ME patients. Although we were not able to conduct a formal statistical analysis secondary to the small number of SHT/PH-2 and ME patients, we noted that all the SHT/PH-2 patients had good collateral scores whereas all the ME patients had poor collateral scores. This is a new observation although limited in significance due to the small sample size. Reperfusion due to recanalization of the primary occlusion or through collateral vessels³⁷ is known to contribute to the development of SHT/PH-2¹⁴ while ME is likely to be caused by a lack of reperfusion. In a prospective study it would be interesting to investigate the role of reperfusion in BBB function and the development of SHT and ME.³⁸ One would have to obtain follow-up imaging at two separate time points, first a reperfusion scan soon after treatment (but before the development of PH-2 or ME) and a later follow-up scan to assess the development of PH-2 or ME.

In general, our study is limited due to the fact that it was retrospective and conducted at only one institution. Moreover, we studied a relatively small population of only 32 patients and only 3 patients with SHT/PH-2 and 3 patients with ME. Despite the small sample size we still demonstrated promising sensitivity and specificity and statistically significant results in the multivariate analysis. One could also argue the fact that we combined SHT/PH-2 and ME patients together as a single outcome. We think this is reasonable given that both SHT/PH-2 and ME are devastating complications with ischemia-induced BBB damage as a central component of their pathogenesis.^{14, 15} Surely both complications also need to be separately evaluated in a larger study.

With regards to the clinical utility of BBBP imaging, we would like to emphasize that the ultimate goal of using BBBP imaging for prediction of complications is to prevent them. Prevention may be realized by withholding rtPA treatment to prevent SHT and perform surgical treatment to prevent ME. Identifying patients with a low risk of complications may result in an extension of the treatment time window and increase administration rate of rtPA.

Conclusion

Abnormally elevated BBBP can predict SHT and ME in acute stroke patients. Future research will need to clarify whether treatment decisions based on BBBP measurements improve outcome and reduce the occurrence of SHT and ME.

References

1. Barber PA, Zhang J, Demchuk AM, Hill MD, Buchan AM. Why are stroke patients excluded from tpa therapy? An analysis of patient eligibility. *Neurology*. 2001;56:1015-1020
2. Berger C, Fiorelli M, Steiner T, Schabitz WR, Bozzao L, Bluhmki E, Hacke W, von KR. Hemorrhagic transformation of ischemic brain tissue: Asymptomatic or symptomatic? *Stroke*. 2001;32:1330-1335
3. Hofmeijer J, Algra A, Kappelle LJ, van der Worp HB. Predictors of life-threatening brain edema in middle cerebral artery infarction. *Cerebrovascular Diseases*. 2008;25:176-184
4. Hacke W, Donnan G, Fieschi C, Kaste M, von KR, Broderick JP, Brott T, Frankel M, Grotta JC, Haley EC, Jr., Kwiatkowski T, Levine SR, Lewandowski C, Lu M, Lyden P, Marler JR, Patel S, Tilley BC, Albers G, Bluhmki E, Wilhelm M, Hamilton S. Association of outcome with early stroke treatment: Pooled analysis of atlantis, ecass, and ninds rt-pa stroke trials. *Lancet*. 2004;363:768-774
5. Hacke W, Kaste M, Bluhmki E, Brozman M, Davalos A, Guidetti D, Larrue V, Lees KR, Medeghri Z, Machnig T, Schneider R, von Kummer R, Wahlgren N, Toni D. Thrombolysis with alteplase 3 to 4.5 hours after acute ischemic stroke. *N Engl J Med*. 2008;359:1317-1329
6. Albers GW, Olivot JM. Intravenous alteplase for ischaemic stroke. *Lancet*. 2007;369:249-250
7. Hofmeijer J, van der Worp HB, Kappelle LJ. Treatment of space-occupying cerebral infarction. *Crit Care Med*. 2003;31:617-625
8. Rieke K, Schwab S, Krieger D, von Kummer R, Aschoff A, Schuchardt V, Hacke W. Decompressive surgery in space-occupying hemispheric infarction: Results of an open, prospective trial. *Crit Care Med*. 1995;23:1576-1587
9. Hofmeijer J, Kappelle LJ, Algra A, Amelink GJ, van Gijn J, van der Worp HB. Surgical decompression for space-occupying cerebral infarction (the hemicraniectomy after middle cerebral artery infarction with life-threatening edema trial [hamlet]): A multicentre, open, randomised trial. *Lancet Neurol*. 2009;8:326-333
10. Juttler E, Schwab S, Schmiedek P, Unterberg A, Hennerici M, Woitzik J, Witte S, Jenetzky E, Hacke W. Decompressive surgery for the treatment of malignant infarction of the middle cerebral artery (destiny): A randomized, controlled trial. *Stroke*. 2007;38:2518-2525
11. Vahedi K, Vicaut E, Mateo J, Kurtz A, Orabi M, Guichard JP, Boutron C, Couvreur G, Rouanet F, Touze E, Guillon B, Carpentier A, Yelnik A, George B, Payen D, Bousser MG. Sequential-design, multicenter, randomized, controlled trial of early decompressive craniectomy in malignant middle cerebral artery infarction (decimal trial). *Stroke*. 2007;38:2506-2517
12. Schwab S, Steiner T, Aschoff A, Schwarz S, Steiner HH, Jansen O, Hacke W. Early hemicraniectomy in patients with complete middle cerebral artery infarction. *Stroke*. 1998;29:1888-1893
13. Lampl Y, Sadeh M, Lorberboym M. Prospective evaluation of malignant middle cerebral artery infarction with blood-brain barrier imaging using tc-99m dtpa spect. *Brain Res*. 2006;1113:194-199
14. Wang X, Lo EH. Triggers and mediators of hemorrhagic transformation in cerebral ischemia. *MolNeurobiol*. 2003;28:229-244
15. Zador Z, Stiver S, Wang V, Manley GT. Role of aquaporin-4 in cerebral edema and stroke. *Handb Exp Pharmacol*. 2009:159-170
16. Aviv RI, d'Esterre CD, Murphy BD, Hopyan JJ, Buck B, Mallia G, Li V, Zhang L, Symons SP, Lee TY. Hemorrhagic transformation of ischemic stroke: Prediction with ct perfusion. *Radiology*. 2009;250:867-877

17. Bang OY, Buck BH, Saver JL, Alger JR, Yoon SR, Starkman S, Ovbiagele B, Kim D, Ali LK, Sanossian N, Jahan R, Duckwiler GR, Vinuela F, Salamon N, Villablanca JP, Liebeskind DS. Prediction of hemorrhagic transformation after recanalization therapy using t2*-permeability magnetic resonance imaging. *Ann Neurol.* 2007;62:170-176
18. Ding G, Jiang Q, Li L, Zhang L, Gang Zhang Z, Ledbetter KA, Ewing JR, Li Q, Chopp M. Detection of bbb disruption and hemorrhage by gd-dtpa enhanced mri after embolic stroke in rat. *Brain Res.* 2006;1114:195-203
19. Hjort N, Wu O, Ashkanian M, Solling C, Mouridsen K, Christensen S, Gyldensted C, Andersen G, Ostergaard L. Mri detection of early blood-brain barrier disruption: Parenchymal enhancement predicts focal hemorrhagic transformation after thrombolysis. *Stroke.* 2008;39:1025-1028
20. Wintermark M, Flanders AE, Velthuis B, Meuli R, van Leeuwen M, Goldsher D, Pineda C, Serena J, van der Schaaf I, Waaijer A, Anderson J, Nesbit G, Gabriely I, Medina V, Quiles A, Pohlman S, Quist M, Schnyder P, Bogousslavsky J, Dillon WP, Pedraza S. Perfusion-ct assessment of infarct core and penumbra: Receiver operating characteristic curve analysis in 130 patients suspected of acute hemispheric stroke. *Stroke.* 2006;37:979-985
21. Dankbaar JW, Hom J, Schneider T, Cheng SC, Lau BC, van der Schaaf I, Virmani S, Pohlman S, Dillon WP, Wintermark M. Dynamic perfusion ct assessment of the blood-brain barrier permeability: First pass versus delayed acquisition. *AJNR Am J Neuroradiol.* 2008;29:1671-1676
22. Dankbaar JW, Hom J, Schneider T, Cheng SC, Lau BC, van der Schaaf I, Virmani S, Pohlman S, Wintermark M. Age- and anatomy-related values of blood-brain barrier permeability measured by perfusion-ct in non-stroke patients. *J Neuroradiol.* 2009;36:219-227
23. Bisdas S, Hartel M, Cheong LH, Koh TS. Detection of early vessel leakiness in acute ischemic stroke using computed tomography perfusion may indicate hemorrhagic transformation. *Acta Radiol.* 2007;48:341-344
24. Dankbaar JW, Hom J, Schneider T, Cheng SC, Lau BC, van der Schaaf I, Virmani S, Pohlman S, Dillon WP, Wintermark M. Accuracy and anatomical coverage of perfusion ct assessment of the blood-brain barrier permeability: One bolus versus two boluses. *Cerebrovasc Dis.* 2008;26:600-605
25. Wintermark M, Maeder P, Thiran JP, Schnyder P, Meuli R. Quantitative assessment of regional cerebral blood flows by perfusion ct studies at low injection rates: A critical review of the underlying theoretical models. *Eur Radiol.* 2001;11:1220-1230
26. Axel L. Tissue mean transit time from dynamic computed tomography by a simple deconvolution technique. *Invest Radiol.* 1983;18:94-99
27. Patlak CS, Blasberg RG. Graphical evaluation of blood-to-brain transfer constants from multiple-time uptake data. Generalizations. *J Cereb Blood Flow Metab.* 1985;5:584-590
28. Tan JC, Dillon WP, Liu S, Adler F, Smith WS, Wintermark M. Systematic comparison of perfusion-ct and ct-angiography in acute stroke patients. *Ann Neurol.* 2007;61:533-543
29. Wolpert SM, Bruckmann H, Greenlee R, Wechsler L, Pessin MS, del Zoppo GJ. Neuroradiologic evaluation of patients with acute stroke treated with recombinant tissue plasminogen activator. The rt-pa acute stroke study group. *AJNR Am J Neuroradiol.* 1993;14:3-13
30. Larrue V, von Kummer RR, Muller A, Bluhmki E. Risk factors for severe hemorrhagic transformation in ischemic stroke patients treated with recombinant tissue plasminogen activator: A secondary analysis of the european-australasian acute stroke study (ecass ii). *Stroke.* 2001;32:438-441

31. Intracerebral hemorrhage after intravenous t-pa therapy for ischemic stroke. The ninds t-pa stroke study group. *Stroke*. 1997;28:2109-2118
32. Paciaroni M, Agnelli G, Corea F, Ageno W, Alberti A, Lanari A, Caso V, Micheli S, Bertolani L, Venti M, Palmerini F, Biagini S, Comi G, Previdi P, Silvestrelli G. Early hemorrhagic transformation of brain infarction: Rate, predictive factors, and influence on clinical outcome: Results of a prospective multicenter study. *Stroke*. 2008;39:2249-2256
33. Montaner J, Molina CA, Monasterio J, Abilleira S, Arenillas JF, Ribo M, Quintana M, Alvarez-Sabin J. Matrix metalloproteinase-9 pretreatment level predicts intracranial hemorrhagic complications after thrombolysis in human stroke. *Circulation*. 2003;107:598-603
34. Tsuji K, Aoki T, Tejima E, Arai K, Lee SR, Atochin DN, Huang PL, Wang X, Montaner J, Lo EH. Tissue plasminogen activator promotes matrix metalloproteinase-9 upregulation after focal cerebral ischemia. *Stroke*. 2005;36:1954-1959
35. Yepes M, Roussel BD, Ali C, Vivien D. Tissue-type plasminogen activator in the ischemic brain: More than a thrombolytic. *Trends Neurosci*. 2009;32:48-55
36. Serena J, Blanco M, Castellanos M, Silva Y, Vivancos J, Moro MA, Leira R, Lizasoain I, Castillo J, Davalos A. The prediction of malignant cerebral infarction by molecular brain barrier disruption markers. *Stroke*. 2005;36:1921-1926
37. Soares BP, Chien JD, Wintermark M. Mr and ct monitoring of recanalization, reperfusion, and penumbra salvage: Everything that recanalizes does not necessarily reperfuse! *Stroke*. 2009;40:S24-27
38. Wintermark M, Albers GW, Alexandrov AV, Alger JR, Bammer R, Baron JC, Davis S, Demaerschalk BM, Derdeyn CP, Donnan GA, Eastwood JD, Fiebach JB, Fisher M, Furie KL, Goldmakher GV, Hacke W, Kidwell CS, Kloska SP, Kohrmann M, Koroshetz W, Lee TY, Lees KR, Lev MH, Liebeskind DS, Ostergaard L, Powers WJ, Provenzale J, Schellinger P, Silbergleit R, Sorensen AG, Wardlaw J, Wu O, Warach S. Acute stroke imaging research roadmap. *AJNR Am J Neuroradiol*. 2008;29:e23-30



General discussion



13

In this thesis the use of CT-perfusion (CTP) imaging in the evaluation of the most severe complications of subarachnoid hemorrhage (SAH) and ischemic stroke was explored. These complications are delayed cerebral ischemia (DCI) after SAH and damage to the blood-brain barrier (BBB) after ischemic stroke causing hemorrhagic transformation (HT) and malignant edema (ME). In part 1 of this thesis we evaluated the pathogenesis of DCI with CTP, the diagnosis of DCI with CTP, and DCI treatment evaluation with cerebral perfusion measurements. In part 2 we looked at the optimal use of CTP for BBB permeability (BBBP) measurement, factors influencing BBB integrity in stroke and non-stroke patients, BBB integrity in infarcted, ischemic and non-ischemic tissue, and at the predictive value of BBBP measurements for HT and ME.

In this chapter major findings, implications, limitations and future directions of the two topics will be discussed.

Part 1

Complications of subarachnoid hemorrhage: a CT perfusion evaluation of delayed cerebral ischemia

Major findings and implications

Delayed cerebral ischemia (DCI) is a feared complication of subarachnoid hemorrhage (SAH). With CT-perfusion (CTP) we can visualize the combined result of all factors influencing cerebral perfusion and thereby causing DCI. We studied normal values of perfusion with CTP, the use of CTP to evaluate the pathogenesis of DCI, the value of CTP in diagnosing DCI, and the effect of triple-H treatment on cerebral perfusion.

In *Chapter 2* we presented normal absolute values of cerebral perfusion measured with CTP in individuals without intracranial pathology. To reduce observer dependent variability we also introduced an innovative relative measurement of cerebral perfusion by calculating ratios between different ipsilateral flow territories. The absolute values in cortical gray matter, basal ganglia, and white matter measured with CTP in our population were comparable to values in the literature measured with the gold standard ^{133}Xe inhalation, and had a narrow confidence interval.¹ This implies that cerebral perfusion can be accurately estimated with CTP. We found that perfusion was lower in cerebral white matter compared to gray matter and basal ganglia. This difference has been previously described¹⁻⁵ and can be explained by differences in microvascular density: the higher the microvascular density the higher the cerebral blood flow (CBF).⁶⁻⁸ Although the mean values from CTP seem accurate, quantitative perfusion measurements on an individual level can be quite variable.^{9, 10} The alternative relative values between ipsilateral flow territories, presented to overcome this problem, indicate that there are normally small differences between perfusion in different cerebral flow territories (all ratios > 0.88). Deviations from these normal ratios, may indi-

cate pathology. Our alternative relative approach is likely to have advantages over conventional left to right comparison when studying (possible) bilateral perfusion abnormalities like DCI after SAH^{11, 12} or bilateral carotid artery stenosis. If more than one flow territory is affected within one hemisphere, the conventional left to right comparison may however be more helpful. In complicated cases with multiple locations of abnormal perfusion, visual interpretation may prove to be the only possible way to analyze the CTP data.

To study the pathogenesis of DCI we evaluated the effect of vasospasm on cerebral perfusion (*Chapter 3*), the relationship between vasospasm and DCI (*Chapter 3*), and the change in cerebral perfusion around the time of DCI (*Chapter 4*).

In *Chapter 3* we found that vasospasm caused a decrease in perfusion in the flow territory behind the spastic segment but also that large vessel vasospasm is not present in almost half of the DCI patients. These findings are confirmed by other studies,¹³⁻¹⁵ suggesting that vasospasm alone is not sufficient to cause DCI and that a multifactorial origin of DCI is more plausible. Other factors that have been suggested to contribute to the development of DCI are the absence of collateral blood supply, disturbed cerebral autoregulation, and the presence of inflammatory reactions causing micro-emboli and microvascular vasospasm.^{12, 16-20}

In *Chapter 4* we observed several differences in cerebral perfusion between DCI patients and clinically stable patients at different time-points around DCI.

CBF was lower and MTT higher in DCI patients compared to no-DCI patients before, during, and after DCI, with the largest difference between the groups at the time of DCI, while CBV remained relatively constant in both groups. Furthermore, MTT asymmetry develops in MTT at the time of DCI and decreases after DCI. Auto-regulation is often disturbed in SAH patients.²⁰ As a result CBV may not be adjusted appropriately to changes in MTT, which could explain the stable CBV, with increasing MTT and decreasing CBF in DCI patients towards the time of DCI. In ischemic stroke a prolonged MTT in the absence of a decrease in CBV indicates areas of possibly reversible ischemia since blood is still flowing to the ischemic region.²¹⁻²⁴ The increased MTT and constant CBV in our DCI patients could therefore indicate that the ischemia is still reversible in the measured area at the time of DCI. This would also explain why absolute and relative MTT and CBF partially recovered after DCI.^{16, 25} The partial recovery in the measured area can be either spontaneous or due to hypertensive treatment.

The absolute MTT gradually increased towards DCI while MTT asymmetry increased more prominently and occurred after absolute values had already worsened. This suggests that patients with diffusely worse absolute perfusion parameters may be more susceptible to additional changes in perfusion. In patients with worse absolute perfusion, vasospasm, micro-thrombi, or a failing collateral blood supply may lead to additional focal perfusion abnormalities resulting in increased asymmetry and neurologic worsening.^{12, 18, 19}

To diagnose DCI we evaluated the diagnostic value of non-contrast CT (NCT), vasospasm on CT-angiography (CTA) and qualitative assessment of CTP (by reading

the CTP colormaps for CBV, CBF, and MTT) for DCI at the time of clinical deterioration (*Chapter 5*). We also performed a study to obtain quantitative diagnostic threshold values of cerebral perfusion from CTP (*Chapter 6*). We studied both absolute and relative (interhemispheric asymmetry) values (*Chapter 6*).

In *Chapter 5* we found that qualitative assessment of CTP colormaps makes it possible to distinguish patients with DCI from patients with other causes of deterioration. We also confirmed that although NCT is necessary to rule out rebleed or hydrocephalus it is not sensitive enough to detect early ischemia in DCI patients and that macrovascular vasospasm on CTA has poor diagnostic value for DCI. In *Chapter 6*, quantitative perfusion measurements showed decreased absolute perfusion and a larger interhemispheric asymmetry in patients with DCI compared to patients with no deterioration after SAH. Furthermore, we found that threshold values of both absolute perfusion measurements and interhemispheric asymmetry in SAH patients can possibly be used to diagnose DCI. Absolute MTT values and interhemispheric MTT differences had the best diagnostic properties to distinguish patients with DCI from clinically stable patients.

When looking at the diagnostic properties of qualitative assessment of CTP colormaps (*Chapter 5*) and quantitative threshold values (both absolute and relative, *Chapter 6*) of CTP for DCI, it appears that the visual assessment (eyeballing) of colormaps has better diagnostic properties than absolute or relative threshold values. Although the populations of both chapters are not exactly the same, this observation is plausible for two reasons. Firstly, there is an extensive list of co-morbidity in SAH patients that can influence perfusion. These co-morbidities may be hard to distinguish from DCI when using absolute measurements without interpretation of the CTP colormaps. Secondly, eyeballing colormaps results in identifying the most abnormal region of perfusion while the standard measurements we used for the quantitative analysis were not centered to the abnormality. This could have resulted in less abnormal findings with the quantitative method. The advantage of quantitative threshold values is, that they make it possible to automatically highlight areas of ischemia (marking pixels above and below threshold). In both the qualitative assessment of CTP colormaps (*Chapter 5*) and quantitative assessment of CTP images (*Chapter 6*), the perfusion parameter MTT proved to be most useful for diagnosing DCI. As mentioned earlier a prolonged MTT in the absence of a severe decrease in CBF or CBV may indicate areas of possibly reversible ischemia.²²⁻²⁴ Our findings thus imply that the perfusion deficits measured in our DCI patients could still be reversible at the time of deterioration.

As suggested earlier DCI may be partly reversible due to treatment. In *Chapter 7* we performed a systematic review of the literature on the effect of a widely applied treatment for DCI, triple-H and its components, on CBF, the intended substrate of this intervention. We gave a quantitative summary showing that there is no good evidence that CBF improves due to the intervention. From all components of triple-H, induced hypertension seems to be the most promising. Our findings imply that for three decades a treatment strategy with potentially severe complications has been applied that has not been proven to achieve its hypothetical goal.

Limitations

The evaluation of DCI with CTP has some limitations. First, absolute perfusion measurements can be quite variable. In the software we used for CTP analysis there are several observer dependent post-processing steps that can influence the quantitative measurements.^{9, 10, 26, 27} The measurements can furthermore be influenced by partial volume effects of vessels and image noise. The vessels are generally removed by applying a threshold value to the data. However some pixels that are just below the threshold may still contain vessels and thereby disturb the quantitative measurement. Image noise is increased by movement and metal artifacts. These are both factors that are inherent to the often restless SAH patients with intracranial coils or clips after aneurysm treatment. Besides influencing quantitative measurements, movement and metal artifacts can also mimic perfusion abnormalities which can be wrongly interpreted by inexperienced readers during qualitative assessment.

Another important issue of using quantitative measurements to diagnose DCI is the location of the measurement. Ideally we would like to measure perfusion only in the areas where DCI is occurring. However, this would mean that the image needs to be qualitatively interpreted to decide in what area DCI is occurring before a region of interest can be drawn. This type of measurement is likely to be influenced by observer bias. The standardized measurements we used throughout this thesis are the necessary first step to objectively judge the diagnostic value of quantitative CTP measurements. Although more objective, these standardized measurements may have resulted in underestimation of perfusion abnormalities. DCI may only have affected part or none of the standard regions of interest. DCI may even occur outside the scanned area since the used CT scanners have limited coverage for CTP and not the entire brain is visualized. The range is limited to 2.4 cm on 16 slice scanners and 4 cm on 64 slice scanners. Scanners with larger detector ranges (128 to 320 slice) have increased coverage and are currently available. In *Chapter 9*, in part 2 of this thesis, a method to increase coverage on low range scanners is discussed. This method, where two CTP acquisitions at two different anatomical levels using two injections of contrast material are made, is already being applied in ischemic stroke patients. We did not yet apply this double acquisition method in SAH patients since the usefulness of CTP in this population had not been previously established. The problem of limited coverage is of course also an issue when qualitatively assessing CTP images.

The problems inherent to quantitative CTP measurements as described above have forced us to make limiting decisions regarding the selection of our populations. Since there can be several causes other than DCI for clinical deterioration and decreased perfusion in SAH patients, we only selected patients with DCI and clinically stable patients to prove that ischemia can be identified in SAH patients by quantitative assessment. All patients with other causes for deterioration were excluded. This selection of patients made it impossible to calculate positive and negative predictive values.

One last issue that needs to be addressed concerns the differences in cerebral perfusion between DCI patients and clinically stable patients before, during, and after DCI. Since we took DCI as the center point of our time-line, the time points before DCI are not at a fixed time after SAH but relative to DCI. Therefore, we can not make any comments regarding the predictive value of CTP measurements before DCI. Predicting DCI was not a subject in this thesis. The use of CTP for this purpose has however previously been evaluated, with the conclusion that CTP is a useful tool to predict DCI.^{28, 29}

Future directions

To optimize the use of CTP for the evaluation of DCI further investigations are required. It would be of great value to reconstruct CTA and NCT images from the CTP dataset to reduce scan time, the amount of contrast agent and radiation dose. In that way information on vasospasm, arterial patency after aneurysm treatment, presence of hydrocephalus, parenchymal hemorrhage or rebleed, as well as the cerebral perfusion status would be available from a single CTP acquisition. New CT scanners can provide full brain coverage and studies exploring these options are currently being conducted.

Our findings and previous studies point towards a multifactorial process and other tools than CTP may be needed to further unravel the pathogenesis of DCI. The combined result of the different pathologic processes leading to DCI may be visualized by CTP but the processes itself may not. Studying the different processes separately may be interesting since reversible ischemia may for a larger part be caused by vasospasm while micro-emboli or insufficient collaterals may play a larger part in irreversible ischemia.^{12, 16-19} High resolution anatomical imaging may be able to show small artery vasospasm,³⁰ selective arterial spin labeling techniques could visualize the contribution of collateral circulation to cerebral perfusion,³¹ and neuro-inflammatory processes leading to micro-emboli could be identified with cellular and molecular MR imaging.³²

The main goal of diagnosing DCI is to be able to make proper treatment decisions and to test treatment options. To use CTP in the diagnosis of DCI several issues need further evaluation. Firstly, the reproducibility of the qualitative assessment of the CTP colormaps needs to be investigated, both with experienced and properly instructed inexperienced readers. Secondly, the obtained quantitative threshold values need to be evaluated in a population that contains all SAH patients, including patients with clinical deterioration not caused by DCI. Combining the quantitative threshold, the qualitative interpretation of colormaps, clinical information and NCT findings should make it possible for the radiologist to positively identify DCI. Thirdly, it would be interesting to see whether we can discriminate between reversible and irreversible areas of ischemia at the time of deterioration. Standardized follow-up imaging showing permanent infarction would be required and is currently collected in all our SAH patients.

When DCI is properly diagnosed treatment options can be evaluated. As shown in this thesis there is no proper evidence that triple-H or its components can improve cerebral perfusion. Other treatment strategies like transluminal angioplasty and vasodilating drugs are also not proven to be efficient, but are currently applied in several specialized centers.^{33, 34} The evaluation of cerebral perfusion after randomized assignment to treatment with a technique as fast, cheap, and generally available as CTP, may be a practical first step towards an evidence based treatment for DCI.

Part 2

Complications of ischemic stroke: a CT perfusion evaluation of blood-brain barrier damage

Major findings and implications

Blood-brain barrier (BBB) damage is the mechanism by which hemorrhagic transformation (HT) and malignant edema (ME) occur after acute ischemic stroke.³⁵⁻³⁷ The amount of damage to the BBB can be assessed by measuring the permeability of the BBB (BBBP) with CT-perfusion (CTP), and could be helpful in predicting which patients will develop HT or ME.³⁸⁻⁴² Since BBBP measurement is a relatively new application of CTP, we first evaluated the optimal use of CTP for the assessment of BBB permeability (BBBP) in acute ischemic stroke patients. Then we evaluated factors influencing BBB integrity in stroke and non-stroke patients; BBB integrity in infarcted, ischemic and non-ischemic tissue; and the predictive value of BBBP measurements for HT and ME.

To calculate BBBP from CTP values the Patlak model can be applied, which is a relatively simple and frequently applied model to calculate contrast transfer across the BBB.^{43,44} In *Chapter 8* we showed that only the delayed phase of the CTP acquisition (and not the first-pass) respects the assumptions of the Patlak model.⁴⁴ BBBP measurements extracted from first-pass CTP data results in wrongly calculated higher BBBP values compared to values obtained from the delayed phase. This implies that first-pass data should not be used to calculate BBBP with the Patlak model in patients with acute ischemic stroke. To increase the anatomical coverage of CTP, in CT scanners with limited coverage, two slabs at different anatomical positions are made in acute ischemic stroke patients. This acquisition requires two contrast bolus injections. In *Chapter 9* we applied the Patlak model to the delayed phase of contrast injection of both boluses and analyzed whether the contrast material from the first bolus of contrast negatively influences measurements of BBBP values from the second bolus. We showed that the first bolus did not influence measurements from the second bolus if the interval between the two boluses is four minutes. This means that a second bolus can be used to increase anatomical coverage of BBBP measurements with CTP when applying the Patlak model.

In *Chapter 10* we presented normal ranges of BBBP values in cortical gray matter, basal ganglia, and cerebral white matter, calculated from delayed phase CTP data using the Patlak model. We furthermore showed that BBBP is increased in patients with hypertension and diabetes type II and that aspirin use seems to protect against BBB damage. The protective effect of aspirin and the damaging effect of hypertension and diabetes have been previously described.⁴⁵⁻⁴⁸ Other known factors that can influence BBB integrity showed no significant effect in our multivariate analysis.⁴⁹⁻⁵²

In *Chapter 11* we analyzed the difference in BBBP between infarcted, ischemic and non-ischemic tissue in acute ischemic stroke patients and the influence of different patient characteristics on BBBP. We found that BBBP is increased in infarcted and ischemic brain tissue compared to non-ischemic tissue on the admission CTP scan. This confirms that ischemia can result in BBB damage.⁵³ The presence of collateral blood supply to the area behind the occluded vessel and the duration of the occlusion are said to influence the amount of irreversible cerebral damage before the patient arrives at the emergency department.⁵⁴⁻⁵⁶ We found that patients with more than 50% collateral filling had lower BBBP values than patients with less collateral filling. Good collateral supply therefore seems to protect against BBB damage. This may explain why there is a relationship between more collateral filling and a lower incidence of hemorrhagic transformation.⁵⁴ We did not find a relationship between the time since symptom onset and BBBP. This may be caused by the fact that our patients were all admitted relatively soon (2 hours) after symptom onset. In this early stage the relationship between time and damage may not be large enough to be found in a relatively small sample. The relationship of a previous history of hypertension or diabetes that we found in non-stroke patients could not be reproduced in ischemic stroke patients. This may again be a result of the small sample size.

Chapter 12 we evaluated the predictive value of BBBP measurements on admission for HT and ME in acute ischemic stroke patients. We found that patients in whom severe BBBP damage leads to HT or ME can be accurately identified with BBBP measurements from the delayed phase of CTP on admission. Furthermore, we found that only patients with abnormally elevated BBBP, older than 65 years that received rtPA developed HT or ME. This suggests that patients with elevated BBBP older than 65 years may not benefit from rtPA treatment. As for ME, rtPA may have been the last drop in causing ME.

Limitations

There are several limitations regarding our findings.

Firstly, we have not compared the BBBP values that we calculated to a gold standard. The Patlak model has been validated for dynamic MR imaging techniques using intravenous contrast, but not for CTP.⁴³ Also we have not compared our measurements to measurements calculated with different mathematical models.⁵⁷⁻⁵⁹ However, studies applying other mathematical models showed similar re-

relationships between BBBP, patient characteristics and outcome in ischemic stroke patients.^{60, 61} This strengthens our confidence in the obtained findings.

A second limitation to our findings is that all data was collected retrospectively. There are some patient characteristics that have been reported to affect BBBP that could not be confirmed or analyzed because the information was not well documented. Alcohol⁴⁹ and nicotine⁵⁰ have been reported to damage the BBBP, while statin-use may have protective effects on BBBP.^{51, 52} Furthermore, we were not able to investigate the way reperfusion and rtPA treatment influence BBB integrity due to the lack of standardized follow up imaging right after treatment. Both factors have been suggested to increase BBBP and thereby cause HT.^{62, 63} Treatment with rtPA can cause a direct upregulation of a protease (MMP-9) which damages the vasculature.^{62, 64-66} Elevated levels of this protease have also been demonstrated in ischemic stroke patients who develop ME.⁶⁴

A third limitation is the small number of patients, especially patients with our final outcome measurements, symptomatic HT and ME. We retrospectively collected all data from a database spanning a period of almost three years. No more than three patients with symptomatic HT and three with ME were identified with a complete dataset to do the analysis in *Chapter 12*. Due to the small number of outcomes we combined symptomatic HT and ME. We think this is reasonable given that both symptomatic HT and ME are devastating complications with ischemia-induced BBB damage as a central component of their pathogenesis.³⁵⁻³⁷ However, to truly make individualized treatment decisions these two complications need to be separated which requires a much larger study group with a larger number of outcomes.

Future directions

Further investigations are required to optimize the use of CTP for the evaluation of blood-brain barrier damage and prediction of symptomatic HT and ME.

Firstly, different mathematical models to calculate BBBP from CTP data should be compared to each other and a gold standard. Also the reproducibility of the calculated values should be determined. A virtual brain perfusion phantom, which is currently under development in our department, could serve the purpose of a gold standard. The true permeability can first be interactively defined in such a phantom, and then different models can be tested to see whether they can reproduce the implemented permeability values.

Secondly, the threshold values we found to predict symptomatic HT and ME need to be validated. A multi-center study is currently underway and can collect a sufficient amount of patients to prospectively study the predictive value of BBBP measurements on symptomatic HT and ME separately with enough statistical power. We also will need to clarify whether treatment decisions based on BBBP measurements improve outcome. This again needs to be done separately for symptomatic HT and ME.

Thirdly, a prospective multi-center study should evaluate factors that can influence BBB integrity before ischemic stroke and before the occurrence of complications after stroke, that could not be properly analyzed in our retrospective study. Information on alcohol, nicotine, statin and aspirin use should be collected

together with information on blood glucose, previous history of hypertension, diabetes and other cardiovascular risk factors.^{45, 47, 49-52, 67-70} Furthermore, the changes in BBBP between admission and follow-up in relation to the amount of reperfusion and the use of rtPA treatment should be investigated. Identifying risk factors, protective agents, and predictive parameters will make it possible to create an individual risk profile for the development of HT and ME.

References

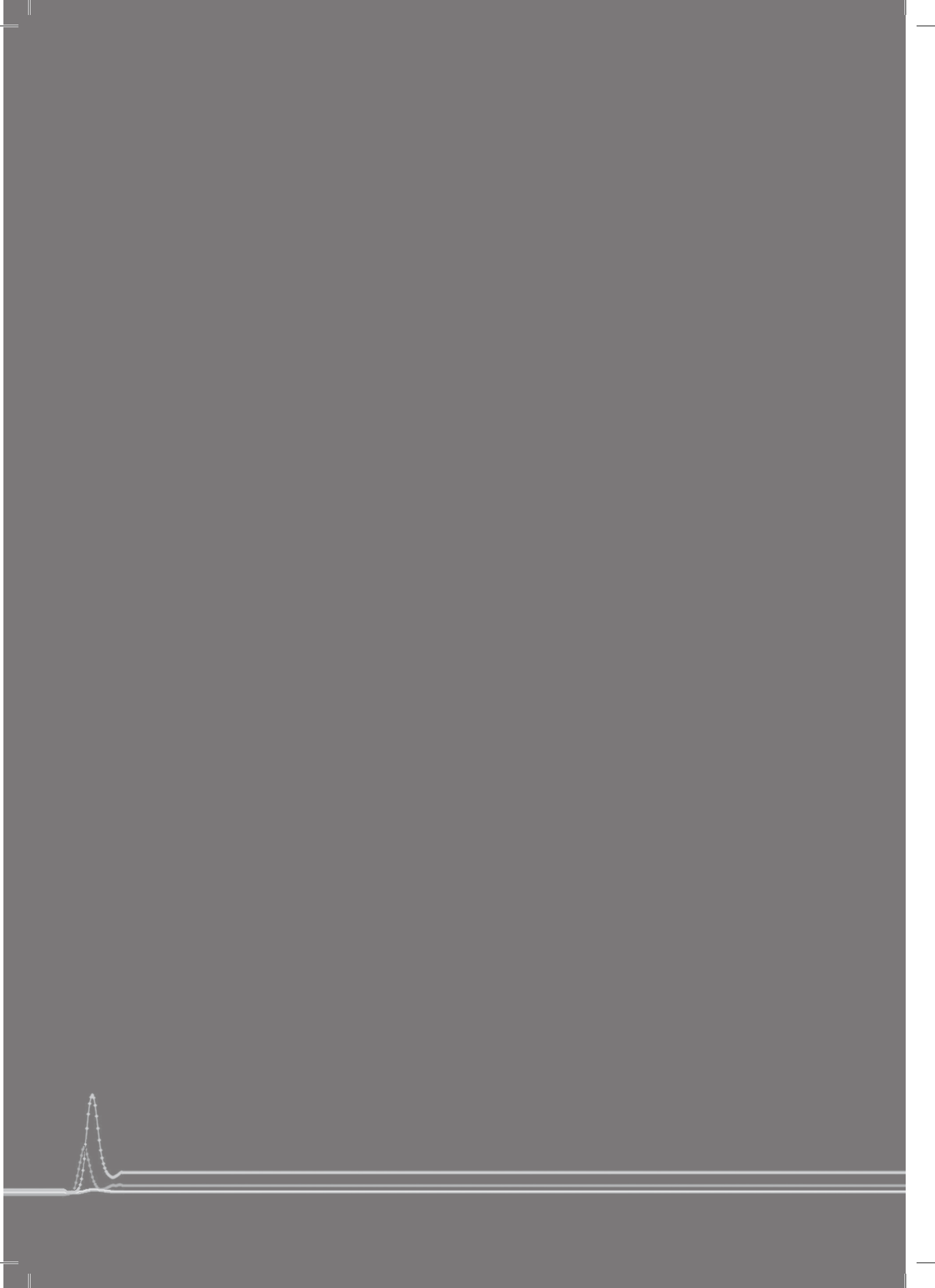
1. Kawamura J, Meyer JS, Ichijo M, Kobari M, Terayama Y, Weathers S. Correlations of leuko-ara-
iosis with cerebral atrophy and perfusion in elderly normal subjects and demented patients. *J
Neurol Neurosurg Psychiatry*. 1993;56:182-187
2. Biagi L, Abbruzzese A, Bianchi MC, Alsop DC, Del Guerra A, Tosetti M. Age dependence of cere-
bral perfusion assessed by magnetic resonance continuous arterial spin labeling. *J Magn Reson
Imaging*. 2007;25:696-702
3. Ito H, Kanno I, Kato C, Sasaki T, Ishii K, Ouchi Y, Iida A, Okazawa H, Hayashida K, Tsuyuguchi N,
Kuwabara Y, Senda M. Database of normal human cerebral blood flow, cerebral blood volume,
cerebral oxygen extraction fraction and cerebral metabolic rate of oxygen measured by positron
emission tomography with 15o-labelled carbon dioxide or water, carbon monoxide and oxygen:
A multicentre study in japan. *Eur J Nucl Med Mol Imaging*. 2004;31:635-643
4. Leenders KL, Perani D, Lammertsma AA, Heather JD, Buckingham P, Healy MJ, Gibbs JM, Wise
RJ, Hatazawa J, Herold S, et al. Cerebral blood flow, blood volume and oxygen utilization. Normal
values and effect of age. *Brain*. 1990;113 (Pt 1):27-47
5. Parkes LM, Rashid W, Chard DT, Tofts PS. Normal cerebral perfusion measurements using ar-
terial spin labeling: Reproducibility, stability, and age and gender effects. *Magn Reson Med*.
2004;51:736-743
6. Cavaglia M, Dombrowski SM, Drazba J, VasANJI A, Bokesch PM, Janigro D. Regional variation in
brain capillary density and vascular response to ischemia. *Brain Res*. 2001;910:81-93
7. Nonaka H, Akima M, Hatori T, Nagayama T, Zhang Z, Ihara F. Microvasculature of the human
cerebral white matter: Arteries of the deep white matter. *Neuropathology*. 2003;23:111-118
8. Suzuki M, Obara K, Sasaki Y, Matoh K, Kitabatake A, Sasaki K, Nunosawa F. Comparison of
perivascular astrocytic structure between white matter and gray matter of rats. *Brain Res*.
2003;992:294-297
9. Kealey SM, Loving VA, DeLong DM, Eastwood JD. User-defined vascular input function
curves: Influence on mean perfusion parameter values and signal-to-noise ratio. *Radiology*.
2004;231:587-593
10. van der Schaaf I, Vonken EJ, Waaijer A, Velthuis B, Quist M, van Osch T. Influence of partial vol-
ume on venous output and arterial input function. *AJNR Am J Neuroradiol*. 2006;27:46-50
11. Romano JG, Rabinstein AA, Arheart KL, Nathan S, Campo-Bustillo I, Koch S, Forteza AM. Micro-
emboli in aneurysmal subarachnoid hemorrhage. *J Neuroimaging*. 2008
12. Stein SC, Levine JM, Nagpal S, LeRoux PD. Vasospasm as the sole cause of cerebral ischemia:
How strong is the evidence? *NeurosurgFocus*. 2006;21:E2
13. Aralasmak A, Akyuz M, Ozkaynak C, Sindel T, Tuncer R. Ct angiography and perfusion imaging
in patients with subarachnoid hemorrhage: Correlation of vasospasm to perfusion abnormality.
Neuroradiology. 2009;51:85-93
14. Binaghi S, Colleoni ML, Maeder P, Uske A, Regli L, Dehdashti AR, Schnyder P, Meuli R. Ct angiog-
raphy and perfusion ct in cerebral vasospasm after subarachnoid hemorrhage. *AJNR AmJNeu-
roradiol*. 2007;28:750-758
15. Wintermark M, Dillon WP, Smith WS, Lau BC, Chaudhary S, Liu S, Yu M, Fitch M, Chien JD,
Higashida RT, Ko NU. Visual grading system for vasospasm based on perfusion ct imaging:
Comparisons with conventional angiography and quantitative perfusion ct. *Cerebrovasc Dis*.
2008;26:163-170

16. Weidauer S, Lanfermann H, Raabe A, Zanella F, Seifert V, Beck J. Impairment of cerebral perfusion and infarct patterns attributable to vasospasm after aneurysmal subarachnoid hemorrhage: A prospective mri and dsa study. *Stroke*. 2007;38:1831-1836
17. Weidauer S, Vatter H, Beck J, Raabe A, Lanfermann H, Seifert V, Zanella F. Focal laminar cortical infarcts following aneurysmal subarachnoid hemorrhage. *Neuroradiology*. 2008;50:1-8
18. Vergouwen MD, Vermeulen M, Coert BA, Stroes ES, Roos YB. Microthrombosis after aneurysmal subarachnoid hemorrhage: An additional explanation for delayed cerebral ischemia. *J Cereb Blood Flow Metab*. 2008;28:1761-1770
19. Romano JG, Rabinstein AA, Arheart KL, Nathan S, Campo-Bustillo I, Koch S, Forteza AM. Microemboli in aneurysmal subarachnoid hemorrhage. *J Neuroimaging*. 2008;18:396-401
20. Jaeger M, Schuhmann MU, Soehle M, Nagel C, Meixensberger J. Continuous monitoring of cerebrovascular autoregulation after subarachnoid hemorrhage by brain tissue oxygen pressure reactivity and its relation to delayed cerebral infarction. *Stroke*. 2007;38:981-986
21. Donnan GA, Baron JC, Ma H, Davis SM. Penumbra selection of patients for trials of acute stroke therapy. *Lancet Neurol*. 2009;8:261-269
22. Parsons MW, Pepper EM, Bateman GA, Wang Y, Levi CR. Identification of the penumbra and infarct core on hyperacute noncontrast and perfusion ct. *Neurology*. 2007;68:730-736
23. Schaefer PW, Roccatagliata L, Ledezma C, Hoh B, Schwamm LH, Koroshetz W, Gonzalez RG, Lev MH. First-pass quantitative ct perfusion identifies thresholds for salvageable penumbra in acute stroke patients treated with intra-arterial therapy. *AJNR Am J Neuroradiol*. 2006;27:20-25
24. Wintermark M, Flanders AE, Velthuis B, Meuli R, van Leeuwen M, Goldsher D, Pineda C, Serena J, van der Schaaf I, Waaijer A, Anderson J, Nesbit G, Gabriely I, Medina V, Quiles A, Pohlman S, Quist M, Schnyder P, Bogousslavsky J, Dillon WP, Pedraza S. Perfusion-ct assessment of infarct core and penumbra: Receiver operating characteristic curve analysis in 130 patients suspected of acute hemispheric stroke. *Stroke*. 2006;37:979-985
25. Conditte-Auliac S, Bracard S, Anxionnat R, Schmitt E, Lacour JC, Braun M, Meloneto J, Cordebar A, Yin L, Picard L. Vasospasm after subarachnoid hemorrhage: Interest in diffusion-weighted mr imaging. *Stroke*. 2001;32:1818-1824
26. Sanelli PC, Lev MH, Eastwood JD, Gonzalez RG, Lee TY. The effect of varying user-selected input parameters on quantitative values in ct perfusion maps. *Acad Radiol*. 2004;11:1085-1092
27. Soares BP, Dankbaar JW, Bredno J, Cheng S, Bhogal S, Dillon WP, Wintermark M. Automated versus manual post-processing of perfusion-ct data in patients with acute cerebral ischemia: Influence on interobserver variability. *Neuroradiology*. 2009;51:445-451
28. van der Schaaf I, Wermer MJ, van der Graaf Y, Hoff RG, Rinkel GJ, Velthuis BK. Ct after subarachnoid hemorrhage: Relation of cerebral perfusion to delayed cerebral ischemia. *Neurology*. 2006;66:1533-1538
29. van der Schaaf I, Wermer MJ, van der Graaf Y, Velthuis BK, van de Kraats CI, Rinkel GJ. Prognostic value of cerebral perfusion-computed tomography in the acute stage after subarachnoid hemorrhage for the development of delayed cerebral ischemia. *Stroke*. 2006;37:409-413
30. Zwanenburg JJ, Hendrikse J, Takahara T, Visser F, Luijten PR. Mr angiography of the cerebral perforating arteries with magnetization prepared anatomical reference at 7 t: Comparison with time-of-flight. *J Magn Reson Imaging*. 2008;28:1519-1526
31. van Laar PJ, van der Grond J, Hendrikse J. Brain perfusion territory imaging: Methods and clinical applications of selective arterial spin-labeling mr imaging. *Radiology*. 2008;246:354-364

32. Jin AY, Tuor UI, Rushforth D, Filfil R, Kaur J, Ni F, Tomanek B, Barber PA. Magnetic resonance molecular imaging of post-stroke neuroinflammation with a p-selectin targeted iron oxide nanoparticle. *Contrast Media Mol Imaging*. 2009
33. Rabinstein AA, Friedman JA, Weigand SD, McClelland RL, Fulgham JR, Manno EM, Atkinson JL, Wijidicks EF. Predictors of cerebral infarction in aneurysmal subarachnoid hemorrhage. *Stroke*. 2004;35:1862-1866
34. Smith WS, Dowd CF, Johnston SC, Ko NU, DeArmond SJ, Dillon WP, Setty D, Lawton MT, Young WL, Higashida RT, Halbach VV. Neurotoxicity of intra-arterial papaverine preserved with chlorobutanol used for the treatment of cerebral vasospasm after aneurysmal subarachnoid hemorrhage. *Stroke*. 2004;35:2518-2522
35. Lampl Y, Sadeh M, Lorberboym M. Prospective evaluation of malignant middle cerebral artery infarction with blood-brain barrier imaging using tc-99m dtpa spect. *Brain Res*. 2006;1113:194-199
36. Wang X, Lo EH. Triggers and mediators of hemorrhagic transformation in cerebral ischemia. *MolNeurobiol*. 2003;28:229-244
37. Zador Z, Stiver S, Wang V, Manley GT. Role of aquaporin-4 in cerebral edema and stroke. *Handb Exp Pharmacol*. 2009:159-170
38. Bisdas S, Hartel M, Cheong LH, Koh TS. Detection of early vessel leakiness in acute ischemic stroke using computed tomography perfusion may indicate hemorrhagic transformation. *Acta Radiol*. 2007;48:341-344
39. Ding G, Jiang Q, Li L, Zhang L, Gang Zhang Z, Ledbetter KA, Ewing JR, Li Q, Chopp M. Detection of bbb disruption and hemorrhage by gd-dtpa enhanced mri after embolic stroke in rat. *Brain Res*. 2006;1114:195-203
40. Hjort N, Wu O, Ashkanian M, Solling C, Mouridsen K, Christensen S, Gyldensted C, Andersen G, Ostergaard L. Mri detection of early blood-brain barrier disruption: Parenchymal enhancement predicts focal hemorrhagic transformation after thrombolysis. *Stroke*. 2008;39:1025-1028
41. Kim EY, Na DG, Kim SS, Lee KH, Ryoo JW, Kim HK. Prediction of hemorrhagic transformation in acute ischemic stroke: Role of diffusion-weighted imaging and early parenchymal enhancement. *AJNR AmJNeuroradiol*. 2005;26:1050-1055
42. Latour LL, Kang DW, Ezzeddine MA, Chalela JA, Warach S. Early blood-brain barrier disruption in human focal brain ischemia. *AnnNeurol*. 2004;56:468-477
43. Ewing JR, Knight RA, Nagaraja TN, Yee JS, Nagesh V, Whitton PA, Li L, Fenstermacher JD. Patlak plots of gd-dtpa mri data yield blood-brain transfer constants concordant with those of 14c-sucrose in areas of blood-brain opening. *Magn Reson Med*. 2003;50:283-292
44. Patlak CS, Blasberg RG, Fenstermacher JD. Graphical evaluation of blood-to-brain transfer constants from multiple-time uptake data. *JCerebBlood Flow Metab*. 1983;3:1-7
45. Alvarez-Guerra M, Hannaert P, Hider H, Chiavaroli C, Garay RP. Vascular permeabilization by intravenous arachidonate in the rat peritoneal cavity: Antagonism by antioxidants. *Eur J Pharmacol*. 2003;466:199-205
46. Serhan CN, Takano T, Chiang N, Gronert K, Clish CB. Formation of endogenous "Antiinflammatory" Lipid mediators by transcellular biosynthesis. Lipoxins and aspirin-triggered lipoxins inhibit neutrophil recruitment and vascular permeability. *Am J Respir Crit Care Med*. 2000;161:S95-S101
47. Al-Sarraf H, Philip L. Effect of hypertension on the integrity of blood brain and blood csf barriers, cerebral blood flow and csf secretion in the rat. *Brain Res*. 2003;975:179-188

48. Starr JM, Wardlaw J, Ferguson K, MacLulich A, Deary IJ, Marshall I. Increased blood-brain barrier permeability in type ii diabetes demonstrated by gadolinium magnetic resonance imaging. *J Neural Neurosurg Psychiatry*. 2003;74:70-76
49. Haorah J, Knipe B, Gorantla S, Zheng J, Persidsky Y. Alcohol-induced blood-brain barrier dysfunction is mediated via inositol 1,4,5-triphosphate receptor (ip3r)-gated intracellular calcium release. *J Neurochem*. 2007;100:324-336
50. Hawkins BT, Abbruscato TJ, Egleton RD, Brown RC, Huber JD, Campos CR, Davis TP. Nicotine increases in vivo blood-brain barrier permeability and alters cerebral microvascular tight junction protein distribution. *Brain Res*. 2004;1027:48-58
51. Ifergan I, Wosik K, Cayrol R, Kebir H, Auger C, Bernard M, Bouthillier A, Moumdjian R, Duquette P, Prat A. Statins reduce human blood-brain barrier permeability and restrict leukocyte migration: Relevance to multiple sclerosis. *Ann Neurol*. 2006;60:45-55
52. Mooradian AD, Haas MJ, Batejko O, Hovsepian M, Feman SS. Statins ameliorate endothelial barrier permeability changes in the cerebral tissue of streptozotocin-induced diabetic rats. *Diabetes*. 2005;54:2977-2982
53. McColl BW, Carswell HV, McCulloch J, Horsburgh K. Extension of cerebral hypoperfusion and ischaemic pathology beyond mca territory after intraluminal filament occlusion in c57bl/6j mice. *Brain Res*. 2004;997:15-23
54. Christoforidis GA, Karakasis C, Mohammad Y, Caragine LP, Yang M, Slivka AP. Predictors of hemorrhage following intra-arterial thrombolysis for acute ischemic stroke: The role of pial collateral formation. *AJNR Am J Neuroradiol*. 2009;30:165-170
55. Christoforidis GA, Mohammad Y, Kehagias D, Avutu B, Slivka AP. Angiographic assessment of pial collaterals as a prognostic indicator following intra-arterial thrombolysis for acute ischemic stroke. *AJNR Am J Neuroradiol*. 2005;26:1789-1797
56. Tan JC, Dillon WP, Liu S, Adler F, Smith WS, Wintermark M. Systematic comparison of perfusion-ct and ct-angiography in acute stroke patients. *Ann Neurol*. 2007;61:533-543
57. Bisdas S, Donnerstag F, Berding G, Vogl TJ, Thng CH, Koh TS. Computed tomography assessment of cerebral perfusion using a distributed parameter tracer kinetics model: Validation with h(2)(15)o positron emission tomography measurements and initial clinical experience in patients with acute stroke. *J Cereb Blood Flow Metab*. 2008;28:402-411
58. Koh TS, Cheong LH, Hou Z, Soh YC. A physiologic model of capillary-tissue exchange for dynamic contrast-enhanced imaging of tumor microcirculation. *IEEE Trans Biomed Eng*. 2003;50:159-167
59. Larson KB, Markham J, Raichle ME. Tracer-kinetic models for measuring cerebral blood flow using externally detected radiotracers. *J Cereb Blood Flow Metab*. 1987;7:443-463
60. Aviv RI, d'Esterre CD, Murphy BD, Hopyan JJ, Buck B, Mallia G, Li V, Zhang L, Symons SP, Lee TY. Hemorrhagic transformation of ischemic stroke: Prediction with ct perfusion. *Radiology*. 2009;250:867-877
61. Bisdas S, Hartel M, Cheong LH, Koh TS, Vogl TJ. Prediction of subsequent hemorrhage in acute ischemic stroke using permeability ct imaging and a distributed parameter tracer kinetic model. *JNeuroradiol*. 2007;34:101-108
62. Su EJ, Fredriksson L, Geyer M, Folestad E, Cale J, Andrae J, Gao Y, Pietras K, Mann K, Yepes M, Strickland DK, Betsholtz C, Eriksson U, Lawrence DA. Activation of pdgf-cc by tissue plasminogen activator impairs blood-brain barrier integrity during ischemic stroke. *Nat Med*. 2008;14:731-737

63. Warach S, Latour LL. Evidence of reperfusion injury, exacerbated by thrombolytic therapy, in human focal brain ischemia using a novel imaging marker of early blood-brain barrier disruption. *Stroke*. 2004;35:2659-2661
64. Serena J, Blanco M, Castellanos M, Silva Y, Vivancos J, Moro MA, Leira R, Lizasoain I, Castillo J, Davalos A. The prediction of malignant cerebral infarction by molecular brain barrier disruption markers. *Stroke*. 2005;36:1921-1926
65. Tsuji K, Aoki T, Tejima E, Arai K, Lee SR, Atochin DN, Huang PL, Wang X, Montaner J, Lo EH. Tissue plasminogen activator promotes matrix metalloproteinase-9 upregulation after focal cerebral ischemia. *Stroke*. 2005;36:1954-1959
66. Yepes M, Roussel BD, Ali C, Vivien D. Tissue-type plasminogen activator in the ischemic brain: More than a thrombolytic. *Trends Neurosci*. 2009;32:48-55
67. Demchuk AM, Morgenstern LB, Krieger DW, Linda Chi T, Hu W, Wein TH, Hardy RJ, Grotta JC, Buchan AM. Serum glucose level and diabetes predict tissue plasminogen activator-related intracerebral hemorrhage in acute ischemic stroke. *Stroke*. 1999;30:34-39
68. Dietrich WD, Alonso O, Busto R. Moderate hyperglycemia worsens acute blood-brain barrier injury after forebrain ischemia in rats. *Stroke*. 1993;24:111-116
69. Kagansky N, Levy S, Knobler H. The role of hyperglycemia in acute stroke. *Arch Neurol*. 2001;58:1209-1212
70. Ribo M, Molina CA, Delgado P, Rubiera M, Delgado-Mederos R, Rovira A, Munuera J, Alvarez-Sabin J. Hyperglycemia during ischemia rapidly accelerates brain damage in stroke patients treated with tpa. *J Cereb Blood Flow Metab*. 2007;27:1616-1622



Nederlandse samenvatting



In dit proefschrift worden de complicaties van twee subtypes van beroertes bestudeerd met een techniek waarmee de doorbloeding van de hersenen kan worden afgebeeld. De gebruikte techniek heet CT-perfusie (CTP). De twee subtypes van beroerte die worden bestudeerd zijn ten eerste subarachnoidale bloedingen (SAB) met als complicatie het optreden van secundaire ischemie en ten tweede acute herseninfarcten met als complicatie beschadiging van de bloed hersen-barriere die tot bloeding in het geïnfarceerde gebied (hemorragische transformatie, HT) kan leiden of ernstige zwelling van het brein (maligne oedeem, MO).

Deel 1

Complicaties van subarachnoidale bloedingen: een evaluatie van secundaire ischemie met CT-perfusie

Ongeveer 5% van alle beroertes is een subarachnoidale bloeding (SAB).^{1, 2} Ongeveer de helft van alle patiënten met een SAB komt te overlijden in de eerste maand.^{2, 3} Tevens is de helft van de patiënten jonger dan 55 jaar waardoor het verlies in productieve levensjaren door deze ziekte hoog is.⁴ De prognose van patiënten met SAB wordt aanzienlijk slechter als de complicatie secundaire ischemie (DCI) optreedt.^{3, 5} DCI wordt gekenmerkt door een daling van het bewustzijn of nieuwe focale uitval. Het treedt met name op in de eerste twee weken na de bloeding.⁵ Behandeling bestaat uit hypertensieve therapie, hypervolemie en/of hemodilutie (samen triple-H therapie). Deze behandeling is echter niet zonder risico's en tevens niet bewezen werkzaam.⁶ Daar komt bij dat de diagnose DCI moeilijk te stellen is doordat er diverse andere factoren een gedaald bewustzijn of focale uitval kunnen veroorzaken bij SAB patiënten. Het testen van bestaande behandelingen en het ontwikkelen van nieuwe behandelingen is daardoor uiterst lastig. Het ontwikkelen van een nauwkeurig diagnostisch middel en het verhelderen van het ontstaan van DCI zou daarom erg zinvol zijn.

Gezien het feit dat ischemie wordt veroorzaakt door verminderde perfusie van de hersenen, lijkt het logisch dat het aantonen van deze verminderde perfusie diagnostisch is voor DCI. Verder zouden veranderingen in de perfusie rondom het ontstaan van DCI ons wellicht informatie kunnen verschaffen over het ontstaan van DCI. CTP is een nauwkeurige, goedkope en snelle techniek voor het meten van de hersenperfusie (cerebral blood volume (CBV); mean transit time (MTT); cerebral blood flow (CBF=CBV/MTT); time to peak (TTP)).⁷

Het doel van deel één van dit proefschrift is het bestuderen van de pathogenese van DCI met CTP, het diagnosticeren van DCI met CTP en het bestuderen van het effect van behandeling op hersenperfusie.

In *hoofdstuk 2* presenteren we absolute hersenperfusie metingen in patiënten zonder intracraniele pathologie om een idee te krijgen van wat normaal is. Tevens presenteren we een innovatieve manier om relatieve metingen te verkrijgen door normale verhoudingen van perfusie tussen verschillende stroomgebieden in het brein vast te stellen. Met deze relatieve metingen verwachten we minder hinder

te ondervinden van variatie die door waarnemer afhankelijke bewerkingsstappen wordt veroorzaakt.⁸ De absolute gemiddelde waarden die wij vonden in grijze stof, witte stof en de basale kernen hebben een smal betrouwbaarheidsinterval en komen overeen met waarden in de literatuur die bepaald zijn met de gouden standaard (¹³³Xe inhalatie).⁹ Tevens bleek de perfusie in de witte stof lager te zijn dan in de grijze stof, wat verklaard kan worden door een verschil in microvasculaire dichtheid.¹⁰ De relatieve metingen lieten zien dat er slechts kleine verschillen zijn in de verschillende perfusieparameters tussen de verschillende stroomgebieden. Onze alternatieve relatieve meetmethode zou een voordeel kunnen hebben boven de reguliere relatieve methode (link/rechts vergelijking) bij het bestuderen van afwijkingen waar bilaterale perfusievermindering voor kan komen. DCI en bilaterale carotisstenoses zijn hier voorbeelden van.

Om de pathogenese van DCI beter te begrijpen hebben we het effect van vaatspasmen (een veelvuldig gedocumenteerd fenomeen dat als oorzaak wordt gezien van DCI) op hersenperfusie bestudeerd en de relatie tussen vaatspasme en DCI bekeken (*hoofdstuk 3*). Tevens hebben we verschillen in perfusie tussen patiënten met en zonder DCI rondom het ontstaan van DCI bekeken (*hoofdstuk 4*). *Hoofdstuk 3* laat zien dat in het stroomgebied van een spastisch vaatsegment de perfusie is verminderd. Tevens blijkt echter dat bijna de helft van de patiënten met DCI geen vaatspasme heeft. Deze bevindingen suggereren dat vaatspasme alleen niet voldoende perfusie vermindering veroorzaakt om DCI te veroorzaken. Blijkbaar spelen er ook andere factoren een rol. Factoren die in deze context zijn genoemd als alternatieve oorzaak voor DCI zijn: de afwezigheid van collaterale vaten, een verstoorde autoregulatie en de aanwezigheid van ontstekingsreacties die micro-emboli en microvasculair vaatspasme kunnen veroorzaken.¹¹⁻¹⁶

Hoofdstuk 4 laat zien dat de absolute waardes van CBF en MTT minder gunstig zijn in patiënten met DCI voor, tijdens en na DCI. CBF en MTT verslechteren geleidelijk tot het tijdstip van DCI en herstellen daarna enigszins. De asymmetrie van MTT neemt duidelijk toe ten tijde van DCI met een gedeeltelijk herstel erna in patiënten met DCI. In patiënten zonder DCI blijft MTT asymmetrie constant en lager dan in DCI patiënten. Tevens blijkt het absolute CBV en de CBV asymmetrie vergelijkbaar te zijn tussen DCI patiënten en patiënten zonder DCI. Deze bevindingen wekken de indruk dat DCI optreedt door focale verslechtering (toenemende asymmetrie) in patiënten die enige dagen voor het ontstaan van DCI een slechtere absolute perfusie hebben. Tevens duidt de bevinding dat CBV niet verschillend is tussen DCI patiënten en patiënten zonder DCI erop dat in de gemeten gebieden geen infarcering optreedt.¹⁷⁻¹⁹ Het herstel van zowel absolute MTT als MTT asymmetrie duidt erop dat in de gemeten gebieden de ischemie reversibel was. De reversibele aard van de ischemie kan zowel spontaan zijn als veroorzaakt worden door behandeling met hypertensieve therapie. Om dit te kunnen vaststellen is echter het gerandomiseerd geven van therapie noodzakelijk. Het onderscheiden van factoren die in de periode voor DCI voor verminderde perfusie zorgen van factoren die tijdens DCI de verhoogde asymmetrie veroorzaken, is een onderwerp voor toekomstig onderzoek.

Om DCI te diagnosticeren hebben we de diagnostische waarde van non-contrast CT (NCT), kwalitatieve beoordeling van CTP en vaatspasme op CT-angiografie voor het vaststellen van DCI ten tijde van klinische achteruitgang bij SAB patiënten bestudeerd (*hoofdstuk 5*). Tevens hebben we voor cerebrale perfusie, kwantitatieve diagnostische drempelwaarden voor DCI verkregen (*hoofdstuk 6*). *Hoofdstuk 5* laat zien dat je door het kwalitatief beoordelen van CTP kleurenafbeeldingen goed onderscheid kan maken tussen patiënten met en zonder DCI ten tijde van klinische achteruitgang van SAB patiënten. Tevens bevestigen we dat NCT niet sensitief is voor het aantonen van ischemie en dat vaatspasme op CTA van weinig diagnostische waarde is voor DCI. In *hoofdstuk 6* laten we zien dat patiënten met DCI lagere absolute perfusie en hogere perfusie asymmetrie hebben dan patiënten zonder DCI. Tevens laten we zien dat zowel absolute als relatieve (asymmetrie) perfusie metingen gebruikt kunnen worden om DCI te diagnosticeren. Absolute MTT en MTT asymmetrie bleken de beste diagnostische kwaliteiten te hebben om patiënten met DCI te kunnen onderscheiden van klinisch stabiele patiënten.

Als men de resultaten van de kwalitatieve beoordeling (*hoofdstuk 5*) naast de kwantitatieve beoordeling bekijkt, lijken de kwalitatieve beoordelingen betere diagnostische eigenschappen te hebben. Ondanks het feit dat de populaties niet geheel hetzelfde zijn, lijkt deze observatie plausibel om de volgende twee redenen. Ten eerste is er een lange lijst met co-morbiditeit die bij patiënten met een SAB de perfusie kan beïnvloeden. Deze co-morbiditeit zal moeilijk van DCI te onderscheiden zijn als puur naar kwantitatieve metingen gekeken wordt en vereist kwalitatieve beoordeling. Ten tweede wordt bij kwalitatieve beoordeling het gebied met de meest afwijkende perfusie geselecteerd, terwijl metingen in vooraf geselecteerde gebieden, zoals deze heeft plaatsgevonden in onze kwantitatieve beoordeling, tot gevolg hebben dat niet altijd in de kern van de afwijking wordt gemeten. De kwantitatieve beoordeling zal daardoor tot minder afwijkende waarden hebben geleid. Het grote voordeel van de kwantitatieve drempelwaarden in *hoofdstuk 6* is dat ze het mogelijk maken om automatisch pixels te markeren waar de perfusie afwijkend is. Het zal echter zo zijn dat de gemarkeerde beelden nog geïnterpreteerd dienen te worden door een radioloog die beschikking heeft over klinische informatie om vast te stellen of de gevonden abnormale perfusie DCI representeert. Dit zal uit toekomstig onderzoek moeten blijken.

Zowel de kwantitatieve als de kwalitatieve bevindingen laten zien dat MTT de beste parameter is voor het vaststellen van DCI. In patiënten met een herseninfarct is gebleken dat deze parameter in afwezigheid van een duidelijke verslechtering van het CBV of de CBF een ischemisch gebied voorstelt dat nog niet irreversibel beschadigd is.¹⁷⁻¹⁹ Hieruit zouden we kunnen opmaken dat de afwijkingen die we bij DCI zien ook nog mogelijk reversibel zijn ten tijde van de meting (bij klinische achteruitgang). Onderscheid tussen reversibele en irreversibele ischemie bij patiënten met DCI dient in de toekomst gemaakt te worden.

In *hoofdstuk 7* hebben we alle beschikbare literatuur doorzocht naar bewijs voor de hypothese dat behandeling van patiënten met DCI met triple-H of de verschillende onderdelen ervan, leidt tot een verbetering van de CBF. Verbetering van de CBF is het beoogde doel van deze behandeling. We laten zien dat er geen goed bewijs is hiervoor. Enkel bevindingen uit niet gecontroleerde studies laten zien dat de CBF toeneemt na toediening van met name hypertensieve therapie. Door het ontbreken van een controle groep staat het echter niet vast dat dit niet een spontane verandering is. Gerandomiseerde studies naar het effect van hypertensieve therapie op CBF zijn in de toekomst wenselijk.

Deel 2

Complicaties van herseninfarcten: een evaluatie van schade aan de bloed-hersenbarrière met CT-perfusie

Ongeveer 87% van alle beroertes is een herseninfarct.¹ Ongeveer een derde van alle patiënten met een herseninfarct sterft binnen een jaar.² De gemiddelde leeftijd ligt rond de 75 jaar.² Dit is aanzienlijk hoger dan de gemiddelde leeftijd van een SAB. Net als bij een SAB wordt de prognose van patiënten met een herseninfarct aanzienlijk slechter door het optreden van complicaties van het infarct. Een herseninfarct wordt veroorzaakt door een afsluiting van een arterie in of naar het hoofd. De afsluiting wordt veroorzaakt door een embolus die uit het hart of van een atherosclerotische plaque afkomstig is of door chronisch vaatlijden.²⁰ De ischemie en infarcering die in het gebied achter de afsluiting optreedt kan leiden tot schade aan de bloed-hersenbarrière.²¹ De schade aan de bloed-hersenbarrière kan leiden tot twee belangrijke complicaties, namelijk hemorragische transformatie (HT) en maligne oedeem (MO).²²⁻²⁵ Door vroege schade aan de bloed-hersenbarrière op te sporen kan het optreden van deze complicaties wellicht voorspeld worden. Dit kan belangrijke consequenties hebben voor de behandeling. De behandeling van een herseninfarct bestaat uit het toedienen van rtPA. Dit is zelf een risico factor voor het krijgen van HT.²⁶ Patiënten die een hoog risico hebben op het krijgen van HT zijn daarom wellicht beter af als ze geen rtPA krijgen. Voor behandeling van MO is het waarschijnlijk van belang dat er zo vroeg mogelijk wordt ingegrepen, zelfs vóór het ontstaan van symptomen. De behandeling van MO bestaat uit het chirurgisch verwijderen van een deel van de schedel om inklemming te voorkomen die door de het MO kan worden veroorzaakt.²⁷

Met CTP kan de doorgankelijkheid (permeabiliteit) van de bloed-hersenbarrière worden gemeten. Het doel van deel twee van dit proefschrift is het vaststellen van het optimale gebruik van CTP voor de bloed-hersenbarrière permeabiliteit (BHBP), het evalueren van factoren die BHBP beïnvloeden in patiënten met een herseninfarct en patiënten zonder een herseninfarct en de voorspellende waarde van BHBP voor het ontstaan van HT en MO in patiënten met een herseninfarct.

BHBP kan uit CTP data worden berekend met behulp van het Patlak model.²⁸ Dit is een relatief eenvoudig en vaak gebruikt mathematische model dat het progressief uittreden van contrast buiten de vaten beschrijft. In *hoofdstuk 8* laten we zien dat bij gebruikmaking van het Patlak model alleen een verlengde acquisitie na contrasttoediening (en niet de eerste passage) geschikt is voor het bepalen van BHBP uit CTP data. De eerste passage respecteert niet de aannames van het Patlak model en zorgt voor foutief berekende hoge waarden.

Om de anatomische dekking van CTP te vergroten kunnen bij patiënten met een herseninfarct twee opnames worden gemaakt op twee verschillende anatomische niveaus in de hersenen. Hierbij wordt tevens tweemaal contrast toegediend. Omdat we niet weten hoe de eerste contrasttoediening BHBP metingen van de tweede contrasttoediening beïnvloedt, hebben we dit in *hoofdstuk 9* vergeleken. *Hoofdstuk 9* laat zien dat de aannames voor het Patlak model voor beide contrasttoedieningen evengoed worden gerespecteerd. Tevens blijkt de eerste contrasttoediening geen negatieve invloed te hebben op de metingen van de tweede contrasttoediening en kan de anatomische dekking dus ook voor BHBP metingen op deze manier uitgebreid worden.

Hoofdstuk 10 geeft een overzicht van normale variaties in BHBP in de hersencortex, basale kernen en witte stof, zoals berekend met het Patlak model uit CTP data. Tevens wordt een overzicht gegeven van factoren die BHBP beïnvloeden in patiënten zonder een herseninfarct. Diabetes type II en hypertensie blijken een ongunstig effect te hebben terwijl het gebruik van aspirine een beschermende werking lijkt te hebben.

Hoofdstuk 11 beschrijft de verschillen in BHBP bij binnenkomst tussen geïnfarceerd, ischemisch en niet-ischemisch hersenweefsel van patiënten met een herseninfarct. Tevens wordt de invloed van verschillende patiënteigenschappen op BHBP in deze groep beschreven. De resultaten laten zien dat geïnfarceerd en ischemisch weefsel en hogere BHBP hebben dan niet-ischemisch weefsel. Dit is in overeenstemming met het feit dat ischemie voor beschadiging van de BHB zorgt.^{29, 30} Uit de resultaten blijkt ook dat patiënten met een goede collaterale circulatie lagere BHBP waarden hebben dan patiënten met een slechte collaterale circulatie. Het is bekend dat een goede collaterale circulatie de ischemische schade kan beperken. Verder is er een verband tussen het ontstaan van HT en een slechte collaterale circulatie dat door onze bevindingen verklaard zou kunnen worden.³¹

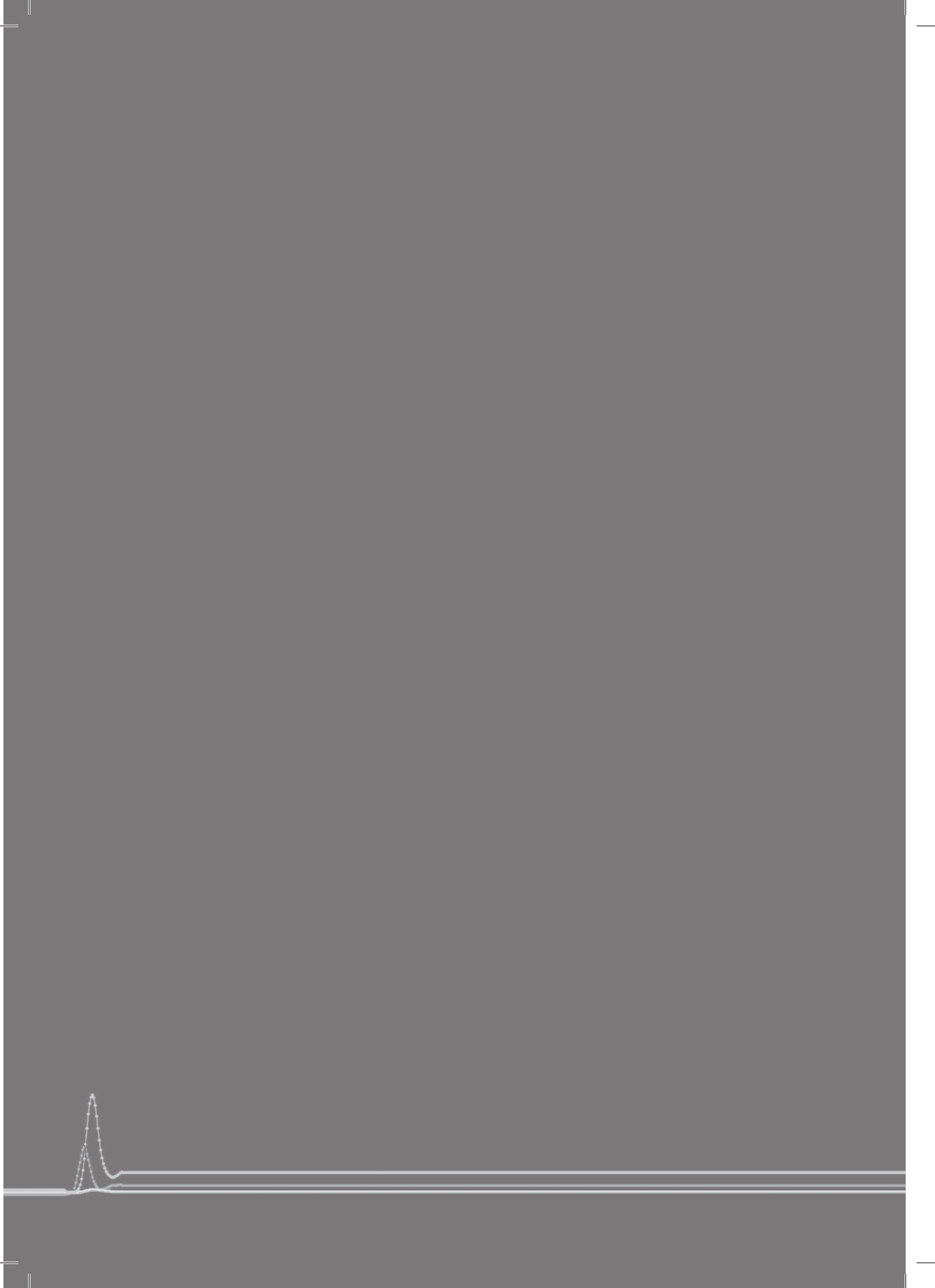
In *hoofdstuk 12* wordt naar de voorspellende waarde gekeken van BHBP metingen op de binnenkomst CTP scan voor het ontstaan van de complicaties symptomatische HT (SHT) en MO na een herseninfarct. Omdat de gegevens retrospectief zijn verzameld, was het aantal patiënten met HT en MO erg gering (beide 3 patiënten). Omdat beide complicaties het gevolg zijn van schade aan de BHB hebben we ervoor gekozen om de twee complicaties samen te nemen als uitkomst maat. Uit onze resultaten blijkt dat het volume aan gebieden met een verhoogde BHBP als goede voorspeller kan dienen voor het ontstaan van SHT of MO. Alleen patiënten ouder dan 65 met abnormaal verhoogde BHBP waardes

die rtPA gebruikten, ontwikkelden HT of MO (sensitiviteit en specificiteit 100%). Dit suggereert dat patiënten ouder dan 65 met verhoogde BHBP geen baat hebben van rtPA behandeling. Voor patiënten die MO ontwikkelen zou kunnen gelden dat rtPA de druppel is die de emmer doet overlopen. Er kan niet worden geconcludeerd dat patiënten die ouder zijn dan 65, verhoogde BHBP waarden en rtPA gebruiken vroege craniotomie moeten krijgen om de schade van MO te beperken. De helft van die patiënten ontwikkelt immers geen MO. Prospectieve studies zijn nodig om voldoende patiënten te verzamelen met SHT en MO om de twee groepen afzonderlijk van elkaar te kunnen analyseren. Tevens zouden de invloed van rtPA en reperfusie op toename van de BHBP kunnen worden onderzocht om het ontstaan van SHT en MO verder te verduidelijken.

References

1. Lloyd-Jones D, Adams R, Carnethon M, De Simone G, Ferguson TB, Flegal K, Ford E, Furie K, Go A, Greenlund K, Haase N, Hailpern S, Ho M, Howard V, Kissela B, Kittner S, Lackland D, Lisabeth L, Marelli A, McDermott M, Meigs J, Mozaffarian D, Nichol G, O'Donnell C, Roger V, Rosamond W, Sacco R, Sorlie P, Stafford R, Steinberger J, Thom T, Wasserthiel-Smolter S, Wong N, Wylie-Rosett J, Hong Y. Heart disease and stroke statistics--2009 update: A report from the american heart association statistics committee and stroke statistics subcommittee. *Circulation*. 2009;119:480-486
2. Thrift AG, Dewey HM, Sturm JW, Srikanth VK, Gilligan AK, Gall SL, Macdonell RA, McNeil JJ, Donnan GA. Incidence of stroke subtypes in the north east melbourne stroke incidence study (nemesi): Differences between men and women. *Neuroepidemiology*. 2009;32:11-18
3. Nieuwkamp DJ, Setz LE, Algra A, Linn FH, de Rooij NK, Rinkel GJ. Changes in case fatality of aneurysmal subarachnoid hemorrhage over time, according to age, sex, and region: A meta-analysis. *Lancet Neurol*. 2009;8:635-642
4. Johnston SC, Selvin S, Gress DR. The burden, trends, and demographics of mortality from subarachnoid hemorrhage. *Neurology*. 1998;50:1413-1418
5. van Gijn J, Kerr RS, Rinkel GJ. Subarachnoid hemorrhage. *Lancet*. 2007;369:306-318
6. Treggiari MM, Deem S. Which h is the most important in triple-h therapy for cerebral vasospasm? *Curr Opin Crit Care*. 2009;15:83-86
7. Hoeffner EG, Case I, Jain R, Gujar SK, Shah GV, Deveikis JP, Carlos RC, Thompson BG, Harrigan MR, Mukherji SK. Cerebral perfusion ct: Technique and clinical applications. *Radiology*. 2004;231:632-644
8. Kealey SM, Loving VA, DeLong DM, Eastwood JD. User-defined vascular input function curves: Influence on mean perfusion parameter values and signal-to-noise ratio. *Radiology*. 2004;231:587-593
9. Kawamura J, Meyer JS, Ichijo M, Kobari M, Terayama Y, Weathers S. Correlations of leuko-ariosis with cerebral atrophy and perfusion in elderly normal subjects and demented patients. *J Neurol Neurosurg Psychiatry*. 1993;56:182-187
10. Cavaglia M, Dombrowski SM, Drazba J, VasANJI A, Bokesch PM, Janigro D. Regional variation in brain capillary density and vascular response to ischemia. *Brain Res*. 2001;910:81-93
11. Weidauer S, Lanfermann H, Raabe A, Zanella F, Seifert V, Beck J. Impairment of cerebral perfusion and infarct patterns attributable to vasospasm after aneurysmal subarachnoid hemorrhage: A prospective mri and dsa study. *Stroke*. 2007;38:1831-1836
12. Weidauer S, Vatter H, Beck J, Raabe A, Lanfermann H, Seifert V, Zanella F. Focal laminar cortical infarcts following aneurysmal subarachnoid hemorrhage. *Neuroradiology*. 2008;50:1-8
13. Vergouwen MD, Vermeulen M, Coert BA, Stroes ES, Roos YB. Microthrombosis after aneurysmal subarachnoid hemorrhage: An additional explanation for delayed cerebral ischemia. *J Cereb Blood Flow Metab*. 2008;28:1761-1770
14. Romano JG, Rabinstein AA, Arheart KL, Nathan S, Campo-Bustillo I, Koch S, Forteza AM. Microemboli in aneurysmal subarachnoid hemorrhage. *J Neuroimaging*. 2008;18:396-401
15. Stein SC, Levine JM, Nagpal S, LeRoux PD. Vasospasm as the sole cause of cerebral ischemia: How strong is the evidence? *NeurosurgFocus*. 2006;21:E2

16. Jaeger M, Schuhmann MU, Soehle M, Nagel C, Meixensberger J. Continuous monitoring of cerebrovascular autoregulation after subarachnoid hemorrhage by brain tissue oxygen pressure reactivity and its relation to delayed cerebral infarction. *Stroke*. 2007;38:981-986
17. Parsons MW, Pepper EM, Bateman GA, Wang Y, Levi CR. Identification of the penumbra and infarct core on hyperacute noncontrast and perfusion ct. *Neurology*. 2007;68:730-736
18. Schaefer PW, Roccatagliata L, Ledezma C, Hoh B, Schwamm LH, Koroshetz W, Gonzalez RG, Lev MH. First-pass quantitative ct perfusion identifies thresholds for salvageable penumbra in acute stroke patients treated with intra-arterial therapy. *AJNR Am J Neuroradiol*. 2006;27:20-25
19. Wintermark M, Flanders AE, Velthuis B, Meuli R, van Leeuwen M, Goldsher D, Pineda C, Serena J, van der Schaaf I, Waaijer A, Anderson J, Nesbit G, Gabriely I, Medina V, Quiles A, Pohlman S, Quist M, Schnyder P, Bogousslavsky J, Dillon WP, Pedraza S. Perfusion-ct assessment of infarct core and penumbra: Receiver operating characteristic curve analysis in 130 patients suspected of acute hemispheric stroke. *Stroke*. 2006;37:979-985
20. Donnan GA, Fisher M, Macleod M, Davis SM. Stroke. *Lancet*. 2008;371:1612-1623
21. Latour LL, Kang DW, Ezzeddine MA, Chalela JA, Warach S. Early blood-brain barrier disruption in human focal brain ischemia. *AnnNeurol*. 2004;56:468-477
22. Lampl Y, Sadeh M, Lorberboym M. Prospective evaluation of malignant middle cerebral artery infarction with blood-brain barrier imaging using tc-99m dtpa spect. *Brain Res*. 2006;1113:194-199
23. Sandoval KE, Witt KA. Blood-brain barrier tight junction permeability and ischemic stroke. *Neurobiol Dis*. 2008;32:200-219
24. Serena J, Blanco M, Castellanos M, Silva Y, Vivancos J, Moro MA, Leira R, Lizasoain I, Castillo J, Davalos A. The prediction of malignant cerebral infarction by molecular brain barrier disruption markers. *Stroke*. 2005;36:1921-1926
25. Wang X, Lo EH. Triggers and mediators of hemorrhagic transformation in cerebral ischemia. *MolNeurobiol*. 2003;28:229-244
26. Su EJ, Fredriksson L, Geyer M, Folestad E, Cale J, Andrae J, Gao Y, Pietras K, Mann K, Yepes M, Strickland DK, Betsholtz C, Eriksson U, Lawrence DA. Activation of pdgf-cc by tissue plasminogen activator impairs blood-brain barrier integrity during ischemic stroke. *Nat Med*. 2008;14:731-737
27. Hofmeijer J, Kappelle LJ, Algra A, Amelink GJ, van Gijn J, van der Worp HB. Surgical decompression for space-occupying cerebral infarction (the hemicraniectomy after middle cerebral artery infarction with life-threatening edema trial [hamlet]): A multicentre, open, randomised trial. *Lancet Neurol*. 2009;8:326-333
28. Patlak CS, Blasberg RG, Fenstermacher JD. Graphical evaluation of blood-to-brain transfer constants from multiple-time uptake data. *JCerebBlood Flow Metab*. 1983;3:1-7
29. Gasparotti R, Grassi M, Mardighian D, Frigerio M, Pavia M, Liserre R, Magoni M, Mascaro L, Padovani A, Pezzini A. Perfusion ct in patients with acute ischemic stroke treated with intra-arterial thrombolysis: Predictive value of infarct core size on clinical outcome. *AJNR Am J Neuroradiol*. 2009;30:722-727
30. McColl BW, Carswell HV, McCulloch J, Horsburgh K. Extension of cerebral hypoperfusion and ischaemic pathology beyond mca territory after intraluminal filament occlusion in c57bl/6j mice. *Brain Res*. 2004;997:15-23
31. Christoforidis GA, Karakasis C, Mohammad Y, Caragine LP, Yang M, Slivka AP. Predictors of hemorrhage following intra-arterial thrombolysis for acute ischemic stroke: The role of pial collateral formation. *AJNR Am J Neuroradiol*. 2009;30:165-170



Dankwoord



Een grote groep mensen heeft bijgedragen aan de totstandkoming van dit proefschrift. Ik ben iedereen daar uiteraard erg Dankbaar voor.

Professor dr. G.J.E Rinkel, mijn eerste promotor, Gabriel ik heb genoten van onze leuke samenwerking en hoop deze nog lang te kunnen voortzetten. Ik wil je bedanken voor je inzichten, realisme, doortastendheid en expertise waar ik veel van heb kunnen leren. Met jou is alles bespreekbaar. Voordat ik met jou samenwerkte had ik vaak het gevoel dat wetenschappelijke besprekingen nooit tot actie leiden. Dat gevoel is geheel verdwenen.

Professor dr. W.P.Th.M. Mali, mijn tweede promotor, ik wil u bedanken voor uw begeleiding en met name voor het vertrouwen dat u mij al had geschonken voordat ik was begonnen. Ik hoop dat ik aan de verwachtingen heb voldaan.

Dr. I.C. Irene van der Schaaf, mijn eerste co-promotor, Irene ik wil je bedanken voor al je inzet en het overdragen van je kennis, motivatie en enthousiasme. Maar met name wil ik je bedanken voor het feit dat je mij de baan als promovendus hebt bezorgd, het project waaraan ik gewerkt heb in het UMC Utrecht hebt geschreven, de contacten en financiën voor mijn verblijf in San Francisco hebt geregeld, en hebt bijgedragen aan alle hoofdstukken in dit proefschrift. Kortom, zonder jou geen Dr. J.W. Dankbaar. Ik mag mijzelf gelukkig prijzen dat je mijn co-promotor was. Onze samenwerking was efficiënt, praktisch en gezellig, zeker na je bezoek in San Francisco. Je directheid en concreetheid is zeker aan mij besteed en ik ben je daar dankbaar voor.

Dr. B.K. Velthuis, mijn tweede co-promotor, Birgitta ik wil je bedanken voor de rust die je uitstraalt. Ik vind het bijzonder hoe je zoveel projecten tegelijk kan uitvoeren. Het was altijd prettig om snel even wat met je te kunnen overleggen en ik heb me nooit bezwaard gevoeld je hulp in te schakelen. Ondanks het feit dat ik de Amerikaanse schrijfstijl prefereer boven de Britse, waren je aanvullingen aan dit proefschrift onmisbaar.

Max Wintermark, to you my special thanks, you supervised my research fellowship at the University of California, San Francisco, and did that with great enthusiasm. Without you, this thesis would be only half of what it is now. I really enjoyed my stay both professionally and personally. You taught me a lot about efficiency in research, which in my opinion is one of the most important things. It has been a great privilege to work with you and I'm hoping we will stay in touch for many more years.

Nicolien de Rooij, bedankt voor het samen met mij opzetten en sturen van de DECIDE studie. Ik hoop dat je ook snel je proefschrift kan schrijven met de resultaten van onze studie.

Ewoud Smit, bedankt voor het met mij delen van je intelligentie, enthousiasme en altruïsme. Jij staat altijd voor iedereen klaar om problemen op te lossen. Hier-

bij vergeet je soms dat je zelf ook nog moet promoveren. Ewoud, je bent een van de weinige wetenschappers die de tijdrovende stappen op zich neemt die nodig zijn voor het verbeteren van een groter geheel waar iedereen van kan mee profiteren. Tijdsdruk en eigenbelang weerhouden anderen, ik denk ook mijzelf, hiervan. Dankjewel.

Jason Hom, I would like to thank you for writing all the papers with me for Max. I enjoyed your company in Vancouver and of course at UCSF.

Dr. C.J.M. Frijns, Rinie bedankt voor het uitvoeren van één van de belangrijkste onderdelen van de DECIDE studie. Zonder te weten wie er ziek is en wie niet had ik geen enkel stuk kunnen schrijven.

Dr. A.S. Slooter, Arjen dankjewel voor je hulp bij onze review en het opzetten van de hypertensie trial. Ik hoop dat er nog mooie resultaten uit zullen komen.

Prof. dr. W.M. Prokop, Mathias heel erg bedankt voor je begeleiding en gedachten. De snelheid van je gedachtegang is duizelingwekkend, maar erg motiverend. Ik vind het zeer jammer dat jij niet direct betrokken bent bij mijn opleiding tot radioloog.

Dr. H.W.A.M. de Jong, Hugo ik vind het prettig om met je samen te werken. Je bent doelgericht en praktisch ingesteld. Dankjewel voor je bijdrage en ik hoop dat we nog eens samen gaan publiceren.

Su-Chun Chen, thank you for doing the complicated statistics that come with the multivariate analysis in several of our papers. You were able to translate some of the statistics to the common language for me.

Thomas Schneider, Scott Pohlman, Bruno Soares, Sunny Virmany, Benison Lau, thank you for contributing to our papers which are now chapters of my thesis.

Bill Dillon, thank you for making my stay at UCSF possible and receiving me with such enthusiasm and kindness.

Joerg Bredno, thank you for helping me with my software problems and making all the practical adjustments.

Sandeep Arora and also Andre Furtado, thank you for making my stay at UCSF as nice as it was. I appreciated our discussions at breakfast, lunch and diner a lot.

Alan Riordan, thank you for creating a proper way to validate perfusion measurements. I enjoy working with you.

Dankwoord

Drs. L.M. Ramos, Dr. D.R. Rutgers en Drs. T.D.Witkamp, de neuroradiologen van het AZU, Lino, Dik, en Theo hartelijk dank voor jullie medewerking aan de DECIDE studie en de leerzame neuroradiologie besprekingen.

Henk, Karin, Angelique, Bas, Loes, Amanda, Irma, Sebastiaan, Jenneke, Selina, Wouter, Judith en alle andere röntgen laboranten, bedankt voor het helpen scannen van al mijn onderzoekspatiënten en het honoreren van al mijn verzoekjes. Ik werk met veel plezier met jullie samen en ben blij dat ik dat nog een aantal jaren zal blijven doen.

Hetzelfde geldt voor de verpleegkundigen van de afdeling neurologie, heel erg bedankt voor al jullie inspanningen die mijn promotieonderzoek met zich mee heeft gebracht.

Trial bureau radiologie, Anneke en Cees, bedankt voor het plannen van mijn scans en het doorspitten van databases.

Trial bureau neurologie, Sanne, Marrit, Merel, Paut en Dorien, bedankt voor jullie hulp.

Fotografie, Eugene, Karin, Roy, en Jan bedankt voor het maken van alle stickers, placemats, ingescande documenten, foto's en gezelligheid. Roy, natuurlijk ook hartelijk dank voor het verzorgen van de lay-out van dit proefschrift.

Stafsecretariaat radiologie, Linda, Marja, Amanda en Selma, bedankt voor alle behulpzame antwoorden op de soms wat domme vragen van mijn kant. Ik heb altijd met veel plezier even een korte omweg gemaakt om jullie een goedemorgen te wensen of een praatje te maken.

Marjorie Bootsma, dankjewel voor het in goede banen leiden van de aanmelding van mijn proefschrift en voor het bemachtigen van plekje in de agenda van Gabriel.

Technische cluster, Kees, Sven, Martijn, Rudy, Karel en John, bedankt voor het faciliteren van mijn onderzoek en de hulp bij alle technische problemen die ik ben tegen gekomen. Kees, zonder de twee schermen die je voor me hebt geregeld was mijn onderzoek minder efficiënt verlopen.

Professor dr. Y. van der Graaf en Professor dr. L.J. Kappelle, hartelijk dank voor het helpen schrijven van mijn AGIKO voorstel, zonder jullie was het vast nooit goedgekeurd. Tevens bedankt voor het willen plaatsnemen in mijn beoordelingscommissie.

Alle assistenten van de radiologie, neurologie en neurochirurgie, bedankt voor het helpen uitvoeren van de DECIDE studie.

Mijn research collega's en kamergenoten, Bart-Jan, Ricardo, Lisa, Rianne, Marianne, Reinout, Annemarie, Mies, Tom, Alexander, Tim, Niek, Malou, Anja, Audrey, Thomas, Beatrijs, Onno, Cecile, Liesbeth, Jet en de rest, bedankt voor jullie steun en luisterend oor bij al mijn vragen en frustraties en natuurlijk voor het al die jaren meeluisteren naar mijn muziek. Bedankt ook voor de koptelefoon.

Vrienden, Bult, Wiep bedankt voor jullie vriendschap en het paranimfen. Zonder paranimfen geen promotie en zonder vrienden geen leven.

Papa, mama en Annelies, het is een voorrecht om een Dankbaar te zijn. Ik kan me geen betere, leukere of lievere familie voorstellen. Ik ben jullie dankbaar voor wie ik ben.

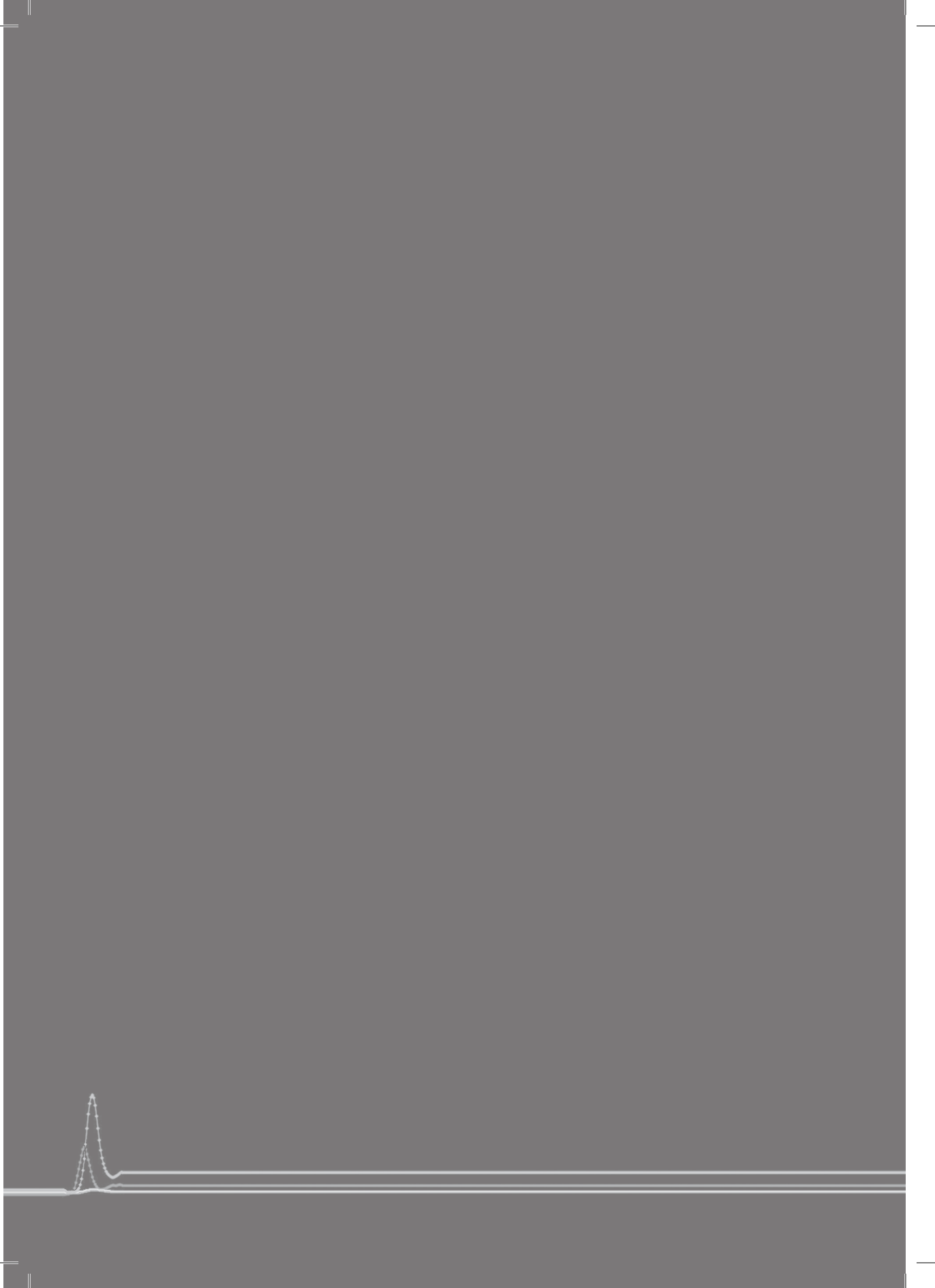
Caroline, bedankt dat je er bent. Ik hoop dat we samen nog lang en gelukkig leven.



Curriculum vitae



Jan Willem Dankbaar was born on the 1st of July 1979 in Amsterdam, the Netherlands, there he spent his first two and a half years trying to learn Dutch. He then moved to Berlin, Germany, trying to learn German for the next six years, before returning to the Netherlands where he spent the following nine years of his life in Maastricht. He graduated from secondary school in 1997 at the Jeanne d'Arc College, Maastricht. In 1997 he temporary started studying Pharmacy at the University of Utrecht because a spot at medical school was not yet available. In 2000 he then started studying medicine at the University of Amsterdam, while he continued finishing Pharmacy in Utrecht where he graduated in 2003. In April 2007 he graduated from medical school and could immediately start as a PhD student at the University Medical Center Utrecht on a project written by Dr. I.C. van der Schaaf. In September 2007 he started a 7 month research fellowship with Dr. M. Wintermark at the University of California San Francisco. In March 2009 he received a grant (AGIKO stipendium) that was awarded by the Netherlands Organization of Health Research and Development (ZonMw) to continue his PhD. In March 2010 he started as a resident in Radiology at the University Medical Center Utrecht under supervision of Professor dr. J.P.J. van Schaik.



List of publications



Journal articles

Dankbaar JW, Hom J, Schneider T, Cheng S, Lau BC, van der Schaaf IC, Virmani S, Pohlman S, Dillon WP, Wintermark M. Dynamic Perfusion-CT Assessment of the Blood-Brain Barrier Permeability: First-Pass Versus Delayed Acquisition. *AJNR Am J Neuroradiol*. 2008 Oct;29(9):1671-6.

Dankbaar JW, Hom J, Schneider T, Cheng S, Lau BC, van der Schaaf IC, Virmani S, Pohlman S, Dillon WP, Wintermark M. Accuracy and Anatomical Coverage of Perfusion-CT Assessment of the Blood-Brain Barrier Permeability: One Bolus versus Two Boluses. *Cerebrovascular Diseases*. 2008 Oct 23;26(6):600-605

Dankbaar JW, Hom J, Schneider T, Cheng S, Lau BC, van der Schaaf IC, Virmani S, Pohlman S, Dillon WP, Wintermark M. Dynamic Perfusion-CT Assessment of Blood-Brain Barrier Permeability in Non-stroke Patients: Differences between Anatomical Regions of the Brain. *Journal of Neuroradiology*. 2009 feb 27

Hom J, **Dankbaar JW**, Schneider T, Cheng S, Bredno J, Wintermark M. Optimal Duration of Acquisition for Dynamic Perfusion-CT Assessment of Blood-Brain Barrier Permeability. *AJNR Am J Neuroradiol*. 2009 Apr 15.

Dankbaar JW, de Rooij NK, Frijns CJM, Velthuis BK, Rinkel GJE, van der Schaaf IC. Diagnosing delayed cerebral ischemia with different CT modalities in SAH patients with clinical deterioration. *Stroke*. 2009 Nov;40(11):3493-8.

Soares BP, **Dankbaar JW**, Bredno J, Cheng SC, Bhogal S, Dillon WP, Wintermark M. Automated versus Manual Post-Processing of Perfusion-CT Data in Patients with Acute Cerebral Ischemia: Influence on Interobserver Variability. *Neuroradiology*. 2009 Jul;51(7):445-51.

Dankbaar JW, Rijdsdijk M, van der Schaaf IC, Velthuis BK, Rinkel GJE. Relationship between vasospasm and cerebral perfusion after aneurysmal subarachnoid hemorrhage. *Neuroradiology*. 2009 Dec;51(12):813-9.

Dankbaar JW, Slooter AJC, Rinkel GJE, van der Schaaf IC. Effect of hyperdynamic treatment on cerebral perfusion in patients with aneurysmal subarachnoid hemorrhage: a systematic review. *Critical Care*. 2010 Feb 22;14(1):R23.

Dankbaar JW, Franssen FAR, Tiehuis AM, Velthuis BK, van der Schaaf IC. Normal values of Cerebral Perfusion measured with CT- perfusion: quantitative values and inter-territorial ratios. *Submitted*

Dankbaar JW, Hom J, Schneider T, Cheng S, Bredno J, Lau BC, van der Schaaf IC, Wintermark M. Dynamic Perfusion-CT Assessment of Early Changes in Blood-Brain Barrier Permeability of Acute Ischemic Stroke Patients. *Submitted*

Hom J, **Dankbaar JW**, Soares BP, Schneider T, Cheng S, Bredno J, Lau BC, Smith W, Dillon WP, Wintermark M. Blood-Brain Barrier Permeability Measurements with Perfusion-CT as a Predictor of Symptomatic Hemorrhagic Transformation in Acute Ischemic Stroke. *Submitted*

Dankbaar JW, de Rooij NK, Smit EJ, Velthuis BK, Frijns CJM, Rinkel GJE, van der Schaaf IC. Changes in cerebral perfusion around the time of delayed cerebral ischemia in subarachnoid hemorrhage patients. *Submitted*

Dankbaar JW, de Rooij NK, Rijdsdijk M, Velthuis BK, Frijns CJM, Rinkel GJE, van der Schaaf IC. Diagnostic threshold values of cerebral perfusion measured with CT for delayed cerebral ischemia after aneurysmal subarachnoid hemorrhage. *Accepted, Stroke. 2010*

Conference proceedings (abstracts)

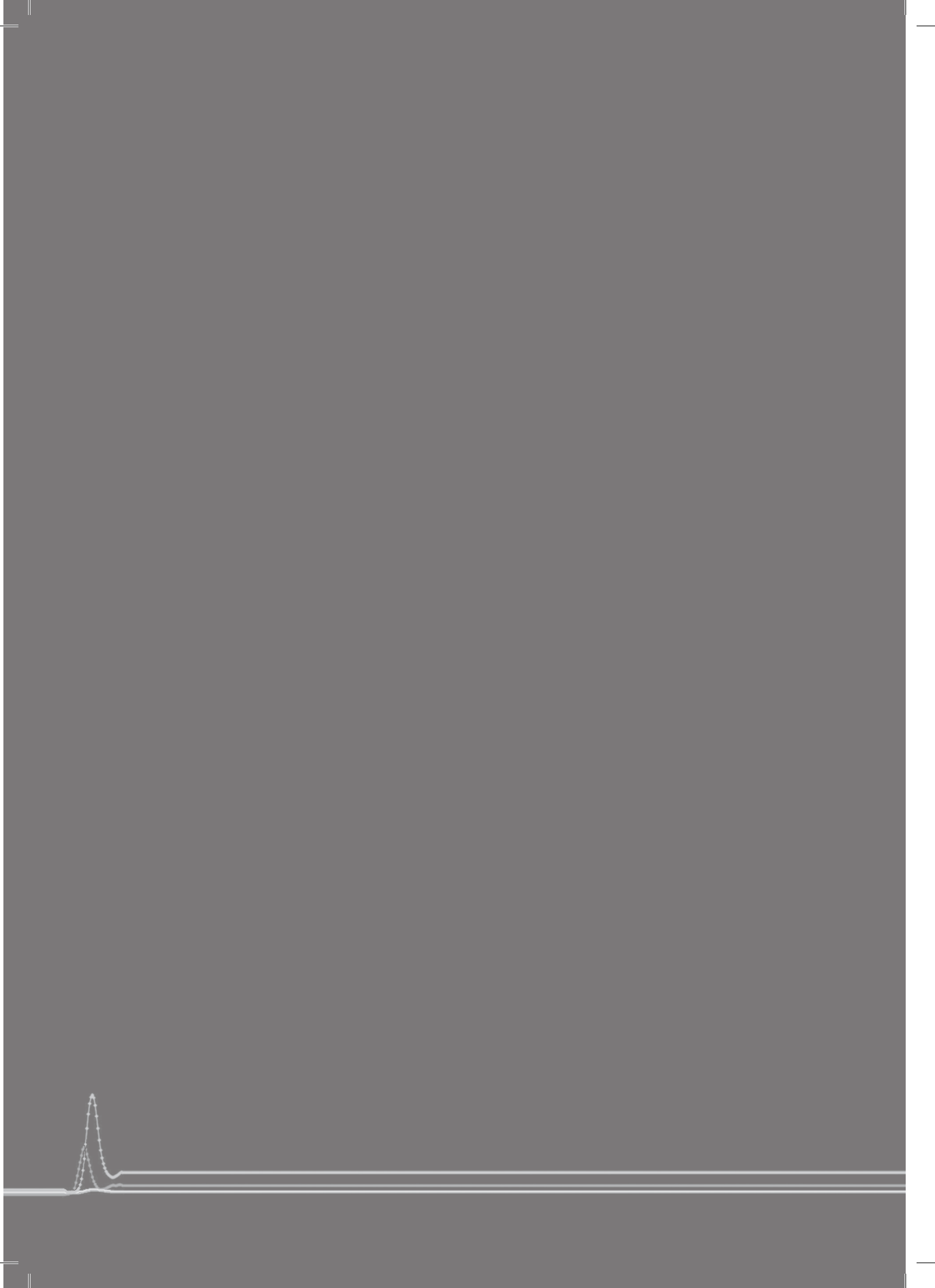
Hom J, **Dankbaar JW**, Soares BP, Schneider T, Cheng S, Bredno J, Lau BC, Smith W, Dillon WP, Wintermark M. Blood-Brain Barrier Permeability Measurements with Perfusion-CT as a Predictor of Symptomatic Hemorrhagic Transformation in Acute Ischemic Stroke. *International Stroke Conference, San Antonio, USA. 2010.*

Dankbaar JW, de Rooij NK, Frijns CJM, Velthuis BK, Rinkel GJE, van der Schaaf IC. Diagnosing delayed cerebral ischemia with different CT modalities in subarachnoid hemorrhage patients with clinical deterioration. *34th European Society of Neuroradiology Meeting, Athens, Greece. 2009.*

Dankbaar JW, Slooter AJC, Rinkel GJE, van der Schaaf IC. Effect of hemodynamic therapy on cerebral perfusion in SAB patients with DCI: a meta-analysis. *ASNR American Society of Neuroradiology 47th Annual Meeting, Vancouver, Canada. 2009.*

Dankbaar JW, Hom J, Schneider T, Cheng S, Lau BC, van der Schaaf IC, Virmani S, Pohlman S, Dillon WP, Wintermark M. Dynamic Perfusion CT Assessment of the Blood-Brain Barrier Permeability in Acute Stroke Patients: Delayed Acquisition More Accurate than First-Pass. *94th Scientific Assembly and Annual Meeting of the Radiological Society of North America, Chicago, USA. 2008.*

Dankbaar JW, Hom J, Schneider T, Cheng S, Lau BC, van der Schaaf IC, Virmani S, Pohlman S, Dillon WP, Wintermark M. Dynamic Perfusion CT Assessment of the Blood-Brain Barrier Permeability in Acute Stroke Patients: Delayed Acquisition More Accurate than First-Pass. *ASNR American Society of Neuroradiology 46th Annual Meeting, New Orleans, USA. 2008.*



Color figures



Chapter 3

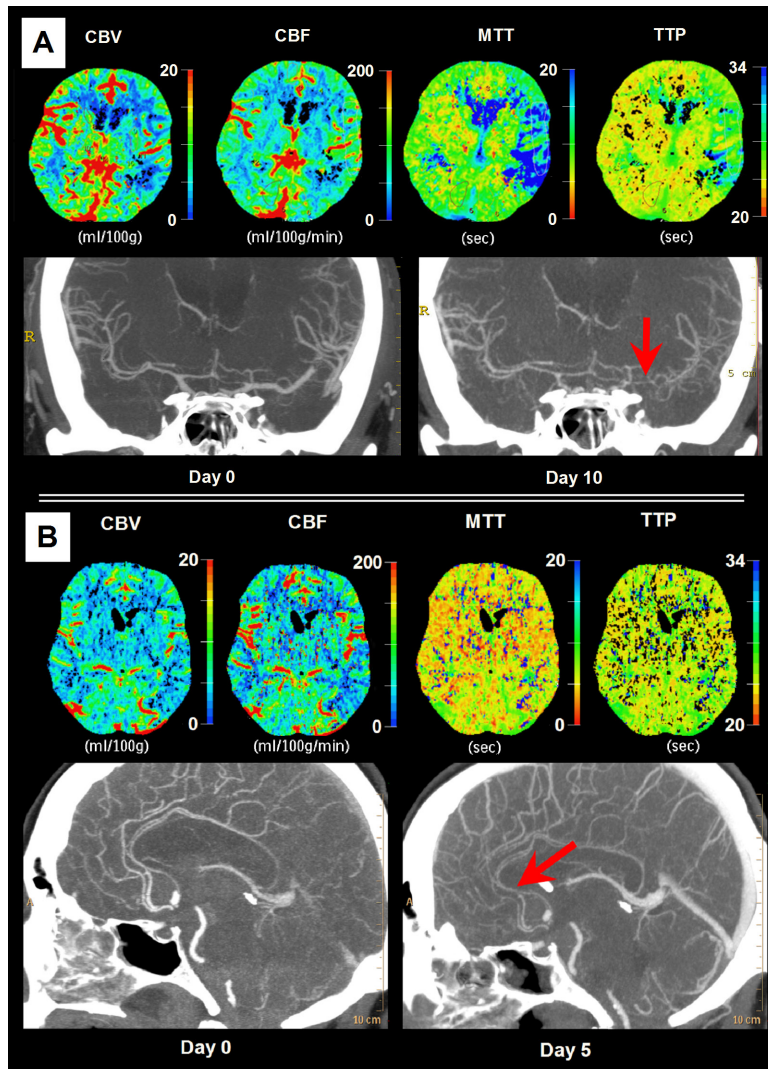


Figure 2 CTA vasospasm and its effect on cerebral perfusion as seen on CTP colour maps: (A) 43 year old man, 10 days after SAH with vasospasm (red arrow) in the left middle cerebral artery and an area of low perfusion in the flow territory of this artery (most visible on the MTT map); (B) 60 year old woman, 5 days after SAH with vasospasm (red arrow) in all anterior cerebral arteries (ACA; note the presence of an accessory ACA) and no areas of low perfusion in the flow territory of these arteries.

Chapter 4

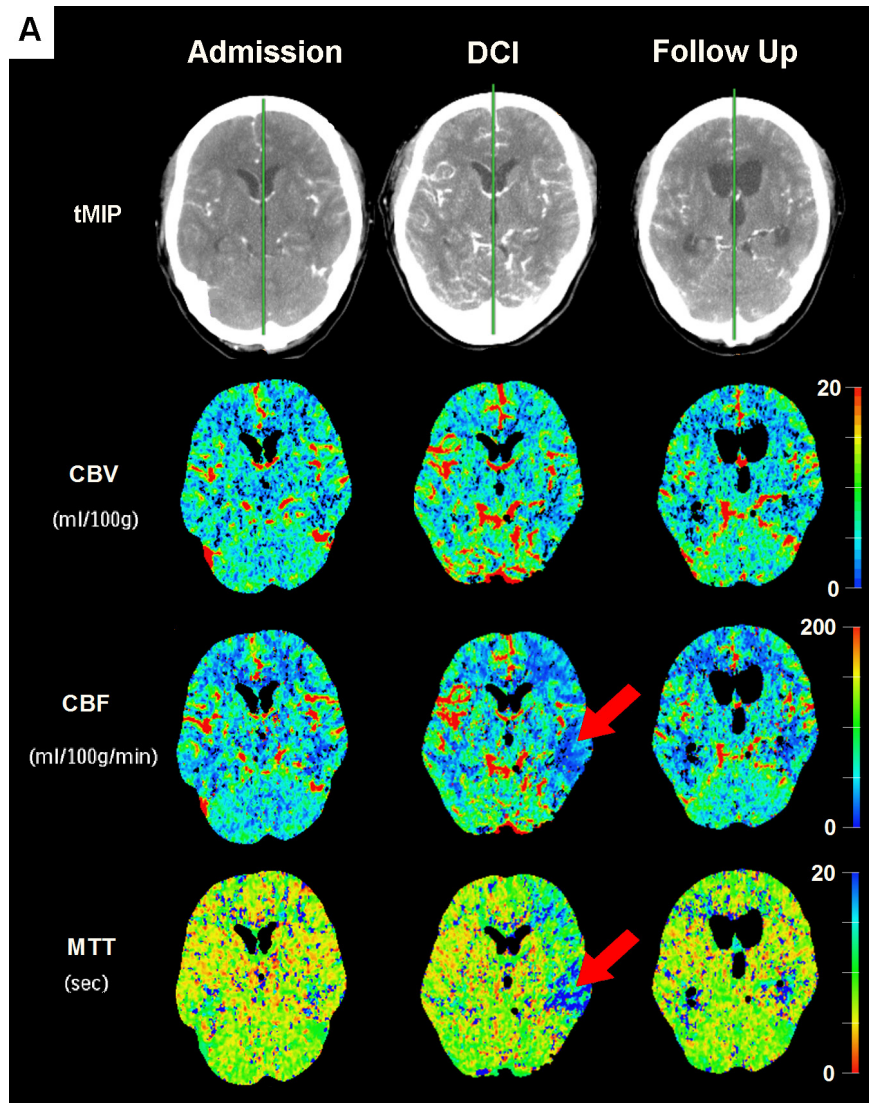


Figure 3 Example of reversible (A) and irreversible (B) ischemia in two patients with delayed cerebral ischemia (DCI). (A) A 49-year-old woman with a ruptured left carotid bifurcation aneurysm that was successfully treated with surgical clip placement. On day seven after hemorrhage the patient developed dysphasia due to DCI. The Cerebral Blood Flow (CBF) and Mean Transit Time (MTT) color map show a perfusion abnormality in the left middle cerebral artery flow territory (red arrows), and no apparent abnormalities on the Cerebral Blood Volume (CBV) map. The symptoms and the CTP abnormalities resolved in the following days, indicating reversible ischemia.

Chapter 4

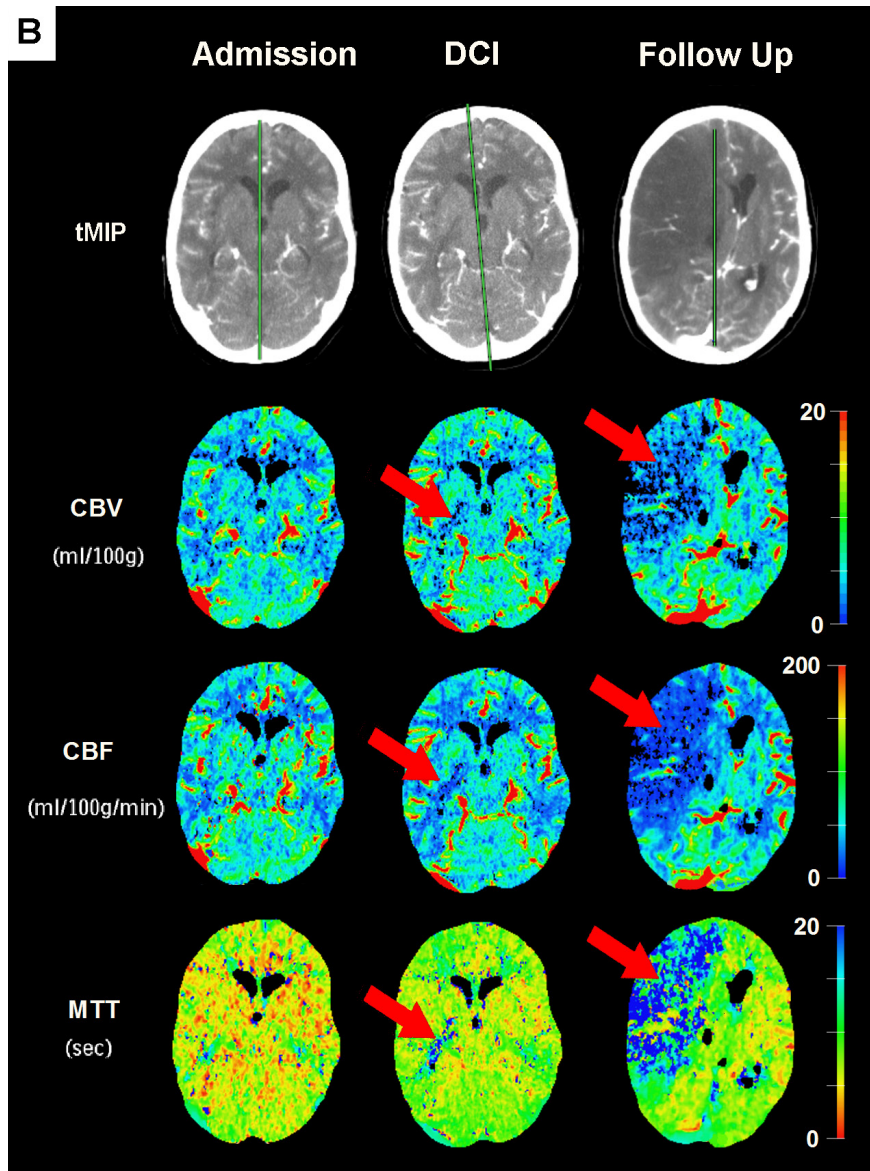


Figure 3 Example of reversible (A) and irreversible (B) ischemia in two patients with delayed cerebral ischemia (DCI). (B) A 52-year-old woman with a ruptured right carotid bifurcation aneurysm that was successfully treated by intravascular coil embolization. One day after embolization the patient developed new focal deficits from DCI, with a perfusion abnormality in the right internal capsule visible on the CBV, CBF and MTT color map (red arrows). The perfusion abnormality progressed to complete right middle cerebral artery infarction on follow up. tMIP = temporal maximal intensity projection.

Chapter 5

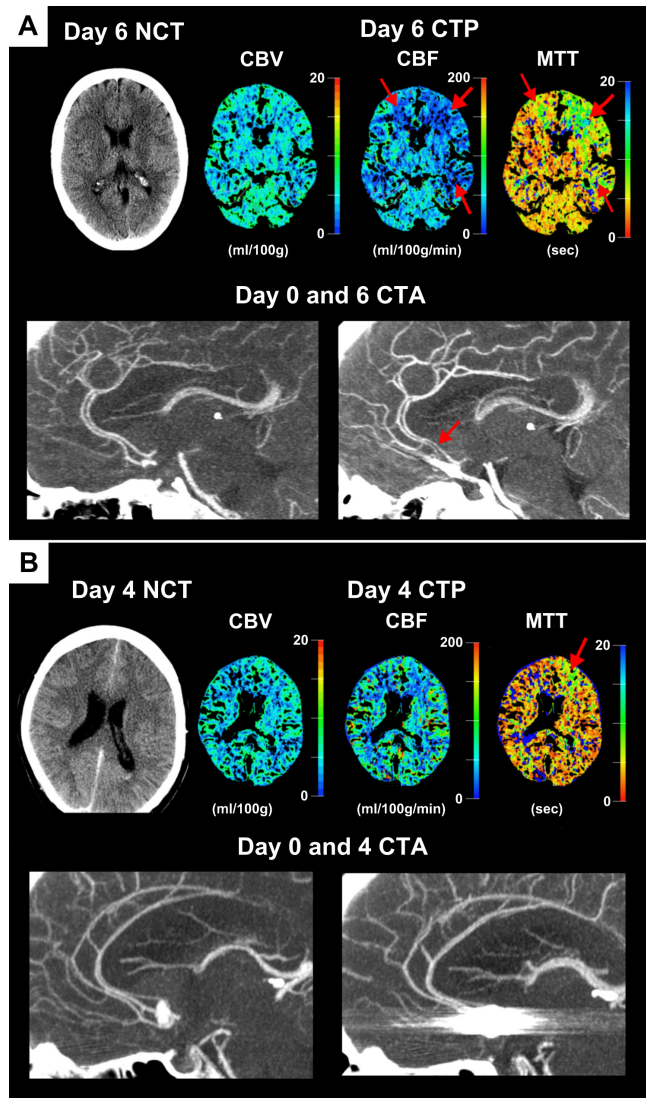


Figure 3 Example of non-contrast CT (NCT), CT-perfusion (CTP) and CT-angiography (CTA) findings in two patients with delayed cerebral ischemia (DCI): (A) 47 year old woman with clinical deterioration 6 days after subarachnoid hemorrhage (SAH) and: no ischemic changes on NCT; low perfusion in the flow territories of both anterior cerebral arteries (ACA) and the left middle cerebral artery on CTP (most visible on the MTT map); and vasospasm in the left ACA on CTA. (B) 59 year old man with clinical deterioration 4 days after SAH and: no ischemic changes on NCT; areas of low perfusion in the flow territory of the left ACA on CTP (most visible on the MTT map); but no vasospasm on CTA.

Chapter 6

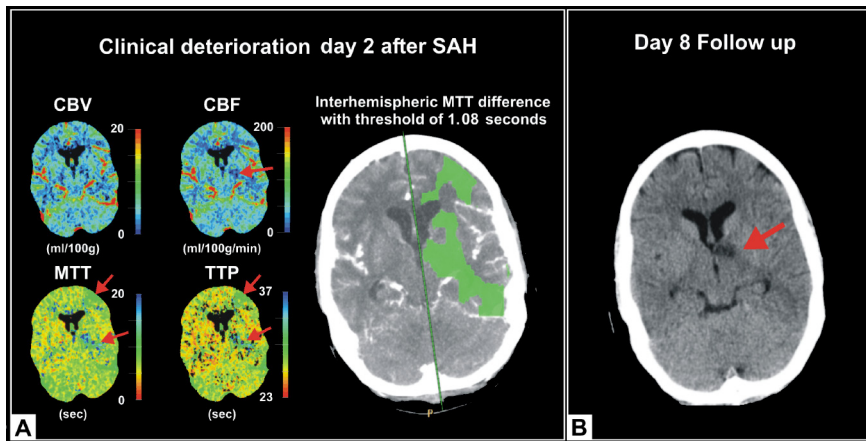


Figure 3 A 51 year old woman who developed dysphasia and a right sided paresis two days after aneurysmal subarachnoid hemorrhage (SAH). The deterioration was eventually diagnosed as delayed cerebral ischemia (DCI). **(A)** The CBF, MTT and TTP map at time of the clinical deterioration show a small perfusion defect in the left internal capsule. The MTT and TTP map furthermore show subtle abnormalities in the left frontal region. Applying the MTT difference threshold shows the perfusion asymmetries more clearly. The patient was not treated with hypertensive treatment. **(B)** On the follow up non-contrast CT 6 days later (day 8 after hemorrhage) permanent infarction is seen in the internal capsule but not in the anterior frontal region, indicating that the ischemia has partially resolved. CBV = cerebral blood volume; CBF = cerebral blood flow; MTT = mean transit time; TTP = time to peak.

Chapter 8

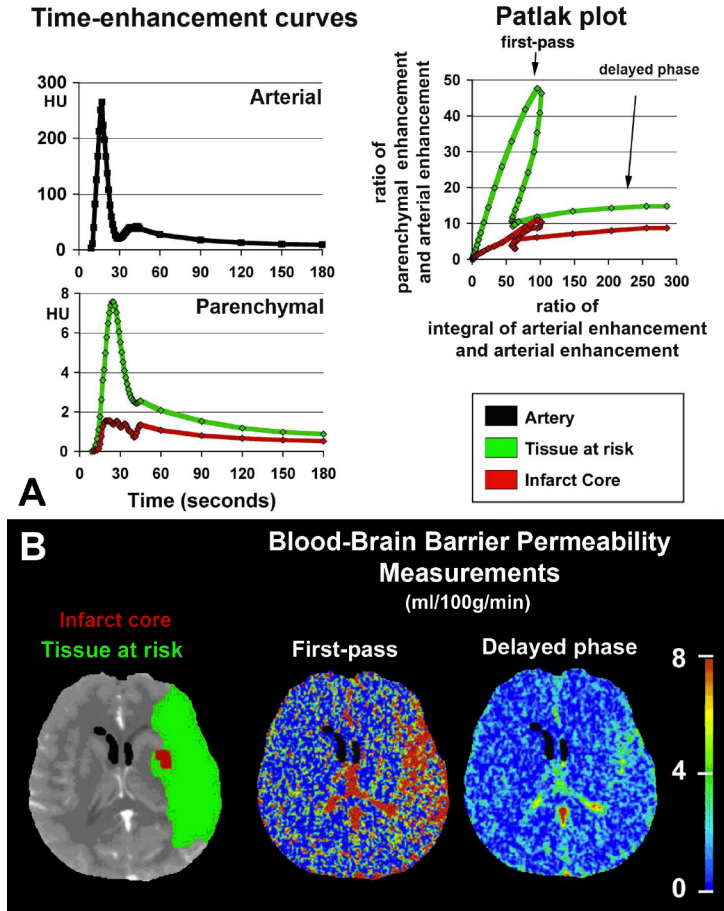


Figure 1 Graphical illustration of the calculation of blood-brain barrier permeability (BBBP) using the Patlak model. (A) The Patlak plots are constructed from the arterial and parenchymal time-enhancements curves. The first-pass component of the Patlak plots is clearly not linear, especially within the tissue at risk (shown in green in (B)), while the delayed phase respects the linear, steady-state assumption of the Patlak model. (B) BBBP maps, at the level of the basal ganglia, are shown. They are extracted from the Patlak plots and performed pixel-by-pixel. The first-pass BBBP map is noisier than delayed phase BBBP map because the quality of the linear fit is less, and results in BBBP values that are overestimated compared to the delayed phase BBBP values. This is true again especially within the tissue at risk (shown in green). The CTP infarct core (shown in red) and at risk brain tissue (shown in green) are automatically calculated by the software using MTT and CBV reported in the literature as the most accurate (CT-perfusion salvageable brain tissue: $MTT > 145\%$ of the contralateral side values plus $CBV \geq 2.0$ ml/100g; CT-perfusion infarct core: $MTT > 145\%$ of the contralateral side values plus $CBV < 2.0$ ml/100g).²⁰

Chapter 9

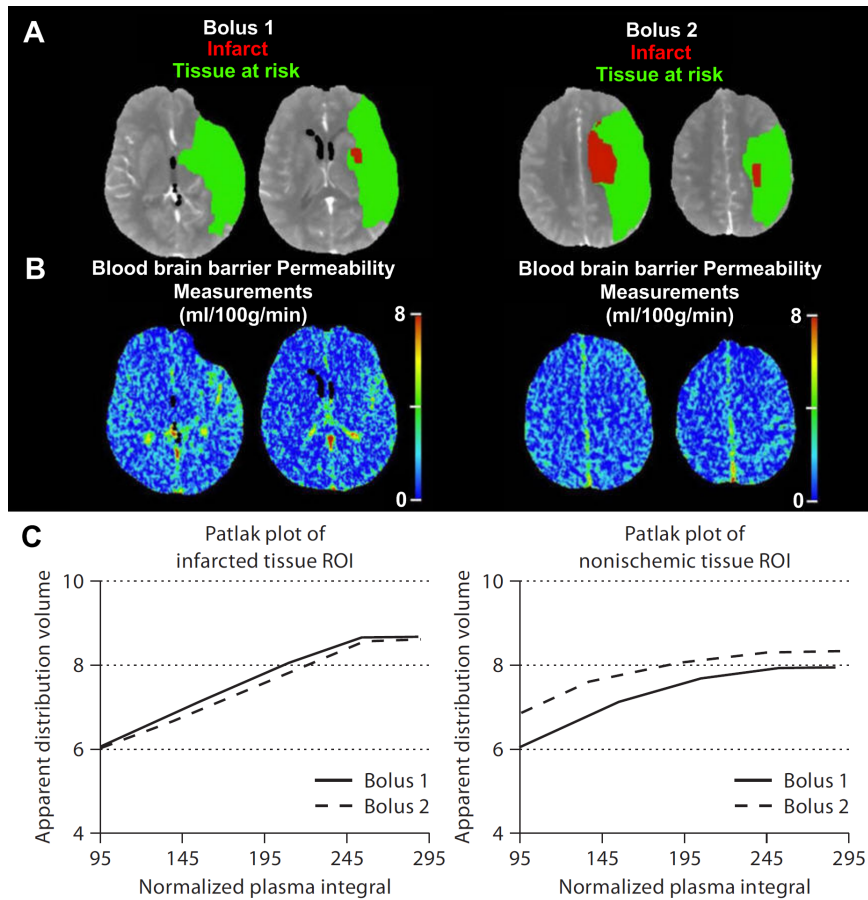


Figure 1 Example of graphical illustration of blood-brain barrier permeability (BBBP), calculated from the slope of a regression line fit to the Patlak plot: (A) CTP infarct core and tissue at risk threshold maps; (B) BBBP color maps, BBBP values from the second bolus (bolus 2) were not lower than the values from the first bolus (bolus 1); (C) Patlak plots that were constructed from arterial and parenchymal time-enhancements curves, in an infarcted tissue ROI and a non-ischemic tissue ROI. These Patlak plots illustrate how small the differences in slope (BBBP) and linearity between bolus 1 and 2 are. Of note, the slope of the plot from the infarcted tissue ROI is steeper than the slope of the non-ischemic tissue ROI.

Chapter 11

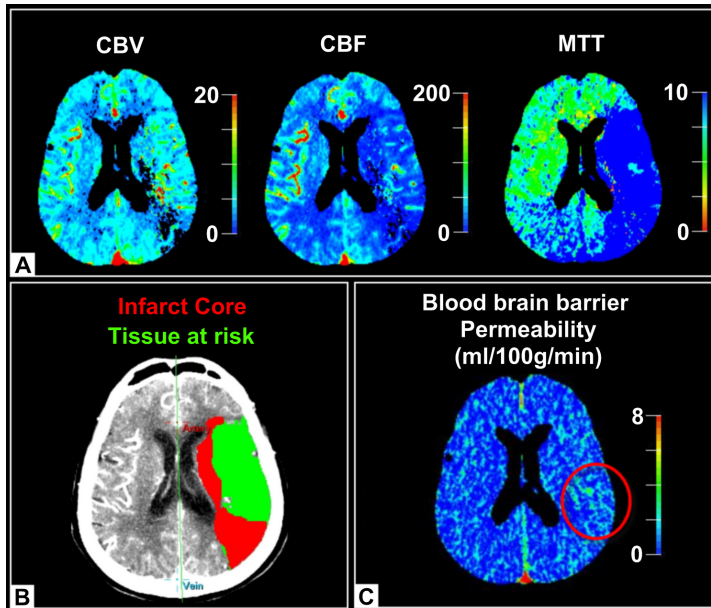


Figure 1 Illustrative case: 59 year old patient with an ischemic stroke in the left middle cerebral artery (MCA) flow territory, admitted within 5 hours after symptom onset with NIH-stroke scale of 14. (A) perfusion maps showing cerebral blood volume (CBV), cerebral blood flow (CBF), and mean transit time (MTT); (B) infarct core in red and penumbra in green determined by perfusion threshold values¹⁶; (C) blood brain barrier permeability (BBBP) map calculated with the Patlak model from delayed phase perfusion data¹² showing an area of increased BBBP in the left MCA flow territory adjacent to the infarct core.

Chapter 12

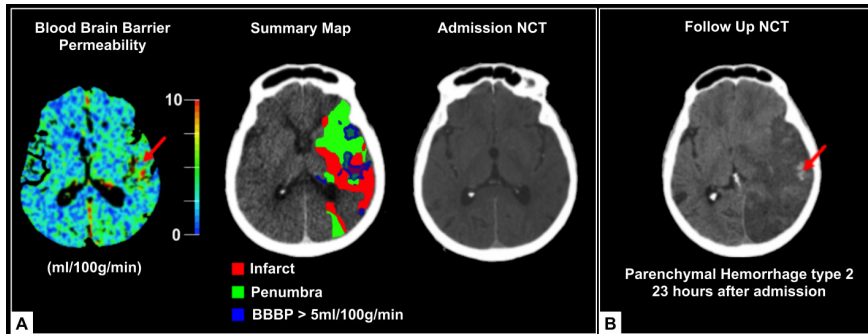


Figure 1 Illustrative case of abnormal permeability resulting in hemorrhagic transformation. (A) A 75 year-old woman with stroke CT imaging work-up approximately two hours after onset of a right sided hemiparesis. The blood brain barrier permeability (BBBP) map shows an area of increased BBBP (red arrow); applying the 5 ml/100gr/min threshold shows a “hotspot” of increased BBBP (automatically delineated in blue by the software) in the infarct core (red area) on the summary map; the non-contrast CT (NCT) revealed no evidence of intracranial hemorrhage. The patients was treated with IV rtPA. (B) 23 hours later, she was in critical condition in the ICU, and NCT imaging follow-up at that time demonstrated parenchymal hematoma type-2 (red arrow). Of note, permeability hotspots occur in both the infarct and penumbra, not just in the infarct, where the vasculature has presumably undergone the most severe ischemia-induced damage. This highlights that permeability imaging provides information above and beyond what is provided by the standard perfusion-CT parameters that can be used to define infarct and penumbra.

